NYLON 4,6 AS MEMBRANE MATERIAL

Polymer Crystallization during Immersion Precipitation

Astrid Bulte

NYLON 4,6 AS MEMBRANE MATERIAL

Polymer Crystallization during Immersion Precipitation

CIP-GEGEVENS KONINKLIJKE BIBLIOTHEEK, DEN HAAG

Bulte, Astrid Maria Wilhelmina

Nylon 4,6 as membrane material : polymer crystallization
during immersion precipitation / Astrid Maria Wilhelmina
Bulte. - [S.l. : s.n.]. - Ill.
Proefschrift Enschede. Met lit. opg.
ISBN 90-9006884-8
Trefw.: nylon / polymeerchemie

Acknowledgement

D.S.M. The Netherlands is gratefully acknowledged for their financial support.

Druk: Alfa Enschede

NYLON 4,6 AS MEMBRANE MATERIAL

Polymer Crystallization during Immersion Precipitation

Proefschrift

ter verkrijging van
de graad van doctor aan de Universiteit Twente,
op gezag van de rector magnificus
prof. dr. Th.J.A. Popma
volgens besluit van het College voor Promoties
in het openbaar te verdedigen
op vrijdag 11 februari 1994 te 15.00 uur

door

Astrid Maria Wilhelmina Bulte

geboren op 21 oktober 1964

te Oldenzaal

Dit proefschrift is goedgekeurd door de promotores prof dr ing H. Strathmann en prof dr C.A. Smolders, en door de assistent-promotor dr ing M.H.V. Mulder.

Voorwoord

De totstandkoming van dit proefschrift is mede afhankelijk geweest van een groot aantal mensen. In eerste instantie wil ik mijn promotores Heiner Strathmann en Kees Smolders bedanken voor hun wetenschappelijke en morele support. Aan Marcel Mulder ben ik meer dan dank verschuldigd, niet alleen voor de technische realisatie van het project, maar ook voor het overbrengen van jouw levenswijsheid, waarin je hebt laten zien dat een heleboel dingen uiteindelijk op hun pootjes terecht komen. Iedereen binnen de groep membraantechnologie heeft bijgedragen tot vier zeer plezierige jaren. Bedankt!

DSM Nederland wil ik bedanken voor de financiering van dit project. De goede en prettige samenwerking, mede tot stand gekomen dankzij Wytze Meindersma, is de vooruitgang van dit project zeker ten goede gekomen. Het organiseren van experimenten, het beschikbaar stellen van chemicaliën en het geven van toestemming tot publicatie, vaak op zeer korte termijn, zijn zaken die zonder problemen zijn verlopen. Stefan Eltink wil ik bedanken voor de motiverende discussies over kristallisatie, die autoritten van zo'n vijf uur volledig compenseerden. Betty Folkers en Stefan Eltink, ik dank jullie beiden voor het optreden als mijn paranimfen.

Betty wil ik tevens bedanken voor de bijzondere prettige manier van samenwerken. Mede door jouw inzet en inbreng zijn een groot aantal experimenten een heel stuk systematischer verlopen. Een woord van dank is zeker op zijn plaats voor John Krol en Erik Naafs, die beiden voor een groot deel aan dit proefschrift hebben bijgedragen. John en Erik ook bedankt voor het uitvoeren van die rotklusjes, die ik jullie vroeg te doen na jullie afstuderen. Frank van Eeten wil ik bedanken voor de enthousiaste en professionele inzet, waarmee je vanuit de Hogeschool Amsterdam je afstudeerwerk bent komen doen. Jean Marc Duval is als kamergenoot gedurende drieëneenhalf jaar een vast steunpunt geweest voor mijn vrolijke en ook wel eens minder plezierige buien. Merci!

Aan de na-mensa-se wandelingen langs het natuurschoon van de Campus met Erik Rolevink, Jeroen Boom en de andere dis-genoten denk ik met plezier terug. Erik, bedankt voor je uitleg en verklaring van menig plantje en Jeroen, dank je voor je altijd relativerende woorden.

Marjo Peeters en Josef Thesing beiden bedankt voor alle begrip, dat er was als ik op een willekeurige tijdstip onze kamer binnenstormde en plotseling van alles en nog wat nodig had. Marjo, dank je voor de last-minute correcties, vooral wat betreft mijn Nederlands.
Verder wil ik alle medewerkers van de faculteit Chemische Technologie bedanken, zonder jullie werkzaamheden en medewerking had ik mijn werk niet kunnen uitvoeren.
Als laatste bedank ik een ieder, die via een niet-technische weg heeft bijgedragen tot het gereedkomen van dit boekje, vooral diegenen die het laatste half jaar tekort zijn gekomen, omdat ik maar één ding voor ogen had: hoofdstukken, hoofdstukken, hoofdstukken....
Remko, vooral jouw support op persoonlijk en wetenschappelijk vlak valt door niemand te overtreffen.

Contents

CHAPTER 1

Aliphatic Polyamides as Membrane Materials; Membrane Formation by Immersion Precipitation

A.M.W. Bulte, M.H.V. Mulder, C.A. Smolders, H. Strathmann

ALIPHATIC POLYAMIDES

Introduction

As researchers understand phenomena of our physical world often these discoveries are the structural elements for the development of new technologies, thus inspired by the ingenuity of nature. The discovery of the molecular nature of macromolecules[1] has allowed the mimicry of natural polymers, such as cotton, starch, proteins and wool. Synthetic polymers could be prepared, based on the principle that macromolecules consist of long chains with repeating monomeric units. Aliphatic polyamides or nylons were among the first macromolecules synthesized. Carothers developed the synthesis of polyamide 6,6 in the laboratories of Dupont de Nemours (U.S.A) in 1935[2], followed by Schlack of I.G. Farbenindustrie Aktieengesellschaft Germany[3], who was able to synthesize polyamide 6 in 1938. Soon these polyamides became known under the name of nylon.

Ironically, major technological achievements are frequently developed during war time. During World War II the production of nylon yarn was used for military purposes, e.g. parachutes, airplane tire cords, glider tow ropes, and military apparel[4]. At the end of the war, nylon production was expanded and the use of nylon in clothing, industrial, and carpet application grew rapidly. In addition, nylon became

important as an engineering plastic. Applications can be found in the automotive industry, as cog-wheels, tubing and tank-caps, and in electrical industry as connectors and switches. Nylons in membrane science emerged in the beginning of the seventies and is currently applied mainly for the preparation of microfiltration membranes. Application and preparation techniques will be described later on.

Properties of the different nylons

A polyamide is a synthetic polymeric amide in which recurring amide groups (-NHCO-) are an integral part of the main polymer chain. A large number of types are available with completely different properties. These polymers can be classified by aliphatic and aromatic polyamides.
The basic aliphatic polyamides are referred to as nylons. The schematic structural formulas of this class of polyamides are given in figure 1.
Aromatic polyamides have an aromatic ring structure in the polymer chain. Well known aromatic polyamides are Nomex, Kevlar and Twaron. Nomex (poly(m-phenylene isophtalamide) contains meta substituted rings. The para substituted polybenzamides (Kevlar and Twaron) show a higher chemical and thermal stability and are mechanically stronger.

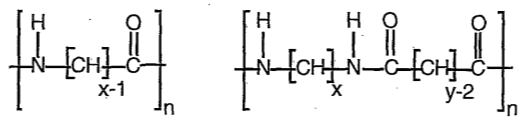

Figure 1. Formulas for basic aliphatic polyamides also known as nylon x or nylon x,y

The basic aliphatic polyamides or nylons are identified by a simple numerical system[4]: one number indicates that the product was prepared from a single monomeric substance and represents the number of carbon atoms in the linear chain of the recurring polymer unit. For example, nylon 6 is manufactured by the ring opening polymerization of caprolactam and polyamide 11 from 11-aminodecanoic acid. When two reactants are used in the polymer manufacture, they are represented by numbers separated by a comma. The first refers to the number of carbon atoms in the diamine

and the second to the number of carbon atoms in the dibasic acid. Thus nylon 6,6 is prepared by the reaction of hexamethylenediamine and adipic acid and nylon 6,12 from hexamethylenediamine and dodecanedioic acid. In 1975 Gaymans[5] was able to synthesize high molecular nylon 4,6 in a two stage process. A prepolymer was synthesized from tetramethylene diamine and adipic acid, followed by condensation in the solid state to a high molecular weight nylon 4,6. The commercial availability of nylon 6,6 and nylon 6 was established just before 1940 by Dupont and I.G. Farben respectively. In 1990 the Dutch State Mines (D.S.M.) introduced nylon 4,6 as an engineering resin called Stanyl. This polymer exhibits superior mechanical, thermal and chemical properties compared to nylon 6,6 and nylon 6, and has found its application as an engineering plastic for e.g. cog-wheels, tubing and tank-caps, and as a membrane material.

The aliphatic polyamides or nylons are structurally regular chains consisting of a series of methylene groups joined together by the strongly hydrogen bonding amide linkage[4]. The hydrogen bonding results in strong intermolecular associations. Symmetrical, hydrogen-bonded linear polyamides are generally highly crystalline with a degree of crystallization varying from 20 - 50%[4]. The nylons owe their good mechanical properties and their chemical stability mainly to this property. Yield stress, tensile strength, module, hardness, and abrasion resistance increase with increasing crystallinity, whereas water sorption and impact strength decrease. The nylons with an even number of carbon atoms in their repeating structure, such as nylon 6,6, nylon 6, nylon 6,10, and nylon 4,6 show the largest degree of crystallinity. The crystal structure is even more regular for nylon 4,6, because in both parts of the repeating unit four carbon atoms lie in between the amide group. This is reflected in the highest melting temperature of the family of nylons (see table 1) and a relatively high tendency towards fast crystallization.

Nylons are known to be resistant to a large number of organic solvents, partly because of their crystalline nature. They are highly resistant to aliphatic and aromatic hydrocarbons[6] as well as to some linear alcohols and aprotic liquids such as n-methylpyrrolidone and dimethylformamide. The chemical stability of nylon 4,6, nylon 6,6 and nylon 6 in various organic liquids is given in table 2. Chemical stability is largely influenced by the degree of crystallization of the polyamides. The literature

data presented in table 2 are valid for samples with a relatively large degree of crystallinity[6].

Table 1. Some physical properties of nylon 4,6, nylon 6,6 and nylon 6[4].

	nylon 4,6	*nylon 6,6*	*nylon 6*
Glass transition (°C)	80	57	50
Melting temperature (°C)	295	265	220
Degree of crystallinity (%)	50	30	20
Density (kg / m³)	1180	1140	1140

Table 2. Chemical resistance of nylon 4,6, nylon 6,6 and nylon 6 towards various pure liquids[6].

liquid	*weight increase (wt %)*		
	nylon 4,6 [a]	*nylon 6,6* [b]	*nylon 6* [b]
methanol	11	9	3
ethanol	9	3	3
toluene	<1	1	1
hexane	<1	<1	<1
acetone	<1	1	3
methyletylketone	<1	1	2
DMF	<1	<1	<1
NMP	4	n.a.	n.a.
methylene chloride	10	n.r.	n.r.
chloroform	18	n.a.	n.a.
acetic acid	22	n.r.	n.r.

a: determined by measuring weight increase of triplicate samples in 48 hours most samples showed no further weight increase.
b: according to reference 6
n.a.: not available
n.r.: dissolved / not resistent

Crystallization and Crystallinity

The crystalline state refers to the ordered polymer regions, whereas the amorphous state is unordered[7]. Polymers may either be completely amorphous or *semicrystalline*, since no polymer is completely crystalline. The ordering of macromolecules in a microscopic crystal lattice resembles the arrangement of low molecular components in a fundamental structural unit composed of atoms, molecules, or ions. In a crystal lattice of a macromolecule, one molecule, however, is part of more unit cells. A schematical representation of several unit cells is given in figure 2. A single crystal consists of chains folded back upon themselves[8] (see figure 2). Such thin platelets are termed lamellae, with dimensions typically of 1000 nm^2 x 15 nm, when grown from dilute polymer solutions. The unit cells for nylon 6, nylon 6,6 and nylon 4,6 are shown in figure 3.

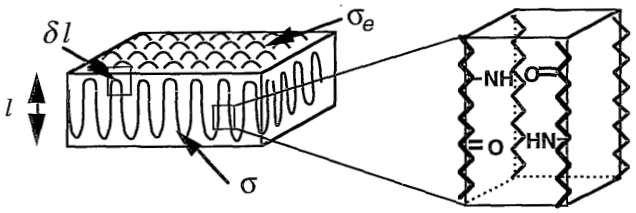

Figure 2. Folded chains in a crystalline structure[9] with the folded surface free energy, σ_e, and the lateral free energy, σ (left-hand side), and a schematical unit cell for a nylon (right-hand side).

Crystallization from polymer melts or from concentrated solutions usually do not lead to the formation of individual lamellae. The crystalline structures that appear under these circumstances are called spherulites (see figure 4): spherical entities that consists both of amorphous and crystalline material. Nylons can show spherulite formation, which under polarized light is observed by the appearance of Maltese crosses[4]. A comprehensive mechanism for spherulitic crystallization has first been reported by Keith and Padden[12] (see figure 4). The growth of a spherulite begins with a crystalline entity, presumably a single crystal nucleus. The nucleus degenerates into sheaf-like structures during the early stages of the spherulitic growth. Axialites[13] form an intermediate stage in the formation of spherulites. The lamellae fan out progressively, and grow away from the plane as the structures begin

to mature. Once the center, indicated with R (see figure 4) has been filled, the branching lamellae grow into a radial direction.

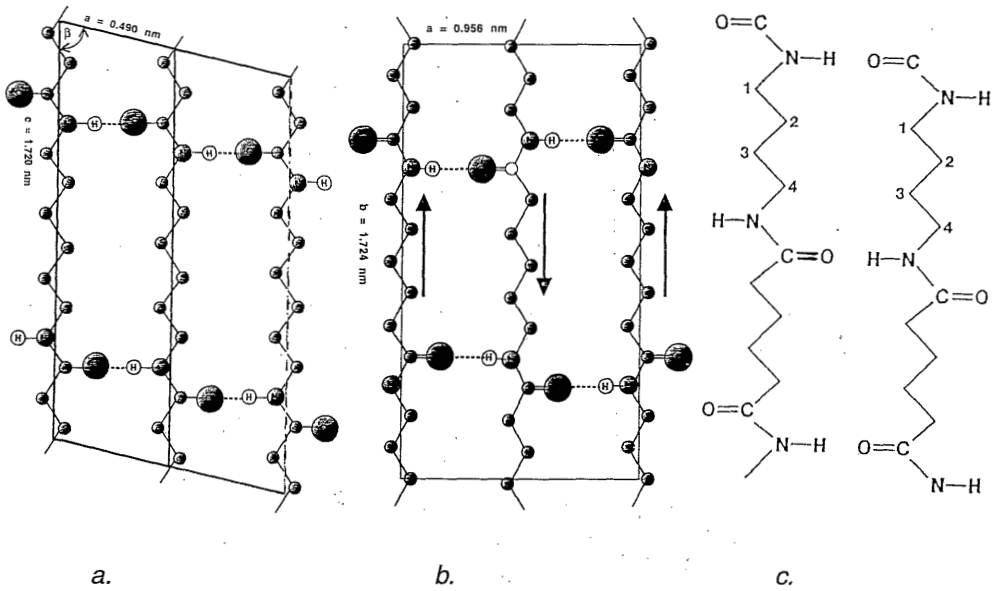

Figure 3. Projections of the unit cells of nylon 6,6 (a), nylon 6 (b)[10] *and nylon 4,6 (c)*[11] *determined by X-ray. The crystal structures are all the stable forms at room temperature. The lattice constants and axis angles are: (a) a=0.49 nm, b=0.54 nm, c=1.72 nm (fiber axis), α=48.5°, β=77° and γ=63.5° for nylon 6,6; (b) a=0.956 nm, b=1.724 nm (fiber axis), c=0.801 nm, α=γ=90° and β=67.5° for nylon 6 (α-structure) and (c) a=0.49 nm, b=0.55 nm, c=1.46 nm, α=48.5°, β=77° and γ=63° for nylon 4,6.*

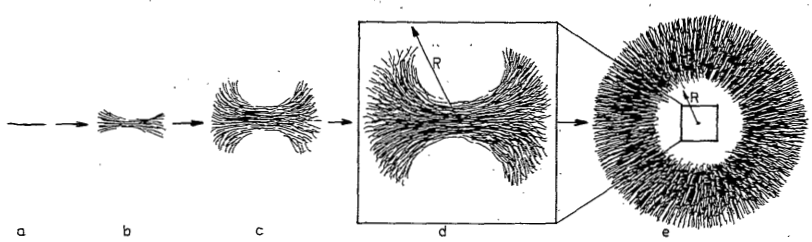

Figure 4. The development of a spherulite according to Keith and Padden[12].

The radius of spherulites grow linearly in time when crystallized from the melt or from solution until neighboring spherulites impinge or by exhaustion of the polymer solution[18,19]. When spherulites are nucleated simultaneously from the melt straight borders are observed (see figure 5).
The exact structure that is obtained strongly depends on the crystallization circumstances. The nuclei can either grow out completely or stop growing at intermediate stages (figure 4) if only a few or relatively large nuclei have been created.
Spherulites in nylons have been studied by Keller[14,15] and Magill[16,17] when grown from a polymer solution. Both spherulitic and axialitic textures have been observed when films were prepared by evaporation of solvent (formic acid or cresol) or by quenching in water.

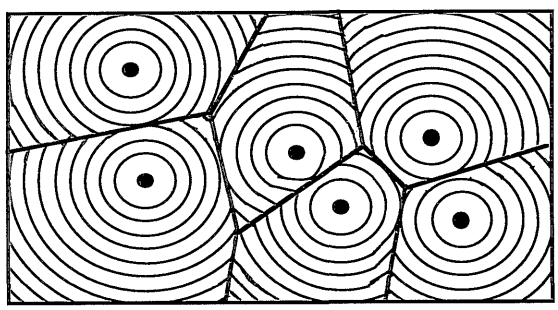

Figure 5. Schematic drawing of the change in the radius of the spherulite during crystallization from the melt.

Nucleation mechanisms have been extensively described by Lauritzen and Hoffman[20]. Nucleation of crystals of macromolecules is a more complex process compared to systems exclusively consisting of low molecular substances because of the strong anisotropy of the crystal structure (see figure 2).
Polymer melts and solutions start to crystallize at much lower temperatures than the equilibrium melting temperature; they supercool. Any crystal must have its beginning as a small nucleus, which is characterized by a large surface area to volume ratio.

Before a thermodynamically stable crystal of sufficient size can be grown, a nucleus must first be formed via an intermediate that is energetically unfavorable: an activation energy is required. This can be described by plotting the free enthalpy change against the size of the nucleus that is created. The nucleus size at which the maximum of the free enthalpy curve occurs (figure 6) corresponds to the size of the critical nucleus.

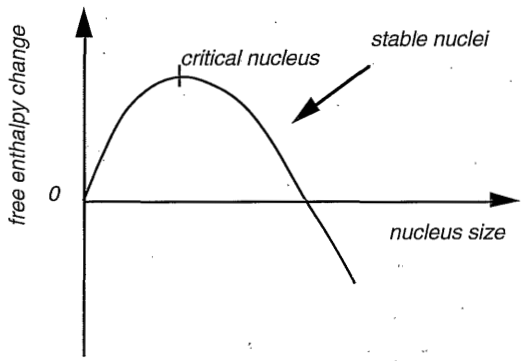

Figure 6. Schematic representation of the change in free enthalpy as a function of size, in the nucleation process.

Only nuclei with a size larger than the critical nucleus size are stable nuclei. Once these nuclei are formed, they spontaneously grow out. Smaller nuclei will have the tendency to disappear. The free enthalpy barrier to crystallization can be overcome by local random concentration fluctuations. The larger the required size of the nucleus, the longer will be the time necessary for the nucleation process. A critical nucleus dimension is related to the surface free energy, σ_e, the melting temperature T_m, the heat of fusion, Δh_f, the undercooling, $\Delta T=T_m-T$, and the density, ρ, according to[20]:

$$l = 2\,\sigma_e T_m / (\Delta h_f \Delta T\,\rho) + \delta l$$

in which 'l' is the lamellar thickness. With typical values T_m =600K, Δh_f = 200 J/g, ρ = 1 g/cm^3 and σ_e = 100 10^{-3}N / m and δl =4 nm (see figure 2), the critical lamellar thicknesses are e.g. 600, 60, 28, 16, 10 and 8 nm for undercoolings of 1, 10, 25, 50, 100 and 150 °C respectively. (For comparison the lateral free surface energy,

σ is about 10^{-3}N / m; see also figure 2.)
At low undercoolings relatively thick lamellae must be created in order to allow continuation of crystallization; this is reflected in a larger radial span R (see figure 4). This fact is also responsible for the appearance of axialites when polymers, e.g.polyethylene, are crystallized from the melt at low undercoolings, whereas complete spherulites are grown when crystallized at lower temperatures.
The surface free energy required for nucleation can be reduced by the presence of another, usually solid, interface (heterogeneous nucleation). The high nucleation free enthalpy involved in the crystallization process usually leads to heterogeneous nucleation.

ALIPHATIC POLYAMIDES AS MEMBRANE MATERIALS

Synthetic membranes and their classification

Membranes are generally defined as selective barriers between two phases. Certain components of solutions or suspensions are allowed to permeate through the membrane, while others are not (see figure 7).
Biological membranes are barriers in living species, showing a complex multicomponent structure with low molecular weight phospholipids as main components. The membranes typically consist of only a few layers of molecules, which are arranged in a liquid crystalline structure. Synthetic polymeric membranes are usually composed of macromolecules of a single type. Transport through biological membranes can take place either by passive or by active transport using the bodies energy sources, whereas in synthetic membranes transport is always passive and an applied driving force is required, i.e. differences in pressure, concentration or electrical potential across the membrane.

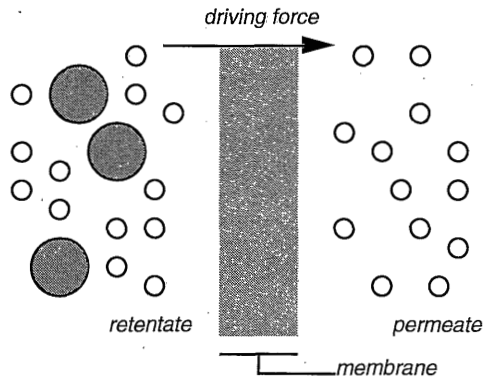

Figure 7. A schematical representation of a selective membrane.

Classification by application

The most important driving force used is a pressure gradient. Pressure driven membrane processes are usually classified into four groups[21]:
1. microfiltration (MF), 2. ultrafiltration (UF) - nanofiltration (NF), 3. reverse osmosis (RO) and 4. gas separation membranes. The separation characteristics are given in table 3 with typical pore sizes and water fluxes of the membranes[22].

Separation in microfiltration and ultrafiltration is based on sieving, whereas separation for reverse osmosis and gas separation is influenced by the differences in solubility and diffusivity of the various feed components in the membrane matrix. These latter membranes do not contain pores and separation is based on the specific material properties of the membrane material. Nanofiltration is a transition area between ultrafiltration and reverse osmosis. The exact mechanism on which this separation is based is yet unknown.

The choice of the membrane material for porous (micro- and ultrafiltration) membranes can be made more or less independently from the separation characteristics of the membrane, since separation is based on the sizes of the pores. For reverse osmosis the choice of the material is dependent in the first place on the intrinsic separation characteristics of the polymer itself.
Important factors for material choice are thermal and chemical stability and

processibility of polymer. Polymers used for the different types of pressure driven separation processes are given in table 4. For some cases advantages and disadvantages of the materials mentioned are presented.

Table 3. Separation regions of four pressure driving membrane processes: microfiltration (MF), ultrafiltration (UF) nanofiltration and reverse osmosis (RO)[22]*. Sizes of some well known and well defined particles are given for comparison.*

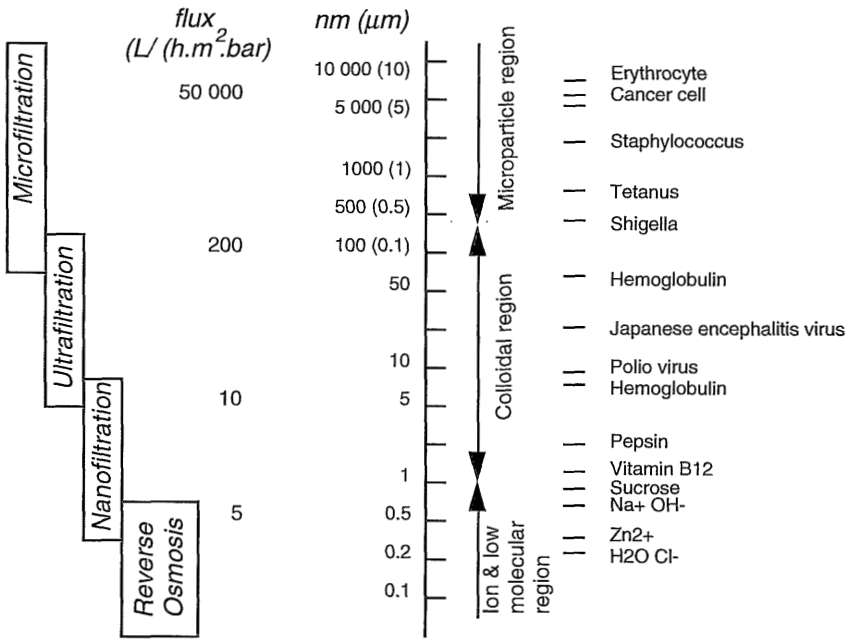

Hydrophilicity and good chemical resistance in non-aqueous media (see also table 2) and in media with a high pH-value are the main advantages for the choice of nylons as a membrane material in micro- and ultrafiltration. Nylon 4,6 exhibits the extra advantage of being steam sterilizable. The material is also expected to be superior in the application in non-aqueous systems. For dense membranes knowledge about intrinsic separation characteristics of the nylons is necessary.

Classification by morphology

Synthetic membranes can be classified by morphology into two types: symmetric (skinless) and asymmetric (skinned) membranes[21]. Asymmetric membranes are generally applied in the field of ultrafiltration, reverse osmosis, pervaporation and gas separation. This can be achieved by making the sub-layer highly porous and the actual selective barrier very thin. Symmetric porous membranes are often used for microfiltration. For this class of separation the resistance for permeation is only a fraction of the total resistance; far more important are the fouling and separation characteristics of the membrane. In recent years, however, asymmetric membranes have become more widely used.

Table 4. Materials used for membranes in pressure driven processes, some advantages and disadvantages[21, 23, 24].

Membrane process	*Material*	*Advantages*	*Disadvantages*
MICROFILTRATION	polyvinylidenefluoride	chemical / thermal / mechanical stability	solubility
	polytetrafluoroethene	chem. / therm. stability	solubility
	cellulosics	good flux, hydrophilicity	chemical resistance, brittle
	polypropylene	chem.stability, hydrophobic	poor heat resistance
	nylon 6 and nylon 6,6	chem./thermal/mechanic., hydrophilic	not autoclavable at 134°C not stable at low pH
	polyetherimide (PVP)	good morphology, hydrophilic	chemical resistance
	polycarbonate		
ULTRAFILTRATION	polysulfone		hydrophobic
	polyacrylonitrile	chemical / thermal stability	
	cellulose esters		chemical resistance, brittle
	polyimide	chemical / thermal stability	
	polyamide (aliphatic / aromatic)		not stable at low pH
	polyvinylidenefluoride		
	poly(phenylene oxide)		
NANOFILTRATION	polyamide (interfacial polymerization)		not stable at low pH
REVERSE OSMOSIS	cellulose derivates	good flux, hydrophilicity	chemical resistance
	aromatic polyamides (composites)	chemical / thermal stability	sensitve to oxidation

Nylon membranes

Nylons offer the advantage of being a hydrophilic material: membranes of this polymer do not require wetting agents. Furthermore, hydrophilic membranes usually show reduced fouling properties. Especially for microfiltration applications in the medical and pharmaceutical field the use of wetting agents may cause problems. A disadvantage of nylon 6 and 6,6 membranes is that these polymers can not be steam sterilized. The better thermal resistance of nylon 4,6 makes steam sterilization possible, because of a considerable larger crystalline content in combination with a higher melting temperature. (The glass temperature of nylon 4,6, at 80°C, does not determine the thermal stability.)

Table 5. Some commercially available microfiltration membranes[26,27].

Type of nylon	Trade name	Manufacturer	Pore size (μm)	Flux (L/(h.m^2.bar)	Remarks
6	Accurel	Membrana (AKZO)	0.45	20 000	bubble point: 1.2 μm
6	Caprone	IPhOCh (CIS)#	0.2		mechanically strong
6 / 6,6-4	co-polyamide	IPhOCh (CIS)	1.2	90 000	
6 / 6,6-4	co-polyamide	IPhOCh (CIS)	0.5	25 000	
6 / 6,6-4	co-polyamide	IPhOCh (CIS)	0.3	10 000	
6	Durapor	Millipore	0.2		mechanically strong
6	GS	Miliipore	0.2		brittle
6	MFA-I	RIST (CIS)	0.2		brittle
6,6 - 6	Prepor-N	Domnick Hunter	0.1		
			0.2		
			0.45	15 000	
6,6	Puropor-Nyaflo	Gelman	0.2	15 000	bubble point: 0.8 μm
			0.45	50 000	bubble point: 1.2 μm
6	PA-SM 11903	Sartorius	1.2	200 000	
6			0.45	30 000 - 50 000	bubble point: 6 μm
6			0.2	15 000	bubble point: 4 μm
6,6	Ultipor NR	Pall	0.2	20 000	sufficient strength
6,6	Ultipor NX		0.45	30 000	bubble point: 1.2 μm
6,6	Zetapor	AMF - Cuno	0.2	18 000	bubble point: 0.9 μm
			0.4 -1.2	24 000	bubble point: 1.2 μm

Institute of Physico-Organic Chemistry of the BSSR Academy of Sciences (Minsk) Commonwealth of Independent States (CIS)

Nylons as membrane material are mainly used for microfiltration applications. An overview of commercially available nylon membranes is listed in table 5 with reported pore sizes and water fluxes as far as they are available. The commercial microfiltration membranes have different pore ratings for the different applications[25]: pore sizes are typically in the range of 0.2 - 0.4 μm for electronic semi-conductor industry, 0.1 μm for Mycoplasma removal, 0.2 μm as 'absolute' sterilizing grade and 0.45 - 0.65 μm for clearance of beverages.

Nylon 6 membranes have been used in both aqueous[28] and non-aqueous ultrafiltration[29,30] applications. Here decane, benzene, dimetyl formamide and n-methylpyrrolidone were used as organic liquids.

The use of various types of aromatic and aliphatic polyamides in reverse osmosis has been reviewed by Blais[31]. The aliphatic polyamides or nylons were found not to be very suitable for desalination. A number of publications discuss properties for reverse osmosis of nylon 6 and nylon 6,6 membranes as well as some modified nylons[32-36]; salt retention values never exceed 80%. On the other hand aromatic polyamide membranes exhibited salt retentions up to 99.9%; membranes of these materials have further been commercialized (e.g. Permasep membranes of Dupont). According to Blais[31] a polymer only exhibits permselectivity if its chains are inherently stiff and capable of hydrogen bonding to give virtual cross-links into networks of low chain mobility. Chain stiffness can seldom be increased in a linear molecule. Sumitomo[36] claims that permselectivity is obtained if the hydrogen bonding between the amide groups is loosened by the sterical hindrance of bulky groups.

The nylons are not very suitable for the gas separation application since the permeability for gases is very low[21], due to the high crystalline content. Dense homogeneous films from nylon 4,6 are difficult to prepare because of the high tendency to crystallization.
The membrane should not necessarily be composed of one material; layers of different materials (composite membranes) are employed in practice[37]. The support on which a thin, dense, separating layer is coated must be resistant to the solvent used for the coating procedure. The chemical resistance of nylon 4,6 makes this polymer ultimately suited as support material. A support for composite membranes often has ultra- or microfiltration characteristics. A number of publications have described the

use of nylons as a hydrophilic matrix[38-39] or as a fabric support[40-42]. Nylons as support layers for gas separation or pervaporation membranes have not been reported.

A general survey of possible applications for this new nylon 4,6 in membrane science is given in figure 8.

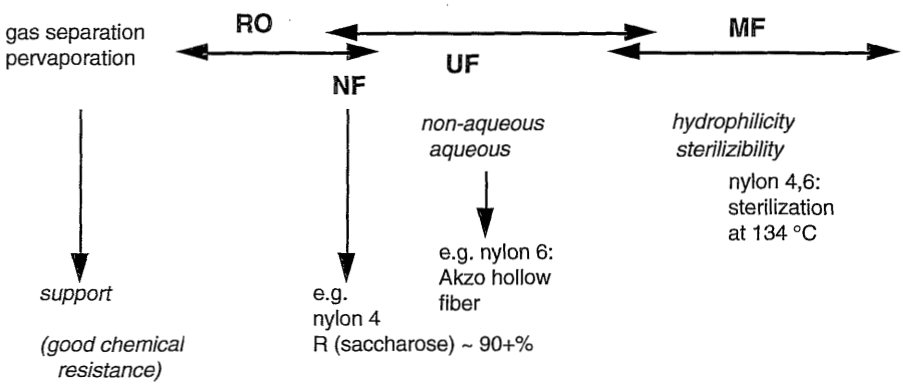

Figure 8. Promising possibilities for application of nylon 4,6 as a membrane material.

MEMBRANE FORMATION

Introduction

For the preparation of synthetic membranes various techniques[21] are available. Ultrafiltration, nanofiltration, reverse osmosis, gas separation and pervaporation membranes can be prepared by coating procedures, such as dip-coating, plasma polymerization, interfacial polymerization and in situ-polymerization, on a microporous support and by phase inversion.

Microfiltration membranes can be prepared by the following methods.
- sintering of polymer particles, such as polyethylene, polytetrafluoroethene, polypropylene, metals, ceramics, graphite and glass.
- stretching of an extruded film or foil perpendicular to the direction of extrusion. The film is made from a semi-crystalline polymer with the amorphous phase in the rubbery state, such as polyethylene, polytetrafluoroethene and polypropylene.
- track-etching; a film or foil (often polycarbonate) is subjected to a high energy particle radiation perpendicular to the film.
- template leaching; one component of a homogeneous film or sheet (e.g. glass membranes) is leached out and a porous matrix is obtained.
- phase inversion.

The last mentioned technique, phase inversion, is suitable for synthesis of membranes with separation properties varying from microfiltration to gas separation membranes. Most commercially available polymeric membranes are obtained by phase inversion. It involves a polymer dissolved in a solvent, that is extruded in the desired configuration. The polymer is precipitated by phase transition either by a change in temperature or by a change in composition of the solution.

Thermally induced phase separation (TIPS) involves the preparation of a polymer solution at elevated temperatures, followed by a cooling step below the stability region. Phase separation, by liquid - liquid demixing (either meta-stable or spinodal), or by crystallization of the polymer or low molecular components[43-49], leads to the formation of a porous structure.

Diffusion induced phase separation (DIPS) can be achieved by three methods[21].
- Precipitation by solvent evaporation.
  This method generally yields dense homogeneous membranes in case of a binary system consisting of polymer and solvent. Porous membranes can be obtained when the polymer is dissolved in a mixture of a volatile solvent and a non-volatile non-solvent for the polymer.
- Precipitation from the vapor phase.
  A polymer solution is contacted with vapor of a non-solvent. The vapor diffuses into the polymer solution resulting in precipitation of the polymer and the formation of a symmetric (skinless) porous membrane.

- Immersion precipitation. A concentrated polymer solution is immersed in a bath containing a liquid non-solvent. The polymer precipitates as a result of diffusion of solvent from the cast polymer solution into the bath and of non-solvent from the bath into the film (see figure 9).

In many cases the processes mentioned are combined. Well know is the use of an evaporation step or a first vapor phase inversion before the film is further precipitated in an immersion precipitation process.

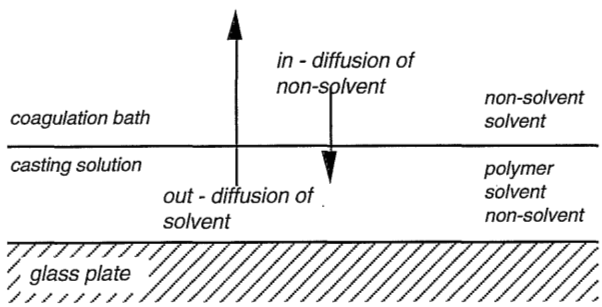

Figure 9. Schematical representation of the immersion precipitation process. The cast polymer solution is coagulated by diffusion of a non-solvent into the casting film and diffusion of solvent out of the film.

Membrane formation with nylons as membrane materials

Nylon membranes are prepared by phase inversion techniques. The choice of a solvent for nylons is restricted to formic acid in most cases (see table 6); cresol, sulphuric acid and hydrochloric acid can also be used as solvents, but with the latter solvents membranes are obtained with poor mechanical properties[50]. Another solvent system, ethanol or methanol in combination with calcium chloride has been known for years[51], but has only recently been reported in literature by Dennisson et al.[52]. for the polymers nylon 6 and nylon 6,6. Besides calcium chloride, the salts calcium nitrate, calcium salicylate and lithium chloride were also used as additives to ethanol and methanol at 60 or 80°C to dissolve the nylon. A variety of non-solvents has

been used, such as water, acetone, dimethyl formamide, methyl ethyl ketone and isopropylalcohol.

Table 6. Overview of the preparation of nylon membranes reported in literature. In all cases formic acid was used as the solvent for the reported nylon.

type of nylon	additives to water bath	minor additives in casting solution	pore size (μm)	waterflux (L/(h.m^{2}bar)	Manu-facturer	Ref.
controlled evaporation						
6,6	-	isopropanol / LiCl	0.2 - 0.8	12 000 - 35 000	Parker Hannifin	53,54
vapor phase inversion						
4,6		methanol /	0.45 - 0.8	1600 - 17 000	Domnick	55,56
4,6 / 6,6		acetic acid / glycerol	0.25 - 1	3400 - 61 000	Hunter	
6,6		glycerol / nylon 6	0.3 -2.7	1600 - 17 000		57
immersion precipitation						
6 / 6,10		glycerol	0.22 - 1.2		AMF	58
6,6		nylon 6-6,10	0.2 - 0.45	9000 - 35000	Gelman	59
6	acetone /			50 - 1800	AKZO	28,60
6	acetic acid / methanol	formamide / methyl - formamide	0.1 - 1		IPhOCS	26,61-67
						26,68
6 / 66-4	ammonia		0.2	2 - 35		50
6	50% formic acid	water	0.09 - 5		Pall	69,70
6,6	formic acid					71
11						70
7						,,
6,9						,,
6,10						,,
6,6 / 6,12						,,
6,12						

Phase inversion with nylons as the membrane forming polymer has not been subject to academic study, since most membranes have been manufactured in industrial research laboratories. Some of the publications describe a membrane morphology that differs from the cellular type of membrane morphology (see figure 12) usually

obtained with immersion precipitation. Marinaccio[58] has described the membrane morphology as '...a box of tennis balls or other non-spherical geometrics fused at their points of contact...'. Artomov and coworkers[61] have shown scanning electron micrographs, in which clear spherical entities with a size of 5 µm were visible. The authors refer to these structures as nodules according to Kesting's description[22]. Precipitation of the polymer solution can very well be affected by crystallization of the polymer. Membrane formation with nylon 4,6, a polymer that is more susceptible to crystallization compared to nylon 6 or nylon 6,6, is very likely to be influenced by crystallization of the polymer.

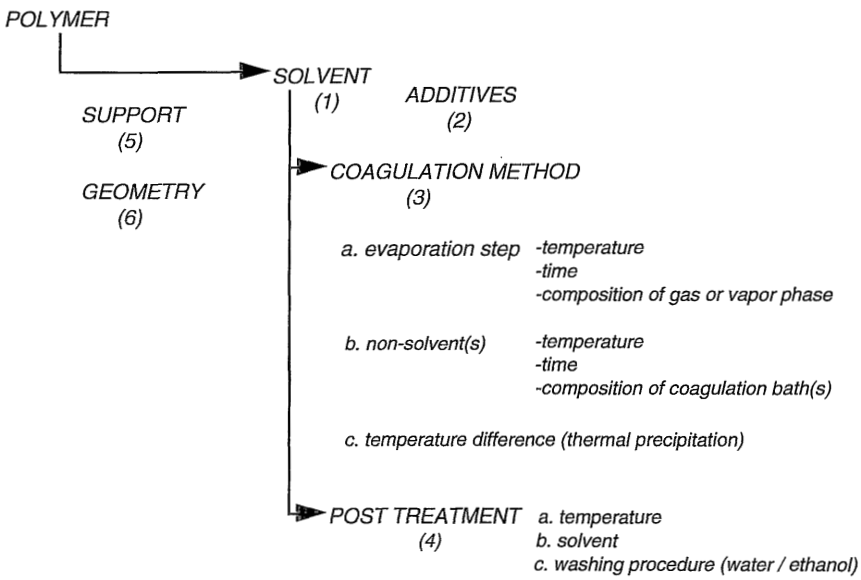

Figure 10. Parameters for membrane formation by means of phase inversion: the membrane morphology is influenced by (1) the choice of solvent, (2) the eventual choice of additives, (3) the coagulation method, (4) the post treatment; also the choice of support material (5) and the cast geometry of the polymer film (6) effects the final membrane structure.

The large number of parameters involved in the phase inversion process (see figure 10) is advantageous for membrane manufacture. By the choice of optimal parameters tailor made membranes with a large variety in morphology can be prepared. These

optimal conditions, however, are frequently determined empirically. From the early start of membrane preparation by means of phase inversion[72] several attempts have been made for modelling the diffusional processes[73-77].

Membrane formation mechanisms for immersion precipitation

In order to understand the immersion precipitation process two major phenomena must be understood: (i) equilibrium thermodynamics, i.e. knowledge about the stability borders of the mostly ternary system and the type of phase separation that occurs, and (ii) kinetics, i.e. insight in the diffusional processes. For the description of the kinetics several mass transfer models for immersion precipitation have been developed.

Thermodynamics

In order to understand the phase behavior of ternary systems, the situation is first described for the more simple binary system consisting of a polymer and a solvent, in which phase separation is induced by a temperature step.

For a binary system the phase diagram can be derived from the free enthalpy of mixing curves versus the volume fraction (see figure 11a and b).

In figure 11b the free enthalpy of the mixture is given as a function of the polymer volume fraction. If this curve would be concave at all compositions the system would exhibit complete miscibility. In this case, however, the curve has a convex part. Polymer solutions with a composition with a polymer volume fraction between α and β can lower their free enthalpy at a temperature T_1 by phase separation into the liquid phases α and β; the corresponding miscibility gap (*liquid-liquid (L-L) phase separation*) is located as is indicated in figure 11a, where the L-L region and the homogeneous region are given as a function of temperature. At lower temperatures β shifts to larger polymer fractions and the miscibility gap becomes larger.

The thermodynamics of a ternary system chosen for membrane formation can be visualized using a triangle diagram (figure 11c). In general the non-solvent (NS) is indicated with component 1, the solvent (S) with component 2 and the membrane forming polymer (P) with component 3. The corners of the triangle represent the pure components.

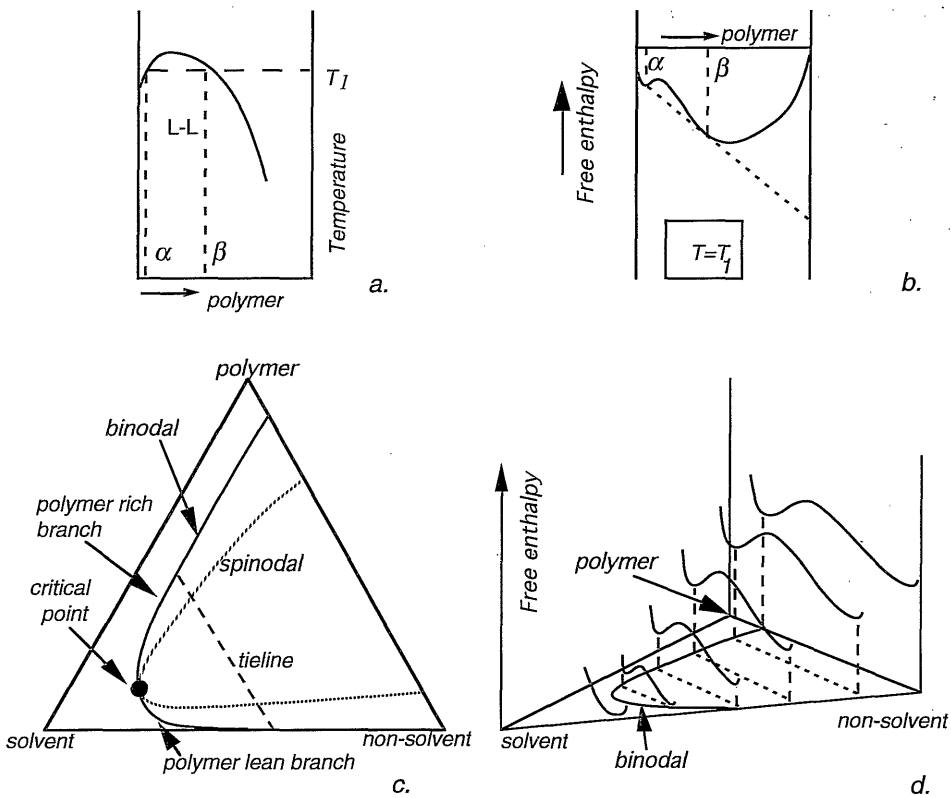

Figure 11. (a) A binary phase diagram. (b) Free enthalpy of the mixture as a function of the polymer volume fraction. (c) A schematic isothermal ternary phase diagram for a membrane forming system consisting of a polymer, a solvent and a non-solvent. (d) Free enthalpy of mixing (G_M) as a function of the ternary composition.

A binary polymer solution is represented by a point on the polymer solvent axis. The solvent and non-solvent are miscible at all compositions. Membrane forming systems generally have a miscibility gap, with the binodal as a stability border (see figure 11c). Inside this region a mixture can lower its free enthalpy by phase separation into two liquid phases analogous to the binary system described above as is indicated in the three dimensional figure 11d.

The location of the binodal curve is asymmetric in the binary and ternary phase diagrams with a critical point (i.e. the point at which the spinodal touches the binodal) near the ordinate (respectively corner) of the low molecular weight component(s). This is characteristic for a system in which one of the components has a high molecular weight. The binodal in such systems has a polymer rich and a polymer lean branch.

A mixture of the three components with a composition in the region between the binodal and the spinodal curve (figure 11c) is metastable. Inside the spinodal region all compositions are unstable; phase separation will take place here by spinodal decomposition. For insight in membrane formation the location of the binodal is most importance. As a result of the diffusion of solvent and non-solvent the composition of the original polymer solution changes. As soon as a part of the film has its composition inside the metastable region phase separation starts by the mechanism of nucleation and growth. This process in most cases determines the final membrane morphology. Since membrane formation generally starts with a medium polymer concentration (~15% or higher) the metastable region is entered at the polymer rich branch of the binodal. Nucleation and growth will take place from the polymer lean phase. A typical membrane morphology is shown in figure 12; the pores result from the growth of the polymer lean phase. This process continues until vitrification of the surrounding polymer rich phase occurs. Spinodal decomposition in membrane formation will only take place under special circumstances. A deep quench inside the instability region can only be accomplished if polymer movement is too slow to respond to the diffusion of the low molecular weight components. This, for example, takes place if two polymers are involved in membrane formation[76].

If a polymer can crystallize, a crystallization line, indicating the equilibrium between the crystalline and amorphous state, is somehow present in the phase diagram. Crystallization of the polymer (which can only be relevant during immersion precipitation) in a ternary mixture will take place if the free enthalpy of mixing can be lowered by phase separation into two phases, i.e. the pure polymer crystal and a liquid phase containing polymer, solvent and non-solvent (*solid - liquid or S-L demixing*).

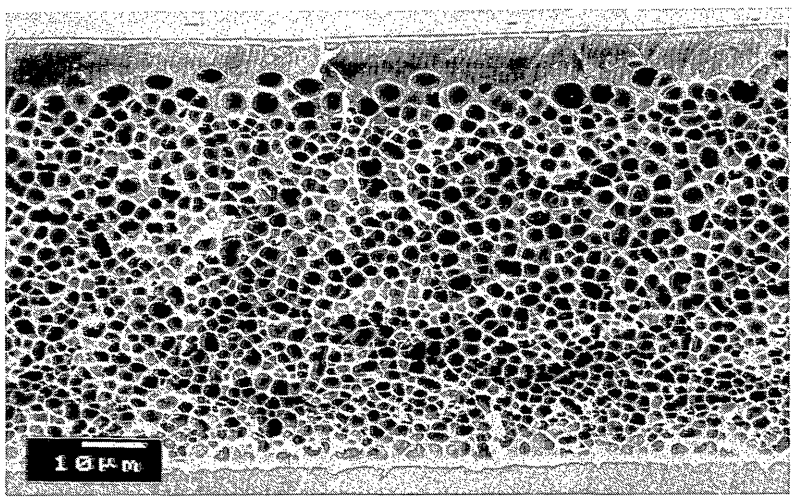

Figure 12. Typical membrane morphology as a result of liquid - liquid phase separation.

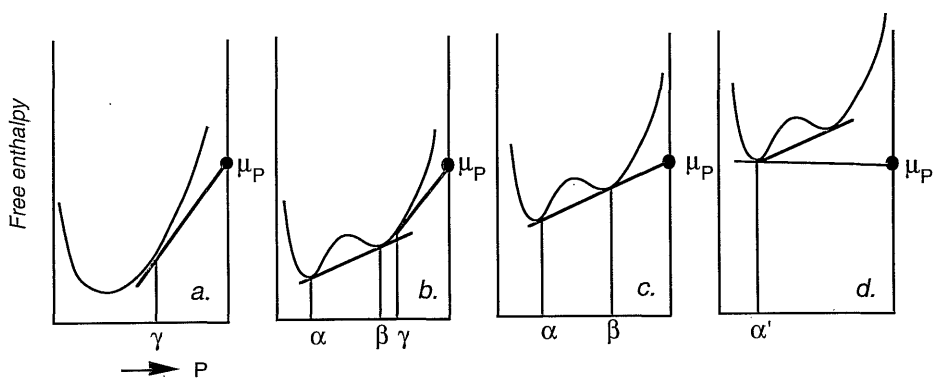

Figure 13. Free enthalpy of the mixture for the liquid state for solvent and polymer: (a) the liquid state is miscible at all compositions with the possibility for crystallization of the polymer above a concentration γ with a value for the chemical potential, μ_P, (b) between α and β L-L phase separation occurs into the phases α and β and above the concentration γ S-L phase separation takes place into the pure crystalline polymer and a phase γ; (c) a three phase equilibrium exists between α,β and pure crystalline polymer; (d) S-L phase separation above polymer concentration α' (<α).

The effect of crystallization of the polymer for the phase diagram is first worked out for a binary system analogous to the situation without crystallization described in figure 11 a and b.
Generally four situations are possible for a binary system, depending on the values for the chemical potentials of the phases relative to each other (see figure 13). In case 'a' the free enthalpy curve for the liquid components is concave indicating that the components in the liquid state are miscible at all compositions. However, mixtures with their compositions in between the pure polymer and γ can lower their free enthalpy by phase separation in the solid crystalline state with a chemical potential, μ_P, and a liquid phase with composition γ. In case 'b' the free enthalpy curve for the liquid state shows a convex part, indicating that a miscibility gap exists for the liquid phases. Mixtures with compositions in between α and β can lower their free enthalpy by L-L phase separation into the phases α and β. The location of the curve for the liquid system relative to the value for the chemical potential, μ_P, for the solid crystalline state is such that only compositions with a relatively large polymer concentration, γ, can be at equilibrium with the pure crystalline polymer. In case 'c' the values for the chemical potential of the three phases α, β and pure crystalline polymer are equal, reflected by the equal tangent line. In this special situation a three phase equilibrium is present. Situation 'd' shows a case in which the free enthalpy of mixing curve for the liquid phases is located 'above' μ_P. Mixtures with their polymer concentration larger than α' can lower their free enthalpy by solid - liquid phase separation. In this case the L-L miscibility gap is located completely inside the crystallization area. Liquid - liquid phase separation can still be obtained by quick cooling .The equilibrium situation, however, will always be a phase separation into the phases α' and polymer crystals. Also for a ternary system such a situation exists.

For the construction of the ternary phase diagram the three dimensional representation of the free enthalpy of mixing as a function of concentration must be used (analogous to figure 11d). μ_P has its location on the polymer ordinate. Near the polymer non-solvent axis the conditions are comparable to the above described case 'd', figure 13. The phase diagram (see figure 14b) gives a S-L region, representing the equilibrium between the pure crystalline polymer and a phase consisting mainly of solvent and non-solvent. Near the polymer solvent axis the situation is like indicated in case 'b', figure 13. At higher polymer concentrations the free enthalpy decreases

by (S -L) phase separation, whereas L-L phase separation takes place at lower polymer concentrations. There is an intermediate region with a three phase equilibrium.

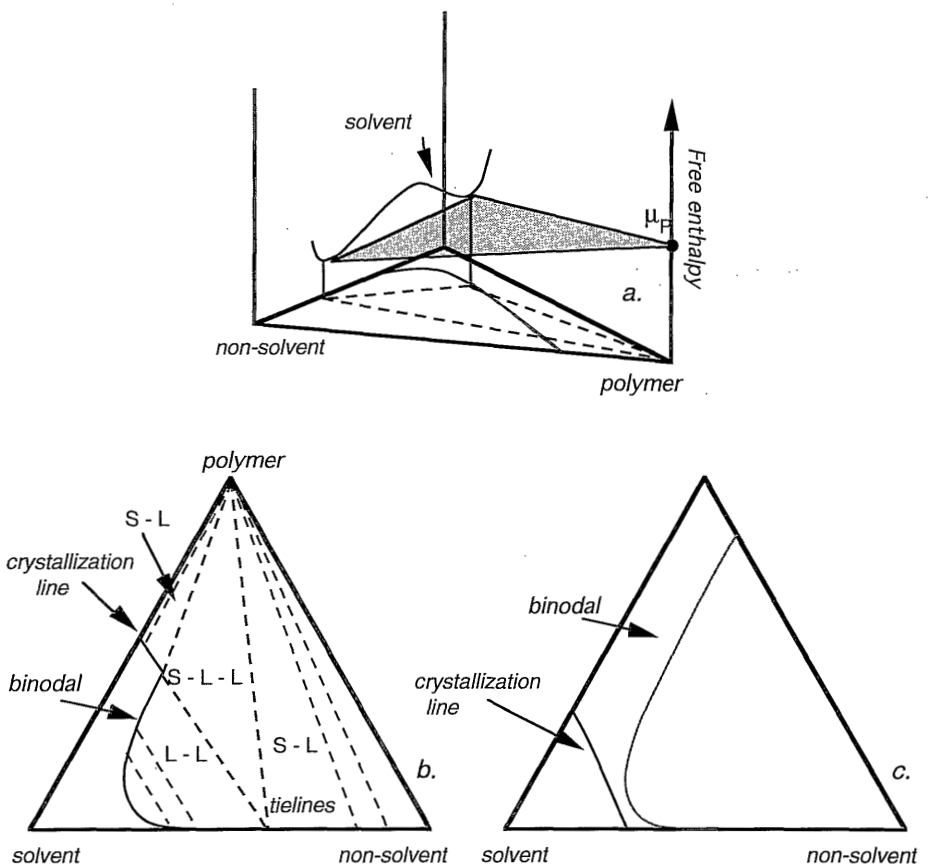

Figure 14. (a) A three dimensional perspective of the phase diagram with the free enthalpy of the mixture shown on the vertical ordinate. One curve is drawn in order to highlight the three phase equilibrium. (b) An isothermal phase diagram for a membrane forming system with crystallization of the polymer. (c) A special situation in which the crystallization line does not intersect the binodal curve.

This situation can be understood by extending figure 13c to a three dimensional plot for a ternary system (figure 14.). This figure is similar to figure 11d but now drawn in a different perspective. The tangents on the polymer rich branch of the free enthalpy of mixing curve for the liquid phase are located in the same plane as the tangent for the polymer lean branch. The complete phase diagram of the ternary system in which crystallization of the polymer is involved is given in figure 14b. If the μ_P value is located much lower than the free enthalpy of mixing curves for the liquid state, the conditions are analogous to the situation shown in figure 13d. Crystallization of the polymer can take place, whereas L-L demixing would never occur at equilibrium conditions. Relatively rapid introduction of non-solvent, however, will also allow L-L demixing. In a ternary system such a situation is reflected in figure 14c.

Equilibrium thermodynamics of a system in which one or more components are polymers can be (semi-quantitatively) described by the Flory-Huggins theory[77,78], based on a relatively simple but very useful lattice theory. The theory is used by many researchers in membrane science[76,77,81-85] in order to describe L-L phase separation. Altena and Smolders[81] were able to compute the location of the binodal curves. The dependence of the location of the miscibility gap on the interaction parameters was reviewed.

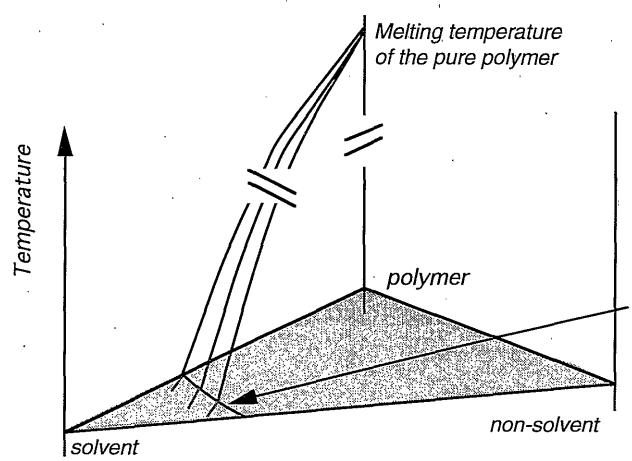

Figure 15. Construction of an isothermal crystallization line from melting point depression curves.

Crystallization of the polymer in binary or ternary systems is caused by melting point depression with respect to the melting point of polymer crystals in the pure polymer. A crystallization line in a ternary phase diagram can be considered as the cross-section of the ternary melting point depression curves with the isothermal plane of interest (see figure 15). For a number of binary systems Flory[79] already determined theoretical and experimental curves for melting point depression, based on the same equations for describing the free enthalpy of mixing. Altena and Smolders[86] and Burghardt and McHugh[87] have investigated melting point depression in ternary membrane forming systems with cellulose acetate and poly(phenylene oxide) respectively.

The influence of the location of the glass transition border on membrane morphology prepared by the immersion precipitation technique has been studied by Li et al.[88]. In most cases of membrane formation L-L phase separation takes place and vitrification of the polymer rich phase occurs by passing the glass transition. Depending on the ternary system of choice vitrification can take place by either a glass transition or crystallization. If the glass transition region (see figure 16) is located outside the binodal region and if crystallization cannot occur, then the immersed polymer film will never become 'solid' (see figure 16b).

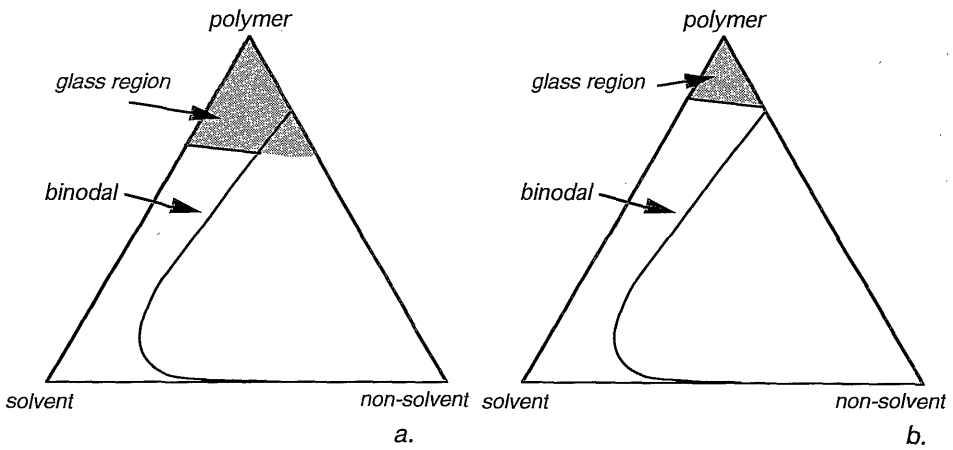

Figure 16. Location of the glass region.

Membrane formation cannot be understood by knowledge of the thermodynamics of the system only. It is important to have insight in the concentration profiles in the polymer film that are a result of the diffusion of solvent and non-solvent. Information about the composition and the velocity by which the binodal region is entered can be obtained by studying the mass transfer during immersion precipitation.

Mass transfer models

Cohen, Tanny and Prager[89] were the first to treat the diffusion of solvent and non-solvent in a comprehensive way, on the basis of the thermodynamics of irreversible processes[90,91]. The membrane forming systems under investigation were: cellulose acetate dissolved in various solvents, coagulated in water, and polystyrene in toluene with ethanol as a non-solvent. Wijmans and Smolders[80] and Tsay and McHugh[83] have shown that their mass transfer equations were not entirely correct. Reuvers and Smolders[73] developed a correct model, in which the parameters were based on the Maxwell-Stefan theory[92]. Usually during membrane formation the solvent flux out of the polymer film and the non-solvent flux into the film are not equal, leading to a shrinkage or an expansion of the film (see figure 9). The Reuvers model incorporated the movement of the interface between bath and film according to Crank[93]. The model distinguished two cases of immersion precipitation that were already known from practice: (i) instantaneous demixing, the polymer film starts to precipitate immediately after immersion in the non-solvent bath and (ii) delayed onset of demixing, in which an induction time occurs between the moment of immersion and the first onset of (L-L) phase separation. The model calculations are applicable as long as no phase separation has taken place. The calculated concentration profiles should be considered as schematical in case of an instantaneous demixing system. Kimmerle[74] developed a more approximate model, based on Fick's law, in which phase separation is incorporated. The Reuvers model was further extended by McHugh and coworkers[83] making use of few assumptions. They claim that a better prediction of the delay time between immersion and the onset of phase separation has been obtained.

One of the boundary conditions of the Reuvers model is the assumption of local equilibrium at every point in the systems and also at the interface between the two

phases. The 'end-point' of a composition path (figure 17) is located on the binodal. The difference between a composition path for instantaneous demixing and for delayed onset of demixing is schematically illustrated in figure 17.
The interfacial polymer concentration and the type of demixing taking place can be related to the final morphology of the membrane. Knowledge of interfacial concentration can give information about the compaction of the skin in the film, resulting in a specific morphology of the top-layer in the final membrane. Instantaneous demixing usually leads to an ultrafiltration type of membrane; delayed onset of demixing mostly gives membranes with a relatively dense top-layer that can be used for gas separation or pervaporation.

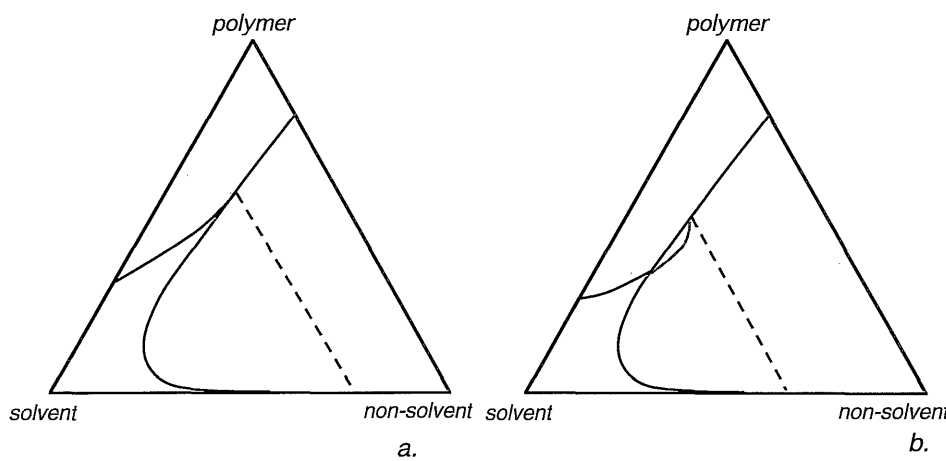

Figure 17. Composition paths according to the model of Reuvers and Smolders[73] for (a) delayed onset of demixing and (b) instantaneous demixing. The 'end' of the path is located on the binodal, reflecting the assumed local equilibrium at the bath - film interface between the polymer rich phase in the film and the polymer lean phase in the bath.

The models described in literature consider situations in which only L-L phase separation occurs, crystallization (or S-L phase separation) has not been taken into account so far. It should be mentioned that only a few polymers are able to crystallize during membrane formation. The vast majority of membrane forming systems exhibit L-L phase separation during immersion precipitation in combination

with vitrification of the phase concentrated in polymer or possibly followed by crystallization in a later stage.
The main difference between previous models and the present treatment of phase separation involving crystallizable polymers occurs in the boundary conditions at the interface and the nucleation of a new phase. Nucleation for a liquid phase in a liquid environment (L-L phase separation) does not require large induction times. In fact this induction time has been reported to be zero[94], indicating that as soon as the stability border is crossed phase separation takes place. For the creation of a solid nucleus in a liquid environment (S-L phase separation) other conditions are valid (see section crystallization and crystallinity). For thermally induced phase separation in binary systems a considerable degree of undercooling and for diffusion induced phase separation a certain degree of supersaturation is necessary to induce crystallization. This fact complicates the understanding of the formation mechanism of membrane structures in ternary systems where S-L phase separation may also occur.

AIMS OF THIS WORK AND STRUCTURE OF THE THESIS

Aim of the present work is firstly to investigate the suitability of nylon 4,6 as a membrane material for various technically relevant applications. In order to prepare membranes with the desired pore sizes and performance the influence of various parameters for membrane formation should be investigated. A second purpose of this work is to study the influence of crystallization on the final membrane morphology. For the membrane formation, the ternary system, nylon 4,6, formic acid and water has been chosen, because of its simplicity, which makes a study on mechanisms possible.

Chapter 2 describes the effect of variation of the membrane forming parameters on morphology and performance. The expected crystalline morphology has indeed been observed, leading to a hypothesis concerning the location of the crystallization line with respect to the binodal. In the first appendix to chapter 2, fluxes of non-aqueous liquids through the membranes are reported. The second appendix describes the

effects on the membrane morphology of different inorganic salts added to the polymer solutions with formic acid as a solvent. Membrane formation with nylon 4,6 in an ethanol, methanol, calciumchloride solvent system has been studied as well and this is described in the third appendix to chapter 2.

Chapter 3 describes the equilibrium thermodynamics of the ternary membrane forming system nylon 4,6, formic acid and water. This system has been compared to nylon 6 and a copolymer of nylon 4,6 and nylon 6, using the Flory Huggins theory. The location of the crystallization lines and the binodals for the three systems is determined in this chapter.

In chapter 4 the Reuvers-Smolders mass transfer model for membrane formation has been extended to conditions in which crystallization of the polymer takes place, in order to explain the observed membrane morphologies. The relation between the results of the mass transfer model and the final membrane morphology is further discussed in chapter 5, in which membrane formation parameters are varied systematically. In order to prepare membranes with a larger variety in pore sizes whilst maintaining the good chemical stability of the membranes the influences of blending with nylon 6 and the copolymer of nylon 4,6 and nylon 6 on morphology and performance of the membranes has been studied. Some aspects mass transfer in a quaternary system with two semi-crystalline polymers are discussed.

REFERENCES

1. H. Staudinger, *Ber.*, 53. 1073 (1920); 57, 1203 (1924).
2. 'Collected Papers of W.H Carothers' in High Polymers: *Monographs on the Chemistry, Physics and Technology of High Polymeric Substances*, Interscience Publishers, Inc., NY, 1940.
3. P. Schlack, K. Kunz, *Chemischer Textilfasern, Filme und Folien* (R. Pummerer), Stuttgart, 629 (1953)
4. H.F. Mark, N.M. Bikales, C.G. Overbeger, G. Menges, *Encyclopedia of Polymer Science and Engineering*, 2nd ed., Wiley NY, vol 11, Polyamides (1985).
5. R.J. Gaymans, T.E.C. van Utteren, J.W.A. van den Berg, J. Schuijer, *J. Polym. Sci., Chem Ed.*, 15, 537 (1977).
6. Vieweg, Müller, *Kunststof Handbuch, Band VI Polyamide*, Carl Hanser Verlag, München 1966.
7. G. Odian, *Principles of Polymerization*, Wiley NY (1981).

8. A. Keller, *Philos. Mag.*, 2, 1171 (1957).
9. L.H. Sperling, *Introduction to Physical Polymer Science*, Wiley NY (1986).
10. H. Tadokoro, *Structure of Crystalline Polymer*, Wiley, NY 1979.
A. Xenopoulos, E.S. Clark, *Nylon Plastics Handbook*(M.I. Kohan Ed.), *Physical Structure*, section 5, 1993.
11. E.D.T. Atkins, M. Hill. S.K. Hong, A. Keller, S. Organ, *Macromolecules*, 25, 917 (1992).
S.J.E.A. Eltink, S. de Boer, J.A.H.M. Moonen, DSM Intenal Report (1992).
12. H.D. Keith, F.J. Padden Jr., *J. Appl. Phys.*, 34, 2409 (1963).
13. D.C. Basset, A. Keller, S. Mitsuhasi, *J. Polymer Sci.*, A1 763 (1963).
14. A. Keller, *J. Polymer Sci.*, 17, 447 (1955).
15. A. Keller, *J. Polymer Sci.*, 26,361 (1959).
16. J. Magill, *J. Polymer Sci.*, A-2, 9, 815 (1971).
17. J. Magill, *J. Polymer Sci.*, A, 3, 1193 (1965).
18. B. Wunderlich, *Macromolecular Physics*, vol. 2, *Crystal Nucleation, Growth, Annealing*, Chapter 5 (1976).
19. F. Khoury, E. Passaglia, *The morphology of Crystalline Synthetic Polymers, Treatise on Solid State Chemistry*, vol. 3 *Crystalline and Noncrystalline Solids* (N.B. Hannay, ed.), Pleneum Press NY (1976).
20. J.D. Hoffman, G.Th. Davis, J.I. Lauritzen,Jr.,*The Rate of Crystallization of Linear Polymers with Chain Folding, Treatise on Solid State Chemistry*, vol. 3 *Crystalline and Noncrystalline Solids* (N.B. Hannay, ed.), Pleneum Press NY (1976).
21. M.H.V. Mulder, *Basic Principles of Membrane Technology*, Kluwer Dordrecht 1991.
22. R.E. Kesting, *Synthetic Polymeric Membranes*, McGraw Hill, NY 1985.
23. T. Berends, *Potential applications of Nylon 4,6 in membrane filters*, Master Thesis University of Twente, June 1989.
24. H.D.W. Roesink, *Microfiltration membrane development and module design*, PhD thesis University of Twente (1989).
25. Membrane & Separation Technology News, September 1989.
26. V. Soldatov, O. Mostovlyanskij, V. Artamov, Synthesis, properties, *Structures and Applications of New Polyamide Microfiltration Membranes*, First Intern. School Artif. Membr., Poland, 17 (1985).
27. R.E. Kesting, L.K. Cunningham, M.C. Morrison, J.F. Ditter, *J. Parenteral Sci. Techn.*, 37, 97 (1983).
28. E. Schindler, *DE Patent* 3138525 A1 (AKZO) (1983).
29. O. Mostovlyanskii, V. Artamov, E. Klementovich, V. Soldatov, *Vestsi Akad. Navuk BSSR, Ser. Khim. Navuk*, 4 31 (1986).
30. D. Malyshev, M. Lazareva, P. Nefedov, V. Baranov, *Khim Volokna*, 6, 15 (1980).
31. P. Blais, *Polyamide Membranes, Reverse Osmosis and Synthetic Membranes*, (S. Sourirajan ed.), NRCC:

Ottawa, Ontario, Canada, 167 (1977).

32. T. Yamabe, S. Yoshida, *Studies on the preparation and Characterization of Nylon Reverse Osmosis Membranes*, 5th Intern, Symp. Fresh Water Sea, 4 (1976).
33. Y. Kurokawa, A. Suzuki, S. Takahahi, A. Takahashi, N. Yui, *Reverse Osmosis Properties of Cellulose Derivatives and 6-Nylon Membranes*, Technology Reports, Tohoku Univ., 44, 1 115 (1979).
34. L. Pilato, L. Litz, J. McGrath, R. Jonson, I. Kochevas, *New Polymer Membrane Technology for Desalination of Sea Water by Reverse Osmosis*, US. Nat Tech. Inform. Serv. PB Rep., No. 222996/1, NTIS 73, 21 (1973).
35. G. Steiner, R. Eaton, T. Kwei, T. Kang, *Diffusion and Reverse Osmosis through Polymer Membranes*, US Clearinghouse Fed. Sci. Tech. Inform., AD, No. 714899, NTIS, 71, 2 (1970).
36. H. Sumitome, H. Kazahiko, *Adv. Polym. Sci.*, 64, 63 (1985).
37. J.M.S. Henis, M.K. Tripodi, *US Patent* 4230483 (1981).
38. D.B Pall, A. Krasnoff, *US Patent* 4431545 (1984)
39. P. Degen, J. Martin, J. Schriefer, B. Shirley, *US Patent* 4693985 (1987).
40. W. Cooper, E. Shea, *US Patent* 3676193 (1972).
41. Alfa-laval Aktiebolag, Improvements in or relating to a tubular filter membrane, *BR Patent* 1374704 (1972).
42. K. Kiyoshi, S. Konomi, *DE Patent* 2453128 (1975).
43. D.R. Lloyd, J.W. Barlow, K.E. Kinzer, *AIChE Symposium Series*, 261, 28 (1988).
44. D.R. Lloyd, K.E. Kinzer, H. Tseng, *J. Membr. Sci.*, 52, 239 (1990).
45. D.R. Lloyd, S.S. Kim, K.E. Kinzer, *J. Membr. Sci.*, 64, 1 (1991).
46. S.S. Kim. D.R. Lloyd, *J. Membr. Sci.*, 13 (1991).
47. G.B.A. Lim, S.S. Kim, Q. Ye, Y.F. Wang, D.R. Lloyd, *J. Membr. Sci.*, 64, 31 (1991).
48. S.S. Kim, G.B.A. Lim, A.A. Alwattari, Y.F. Wang, D.R. Lloyd, *J. Membr. Sci.*, 64, 41 (1991).
49. A.A. Alwattari, D.R. Lloyd, *J. Membr. Sci.*, 64, 55 (1991).
50. M. Bodzek, I. Korus, *Porous Polyamide Membranes*, E.S.M.S.T. Summerschool, Membranes, Processes and Applications, Valladolid, 20 - 24 Sept. Spain (1993).
51. M.H.V. Mulder, *Onderzoek aan nylon 6 membranen*, internal report University of Twente (1976).
52. K.Dennison, B. Kolcinski, S. Krishnan, P. Russell, *US Patent* 50006247 (1991).
53. H. Steadly, A.J. Laccetti, *US Patent* 4770777 (Parker Hannifin) (1988).
54. H. Steadly, Th. Morgan, *WO Patent* 88 / 05686 (Parker Hannifin) (1988).
55. R. Curry, *US Patent* 4788226 (Domnick Hunter) (1988).
56. R. Curry, *WO Patent* 87 / 07849 (Domnick Hunter) (1987).
57. J.F. Ditter, J. Porter, *WO Patent* 86 / 07544 (Domnick Hunter) (1986).

58. P.J. Marinaccio, R.A. Knight, *US Patent* 3876738 (AMF) (1975).

59. R.E. Kesting, *US Patent* 4450126 (Gelman Puropore) (1984).

60. E. Schindler, *DE Patent* 3138525 A1 (AKZO) (1983).

61. V.S Soldatov, V. Artamov, O.A Mostovlyanskii, Proc. 29th Microsymp. Macromolecules, Prague, 171 (1986).

62. T.A. Korshunova, V.A. Artamonov, V.S. Soldatov, *Vestsi Akad. Navuk BSSR, Ser. Khim. Navuk*, 3, 98 (1984).

63. V.A. Artamonov, O.A. Mostovlyanskii, V.S. Soldatov, *Plast. Massy*, 3, 49 (1984).

64. V.A. Artamonov, T.A. Korshunova, E.V. Karpinchik, V.S. Soldatov, *Vesti Akad. BSSR, Ser. Khim. Navuk*, 4, 107 (1984).

65 Y.M. Arkatov, B.Y. Vil'ner, T.A. Korshunaova, V.A. Artamonov, V.S. Soldatov, *Dokl. Akad. Auk BSSR*, 29 (4), 344 (1985).

66. T.A. Korshunova, V.A. Artamonov, V.S. Soldatov, *Plast. Massy*, 9, 18 (1985).

67. T.A. Korshunova, V.A. Artamonov, V.S. Soldatov, *Vesti Akad. Navuk BSSR, Ser. Khim, Navuk*, 1, 82 (1984).

68. S.I. Kuperman, M.A. Agarkova, N.S. Leonova, N.P. Yakovleva, L.A. Vas'kova, O.I. Nachinkin, *Plast. Massy*, 1, 32 (1986).

69. D.B Pall, *US Patent* 4340479 (1982).

70. D.B. Pall, *EP Patent* 0005536 A2 (1979).

71. D.B. Pall, F. Model, *US Patent* 4340480 (1982).

72. S.Loeb, S. Sourirajan, *Advan. Chem. Ser.*, 38, 117 (1962).

73. A.J. Reuvers, J.W.A. van den Berg, C.A. Smolders, *J. Membr.Sci.*, 34, 45 (1987).

74. K. Kimmerle, *Quantitative Betrachtung des Phaseninversionsprozesses bei der Herstellung von Membranen*, PhD thesis, University of Stuttgart (1988).

75. L. Tan, R. Greenberg, W.B. Krantz, R.L. Sani, *Application of Laser Interferometry to Validate a Finite Element Model for Evaporative Casting of Polymeric Membranes*, poster presentation session no. 3 ICOM (1993).

76. Ph. Radovanovics, S.W. Thiel, S.-T. Hwang, *J. Membr. Sci.*, 65, 213 and 231 (1992).

77. C.S. Tsay, A.J McHugh, *J. Polym. Sci., Polym. Phys. Ed.*, 28, 1327 (1990).

78. R.M Boom, *Membranes Prepared from a Polymeric Blend part I: Membranes from Poly(ether Sulfone) and Poly(Vinyl Pyrrolidone)*, PhD thesis University of Twente, Chapter 4 (1992).

79. P.J. Flory, *Principles of Polymer Chemistry*, Cornell, Ithaka (1953).

80. H. Tompa, *Polymer Solutions*, Butterwoths, London (1956).

81. F.W. Altena, C.A. Smolders, *Macromolecules*, 15, 1491 (1982).

82. J.G. Wijmans, J.P.B. Baaij, C.A. Smolders, *J. Membr. Sci.*, 14, 263 (1983).

83. A.J. Reuvers, PD thesis University of Twente, Chapter 6, (1987).

84. R.M. Boom, Th. van den Boomgaard, C.A. Smolders, *Equilibrium Thermodynamics of a Quaternary Membrane Forming System with Two Polymers*, submitted to Macromolecules (1993).

85. S. Li, J. Chengzang, Z. Yunqi, *Desalination*, 62, 79 (1987).

86. F.W. Altena, C.A. Smolders, *J. Polym. Sci., Polym. Symp.*, 69, 1 (1981).

87. W.R. Burghardt, L. Yilmaz, A.J. McHugh, *Polymer*, 28, 2085 (1987).

88. S. Li, PhD thesis University of Twente (1994).

89. C. Cohen, G.B. Tanny, S. Prager, *J. Polym. Sci., Polym. Phys. Ed.*, 17, 477 (1979).

90. S.R. de Groot, P.Mazur, *Non-equilibrium Thermodynamics*, N-Holland Publish. Co., Amsterdam (1962).

91. A. Katchalsky, P.F. Curran, *Nonequilibrium Thermodynamics in Biophysics*, Harvard University Press, Cambridge (1965).

92. J.A. Wesselingh, R. Krishna, *Mass Transfer*, Ellis Horwood Ltd., NY (1990).

93. J. Crank, *The Mathematics of Diffusion*, 2nd Ed., Clarendon Press, Oxford (1975).

94. R.M. Boom, S. Rekveld, U. Cordilia, Th. van den Boomgaard, C.A. Smolders, *Metastable Demixing Phenomena in the Systems PES-NMP-water and PES-NMP-PVP-water*, submitted to *J.Appl. Polym. Sci.* (1992).

CHAPTER 2

Membranes of the Semi-Crystalline Aliphatic Polyamide Nylon 4,6: Formation by Diffusion Induced Phase Separation[1]

A.M.W. Bulte, B. Folkers, M.H.V. Mulder, C.A. Smolders

SYNOPSIS

The preparation of membranes of nylon 4,6 by diffusion induced phase separation (DIPS) using formic acid as a solvent and water as a non-solvent was studied. Nylon 4,6 is a semi-crystalline polymer and phase separation from a solution can occur by solid-liquid (s-l) demixing as well as by liquid-liquid (l-l) demixing. Upon quenching films of solutions with low polymer concentration (<17 wt%) in a non-solvent bath containing water the morphology of the membranes shows a foam-like structure typical for liquid-liquid demixing. When phase separation is induced by water vapor a transition in structure occurs from the cellular type to a morphology typical for solid-liquid phase separated films. At higher polymer concentrations membranes exhibit structures consisting of spheres or smaller crystal-like units resulting from a solid-liquid phase separation process. The addition of 2 wt% of water or more to polymer solutions with low concentration (up till 15 wt%) resulted in solid-liquid demixing as well. In a diffusion induced phase separation process solid-liquid demixing is kinetically competitive with liquid-liquid demixing if nuclei are already present in the starting solutions (heterogeneous nucleation), or if a relatively long time is available for crystal nuclei to be formed. The morphology resulting from s-l demixing is a result of spherulitic crystallization. A certain concentration of nuclei or of precursor particles already present resulted in a small nucleation density during precipitation and thus large spherulites can be grown; at higher polymer and/orwater concentrations the nucleation density has increased resulting in an axialitic morphology of the membranes.

INTRODUCTION

The use of aliphatic polyamides, such as nylon 6, nylon 6,6 and nylon 11, as a membrane material is of growing importance: most applications are found in

[1] J. Appl. Polym. Sci., 50, 13-26 (1993).

microfiltration[1] for which preparation of nylon membranes has been described in patents. It is expected that aliphatic polyamides will be used in a much broader field, because of their favorable mechanical properties and chemical stability.

Membranes can be prepared by various techniques from which immersion precipitation is a widely used technique[2]. A polymer solution is cast as a thin film and subsequently immersed in a non-solvent bath, thereby inducing diffusion induced phase separation (DIPS). The liquid-liquid demixing process that usually takes place for amorphous and low-crystalline polymers has been extensively studied in our laboratory[3-5]. Solid-liquid demixing in membrane formation has also been described by Lloyd et al.[6-7]. They studied the thermally induced phase separation process (TIPS) of isotactic polypropylene and polyethylene solutions. In recent work an extensive study on the different possibilities of demixing processes of a binary system was presented[8-12].

Our objective is to investigate the process of solid-liquid demixing behavior of films cast from a nylon 4,6 solution in a diffusion induced demixing process in a ternary system.

Crystallization phenomena in (quasi) ternary mixtures for membrane formation have been studied in our laboratory by Altena[13] for the system cellulose acetate, dioxane, water, by van Emmerik[14], Koenhen[15] and Wijmans[16] for polyphenylene oxide (PPO) and by Reuvers[17] using both PPO and cellulose acetate as a membrane material. The studies on crystallization in membrane formation started with a systematic study on the behavior of PPO in different solutions[15]. Wijmans[16] studied the ternary system of a solution of PPO in trichloroethane (TCE) with methanol or octanol as non-solvents. Burghardt et al.[18] did the same for methanol, ethanol and octanol; in addition a phase diagram was calculated for ethanol as non-solvent. The phase separation process responsible for membrane formation is liquid-liquid demixing in this case. PPO membranes generally do not show any melting peak in a differential scanning calorimeter (D.S.C.) measurement, indicating that the membrane has a low crystallinity. Both Reuvers[17] and Burghardt[18] found that in some cases crystallization is the thermodynamically preferred phase separation process. The kinetically faster liquid-liquid demixing processes for PPO, however, are in favor compared to the relatively slow crystallization process, if fast quenching conditions are applied for membrane preparation.

The work described on diffusion induced phase separation so far indicates that crystallization can influence the membrane structure but the nature of the demixing process is still unknown. Agglomerates formed during the demixing process are called aggregates[3]. Aggregate formation of lamellar type can be grown from dilute solutions and more complex morphologies e.g. dendrites and spherulites are formed from solutions of medium concentrations upon decreasing the thermodynamic quality of a polymer solution by loss of solvent, by lowering the temperature or by introducing a non-solvent.

From literature it became clear that aliphatic polyamide membranes were formed according to a solid-liquid demixing process[21-21]. In our work nylon 4,6 was chosen as a material for membrane formation because of the promising properties for membrane applications in terms of chemical stability.
The present work is aimed to study:
1. the phenomenological effects of various membrane formation parameters and
2. the features of this polymer as a model system for a process in which both solid-liquid and liquid-liquid demixing can occur during immersion precipitation.

THEORY

Membrane formation in ternary systems

Membrane morphologies obtained by immersion precipitation are usually a result of liquid-liquid demixing of the ternary system polymer, solvent and non-solvent. A dissolved polymer film is cast onto a support. This is then immersed into a bath containing non-solvent. Exchange of solvent and non-solvent leads to instability of the polymer solution. Pores in the final membrane are a result of nuclei that are grown from the polymer lean phase. The morphology of such a membrane can be visualized as a cellular or foam-like structure.

Semi-crystalline polymers

A semi-crystalline polymer in a diluent can decrease its free enthalpy by separation of the homogeneous solution into a phase that consists of a pure crystalline polymer and a remaining phase that is smaller in polymer concentration (solid-liquid demixing). In such a membrane pores are the voids between the crystalline

structures.

The thermodynamic background of solid-liquid demixing is shown for the binary case with one crystallizable polymer and one diluent in figure 1. If no liquid-liquid demixing takes place the free enthalpy of the mixture (G_M) curve is concave and strongly asymmetric for a system with one polymer.

A polymer solution with $\phi_A < \phi_P < 1$, in which ϕp represents the volume fraction of the polymer, can lower its free enthalpy by phase separation into a pure crystalline state ($\phi_P = 1$) and a more diluted phase ($\phi_P = \phi_A$) at a temperature T_A.

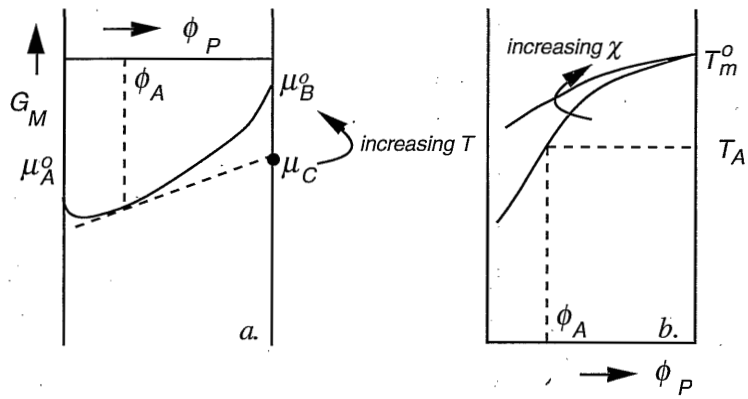

Figure 1.a) Free molar enthalpy of the mixture (G_M) at a temperature T_A as a function of the volume fraction of the polymer (ϕ_P) for a binary system with one diluent and one polymer.b) A binary phase diagram constructed from a G_M - ϕ_P diagram (see a) according to the principle of equal tangent lines.

At equilibrium the chemical potentials of the polymer repeating unit in the liquid phase and in the crystalline polymer must be equal. T_A is called the melting temperature *Tm* of a solution with composition ϕ_A. At temperatures larger than T_A the chemical potential of the crystalline state, μ_C, shifts to larger values. The free enthalpy curve continues to have a similar shape, but at higher temperatures the equilibrium melting temperature shifts to compositions with larger polymer concentrations (see figure 1b).

The complete melting point depression curve can be described according to Flory by:

$$\frac{1}{T_m} - \frac{1}{T_m^o} = \left(\frac{R}{\Delta H_u}\right)\left(\frac{V_u}{V_d}\right)\left(\phi_d - \chi_{pd}\,\phi_d^2\right)$$

in which T_m and $T_m{}^o$ are the melting temperatures of the diluted polymer and of the pure polymer respectively, ΔH_u the heat of fusion per mole of repeating units of polymer, V_d and V_u the molar volume of the diluent and the repeating unit of polymer respectively, ϕ_d is the volume fraction of the diluent and χ_{pd} the interaction parameter polymer-diluent.

The thermodynamic relation of chemical potentials of the crystalline phase and the diluent phase *in a ternary system* is more complicated. Altena et al.[23] derived an expression for the melting point depression of the polymer (3) in a ternary system containing solvent (2) as well as non-solvent (1) using concentration independent Flory Huggins parameters, χ_{12}, χ_{13} and χ_{23}. Burghardt et al.[18] derived a relation for concentration dependent interaction parameters. It is very difficult, however, to obtain all the concentration dependent parameters for a ternary system and therefore we tried to understand the behavior of the melting point depression for a ternary system in a more intuitive manner. It is expected that the lower the equilibrium melting temperature, the better is the solvent for the polymer. This was discussed by Paul[24] using the approach of solubility parameters[25]. In figure 1b it is shown how a melting point depression curve may change with an increasing interaction parameter, χ_{pd}. When the diluent phase contains more non-solvent, the diluent is a poorer solvent for the polymer. With a constant polymer concentration the equilibrium melting temperature increases when the non-solvent content is larger.

For a ternary system a three dimensional plot can be constructed as shown in figure 2. The curve in the polymer-solvent plane (curve A in the left-hand plane of the triangle diagram) represents the melting point depression curve for the polymer-solvent system. Curve B represents polymer solutions in which a certain constant ratio of solvent and non-solvent is present. The cross-section of the different equilibrium lines with the temperature plane at 30°C gives the equilibrium (isothermal) crystallization line in the ternary phase diagram at 30°C. Since the

curves for larger non-solvent concentrations and identical polymer concentration lie at higher T values than the polymer-solvent line, the isothermal crystallization line shifts to lower polymer concentrations for larger non-solvent concentrations.

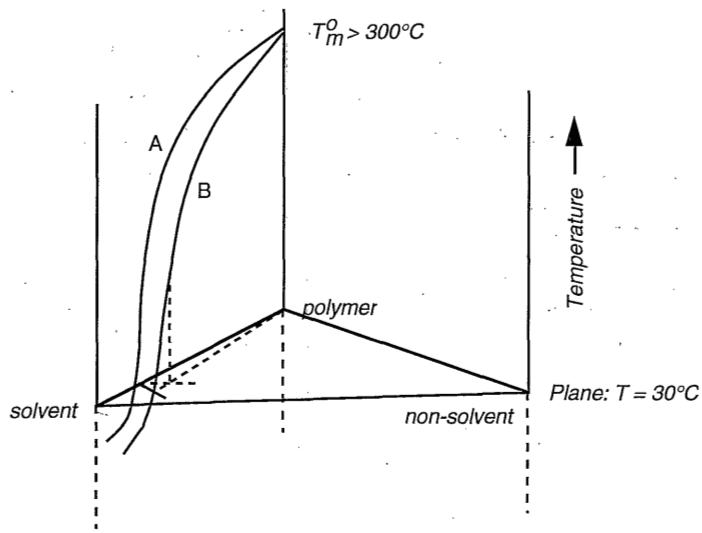

Figure 2. The ternary phase diagram with the equilibrium melting curve as a function of composition and temperature. The solvent polymer plane gives the binary situation of melting point depression. The cross-section at T=30°C gives the isothermal phase diagram with the solid-liquid demixing border at equilibrium conditions.

An equilibrium crystallization line in the phase diagram represents solid-liquid (s-l) demixing. For membrane forming systems also a liquid-liquid demixing gap is present, which results in a liquid-liquid (l-l) demixing process. Figure 3 gives a possible phase diagram for a ternary system in which the polymer can crystallize. Point A represents, as stated, the crystallization of polymer (P) in solvent (S).

The curve A-B is the crystallization curve. Any composition inside the area A-B-P can crystallize into pure polymer P and a composition on curve A-B. Curve B-D-C is the liquid-liquid (l-l) demixing curve: the binodal. Compositions inside the area B-C-D exhibit phase separation into two liquid phases, connected by a tie-line.

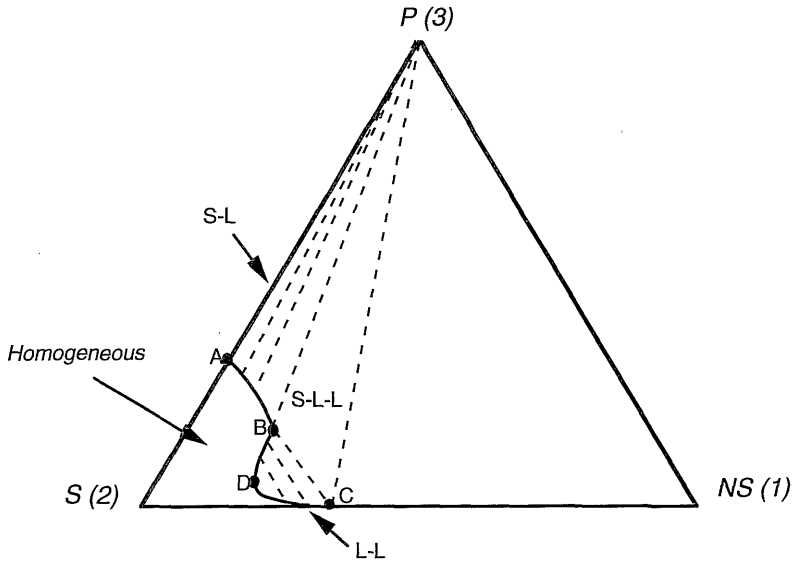

Figure 3. An isothermal ternary phase diagram for a semi-crystalline polymer (P, index:3), a solvent (S,index:2) and a non-solvent (NS, index:1).

Point D is the critical point, where the two equilibrium compositions coincide. Area B-C-P is the area in which three phases are in equilibrium: the compositions indicated with B, C and P. In area P-C-NS phase separation into a solid phase (P) and a liquid phase with a composition on the line C-NS will occur.

It is important to notice that a phase diagram represents equilibrium thermodynamics; kinetic effects are not included. During membrane formation diffusion processes of non-solvent and solvent are continuing; equilibrium is never achieved. At a certain position in the film a composition may thermodynamically be meta-stable, but the time-scale for demixing can be too short for the demixing process to take place. Especially the crystallization process is expected to require a time interval in which polymer chains are allowed to migrate to a growing crystal and to exhibit a surface reaction on the crystal. Besides these consideration a certain degree of supersaturation is necessary.

EXPERIMENTAL

Nylon 4,6 (Stanyl KS 400), kindly supplied by DSM, was dissolved at 30°C in formic acid (Merck, analytical grade 98%) in a concentration range of 10 to 32 wt%. The polymer was dried invacuo for at least 24 hours before use; formic acid was used without further purification. Polymer solutions were cast on a glass plate with a thickness of 0.3 mm. The glass plate with the cast polymer solution was immediately immersed in a water bath. After a sufficient coagulation time the membranes were removed from the glass plate, rolled in filter paper and washed with demineralized water for at least 24 hours.

The morphology of the membranes was examined by Scanning Electron Microscopy (Jeol JSM T 220A). The samples were wetted in ethanol, cryogenically broken and dried in vacuo for at least 6 hours. A thin layer of gold was deposited on top of the sample with a Balzer Union SCD 040 sputtering apparatus (sputtering conditions: 25 mA for 2 minutes).

As a first characterization method, the pure water flux, using ultrafiltrated water, was measured with an AmiconTM set-up at an applied pressure difference of 2 bar. Pore size analysis was performed on a Coulter® Porometer II (ASTM F316-80, 1980; BS 6410: 1984) with Coulter® Porofil as a wetting liquid. The sample holder has a diameter of 25 mm.

Differential scanning calorimetry (Perkin Elmer DSC-4) was used to investigate the crystalline nature of the polymeric membranes.

RESULTS

The effect of enlarging the polymer concentration from 10 to 32 wt% on the ultimate membrane morphology can be clearly observed by electron microscopy (see figure 4). At low polymer concentrations (<17 wt%) liquid-liquid demixing takes place, and the membranes show a cellular morphology. At concentrations between 20 and 30 wt% solid-liquid demixing occurs resulting in a structure, which is formed of spheres. Growth of a nucleus takes place from the polymer-rich phase, that consists of ordered crystalline material, surrounded with a highly concentrated phase of amorphous polymer molecules. Apparently the underlying process is spherulitic crystallization.

Membranes prepared from a polymer solution with a concentration larger than 30 wt% show axialitic crystalline units, which are intermediate stages in the development of a spherulite. The growth of crystalline units to a complete spherulite in this case is inhibited.

Using a polymer concentration of 20 wt% with an increasing amount of water in the initial solution a similar effect can be observed. The membrane is the result of solid-liquid demixing with a spherulitic structure. The spherulite size has decreased from 10 mm to 2 mm when 5 wt% of water (non-solvent) is added to the initial solution. Upon increasing the water concentration in the starting solution the structure changes to a finer morphology. The membrane with 10 wt% of water in the original solution shows an axialitic structure. Such an effect is also shown in figure 5 starting with a 15 wt% polymer solution. The final structure here (15 wt% P, 20wt% water) is better described as a dendritic or leafy structure. Table 1 summarizes the effects of polymer and water concentration on the morphology of the membranes.

The performance of the membranes is shown in table 2. Typical microfiltration membranes were synthesized; 0.1 mm membranes for the use in e.g. the semi-conductor industry, 0.2 mm for an absolute sterilizing grade and 0.45 - 0.65 mm for the use in the beverage industry. Pure water fluxes and air permeability give an indication about the performance of the membranes[26].

While for membranes that result from a liquid - liquid demixed morphology the pores originate from the growth of nuclei of the polymer lean phase, pores in a solid - liquid demixed type of membrane are the voids between the semi-crystalline units. The larger these solid particles are, the larger the voids, resulting in a larger effective pore size in the membrane. Indeed the pore size gives a larger value for a membrane with a larger crystallite size than for membranes with a finer morphology (see the figures 4 and 5 in combination with table 2). Skinless membrane structures were easily prepared with nylon 4,6, while membrane manufacturers of nylon 6 and nylon 6,6 membranes had to use rather high solvent concentrations in the coagulation bath[27,28] or had to induce phase separation by water vapor in order to avoid thick skin layers in the membranes.

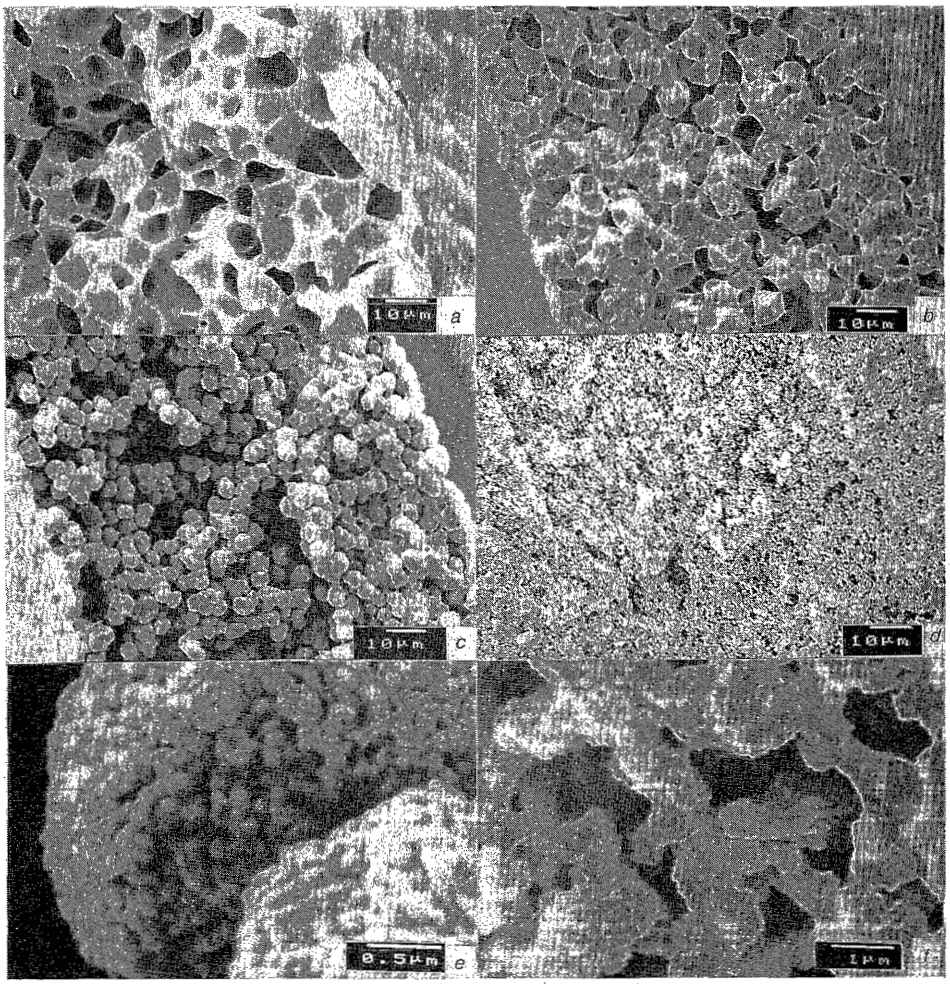

Figure 4.A. Morphology of nylon 4,6 membranes observed by scanning electron microscopy (SEM) starting with different polymer concentrations; the polymer concentration (wt%) is for a: 15%, b: 20%, c: 25%, d: 32%, e. and f. are larger magnifications of the photos c. and d. respectively.

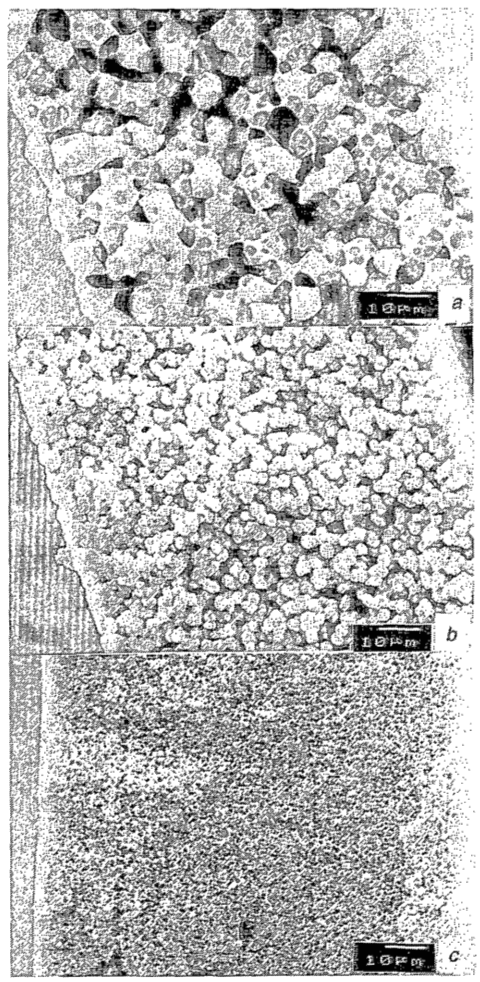

Figure 4.B. Morphology of nylon 4,6 membranes observed by SEM with different water concentrations (wt%) in the polymer solution; the polymer concentration of the initial solution is 20 wt%. The water concentration is for a: 0%, b: 5% and c: 10%.

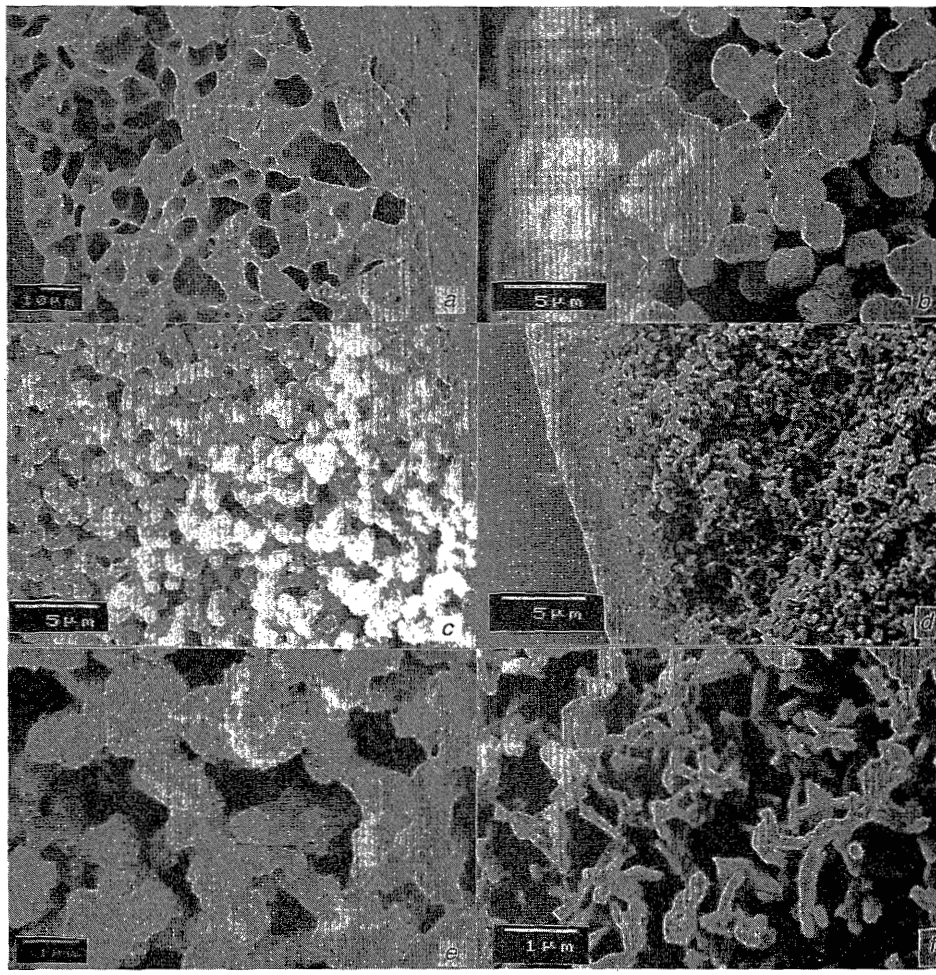

Figure 5. Morphology of nylon 4,6 membranes observed by SEM with 15 wt% of polymer and different water concentration (wt%) in the polymer solution, a: 0%, b: 10%, c: 15%, d: 20%, e. and f. are larger magnifications of the photos c. and d. respectively.

Table 1. The spectrum of the morphology of the membranes obtained by varying the polymer concentration and the water concentration in the original polymer solution.

water concentration (wt%) \ Polymer concentration (wt%)	10	12	15	17	20	25	30	32
0	l-l		l-l	l-l*	s-l*	s-l (sf)	s-l (sf*)	s-l (ax)
2			s-l*					
5	l-l	s-l*	s-l*		s-l (sf)	s-l (sf*)		kin
10	s-l (sf)		s-l (ax)		s-l (ax)	s-l (ax)		
15			s-l (ax)		s-l (ax)	kin		
20	s-l (-)		s-l (de)		kin			
25	un		un					

l-l: liquid-liquid demixed structure,
s-l: solid liquid demixed structure,
l-l*, s-l* : transition from liquid-liquid to solid-liquid demixing,
sf: spherulites, ax: axialites, sf*: transition sf-ax; de: dendrites
un: a solution was not obtained and
kin: occurence of turbidity of the solution after approximately 2 days.

It is obvious that a more interconnected pore structure can be obtained with membranes that result form solid - liquid demixing. Membranes that are prepared via a liquid - liquid demixed very often show isolated pores. Special precaution must very often be taken to improve the connectivity of pores in order to avoid a too high resistance towards permeation of the membrane.

Table 2. Water flux, gas permeability and pore size of Nylon 4,6 membranes with varying as a function of polymer and non-solvent concentrations.

Concentration of Polymer (wt%)	and water (wt%)	Water Flux ($L/m^2.h.bar$)	Air permeability ($L/cm^2.min$) at 2 bar	Pore size (micrometer) max.	average
20	5	15000	6.4	1.0	0.85
20	10	4000	1.6	0.40	0.30
25	0	13000	3.1	0.89	0.62
25	5	1200	0.7	0.40	0.36
25	10	800	0.7	0.20	0.16
27.5	0	2500	0.74	0.74	0.45
30	0	1250	0.33	0.70	0.28
32	0	300	0.16	0.25	0.10

The DSC thermograms of the membranes can be compared with the material as it was received (see figure 6). The polymer shows a large endothermic peak at 297°C; the membranes exhibit smaller but very distinct melting endothermic peaks at somewhat lower temperatures. The membranes prepared are clearly semi-crystalline in nature. The heat of fusion for the membranes is somewhatless than for the polymer as it was received, indicating that the degree of crystallization is somewhat lower for the membranes.

The morphology of the membranes is finer when the polymer concentration or when the water concentration at the same polymer concentration increases. In order to quantify this behavior a *nucleation density* is defined as the total number of entities in the membrane structure per unit area of a cross-section. Nucleation density is the result of nucleation rate and nucleus growth. Assuming that one unit (a spherulite or axialite for solid-liquid demixing or a cell for liquid-liquiddemixing) has grown from one nucleus one can count the number of units per area on a cross section of a SEM picture. Though the structure visualized with SEM is that of a final dry state and

membrane formation takes place in the liquid state, nucleation density as it is described above can be compared when the polymer and/or water concentration is varied. Disapperance of nuclei due to Oswald ripening and/or coalescence is not taken into account.

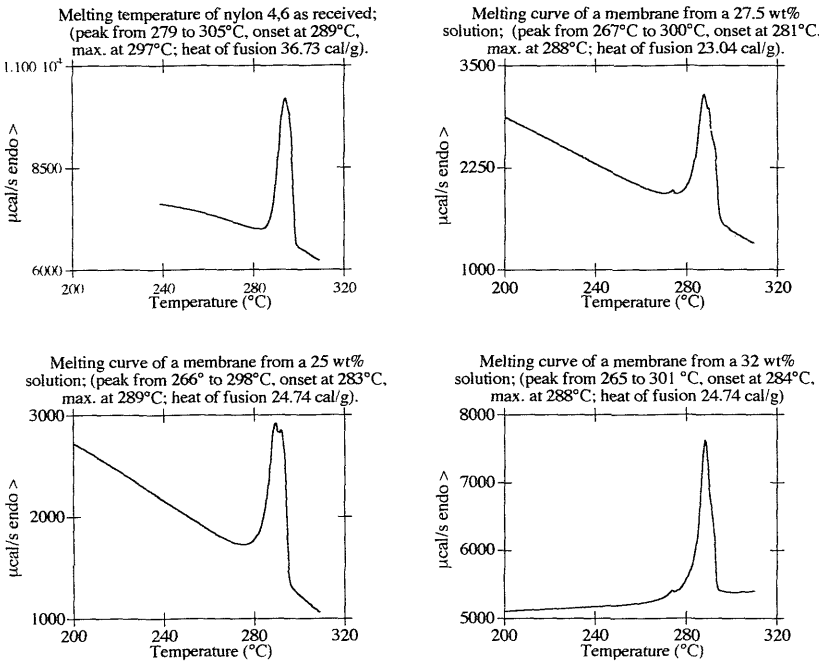

Figure 6. Differential scanning calorimetry of nylon 4,6 and of the membranes prepared from solutions with various polymer concentrations.

In figure 7 the nucleation density is plotted as a function of the composition of the ternary solution from which the membranes were cast. The dots give the nucleation density for a structure obtained by l-l demixing; the unit N then gives the number of cells; the crosses represent the s-l type of demixing. Starting from a low polymer concentration the nucleation density increases non-linearly with an increasing polymer concentration. The same trend is found for an increasing water content in the polymer solution at a constant polymer concentration.

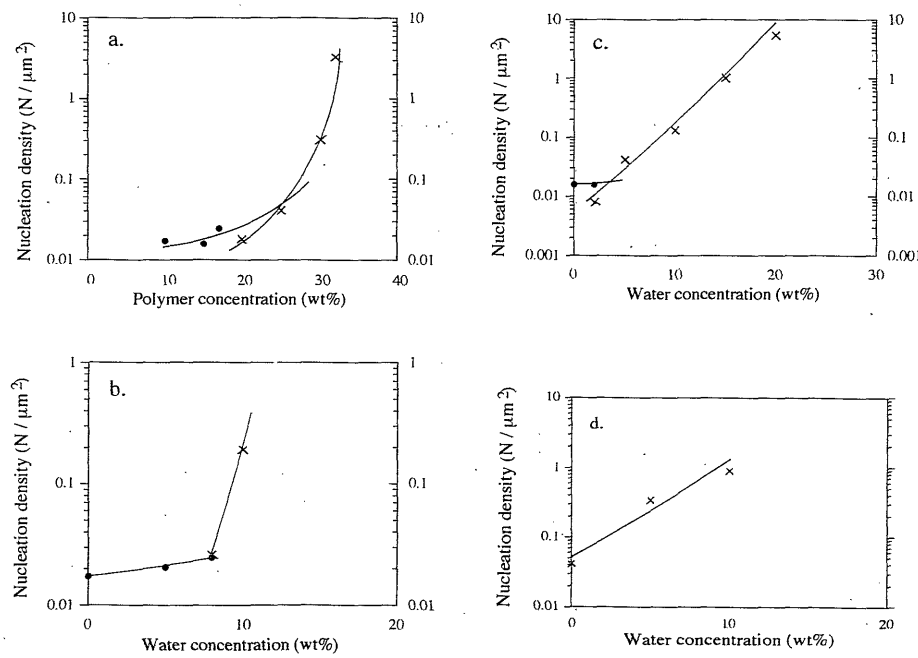

Figure 7. Nucleation density in membranes prepared with diffusion induced phase separation as a function of the composition of the initial solution; a: nucleation density as a function of the initial polymer concentration, b: as a function of water concentration added to a 10 wt% polymer solution, c: as a function of water concentration for a 15 wt% polymer solution and d: for a 25 wt% polymer solution. The dots represent the nucleation density for liquid-liquid demixing, the crosses for solid-liquid demixing.

DISCUSSION

Spherulite formation

As illustrated in figure 4 some membranes showed a spherulitic structure with spherulites that differ in size from 10 mm to 2 mm for membranes with an increasing polymer and/or water concentration in the starting solution. The schematic development of spherulites according to Keith and Padden[29] is shown in figure 8. In the early stages the spherulite has a sheaflike precursor.

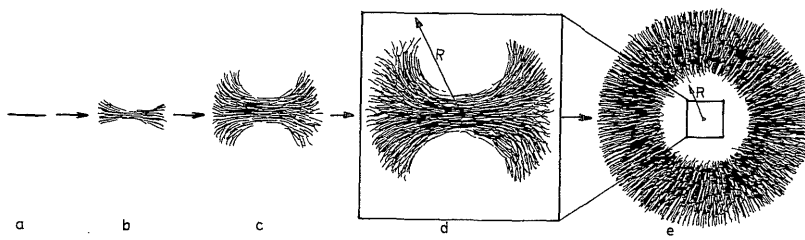

Figure 8. Schematic representation of successive stages in the development of a spherulite (structure e) from a chain-folded precursor crystal (structure a). The structures a to d are drawn at a larger magnification and can be found within the radius R of the spherulite (structure e).

The structures a to d represent the intermediate stages in the development of the spherulite. Neighboring transitional structures can impinge upon the growing units and stop further growth before they attain the spherically symmetric growth stage. The morphology of the polymer sample then is composed of units of axialites.
Spherulite forming materials are multi-component systems in which certain components (impurities of the crystal) are rejected preferentially by the growing crystals. The tips of growing lamellae abstract relatively pure material from the bulk and impurities accumulate between the lamellae. Spherulites are reported to be relatively open. Spherulites that are grown in an environment of polymer in a saturated solution of one liquid in another liquid (e.g. water and formic acid) will reject the low molecular weight components besides the macromolecular impurities. It can be expected that such spherulites have a 'spongy' texture. This morphology is indeed observed for thespherulites shown in figure 4.
The size of the spherulites grown from a pure polymeric melt is generally dependent on the extent of undercooling. At high undercoolings more spherulites are nucleated per unit volume. The larger the nucleation density, the less spherulites are able to grow freely before they reach a neighboring spherulite. For our membrane system apparently the nucleation density increases with increasing polymer concentration and/or increasing water concentration in the polymer dope (see figure 4,5 and 7).
Spherulitic structures in membranes resulting from solid-liquid phase separation of the binary system polypropylene in mineral oils quenched from 245°C to 43°C have

been reported by Lloyd et al.[10]. The spherulite size decreased when membranes were prepared with a lower cooling rate, at a lower temperature or when a nucleating agent, such as adipic acid, was used, because of an increasing nucleation density.
Spherulitic growth of other polyamides from solution has been reported by Keller et al.[30-31] for polyamide 6,6 and polyamide 6,10 from formic acid and cresol, Magill[32-33] for the 'odd-odd' nylons and the 'odd-even' nylons. Films were prepared by evaporation of solvent or by quenching in water.
It is expected that the membrane morphology described by Marinaccio[20] for semi-crystalline nylons is a result of the same type of demixing phenomena as observed by us. The author mentioned that 'aggregation in solution results in film porosity since the film as cast can be thought to consist of interacting aggregation of spherical particles. The larger the sphere the larger the voids in the film. Structurally this is much like a box of tennis balls or other non-spherical geometries fused at their point of contact'. The membrane morphology as it is shown in the SEM photographs of the figures 4 and 5 can be very well visualized with the previous description.
Soldatov et al.[22] investigated the precipitation behavior of nylon 6 films in aqueous acetone. They discussed that with an increasing acetone content a structure conversion occurs: first the film has a cellular morphology; the use of pure acetone results in a structure composed of 'globules' with a size of 3 to 5 mm.
It can be concluded that the phenomena found for nylon 4,6 can be generalized for other aliphatic polyamides, though nylon 4,6 is a much more rapidly crystallizing nylon. Therefore the kinetical crystallization process is likely to give cause to a more pronounced crystalline structure for nylon 4,6 compared to the other aliphatic nylons.

Solid-liquid demixing versus liquid-liquid demixing

A liquid-liquid demixing region is present for the ternary system nylon 4,6, formic acid and water.At low polymer concentrations, e.g. 15 wt% of polymer, the polymer solution at different positions in the film during the diffusion process undergoes phase separation according to a liquid-liquid demixing mechanism. For the cast polymer films at a polymer concentration of 15 wt% both the polymer and the water concentration will increase during the diffusion processes. This means that the composition passes through a region in the phase diagram, in which solid-liquid demixing should occur, for instance when membrane formation was started with a film which contained 20 to 25 wt% of polymer and 5 to 10 wt % of water (see table

1). The final membrane structure, however, differs to a large extent for these two demixing processes. Since a solid-liquid interface has a higher surface energy than a liquid-liquid interface, nucleus formation of a solid phase in a liquid is energetically much more difficult than the formation of a liquid nucleus in a liquid phase. Compositions within the s-l region will not nucleate easily from a homogeneous solution. Solutions with lower polymer concentrations pass through the meta-stable region (solid-liquid demixing can take place thermodynamically) towards the binodal. These solutions remain homogeneous until the l-l binodal is crossed.

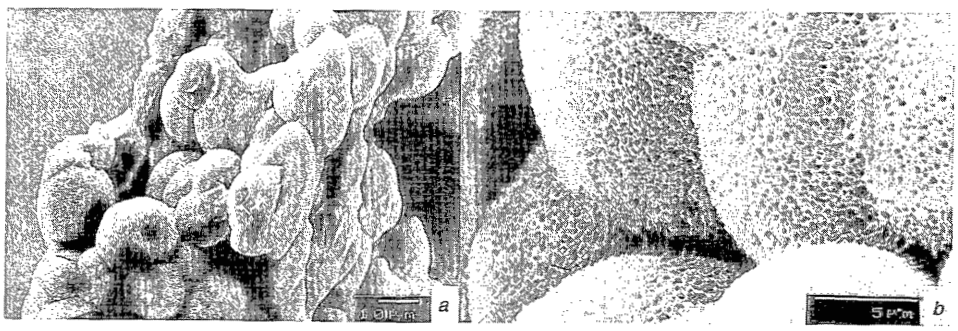

Figure 9. Membrane morphology of a 15 wt% membrane, prepared by a diffusion induced phase separation process by a saturated vapor of water in nitrogen. The right hand photograph is a view of spherulites in the membrane at a higher magnification.

Two effects can explain solid-liquid demixing to take place, despite the fact that nucleation is energetically more difficult.

The first one is that nuclei were already present in the solution; s-l demixing is for instance initiated by small crystallites in the solution. The process of crystal growth takes place by secondary nucleation of polymer molecules on the crystalline nucleus. Especially for the membranes with a large nucleation density (figure 7) that show an axialitic structure it is expected that a large number of small precursor crystallites are already present in the initial solution.

The second possible cause is that the time available for crystallization is large enough to enable solid-liquid demixing to take place before phase separation occurs according to a liquid-liquid demixing mechanism. For the lower polymer

concentrations (<17 wt%) the viscosity of the solution is relatively low. Diffusion processes are fast and therefore the time that the composition in the film is in the s-l demixing gap is too short to allow a crystallization process to take place. If this is the case it is expected that crystallization will occur if the diffusion processes are slowed down. In order to verify this hypothesis a 15 wt% polymer film was precipitated in a saturated water vapor atmosphere. Normally this film exhibits liquid-liquid demixing when allowed to phase separate in a water bath (see figure 4). The morphology of the membrane precipitated from the vapor phase is shown in figure 9. Large spherulites with a size of 20 mm have grown in the membrane. Apparently the crystallization process can take place because of the slower diffusion processes of the in-diffusion of non-solvent and the out-diffusion of solvent. The time available for a composition in the film within the solid-liquid demixing gap is large enough to initiate the process of nucleation and growth of a (solid) nucleus.

For this system (nylon 4,6, formic acid and water) it can be concluded that the crystallization line is always positioned closer to the solvent corner than the binodal, as is schematically shown in figure 10. Thermodynamically cystallization is the favorable phase separation process. In some cases, however, it is possible to surpass the crystallization region, when the kinetic demixing conditions during a diffusion induced phase separation are fast relative to the time necessary for solid-liquid demixing.

Our results for the membrane formation mechanism for the nylon 4,6 membranes are in agreement with results discussed by Wijmans et al.[16] and Reuvers et al.[17]. According to Reuvers crystallization is the thermodynamically most favorable process for the ternary system PPO, trichloroethane, octanol. Demixing processes carried out with a liquid non-solvent usually gives a membrane morphology as a result of liquid-liquid phase separation. Wijmans discussed a series of experiments in which membranes were prepared by phase inversion from the vapor phase using a vapor of octanol as a non-solvent. In contradiction to Wijmans' conclusions the SEM photos show structures that are most likely a result of a crystallization process. The rate of in-diffusion of non-solvent and out-diffusion of solvent in a vapor phase induced demixing process is slow enough to allow crystallization to be the most important phase separation mechanism for the ternary system PPO, trichloroethane and octanol.

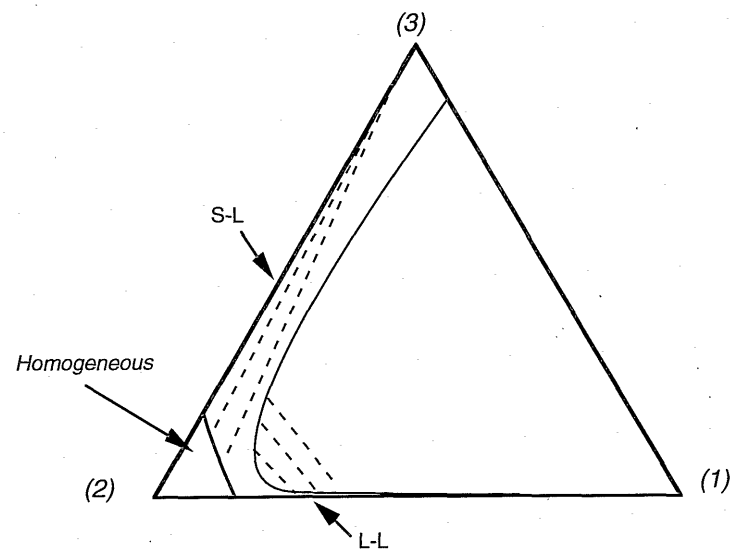

Figure 10. Schematical diagram of the position of the crystallization line and the binodal. At equilibrium conditions only the crystallization line should be drawn. For membrane formation the binodal curve is of importance here because at certain conditions crystallization may not take place as a first step in the phase separation process because of its relatively slow demixing kinetics and/or a not high enough degree of supersaturation.

Solid-liquid demixing is competitive with liquid-liquid demixing in a diffusion induced phase separation process only if nuclei are already present in the solution (heterogeneous nucleation) or if the diffusion processes are slow enough to have enough time available for the nucleation process of a crystalline nucleus. Even while crystallization is thermodynamically the most favorable state liquid-liquid demixing still takes place as a first phase separation process.

CONCLUSIONS

Crystallization (solid-liquid demixing) occurs in the diffusion induced phase separation process for the preparation of nylon 4,6 membranes, resulting in a spherulitic or axialitic morphology of the membrane. Solid-liquid demixing takes

place starting from films of solutions of nylon 4,6 in formic acid with polymer concentrations larger than 17 wt% upon quenching in a water bath. These polyamide membranes exhibited a clear melting peak (D.S.C.). At lower concentrations the membrane morphology is a result of liquid-liquid demixing. Solid-liquid demixing is kinetically competitive with liquid-liquid demixing in a diffusion induced phase separation process if nuclei are already present in the starting solutions (heterogeneous nucleation) or if a relatively long time is available for the process of crystallization. The morphology resulting from s-l demixing is a result of spherulitic crystallization. Spherulites can grow freely if the nucleation density is small. Higher polymer concentrations and lower concentrated polymer solutions containing non-solvent in larger concentrations give a large concentration of nuclei at the start. If nucleation density is large; the precursors for spherulites cannot grow until they attain the symmetric growth stage, which now results in an axialitic structure.

ACKNOWLEDGEMENTS

The authors wish to thank Stephan Eltink for the enlightening discussions and DSM the Netherlands for the funding of this project.

REFERENCES

1. R. Kesting, *Synthetic Polymeric Membranes, A Structural Perspective*, 2nd Ed. Wiley, NY (1985).

2. M.H.V. Mulder,*Basic Principles of Membrane Technology*, Kluwer Dordrecht (1991).

3. F.W. Altena, C.A. Smolders, *Macromolecules*, 15, 1491 (1982).

4. J.G. Wijmans, F.W. Altena, C.A. Smolders, *J. Polym. Sci., Polym. Phys.*, 22, 519 (1984).

5. A.J. Reuvers, C.A. Smolders, *J. Membr. Sci.*, 34, 67 (1987).

6. D. Lloyd, J. Barlow, K. Kinzer, *AIChE Symposium Series*, 261, 28 (1988).

7. D. Lloyd, K. Kinzer, H. Tseng, *J. Membr. Sci.*, 52, 239 (1990).

8. D. Lloyd, S. Kim, K. Kinzer, *J. Membr. Sci.*, 64, 1 (1991).

9. S. Kim, D. Lloyd, *J. Membr. Sci.*, 64, 13 (1991).

10.G. Lim, S. Kim, Q. Ye, Y. Wang, D. Lloyd, *J. Membr. Sci.*, 64, 31 (1991).

11. S. Kim, G. Lim, A. Alwattari, Y. Wang, D. Lloyd, *J. Membr. Sci.*, 64, 41 (1991).

12. A. Alwattari, D. Lloyd, *J. Membr. Sci.*, 64, 55 (1991).
13. F.W. Altena, C.A. Smolders, *J. Polym. Sci., Polym. Symp.*, 69, 1 (1981).
14. P.T. van Emmerik, C.A. Smolders, *J. Polym. Sci., part C*, 38, 73 (1972).
15. D.M. Koenhen, C.A. Smolders, *J. Polym. Sci., Polym. Phys. Ed.*, 15,155 (1977).
16. J.G. Wijmans, H.J.J. Rutten, C.A. Smolders, *J. Polym. Sci., Polym. Phys. Ed.*, 23, 1941 (1985).
17. A.J. Reuvers, *PD Thesis, Appnedix A Chapter 2*, University of Twente, The Netherlands (1987).
18. W.R. Burghardt, L. Yilmaz, A.J. McHugh, *Polymer*, 28 , 2085 (1987).
19. A. Ladbudzinska, A. Wasiak, A. Zianicki, *J. Polym. Sci.*, C16, 2835 (1967).
20. P. Marinaccio, R. Knight, US Patent 387638 (1975).
21. V. Soldatov, V. Artamov, O. Mostovlyanskii, *Proc. 29th Micro Symp. Macromolecules, Prague*, 171 (1986).
22. P.J. Flory, *Principles of Polymer Chemistry*, Cornell University Press, NY 1953.
23. F.W. Altena, J.S. Schröder, R. van de Hulst, C.A. Smolders, *J. Polym. Sci., Polym. Phys. Ed.*, 24, 1725 (1986).
24. D.R. Paul, *J. Appl. Polym. Sci.*, 11, 439 (1967).
25. J.H. Hildebrand, R.L. Scott, *Solubility of Non-electrolytes*, 3rd. Ed., Dover Englewood Cliffs, N.J.(1964).
26. H.D.W. Roesink, *PhD Theis*, University of Twente, The Netherlands (1989).
27. D. Pall, US Patent 4340479 (1982).
28. J.F. Ditter, WO Patent 86 / 07544 (1986).
29. F. Khoury, E. Passaglia, *The Morphology of Crystalline Synthetic Polymers, Treatise on Solid State Chemistry, Vol. 3, Crystalline and Non Crystalline Solids (Ed. N.B. Hannay), Chapter 6, The Morphology of Crystalline Synthetic Polymers*, Plenum Press, NY (1976).
30. A. Keller, *J. Polymer Sci.*, 17, 447 (1955).
31. A. Keller, *J. Polymer Sci.*, 26, 361 (1959).
32. J. Magill, *J. Polymer Sci.*, A, 9, 817 (1971).
33. J. Magill, *J. Polymer Sci.*, A, 3, 1193 (1965).

1st appendix to CHAPTER 2

Performance of Nylon 4,6 Membranes in Non-Aqueous Media

A.M.W. Bulte, B. Folkers, M.H.V. Mulder,
C.A. Smolders, H. Strathmann.

Nylon 4,6 membranes are of special interest for applications in non-aqueous media and therefore the permeability of various organic liquids was tested. In this appendix the alcohol and acetone flux of some membranes described in chapter 2 and four other membranes are compared with the pure water flux of these membranes. Some additional membranes were prepared by coagulation of a solution containing 32 wt% nylon 4,6 (Stanyl KS 400) and 3.5 wt% of water in formic acid in a water bath of different temperatures (0, 30, 50 and 80°C respectively). The water flux of all membranes was measured directly after preparation and rinsing, without drying the membrane. The membranes showed irreversible shrinkage after drying, after which they were stored for a considerable time, 3 months to 1 year. Ethanol and acetone flux was measured after drying and storage of the same samples of the membranes that were used for the determination of the water flux, and were determined by using an Amicon set up with a cell with a smaller diameter: 2 cm instead of 3.5 cm. Special O-rings were used for the measurement of the acetone flux (Kalrez©). The ethanol flux was measured first; then the samples were dried followed by measurement of the acetone flux. The membranes did not show any irreversible shrinkage after the second drying step.

The results are shown in table 1, with the flux expressed in kg / (m^2.h.bar); the pore sizes of the membranes were determined by Coulter porometry. The density of both ethanol and acetone is 0.79 g / cm^3. The values for the ethanol flux were in all cases smaller than those for the water flux; for acetone, which is a milder swelling agent for nylon 4,6 (see chapter 1), these values were higher.

Table 1. Maximum (max.) and average (mean) pore-sizes determined by Coulter Porometry and comparison of the initial water flux with the flux of ethanol, a swelling medium (~9%) and of acetone, a non-swelling agent (<1%) for nylon 4,6, of various nylon 4,6 membranes.

Membrane #	Pore size (μm) max.- mean.	Initial fluxes (kg / (m^2.bar.h) Water	Ethanol (ρ = 0.79 g/cm^3)	Acetone (ρ = 0.79 g/cm^3)
A	0.16 - 0.10	300 ± 30	150 ± 15	630 ±75
B	0.70 - 0.28	1250 ± 400	1100 ± 80	4000 ± 25
C	0.20 - 0.16	800 ± 100	250 ± 60	1000 ± 90
D	0.07 - --	35 ± 3	too close	too close
E	0.07 - --	60 ± 1	25 ± 15	160 ± 70
F	0.07 - --	92 ± 30	50 ± 30	220 ± 80
G	0.11 - 0.08	150 ± 25	100 ± 10	540 ± 65

The casting solution of the membranes was for
A: 32 wt% of polymer and 3 wt% of water,
B: 30 wt% of polymer,
C: 25 wt% of polymer and 10 wt% of water,
D, E, F and G: 32 wt% of polymer and 3.5 wt% of water with the temperature for the coagulation bath 0, 30, 50 and 80°C respectively.

2nd appendix to CHAPTER 2

The Influence of Metal Halides as Additives on the Morphology of Nylon 4,6 Membranes prepared by Immersion Precipitation

A.M.W. Bulte, B. Folkers, M.H.V. Mulder,
C.A. Smolders, H. Strathmann.

SYNOPSIS

Inorganic salts were added to the polymer solution to control the crystallization tendency of nylon 4,6 in the membrane forming process. Alkali halides (especially LiCl and NaCl) improved the performance of the membranes (larger 'flux/pore size' ratio). This can be explained by an enhancement of the porosity. In some cases, especially with $CaCl_2$ and $FeCl_3$, membranes with very thick top-layers and sub-layers with large spherulites were obtained. Only a few ultrafiltration membranes with relatively large pores could be prepared. Coulter porometry and permporometry were used as pore size characterization methods. A nylon 4,6 ultrafiltration membrane was prepared with the largest pores around 80 nm. The membrane had a relatively low number of pores between 20 and 80 nm that mainly determined the water permeation (calculation). This membrane may be a candidate as a support layer in composite membranes for gas separation and pervaporation. The surface porosity and top-layer thickness should be further optimized.

INTRODUCTION

During the demixing process of immersion precipitation crystallization of the polymer, nylon 4,6, appeared to be the most important process for membrane formation. This 'solid - liquid' phase separation is a different demixing process compared to the more common 'liquid - liquid' phase separation. The morphology of the membranes varied from spherulitic to axialitic[1]. This type of morphology was also

reported for membranes from nylon 6,6 and nylon 6[2,3]. The typical cellular structure obtained from the liquid-liquid phase separation process was only found at low polymer concentrations[1].

The effect of alkali halides on the membrane forming system

Alkali halides have shown to influence the crystal structure of nylons[4,5]. The salts have also been used as additives for membrane preparation as reported in patent literature. The addition of inorganic salts to the polymer solution introduces additional variables in the membrane forming system: the type of salt and the concentration. First experiments showed that the addition of LiCl to the polymer solution had a large effect on the membrane morphology. For these membranes a more pronounced dense top-layer could be observed compared to membranes formed without salts in the solution. The morphology of the top-layer was also affected to a large extent depending on the concentration of the salt. The effects of addition of salts was investigated systematically. One of the aims of this study is the development of well defined ultrafiltration membranes with pore sizes smaller than 100 nm in diameter and relatively high surface porosity. Such membranes are interesting for both ultrafiltration applications (especially non-aqueous) and as support layers for pervaporation and gas separation membranes.

Pore size characterization

Two methods are used to characterize the pore size and pore size distribution, permporometry and Coulter® porometry.
The experimental set-up of the permporometer, as described by Eyraud[6] and Katz, was developed by Cuperus[7] in our group. By this method the pore size distribution of the active pores of ultrafiltration (UF) membranes is determined. The technique is based on the controlled blocking of pores by condensation of a vapor, present as a component of a gas mixture, and the simultaneous measurement of the gas flux through the membrane. The capillary condensation process is related to the relative vapor pressure according to the Kelvin relation, and consequently an exact control

of the relative vapor pressure permits a step-wise blocking of pores. The experiments start with a relative pressure equal to one; then all the pores of the membrane are filled and gas transport through the pores of the membrane is not possible. Upon reducing the vapor pressure, pores with a size corresponding to the vapor pressure set, are emptied and become available for gas transport. By measuring the gas transport through the membrane upon decreasing the relative vapor pressure, the pore size distribution of the active pores can be found. The main transport mechanism for gas transport in the nanometer pores is assumed to be Knudsen diffusion. A theoretical pure water flux can be calculated using the Poisseuille equation and the measured pore size distribution, assuming a certain thickness of the top-layer and a tortuosity of one.
The Coulter® Porometer employs a displacement technique to measure the pore size distribution of a membrane. The membrane is first thoroughly wetted with liquid of low surface tension and low vapor pressure, such that all of the pores have been filled with the liquid. Then a gas pressure is applied across the wetted sample. As the pressure of gas increases, it will reach a point where it can overcome the surface tension of the liquid in the largest pores. The liquid is displaced and then a gas flow through these pores can be monitored. Increasing the pressure further allows gas to flow through smaller pores and this continues until all of the pores have been emptied. By monitoring the pressure of gas applied to the membrane and measuring the flow of gas through the membrane when liquid is being expelled, a so called 'wet' run is obtained. If the membrane is tested during 'dry' conditions without liquid in its pores, a so called 'dry' run is obtained. By comparing the flows for the 'wet' run to the 'dry' run, the pore size distribution can be calculated.

Spherulite formation

As has been illustrated in chapter 2[2] some membranes showed a spherulitic structure with spherulites that differ in size from 2 to 10 μm for membranes with a decreasing polymer concentration in the starting solution. At higher initial polymer concentrations incompletely grown spherulites or axialites are observed.

EXPERIMENTAL

Membrane formation

Nylon 4,6 (Stanyl KS 400 kindly supplied by D.S.M. the Netherlands) was dissolved at 30°C in formic acid (Merck, analytical grade 98%) at concentrations of 30 and 32 wt%. The polymer solutions contained 0 to 3 wt% of an inorganic salt (LiCl, NaCl, KCl, LiBr, $MgCl_2$, $CaCl_2$, and $FeCl_3$). Prior to use the polymer and the salts were dried *in vacuo* at 70°C. Membranes were cast on a glass plate with a 0.3 mm casting knife. Immediately after casting the glass plate with the polymer solution was immersed in a coagulation bath containing demineralized water. After a sufficient coagulation time (~30 minutes) the membranes were removed form the glass plate, rolled in filter paper and washed with demineralized water for at least 24 hours.

Flux measurements and pore size characterization

As a first indication of the practical use of a membrane, the pure water flux was tested with an Amicon set-up at an applied pressure of 2 bar using ultrafiltrated water.
Pore size analysis was performed on a Coulter® Porometer II (ASTM F316-80, 1980; BS 6410: 1984). Coulter® Porofil was used as a wetting liquid. The sample holder has a diameter of 25 mm.
In permporometry both sides of one membrane are flushed by a mixture of cyclohexane and nitrogen and air. The oxygen content at the nitrogen outlet is measured by a RETSCH microprocessor oximeter.
The pore size analysis by liquid displacement for one membrane was kindly performed by dr Capanelli and dr I.M. Wienk at the University of Genua (Italy).
The morphology of the membranes was examined by scanning electron microcopy (SEM) (Jeol, magnification 200 - 35000x) The samples were wetted in ethanol, cryogenically broken and dried *in vacuo* for at least 6 hours. A thin layer of gold was deposited on top of the sample with a Balzer Union SCD 040 sputtering apparatus conditions: 25 mA for 2.00 minutes).

RESULTS AND DISCUSSION

Spherulitic crystallization

The addition of inorganic salts to the starting nylon 4,6 solution did effect the final morphology in some special cases. A membrane without salt in the solution resulted in a morphology with axialites[1]. Addition of some salts in specific concentrations changed the morphology to a structure with loosely packed spherulites. In some cases a thick top-layer with densely packed spherulites was observed. In other cases a similar type of morphology as for a (salt free) 32 wt% membrane was observed with a thin top-layer.

Permporometry and liquid displacement

Results of permporometry measurements are shown in figure 1. The largest pores which started to open were around 40 nm (pore radius). This value is in agreement with the bubble point values obtained with the Coulter porometer. In figure 1 the cumulative oxygen flux is plotted against the pore radius. The pore size distribution (number of pores) can be calculated assuming Knudsen diffusion, with a top-layer thickness of 0.2 μm and tortuosity value of 1.)

The contribution to the theoretical pure water flux (figure 1d.) is calculated with the Poisseuille equation. The cumulative total water flux for this membrane was calculated to be 4.5 L/(m^2.bar.h), which is one order of magnitude too low. During the permporometry measurements the driving force for oxygen permeation was not accurately defined. From the theoretical pure water flux calculations with the Poisseuille equation it is clearly shown that a relatively low number of larger pores mainly determined the flux.

The pore size distribution for this membrane can also be compared with the liquid displacement method. The results are shown in the figure 2. Both the results of permporometry and liquid displacement showed bimodal pore size distributions, with a few pores in between 15 and 50 nm and a larger number of pores smaller than 10 nm.

Permporometry is suitable for pore size characterization in the pore range with radii

of 2 - 50 nm. On the other hand, the Coulter measurements can only be carried out when the pores in the membranes are larger than 60 nm diameter; measuring in the upper limit of the apparatus (up to 12 bars) lowers the reliability of the measurements. The permporometry method, however, is a time consuming method compared to Coulter porometry.

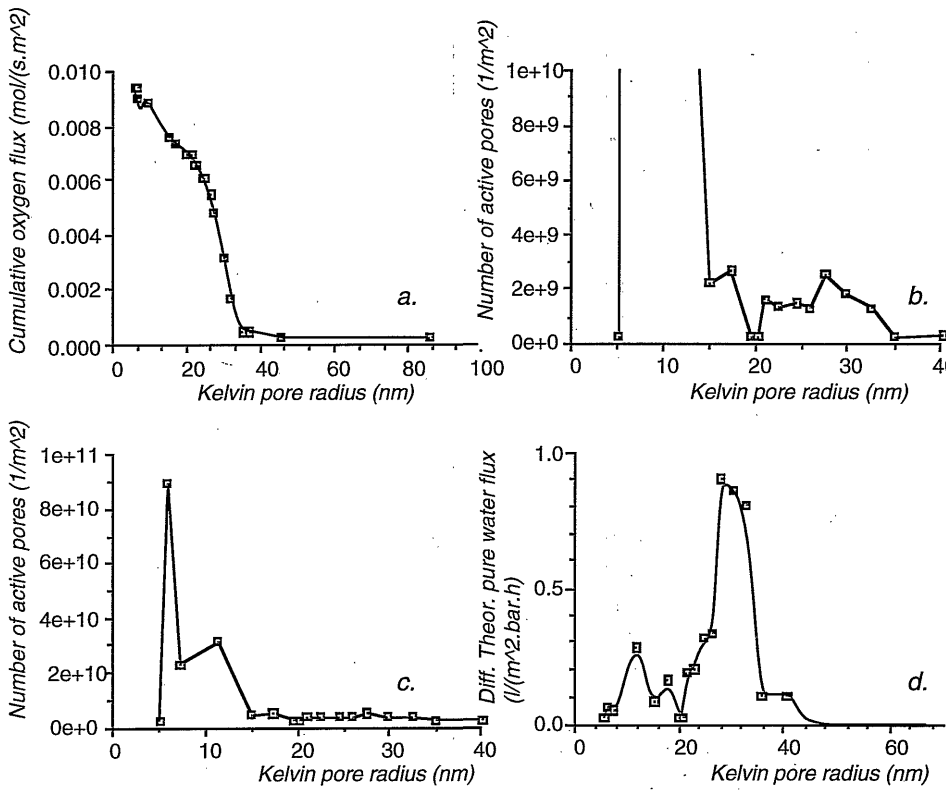

Figure 1. Pore size distribution measured with permporometry for a 32 wt% membrane cast with 0.74 wt% LiCl in the solution; (a) cumulative oxygen permeation (b and c) number distributions (note different scale at ordinate) and (d) theoretical pure water flux contribution as a function of the pore radius.

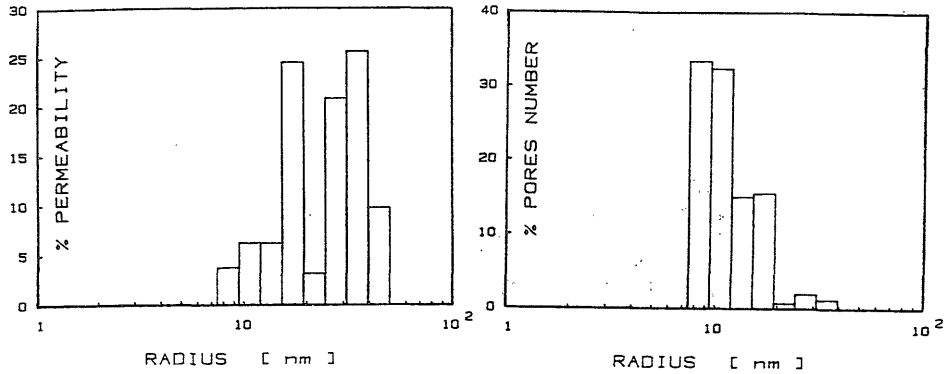

a. *b.*

Figure 2. Pore size distribution measured with the liquid displacement method for a 32 wt% membrane cast with 0.74 wt% LiCl in the solution. Differential liquid permeation (a) and pore number distribution (b) are plotted against pore radius.

The structure of this membrane is shown in figure 3. The cross-section shows a structure composed of axialites. The top-surface shows a spherulitic structure that seems to be much more open than is found by the experiments described above. It can be deduced (figure 3a.) that the densest layer lies underneath the first layer of spherulites.

The effect of inorganic salts

The pure water flux of the membranes prepared from a casting solution of 30 or 32 wt% of nylon 4,6 with increasing LiCl and NaCl content is shown in figure 4. The maximum pore sizes, measured with Coulter porometry, are given in brackets. A large decrease in pure water flux was observed upon increasing the salt concentration up to 2-3 wt% of salt. SEM photographs of the membranes showed a very densely packed thick top-layer (10 μm) with relatively large spherulites in the sub-layer for relatively large salt concentrations. Membranes with a lower amount of salt showed an axialitic structure. Especially the membranes with NaCl had a top- surface of composed very small spheres.

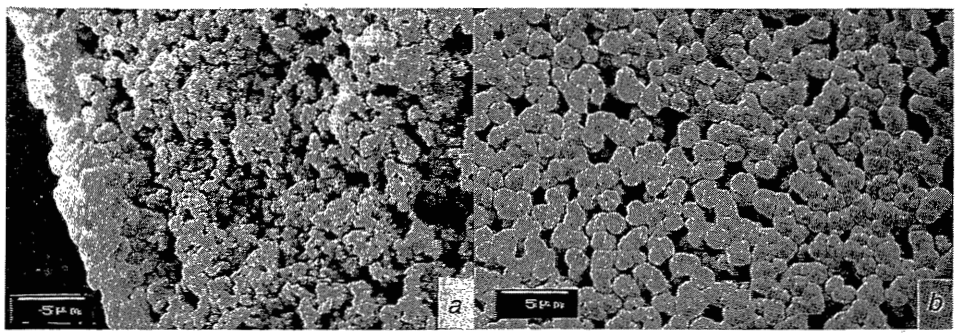

Figure 3. SEM photograph of the cross-section (a) and top-surface (b) of a 32 wt% membrane cast with 0.74 wt% LiCl in the solution.

The membrane prepared from a solution containing 32 wt% of polymer and 0.7wt% of LiCl showed the smallest pores (0.08µm diameter), as measured with permporometry and liquid displacement. It is in fact a membrane in the upper ultrafiltration (UF) or the lower microfiltration (MF) range.
The membranes with fluxes smaller than 10 L/(m^2.bar.h) are not of interest for practical applications. They have a very thick top-layer with a very low number of pores. A typical morphology is shown in figure 8.

A comparison of these (quasi) quaternary systems with the ternary systems without salts shows that the permeability can be improved when salts are added (table 1). For the series prepared from a solution containing 32 wt% of nylon 4,6 three types of morphology can be distinguished (see figure 5). The experimental data using salts as additives in the casting solution are given in table 1. The improved performance in terms of permeability is explained by an increase in porosity. A better packing of the smaller spheres was responsible for this increase as can be observed in figure 6 where 0.8 wt% of NaCl was added to the casting solution.
An overview of the experimental data with various salts used as additives is given in table 2. Upon addition of low concentrations of these salts the pore size was changed and the surface porosity was improved. Higher concentration of LiCl caused a change in morphology to structure III. Addition of $CaCl_2$ gave membranes of a type III morphology only, which were not useful for any practical application. A

top-layer thickness of approximately 10 µm is characteristic for the type III morphology. The membranes cast with magnesium chloride showed a thin top-layer with one layer of spheres. The pore size of these membranes was too small to be determined with Coulter porometry.

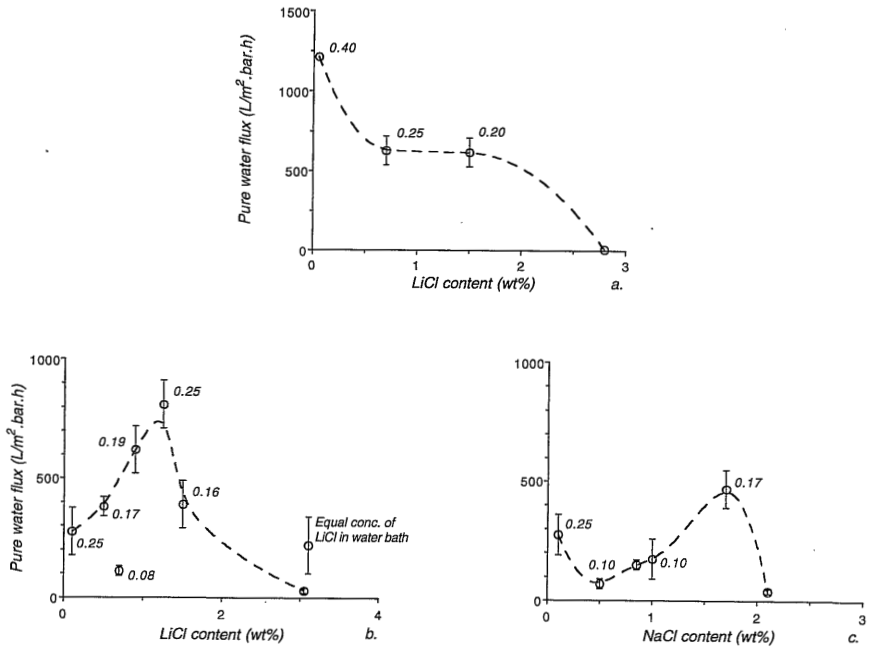

Figure 4. The pure water flux of membranes cast with increasing concentrations of LiCl and NaCl in the solution: (a) LiCl in a 30 wt% solution, (b) LiCl in a 32 wt% solution and (c) NaCl in a 32 wt% solution. The maximum pore sizes measured by Coulter porometry are given as well.

The results of the series cast with nylon 4,6 solutions containing 30 wt% of polymer and various salts are summarized in table 3. The membranes cast from a 30 wt% nylon solution without salt showed an axialitic morphology, schematically given by a structure in between I and II. Addition of different salts resulted in the formation of various membrane structures. The types of morphology are shown in the figures 5 to 8. Examples of a I-type morphology are given in figure 6, of a II-type morphology in figure 7 and of a III type morphology in figure 8.

Table 1 Membranes with and without salts in the casting solution.

polymer conc (wt%)	salt conc (wt%)	flux (L/(m^2.bar.h)	maximum pore size (μm)
32	0	300	0.25
32	1.48 (LiCl)	800	0.25
32	1.63 (NaCl)	500	0.17

Addition of both LiCl and NaCl to the casting solution showed similar effects for both the 30wt% and the 32wt% series. A small amount of salt did not change the morphology. It only resulted in a change in characteristic pore size and consequently in flux. An increase in salt concentration (1.5 wt%) changed the morphology to a spherulitic structure. The top-surface is constructed of irregularly packed spheres.
The effect with KCl was different. While fluxes remained high, the pore size was smaller indicating that the membranes were more porous. In this case the membrane with higher concentrations of salt showed a type I structure, whereas the lower concentrations (1 wt%) showed structure II.
LiBr showed similar effects as shown for LiCl and NaCl. Without addition of salt to the casting solution a type I/II was obtained, that changed to a clear type II morphology for the lower salt concentration (1.1wt%). At higher salt concentration (2.2 wt%) again the type I morphology was observed. Spherulites in the sub- and top-layer were larger (2μm) and more distinctively formed than for KCl.
Membranes cast with $MgCl_2.6H_2O$, $CaCl_2$ and $FeCl_3$ had very thick top-layers. The

membranes with the lowest concentrations had irregularly formed sub-layers, those with the highest concentrations had distinct relatively large spherulites (see e.g. figure 7).

In general, addition of salts showed more pronounced changes of morphology for the membranes cast from a 30 wt% polymer solution compared to those cast from a 32 wt% polymer solution.

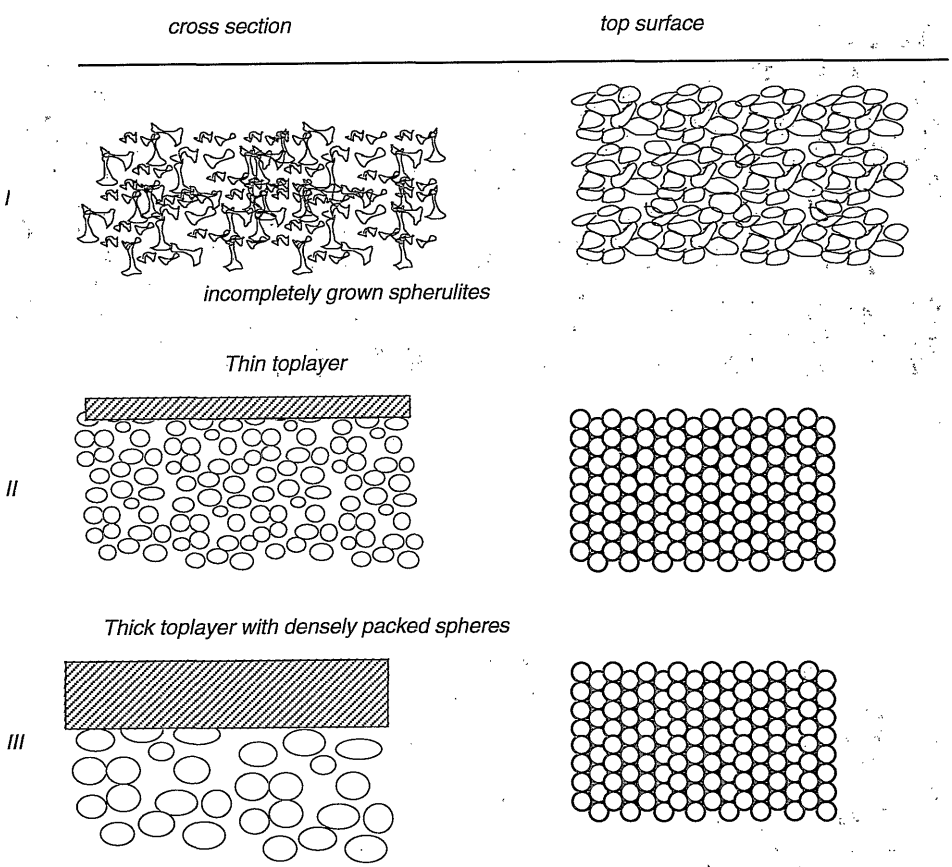

Figure 5. Schematic representation of the three types of morphology for the membranes cast from 32 wt% and 30 wt% polymer solutions when metal halides were added to the casting solutions.

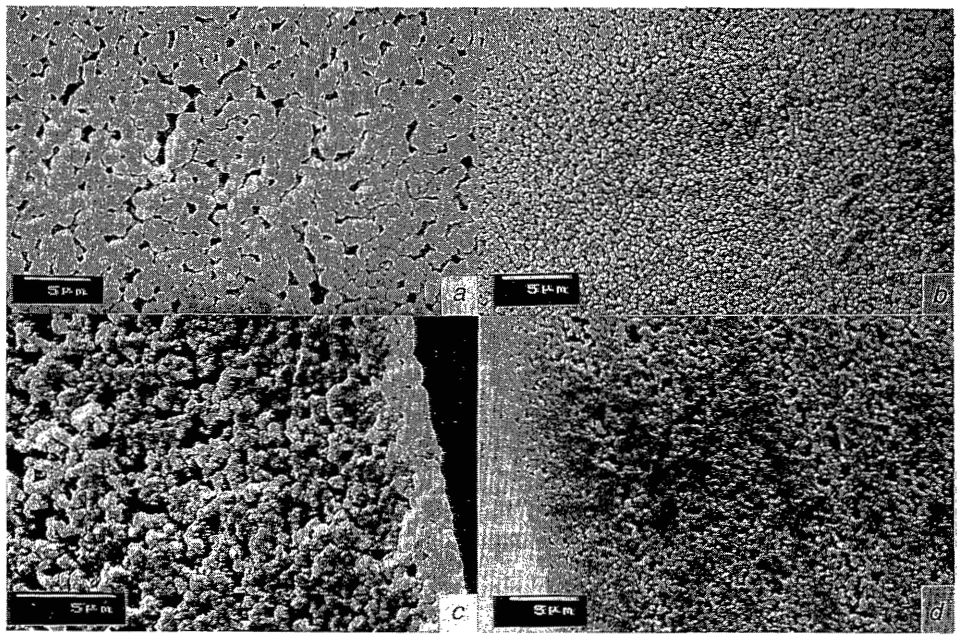

Figure 6. SEM photographs of the top-surface(a and b) and of the cross-section (c and d) of membranes prepared from a 32 wt% nylon 4,6 solution: a. and c. without addition of salt to the casting solution and b. and d. with 0.8 wt% of NaCl. Both are examples of the I type morphology shown in figure 5.

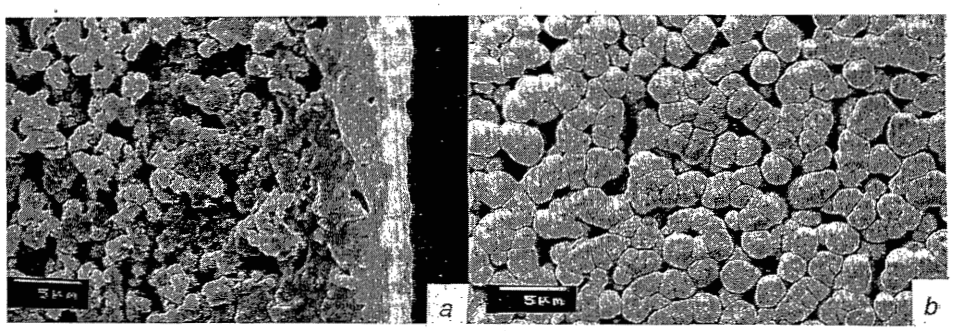

Figure 7. SEM photographs of the cross-section (a) and top-surface (b) of a 30 wt% nylon 4,6 membrane, cast with 1.53 wt% NaCl in the solution. This is an example of the type II morphology.

Table 2. Water flux, pore size and type of morphology for different types and concentrations (in wt%) of salts added to the casting solution containing 32 wt% of nylon 4,6 (the values in brackets in the second column give the ratio of the number of moles of the salt to the number of moles of amide groups in the polymer).

salt	concentration (wt%--ratio)	flux (L/(m^2.bar.h)	max. pore size (μm)	morphology (see figure 5)
-	0	300±80	0.25	I (figure 6)
LiCl	0.74 (0.055)	90±10	0.08	I
	1.48 (0.110)	800±80	0.25	I
NaCl	0.81 (0.044)	130±10	0.10	I (figure 6)
	1.63 (0.088)	450±80	0.17	I
KCl	1.06 (0.045)	515±70	0.16	I
	2.07 (0.088)	410±10	0.16	I
LiBr	1.13 (0.044)	180±30	0.12	I
	2.26 (0.088)	420±80	0.30	III
$MgCl_2$	3.98 (0.062)	430±150	0.23	I
$.6H_20$	7.96 (0.124)	40±10	-	I
$CaCl_2$	1.57 (0.045)	350±80	0.23	III
	3.98 (0.113)	25±10	-	III

Table 3. Water flux, pore size and type of morphology for different types and concentrations (in wt%) of salts added to the casting solution containing 30 wt% of nylon 4,6 (the values in between brackets in the second column give the ratio of the number of moles of the salt to the number of moles of amide groups in the polymer).

salt	concentration (wt%--ratio)	flux ($L/(m^2.bar.h)$)	max. pore size (µm)	morphology (see figure 5)
-	0	1250	0.51	HI
LiCl	0.56 (0.045)	680±100	0.20	I
	1.48 (0.118)	650±100	0.24	II
NaCl	0.76 (0.044)	990±10	0.25	I
	1.53 (0.088)	500±80	0.20	II (figure 7)
KCl	1.06 (0.044)	1000±100	0.34	II
	2.07 (0.088)	1000±10	0.26	I
LiBr	1.13 (0.044)	430±150	0.40	I
	2.26 (0.088)	430±80	0.30	II
$MgCl_2$	3.53 (0.059)	270±100	0.22	IHII
$.6H_20$	7.07 (0.117)	30±15	-	III
$CaCl_2$	1.41 (0.043)	600±300	0.10-0.20	III
	2.97 (0.090)	-	0.11	III
$FeCl_3$	2.17 (0.045)	620±100	0.21	III (figure 8)
	4.34 (0.090)	30±20	0.09	III (figure 8)

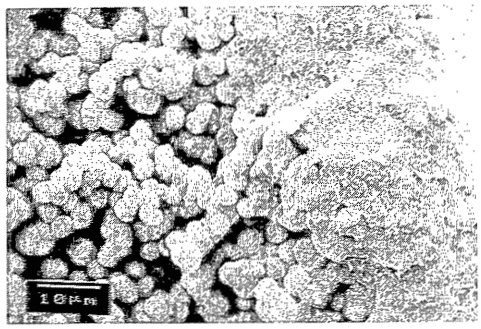

Figure 8. Cross-section of a 30 wt% membrane cast with 2.97 wt% of $FeCl_3$ in the solution. This morphology is an example of the III-type morphology shown in figure 5.

Ultrafiltration membranes and support layers

Favorable support layers for composite membranes have a maximum surface porosity and a narrow pore size distribution without large pores (larger than 100 nm). The top-layer should exhibit a morphology that is easily wetted by the coating solution. The thickness of the top-layer must be kept small in order to avoid a high resistance of the support.

The type I morphology (see figure 5) seems the most promising structure in this respect.

The membranes cast from a 32 wt% polymer solution with addition of LiCl and NaCl (concentration smaller than 1 wt%) seem to have the desired properties (see figure 4), with a top-surface as shown in figure 6b. The layers below the first layer of spheres are rather dense in some cases. This densification of the structure is undesired and adds to the overall resistance for transport. It is therefore more difficult to have the membrane coated. Although the results obtained seem promising for the development of support layers, the top-layer morphology (thickness, porosity and pore size distribution) must still be improved.

Type II morphology can be favorable if the layer of spheres is well packed, if the spheres are smaller than 200 nm and the top-layer thickness less than 2 layers of

spheres (about 0.4μm). The loosely packed larger spheres in the sub-layer will probably not contribute to the overall resistance of the membrane. Such structures have not been prepared so far.
It can be further concluded that the membranes of type III morphology (figure 5) are undesired. Large spheres at the surface result in the creation of large voids which are difficult to cover with a coating layer. In addition the thick top-layer contributes to a large overall resistance towards permeation.
Only a few ultrafiltration (UF) membranes could be prepared, with pore sizes in the upper UF-range. Especially for UF membranes a well defined fine top-layer is essential. Considering the morphology shown in figure 6b it is clear that the relatively large 'units' formed during crystallization hinder the formation of a well defined structure of the top-layer. It is obvious that crystallization should be controlled during the formation of UF membranes. Addition of salts showed that a finer morphology could be obtained (see figure 6). Permporometry experiments were carried out in a liquid-vapor atmosphere of cyclohexane. We have not observed any problems with respect to chemical resistance against this liquid during 5 days of measurement, indicating that excellent performance of nylon 4,6 membranes can be expected.

Mechanism and crystallization effects

Crystallization during the membrane formation process in a (quasi) ternary system can consistently be described by the process of spherulite formation[1]. The lower the polymer concentration the larger the spherulites, since nucleation density has decreased. From a certain polymer concentration (larger than 30 wt%) the nucleation density is so high that the growth of spherulites is hindered. The membrane morphology then consists of axialites. The mechanism involved in these type of membrane formation process can be influenced by the addition of salts. The morphology can be changed from axialitic to spherulitic and vice versa. Thick densely packed top-layers can be formed upon addition of salt with a certain concentration. Addition of small quantities of salt to the casting solutions resulted in relatively large changes in membrane morphology. The alkali halides added to the casting solution did not result in the formation of thick top-layers, except for higher

concentrations of LiCl, whereas the multivalent salts showed a very pronounced effect with respect to the formation of thick top-layers.

The membrane formation mechanism can be influenced by the addition of salts to the casting solution in several ways:
1. Thermodynamic effects. The location of the crystallization line and the binodal is altered by the addition of the fourth component. The interactions between the various components are changed, in particular by the charge effect of the metal halide towards the three components, polyamide, formic acid and water.
2. Kinetic effects. Firstly, the altered interactions will influence the diffusion coefficients of the three components, especially the conformation of the polymer molecules in the solvent is affected by changes in mutual interaction. Secondly, the addition of certain salts, such as calciumchloride, are known to significantly change the crystallization kinetics.
These effects are very complex and difficult to investigate, without even knowing what factors determine the phase inversion behavior of the ternary system.

ACKNOWLEDGEMENTS

The authors wish to thank D.S.M. the Netherlands for financial support. Our gratitude is also expressed to the numerous second year students for their practical assistance and their skills to discuss the work.

REFERENCES

1. A.M.W. Bulte, B. Folkers, M.H.V. Mulder, C.A. Smolders, *Membranes of the Semi-Crystalline Aliphatic Polyamide Nylon 4,6: Formation by Diffusion Induced Phase Separation*, *J. Appl. Polym. Sci.*, 50, 13 - 26 (1993), Chapter 2 of this thesis.
2. H. Steadly, A.J. Laccetti, *US Patent* 4770777 (Parker Hannifin) (1988).
3. H. Steadly, Th. Morgan, *WO Patent* 88 / 05686 (Parker Hannifin) (1988).
4. B. Valenti, E. Bianchi, G. Greppi, A. Tealdi, A. Ciferri, *J. Phys. Chem.*, 77, 389 (1973).
5. B. Valenti, E. Bianchi, A. Tealdi, S. Russo, A. Ciferri, *Macromolecules*, 9, 117 (1976).
6. Ch. Eyraud, M. Betemps, J. Quinson, *Bull. Soc. Chim. France*, 9-10, I-238 (1984).
   A. Mey-Marom, M. Katz, *J. Membr. Sci.*, 27, 119 (1986).
7. F.P.Cuperus, D. Bargeman, C.A. Smolders, *J. Membr. Sci.*, 71, 57 (1992).

3rd Appendix to CHAPTER 2

Membrane Formation with Nylon 4,6; Membranes from Salt / Alcohol Solutions

A.M.W. Bulte, B. Folkers, M.H.V. Mulder,
C.A. Smolders, H. Strathmann

INTRODUCTION

It is generally known that ethanol or methanol in combination with calcium chloride can be used as solvent systems for nylons. These salts are believed to break the strong hydrogen bonds in the polymeric crystals. Only a few publications on these systems are known. Recently the formation of polyamide membranes from alcohol / salt solutions with a variety of non-solvent systems, such as water, acetone, dimethyl formamide (DMF), methylethyl ketone (MEK) and isopropylalcohol was reported by Dennison et al.[1]. Nylon 6,6, nylon 6 and blends of the two polymers were used for membrane preparation. Besides calciumchloride, also calciumnitrate, calcium salicylate and lithium chloride were used as salts. Alcohol / salt solvent systems in stead of formic acid as a solvent have environmental advantages for the preparation of nylon membranes on a large scale. The use of alcohols also enlarges the number of membrane forming parameters[2]. In this appendix the use of methanol and ethanol in combination with calciumchloride as a solvent system for nylon 4,6 is described very briefly. For the membrane preparation different non-solvents were used.

EXPERIMENTAL

Nylon 4,6 (Stanyl KS 400, DSM) was dried *in vacuo* for 24 hours at 70°C and dissolved in methanol with calciumchloride or in ethanol with calciumchloride at 60 and 80 °C respectively under reflux overnight. Thin films were cast on a glass plate

at room temperature and immersed in non-solvent baths containing water, hexane, acetone, propanol, butanol, pentanol or octanol.
The morphology of the membranes was studied with scanning electron microscopy (SEM), Coulter® porometry and gas permeability; the experimental details of these methods have been described in chapter 2.

RESULTS

An overview of the morphology of the membranes prepared is given in the tables 1 and 2 and in the figures 1,2 and 3. Coagulation in water resulted in very brittle films with spherulitic structures. With acetone and hexane as non-solvents porous membranes which were not obtained. After washing with water a porous structure was formed. The films coagulated in acetone and hexane probably still contained the calciumchloride. The films remained transparent; only after washing with water, a white phase separated film was obtained (see figure 1b and 3b).
When ethanol was used in the solvent system, propanol and butanol probably did not act as non-solvents. For the methanol system these chemicals were non-solvents inducing a morphology that resulted from solid - liquid (S - L) demixing. Pentanol and octanol are non-solvents inducing liquid - liquid (L - L) demixing from the very delayed type, resulting in the presence of macrovoids. In the series water, propanol, butanol the nylon showed the tendency towards crystallization of the polymer with methanol as a solvent. Only small samples were prepared and studied on their morphology.

DISCUSSION AND CONCLUSIONS

The use of some coagulants, such as hexane, acetone, propanol and butanol, as a first step in the coagulation process with water as a second step may lead to structures with a very open sub-layer (see e.g. 1.a and b). The membranes were not tested for their performance. Membranes with good properties were obtained with octanol as a non-solvent.

Table 1. Morphology of membranes cast from a methanol / calcium chloride solution prepared at 60°C. S-L stands for a structure formed by crystallization and L-L stands for a cellular morphology.

Polymer concentration (wt%)	$CaCl_2$ concentration (wt%)	Non-solvent	Morphology/Performance
9.1	18.2	water	S-L; very brittle
16.7	16.7	water	S-L; very brittle
		hexane	L-L; and dense
		-after washing with water	larger pores
		acetone	dense, transparent
		-after washing with water	porous, L-L
		propanol	S-L; brittle, spheres 3 - 5 micrometer
		butanol	S-L; presence of threads; spheres 1 - 5 „ MF pores
		pentanol	irregular; cells/spheres
		octanol	dense layer with spheres and macrovoids

Since these membrane forming systems are very complicated with respect to the thermodynamics and kinetics of membrane formation, these systems were not further studied. The influence of the presence of salt (a quaternary system) and the elevated temperature necessary for the solvent systems makes these systems too complicated for fundamental investigations at this stage of knowledge.

Table 2. Morphology of membranes cast from a ethanol / calcium chloride solution prepared at 80°C. S-L stands for a structure formed by crystallization and L-L stands for a cellular morphology.

Polymer concentration (wt%)	$CaCl_2$ concentration (wt%)	non-solvent	Morphology/Performance
7.1	14.2	water	S-L; very brittle
13.3	13.3	water	S-L;
		hexane	L-L; transparent - dense
		-dried in vacuo at 80 °C	,,
		-rinsed with water	large pores in sublayer
		acetone	L-L; with macrovoids
		-dried in vacuo	changing in time
		-rinsed with water	large pores in sublayer
		1-propanol	transparent, dense
		1-butanol	L-L; irregular, dense
		1-pentanol	irregular; brittle
		1-octanol	L-L; macrovoids, top: crystallites P: 6 - 9 L/cm^2/min at 8 bar MF pores (0.35 micrometer)

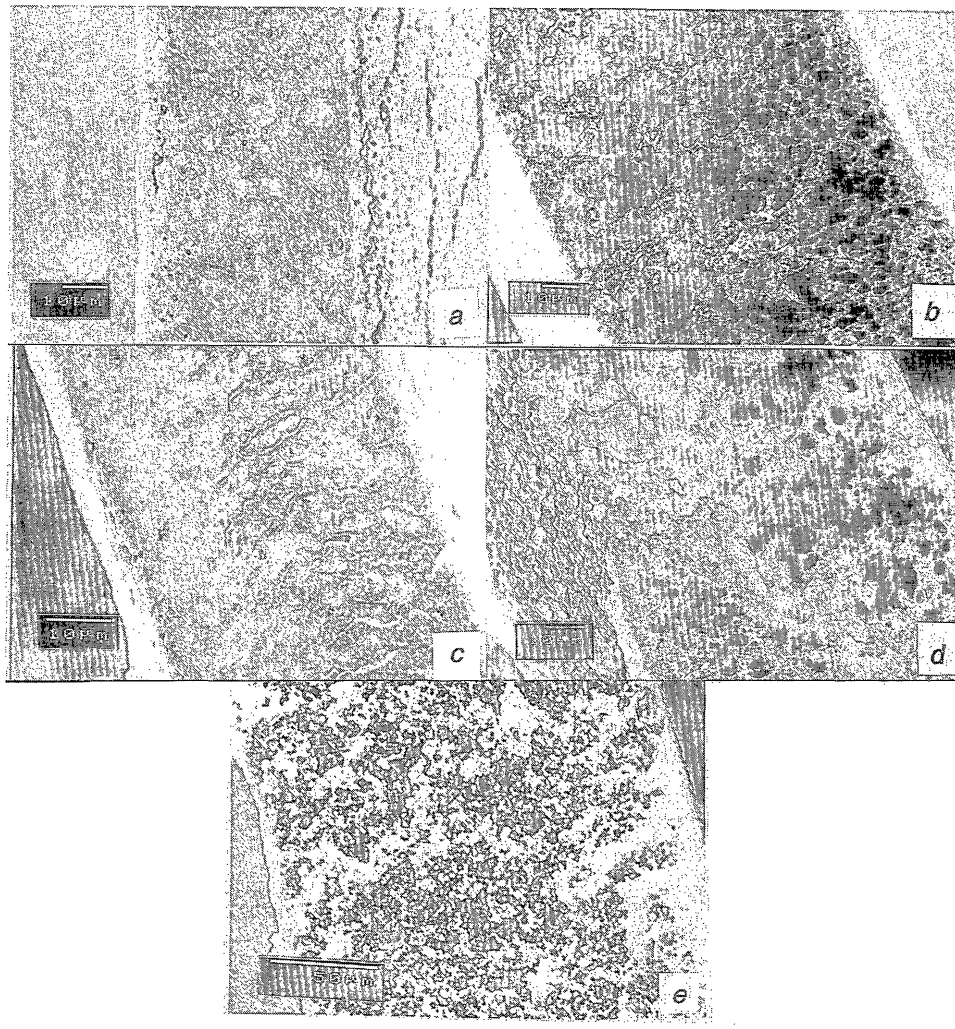

Figure 1. SEM photographs of the membranes cast from methanol and calciumchloride: (a) coagulated in hexane; the influence of rinsing with water is shown in (b); (c) coagulated in acetone; the influence of rinsing with water is shown in (d); (e) coagulated in water.

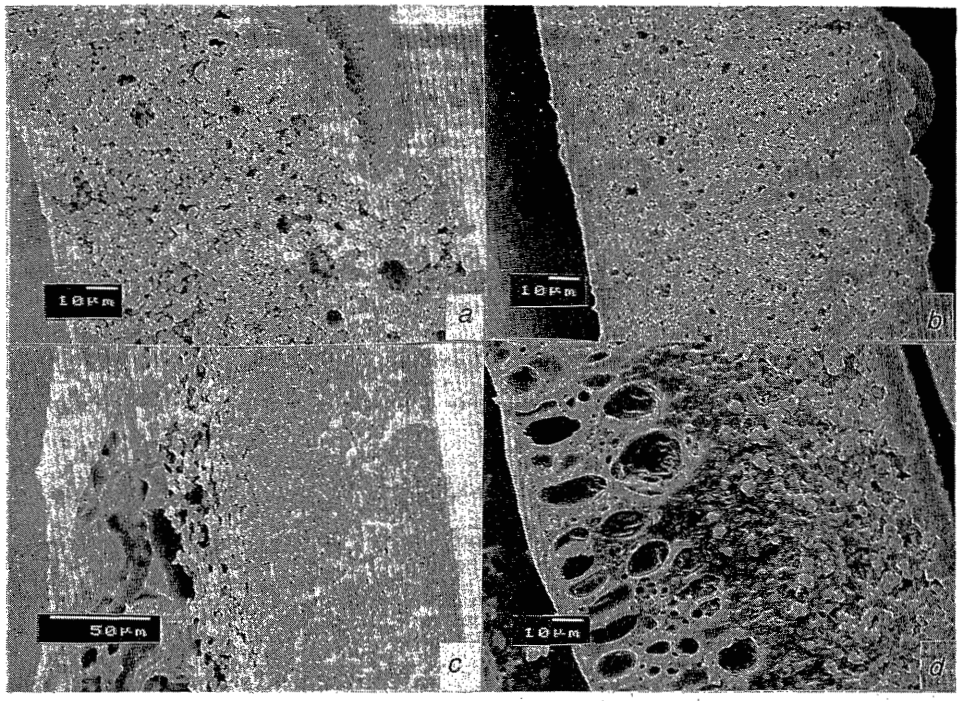

Figure 2. SEM photographs of the membranes cast from methanol and calciumchloride and coagulated in (a) propanol, (b) butanol, (c) pentanol and (d) octanol.

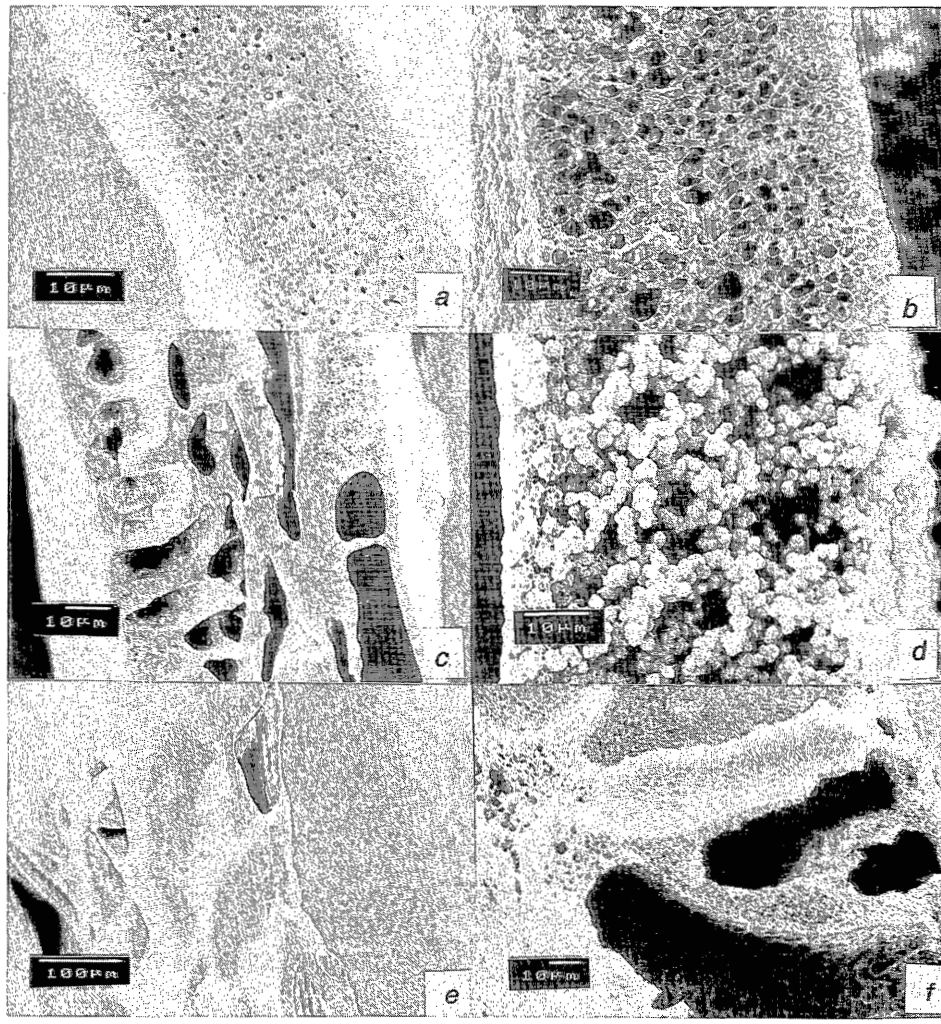

Figure 3. SEM photographs of the membranes cast from ethanol and calciumchloride: (a) coagulated in hexane; the influence of rinsing with water is shown in (b); (c) coagulated in acetone, (d) water, (e) pentanol and (f) octanol.

ACKNOWLEDGEMENTS

The authors wish to thank D.S.M. the Netherlands for financial support.

REFERENCES

1. K.A. Dennison, B.E. Kolcinski, S. Krishnan, P.M. Rusell, *US patent* 5006247 (1991).

2. M.H.V. Mulder, *Onderzoek aan nylon 6 membranen*, internal report University of Twente (1976).

CHAPTER 3

Equilibrium Thermodynamics of the Ternary Membrane Forming System Nylon, Formic Acid and Water

A.M.W. Bulte, E.M Naafs, F. van Eeten, M.H.V. Mulder, C.A. Smolders, H. Strathmann

SYNOPSIS

The binary Flory-Huggins interaction parameters for the ternary membrane forming system nylon 4,6, formic acid and water have been determined from literature data, swelling values and melting point depression. Nylon 4,6, nylon 6 and a copolymer of nylon 4,6 and 6 were examined. The isothermal crystallization boundaries were determined experimentally and the binodal miscibility gap was calculated for these ternary systems. It was found that the crystalline state is the thermodynamically favorable state for each system. Experimental data and calculated phase diagrams were discussed in relation to membrane formation. Though thermodynamic properties of the system dictate the phase separation that can take place, kinetic parameters are of equal significance with respect to membrane formation.

INTRODUCTION

Membrane preparation by means of phase inversion is widely used today both on a laboratory scale and in industry[1]. The concept of phase inversion covers a range of different techniques from which immersion precipitation is the most important one. Here, a thin film of a concentrated solution consisting of a polymer and a solvent is cast on a support. The film is immersed in a non-solvent, which is miscible with the solvent. As a result the non-solvent diffuses into the film and the solvent diffuses out of the film; i.e. a diffusion induced phase separation (DIPS) process takes place. Phase separation may take place if thermodynamic conditions allow a homogeneous

film to demix into two or more phases. Knowledge of the thermodynamic properties of such a ternary system is very important for understanding and predicting membrane formation.
Nylon 4,6 is a semi-crystalline polymer, that has been used as a polymer for membrane preparation. It has been shown that two different phase separation processes were competitive during membrane formation: solid - liquid (S-L) demixing and liquid - liquid (L-L) demixing[2]. Solid - liquid demixing or crystallization leads to membranes with a spherulitic or axialitic morphology. The typical cellular morphology has been observed for liquid - liquid demixing. Other aliphatic polyamides, such as nylon 6, nylon 6,6, nylon 6,10 and nylon 11 are used as membrane materials as well. The preparation and use of these membranes have been described in a number of patents[3-5].

Solid - liquid demixing or crystallization of the polymer in a ternary system can take place because the melting temperature of the pure polymer is depressed by the presence of the two low molecular weight components. Melting point depression of the polymer, leading to isothermal crystallization, can be described with the Flory Huggins theory[6]. Crystallization or solid - liquid demixing results in two separated phases in equilibrium; one phase is the pure crystalline polymer and the other is a more diluted polymer solution. Flory[6] has worked out phase diagrams with experimental data of the melting point depression or dissolution curves (liquidus) for a number of binary systems, deriving the binary interaction parameters for polymer - diluent. It has been shown that the binary melting point depression curve becomes more asymmetric with an increasing difference between molar volume of the low and the high molecular weight component[7-9]. With knowledge of the interaction parameters in a system in which melting point depression occurs, the crystallization line can be calculated.
Altena[10] and Burghardt[11] have attempted to obtain data for the calculation of the equilibrium boundary between the homogeneous phase and the region showing solid - liquid phase separation for (ternary) membrane forming systems. Binary and ternary crystallization curves can be derived if Flory-Huggins interaction parameters for all the components are available.
In liquid - liquid phase separation an equilibrium between two liquid phases exists. In membrane forming systems, in which one polymer is present, the two phases are a polymer rich and a polymer lean phase. The homogeneous region and the miscibility

gap are defined by a binodal curve. Knowledge of the binary Flory-Huggins interaction parameters allows to calculate this binodal as shown by Flory[6,12] and later by Altena[13], Wijmans[14], Reuvers[15] and Boom[16] from our laboratory.
Both solid - liquid and liquid - liquid phase separation can occur in binary and ternary systems. This is clearly shown by Burghardt[17] for a binary situation.
From phenomenological data on membrane formation it has been concluded that for the ternary system nylon 4,6, formic acid and water both solid - liquid demixing and liquid - liquid demixing occurs[2]. A hypothesis was formulated suggesting crystallization being the thermodynamically favorable process. Detailed knowledge about the location of the crystallization line, however, is necessary in order to obtain further insight in the membrane formation of aliphatic polyamides. In order to obtain a better understanding of the influence of the location of the crystallization line on membrane formation, the thermodynamics of nylon 4,6 will be compared with other nylon types.
The aim of this paper is to find a thermodynamic description for three membrane forming systems: nylon 4,6, nylon 6 and a copolymer of the two with 5% of nylon 6 units incorporated, with formic acid as a solvent and water as a non-solvent.

THEORY

Construction of a phase diagram with solid - liquid and liquid - liquid demixing

For a binary system phase diagrams can be derived by plotting the free enthalpy as a function of the volume fraction (see figure 1)[6,17]. In the figures on the left hand side the free enthalpy of the mixture is given as a function of the polymer volume fraction. Polymer solutions with a polymer volume fraction between $\phi\alpha$ and $\phi\beta$ can lower their free enthalpy at a temperature T_1 by phase separation into the liquid phases $\phi\alpha$ and $\phi\beta$; the corresponding miscibility gap (liquid - liquid phase separation) is located as is indicated in figure 1b, where the L-L region and the homogeneous region are given as a function of temperature. At lower temperatures $\phi\beta$ shifts to larger polymer fractions and the miscibility gap becomes larger.

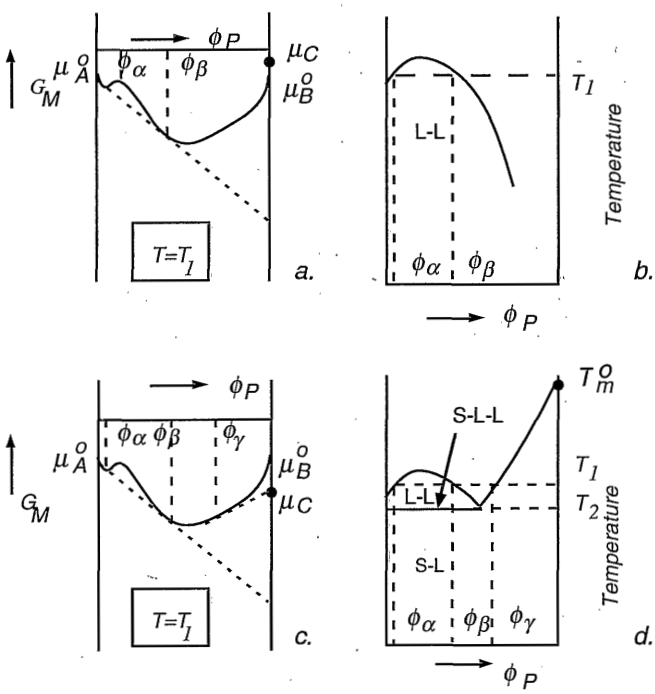

Figure 1. Free enthalpy of the mixture (G_M in J per mole) diagrams as a function of the polymer volume fraction ϕ_P (figures a and c). The binary phase diagrams are schematically given for two different situations: b) liquid - liquid (L-L) demixing (no crystallization occurs), and d) liquid - liquid (L-L) demixing and solid - liquid (S-L) demixing. $\mu_A{}^0$ and $\mu_B{}^0$ are the chemical potentials of the pure state at constant pressure and temperature of the low molecular weight component, A, and the polymer, B, respectively. μ_C is the chemical potential of the crystalline state at a temperature below the melting temperature of the pure polymer. At the melting temperature of the pure polymer ($T_m{}^0$) $\mu_C = \mu_B{}^0$.

The chemical potential of the crystalline phase is represented by a point on the polymer ordinate (μ_C). The location of this point is depends on the choice of polymer and the temperature. When this point is located beneath the molar free enthalpy of the pure liquid polymer ($\mu_B{}^o(P,T)$), solutions with a polymer concentration larger than ϕ_γ can lower their free enthalpy by phase separation into a pure crystalline phase and a phase with composition ϕ_γ. The phase diagram can be constructed as shown in figure 1d. When a homogeneous polymer solution is cooled

to a temperature T_1 two types of phase separation processes can occur (see figure 1d). At higher polymer concentrations crystallization or S-L demixing is responsible for phase separation and at lower concentrations phase separation is controlled by the location of the binodal curve leading to L-L demixing.

At one specific temperature (T_2 in figure 1) the chemical potential of the crystal state lies on the tangent line of the compositions $\phi\alpha$ and $\phi\beta$. At this temperature the three phases, the polymer lean phase, the polymer rich phase and the crystalline state are at equilibrium with each other. Thus in binary systems at a certain temperature a three phase equilibrium (L-L-S) exists.

A liquid solution and a solid crystal (S-L) are the phases present at still lower temperatures ($T<T_2$) if only crystallization of the polymer phase is taken into account.

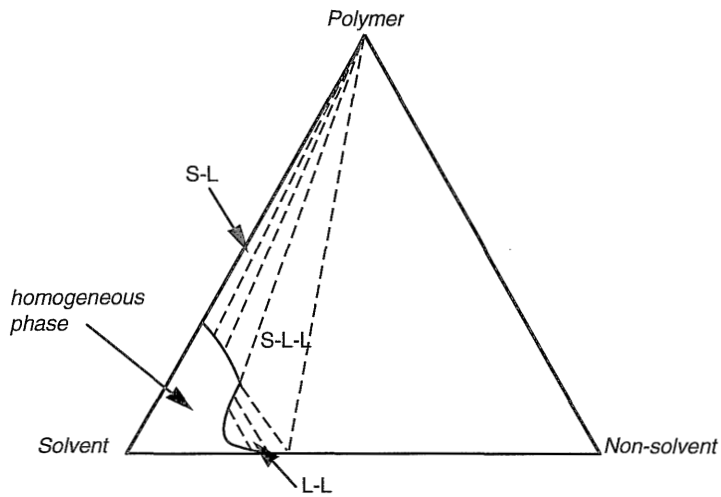

Figure 2. A ternary phase diagram with liquid - liquid demixing and solid - liquid demixing (crystallization of the polymer phase).

A ternary system with a crystallizable polymer

An isothermal three component phase diagram for a polymer (subscript 3), solvent (subscript 2) and a non-solvent (subscript 1) is given in figure 2. At lower polymer concentrations phase separation is controlled by liquid - liquid demixing, whereas at higher concentrations solid - liquid phase separation is involved. The three phase

region (S-L-L) is a plane in a ternary isothermal phase diagram, because there is one degree of freedom additional compared to the binary case. The area on the right hand side near the polymer - non-solvent axis is thermodynamically controlled by solid - liquid phase separation.

Theoretical background of the calculations

The crystallization line

The crystallization line in a phase diagram can be calculated according to theory of melting point depression[6]. At equilibrium between the liquid solution and crystalline polymer, the chemical potentials of the polymer repeating units (μ_u) in both phases must be equal.

$$\mu_u = \mu_u^c \qquad (1)$$

in which μ^c represents the chemical potential of the polymer repeating unit in the crystalline state. The temperature at which this condition is satisfied can be referred to as the melting point T_m, which will depend on the composition of the liquid phase.

The condition of equilibrium between crystalline polymer and the polymer in the solution can be restated as follows:

$$\mu_u - \mu_u^0 = \mu_u^c - \mu_u^0 \qquad (2)$$

In words, the difference between the chemical potential of the crystalline repeating unit and the unit in the standard state, i.e., the pure liquid polymer at the same temperature and pressure, must be equal to the decrease in chemical potential of the polymer unit in the solution relative to the same standard state.

The right hand term is the negative of the free enthalpy of fusion per polymer repeating unit, ΔG_u (the indices u and o stand for the quantities per mole of repeating unit in the polymer and the pure state respectively); with $\Delta H_u / \Delta S_u$ equal to T_m^o the following relation can be obtained:

$$\mu_u^c - \mu_u^0 = -\Delta G_u = -(\Delta H_u - T\Delta S_u) = -\Delta H_u \left(1 - \frac{T}{T_m^o}\right) \qquad (3)$$

where ΔH and ΔS represent the heat and the entropy of fusion respectively.
The left hand term of equation (2) can be obtained from the first derivative of the free enthalpy of mixing with respect to the number of moles of component 3, n_3:

$$\Delta\mu_3 \equiv \left(\frac{\partial \Delta G_m}{\partial n_3}\right)_{P,T,n_j} \qquad (4)$$

with $\Delta\mu_3$ expressed in J per mole of polymer and $\Delta\mu_u$ in J per mole of repeating unit of the polymer.
The free enthalpy of mixing, ΔG_m, for a ternary system can be expressed according to the Flory-Huggins theory.

$$\frac{\Delta G_m}{RT} = n_1 \ln\phi_1 + n_2 \ln\phi_2 + n_3 \ln\phi_3 + g_{12} n_1 \phi_2 + g_{13} n_1 \phi_3 + g_{23} n_2 \phi_3 \qquad (5)$$

The binary interaction parameters g_{ij} are assumed to be concentration dependent.
Rewriting the equations with the ratios of the molar volumes (η) $s = \eta_1/\eta_2$ and $r = \eta_1/\eta_3$ with the indices (1) for non-solvent, (2) for solvent and (3) for polymer and assuming that r -> 0, then according to Altena[10] the following equation can be derived for the melting point depression.

$$\frac{-R}{\Delta H_u}\frac{\eta_u}{\eta_1}\left\{-\phi_1 - s\,\phi_2 + (g_{13}\,\phi_1 + s\,g_{23}\,\phi_2)(\phi_1 + \phi_2) - g_{12}\,\phi_1\,\phi_2 - s\,\phi_2\,v_2\,(1 - v_2)\frac{\delta\, g_{23}}{\delta\, v_2}\right\} - \left(\frac{1}{T_m} - \frac{1}{T_m^0}\right) = 0 \qquad (6)$$

in which η_u is the molar volume per repeating unit in the polymer. It is *assumed* that the binary Flory Huggins parameters g_{ij} are truly binary in ternary and quaternary situations, i.e. that they are only dependent on the components i and j and not on the third component k ($g_{ij} \neq g_{ij}(\phi_k)$; g_{13} is assumed to be constant, since no information about a concentration dependency of a polymer in a non-solvent can be obtained. The interaction parameters are now dependent on the

following composition variables with ϕ_2 and ϕ_3 in the limiting binary cases with components 1-2 and 2-3 only being replaced by u_2 and v_2 respectively for the ternary case:

$$g_{12} = g_{12}(u_2); \quad u_2 = \frac{\phi_2}{(\phi_1 + \phi_2)}$$
$$g_{23} = g_{23}(v_2); \quad v_2 = \frac{\phi_2}{(\phi_2 + \phi_3)} \qquad (7)$$

in which u_2 and v_2 reflect the constant ratio of solvent - non-solvent and the ratio solvent - polymer respectively.

The isothermal crystallization line at a chosen temperature T_m can be calculated if appropriate parameters are selected for ΔH_u and the various interaction parameters g_{ij}, and if $T_m{}^o$ and the molar volumes (η) are known.

The binodal

The approach of Altena[13], Reuvers[15] and Boom[16] will be followed to calculate the liquid - liquid miscibility gap in a ternary system. The chemical potentials for the three components are found by differentiation of equation (5) with respect to n_1, n_2 and n_3, respectively. Liquid - liquid demixing results in phase separation into two liquid phases: a polymer lean phase with $\Delta\mu_i$ of the first phase $(\Delta\mu_i{}^{1st\ phase})$ and a polymer rich phase with $\Delta\mu_i$ of the second phase $(\Delta\mu_i{}^{2nd\ phase})$. At equilibrium the chemical potentials of component i in both phases are equal, their difference being zero. This is approached numerically by minimizing the function F:

$$F = \sum_{i=1}^{3} \left[\frac{\Delta\mu_i^{1st\ phase}}{RT} - \frac{\Delta\mu_i^{2nd\ phase}}{RT} \right]^2 \qquad (8)$$

Evaluation of the interaction parameters

Interaction parameter solvent - non-solvent (g_{12})

The concentration dependent parameter $g_{12}(\phi_2)$ represents the interaction between solvent and non-solvent for this system water (1) and formic acid (2). This parameter can be calculated from literature[18] from the excess free enthalpy of mixing (G^E)

according to equation (9):

$$g_{12}(\phi_2) = \frac{1}{x_1\,\phi_2}\left[\, x_1\, ln\,(\frac{x_1}{\phi_1}) + \; x_2\, ln\,(\frac{x_2}{\phi_2}) + \frac{G^E}{RT}\right]$$

$$G^E = RT \sum_i x_i\, ln\, \gamma_i \qquad (9)$$

in which x_1 and x_2 are the mole fractions, ϕ_1 and ϕ_2 the volume fractions and G^E the excess free enthalpy of mixing and γ_i the acitivity coefficient of component i.
In figure 3 the G^E values are given as a function of the mole fraction of water (1). Strong negative values are obtained over the whole concentration range, indicating that strong interaction forces exist between solvent and non-solvent.

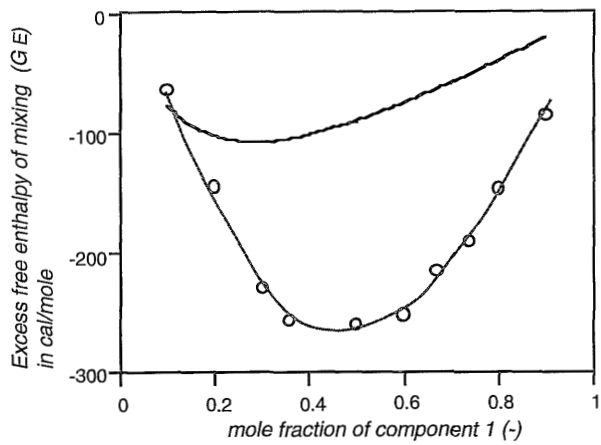

Figure 3. Experimental[18] (points) and theoretical[20] (curve) data for the excess free enthalpy of mixing of formic acid / water mixtures.

Strongly negative values for interaction parameters are not very common. In order to check the validity of the negative values for G^E, excess values were calculated from activity coefficients derived from the Van Laar equation[19], for which appropriate parameters are available[20]. Figure 3 shows data for both the experimental[18] and theoretical[20] excess free enthalpy of mixing. The experimental data were taken form Krasovskii[18] whereas the theoretical data were calculated from the Van Laar

equation with parameters taken from Campbell[19].
The calculated excess free enthalpy of mixing is negative over the whole concentration range, but values are less negative compared to the experimental values. The coefficients used for the calculation of activity coefficient with the Van Laar equation[19] are derived from experimental data for vapor - liquid equilibria. Dimer formation of formic acid molecules in the vapor phase are not taken into account, resulting in a less negative theoretical G^E value.

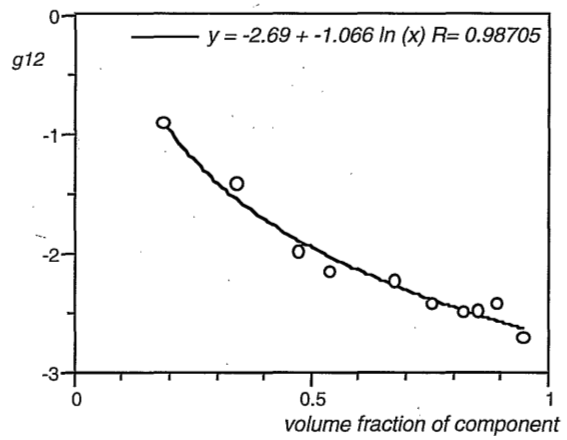

Figure 4. The interaction parameter water - formic acid (g_{12}) as a function of the volume fraction of water.

For our system we use the interaction parameter as has been derived from the experimental values for G^E. In figure 4 the g_{12} interaction parameter derived from these data is given as a function of the volume fraction of water (ϕ_1). The concentration dependency can be described by equation (10) (see also figure 4).

$$g_{12} = -2.69 - 1.066\ ln\ (\phi_1) \qquad 0.2 < \phi_1 < 0.95 \qquad (10)$$

In order to use a binary interaction parameter in a ternary system a composition variable u_2 has been defined (see equation 7); ϕ_1 (or 1- ϕ_2) in equation (10) must then be replaced by (1-u_2).

Interaction parameter non-solvent - polymer (g_{13})

The interaction parameter of non-solvent and polymer can be obtained from the swelling value of the polymer in the non-solvent. At equilibrium swelling conditions the free enthalpy of mixing (ΔG_m) equals zero and g_{13} can be calculated from equation (5) with ϕ_2 is zero. Since it is not possible to determine this parameter as a function of concentration, it is usually taken constant (then also written in literature as χ_{13}). The mass uptake of water in nylon 4,6 films has been determined to be 15 wt%. Since swelling only takes place in the amorphous regions[21] the mass uptake has been corrected for the 50% crystallinity of the polymer samples[22]. An interaction parameter of 1.8 is then calculated. The mass uptake of nylon 6 is 11 wt% at 30% crystallinity. The crystal units in the polymer film can be considered as physical cross-links that will hinder the swelling of the amorphous polymer matrix. Without this hindrance a somewhat higher mass uptake can be expected resulting in lower values for the interaction parameter. For all three nylons a g_{13} value of 1.5 will be used.

$$g_{13} = 1.5 \tag{11}$$

Interaction parameter solvent - polymer (g_{23})

Literature data for the solvent polymer interaction parameter, g_{23}, for the system nylon, formic acid and water are not available. Experimental melting point depression data for the ternary system will be used to fit a g_{23} with equation (6).

Table 1. Physical constants for the studied components

	M (g/mol)	ρ (g/cm^3)	T_m^o (K)	ΔH_u (J/mol r.u.)	η_u (cm^3/mol)
Nylon 4,6	25000#	1.18	623	46000	171
Nylon 4,6*co*6	25000#	1.18	623	46000	171
Nylon 6	25000#	1.14	533	28700	99
Water	18	1.00	-	-	-
Formic Acid	46	1.22	-	-	-

The number average molecular weight, M_n, as reported by the supplier.

The molar volumes (η) of the components are found by taking the the ratio of the molecular weight (M) and the density (ρ). The values for the three components are listed in table 1. $T_m{}^o$ and ΔH_u were taken from literature[20,22]. Isothermal crystallization is calculated at a temperature of 30°C (303 K).

EXPERIMENTAL

Test tubes with mixtures of the three components were prepared and used for laser light transmission in order to determine the cloud point temperatures.

Sample preparation

Nylon 4,6 (Stanyl KS 400), nylon 6 (Ultramid B3) and nylon 4,6 *co* 6 (Stanyl KS 611), kindly supplied by D.S.M. the Netherlands, were dried *in vacuo* for at least 24 hours at 70°C for nylon 4,6 and the copolymer and 30°C for nylon 6 and dissolved in formic acid (Merck analytical grade 98%) with a concentration of 3 to 20 wt% of polymer. Polymer solutions were prepared in erlenmeyers closed with septa. Under continuously stirring demineralized water was added very slowly to the solution at room temperature until the pre-calculated ratio of solvent and non-solvent was reached. Samples were taken from these ternary compositions with a syringe through a septum into glass capillaries, which were frozen in liquid nitrogen, evacuated and sealed. The samples were kept at 8°C until complete demixing occurred (their appearance then was white or opaque). The demixing time varied from several hours to several weeks.

Laser light transmission

Cloud points were measured by using a light transmission technique.
The tubes containing a demixed solution of a certain composition (ϕ_1, ϕ_2 and ϕ_3) were placed in a rotating wheel placed in a thermostated bath at 25°C. The

unit. At the same time the rotating wheel was driven by a small motor at a velocity of 2 rotations per hour. Laser light (He-Ne, 633 nm, 10 mV) passed through the glass capillaries and transmittance was detected and continuously monitored by a recorder. A typical plot obtained from these experiments is given in figure 5. Here a relative peak height of one indicates that there is minimal light transmission through the turbid sample and a relative height of zero indicates that the transmission is maximal, i.e. the solution is completely transparent. The melting temperature is located at the point where the measured line intersects the base line (off-set temperature).

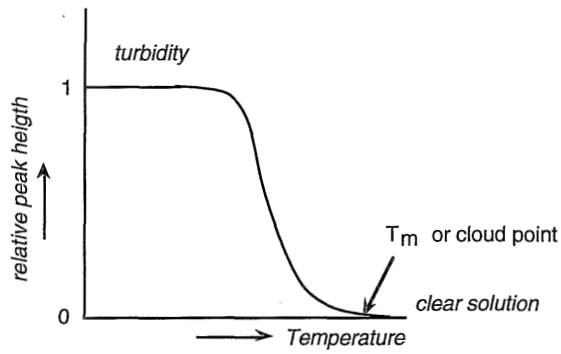

Figure 5. A typical laser light transmission profile.

RESULTS

Cloud point data

The melting temperature of various solutions with varying compositions of the three nylons (from 2-20 vol.% polymer) were determined from cloud point measurements. The measurements were carried out in duplicate with an accuracy of about 2 °C .

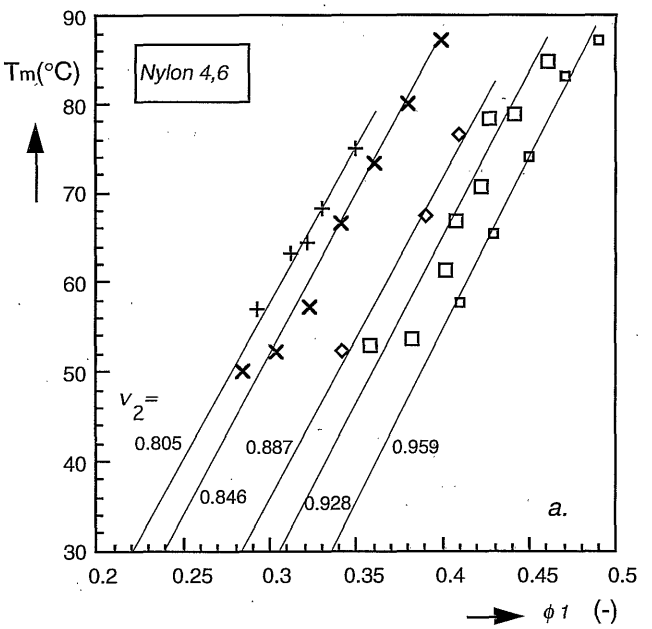
Tm(°C)
Nylon 4,6
90
80
70
60
50
40
30
0.2
0.25
0.3
0.35
0.4
0.45
0.5
$\phi 1$ (-)
v_2=
0.805
0.846
0.887
0.928
0.959
a.

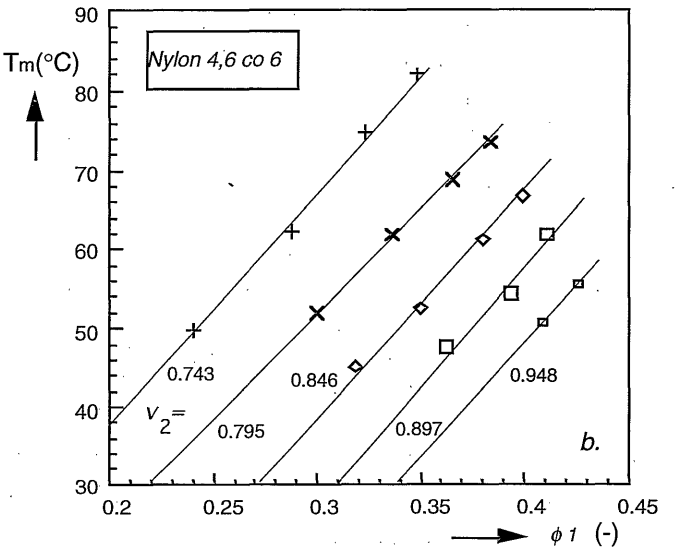
Tm(°C)
Nylon 4,6 co 6
90
80
70
60
50
40
30
0.2
0.25
0.3
0.35
0.4
0.45
$\phi 1$ (-)
v_2=
0.743
0.795
0.846
0.897
0.948
b.

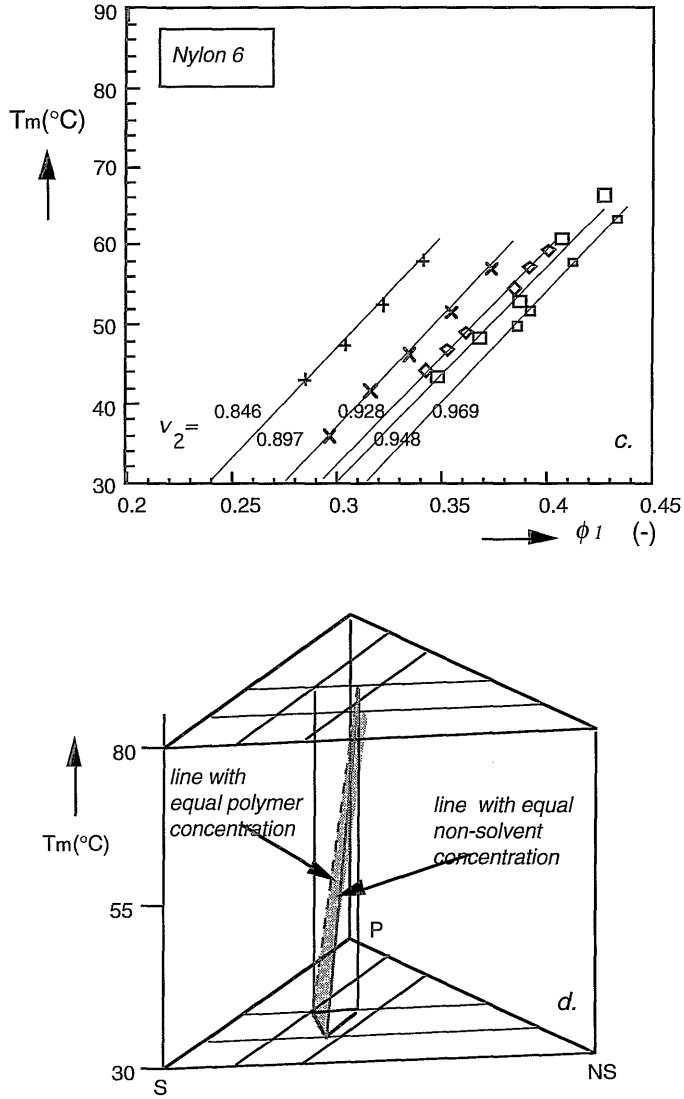

Figure 6: Measured melting temperatures as a function of the volume fraction of water for three different nylons (a: Nylon 4,6; b: Nylon 4,6co6; c: Nylon 6). The lines connect points with the indicated v_2-value. Not all the experimental data are shown in these figures. In figure d the schematical phase diagram as a function of composition and temperature is given.

It was observed visually that the samples did not demix instantaneously during sample preparation. Water could be added to the polymer solution in such quantities that the composition of the samples entered the inhomogeneous region, while turbidity was still not observed. For the samples with the largest cloud-point temperature turbidity only occurred after several hours. Realizing that liquid - liquid demixing is an instantaneous process, it can be concluded that the turbidity of the solutions was caused by solid - liquid demixing.
Figure 6 shows the measured *melting temperatures* as a function of the volume fraction of water (ϕ_1). It can be observed that the melting temperatures increase with increasing polymer- or water fraction at a constant content of the other component. In other words in these directions the solid - liquid demixing area is deeper entered. In addition a linear relationship exists between T_m and ϕ_1 within the range of the experimental data (40 - 80 °C). This dependency of the melting temperature in a ternary system has not been reported yet in literature. A melting temperature of 30°C or lower has not been measured. Apparently the degree of undercooling of approximately 20°C is not large enough to induce crystallization for these nylons. This phenomenon has also been observed with crystallization from the melt. A degree of undercooling of at least 30°C or larger is necessary to induce crystallization within a reasonable time.

Since the aim of these measurements among others is to determine the isothermal crystallization line at T=30°C, it is necessary to extrapolate the experimental data to the axis of T=30°C. This can be achieved by deriving a phenomenological relationship between the melting temperature and the composition of the solution. In order to obtain the most suitable form of such a relationship, the *K*- value (equation 12) of various relations was calculated in a minimization procedure:

$$K = \sum_{all} (T_{m,m} - T_{m,c})^2 \qquad (12)$$

In this equation $T_{m,m}$ is the measured melting temperature and $T_{m,c}$ is the calculated melting temperature. It appeared that the following relationships with no more than three fitting constants gave the lowest *K*- values and thus the best fits:

Nylon 4,6: $Tm,c = -98.65 - 332.9\ ln(v_2) + 367.6\ \phi_1\ v_2$ (°C) (13a)

Nylon 4,6co6: $Tm,c = -100.4 - 301.3\ ln(v_2) + 348.0\ \phi_1\ v_2$ (°C) (13b)

Nylon 6: $Tm,c = -67.31 - 235.3\ ln(v_2) + 294.3\ \phi_1\ v_2$ (°C) (13c)

These are mathematical relations without any physical meaning and they cannot be applied for other ternary systems. In order to give an indication of the quality of these fits, the average absolute values of $T_{m,m} - T_{m,c}$ (ΔT_{av}) and the percentage of points with $T_{m,m} - T_{m,c} < 2$°C and $T_{m,m} - T_{m,c} < 5$°C are given below:

	ΔT_{av} (°C)	$T_{m,m} - T_{m,c}$ < 2°C (%)	< 5°C (%)
Nylon 4,6:	2.3	54	92
Nylon 4,6co6:	1.0	91	100
Nylon 6:	0.6	96	100

Since an empirical relationship has been derived the melting temperature of a mixture can now be calculated accurately as a function of the composition (figure 7). It can be observed that the location of the crystallization line for the different polymers does not differ very much. Moreover it is clear that the copolymer has the largest homogeneous area. This can be understood, considering the fact that the copolymer is no more than 'poisoned' nylon 4,6 and the polymer chains will thus have more difficulty to rearrange into their specific crystalline order[21].

Interaction parameters

The values obtained for the melting temperatures are used for the calculation of the concentration dependent interaction parameter g_{23} of the nylons and formic acid . A spread sheet program with a Newtonian minimizing procedure was used and the best fit was obtained with the following logarithmic functions:

Nylon 4,6: $g_{23} = -3.95 - 1.46 \ln v_2$
Nylon 4,6co6: $g_{23} = -4.32 - 1.32 \ln v_2$
Nylon 6: $g_{23} = -3.91 - 1.59 \ln v_2$ (14)

It is remarkable that the values of the polymer - solvent interaction parameters are highly negative. Such low values are very unusual; the lowest value of a polymer - solvent interaction parameter ever reported was -4.1 for cellulose nitrate with n-propyl acetate as solvent[23]. The negative interaction parameters can partly be explained by the high interaction forces between the nylons and formic acid due to hydrogen bonding. Evaluating the values for g_{23}, it should be realized that the Flory Huggins theory is originally developed for mixtures where the components do not show high mutual interaction forces such as hydrogen bonding and acid - base interactions. It is clear that this condition is not met for the studied systems.

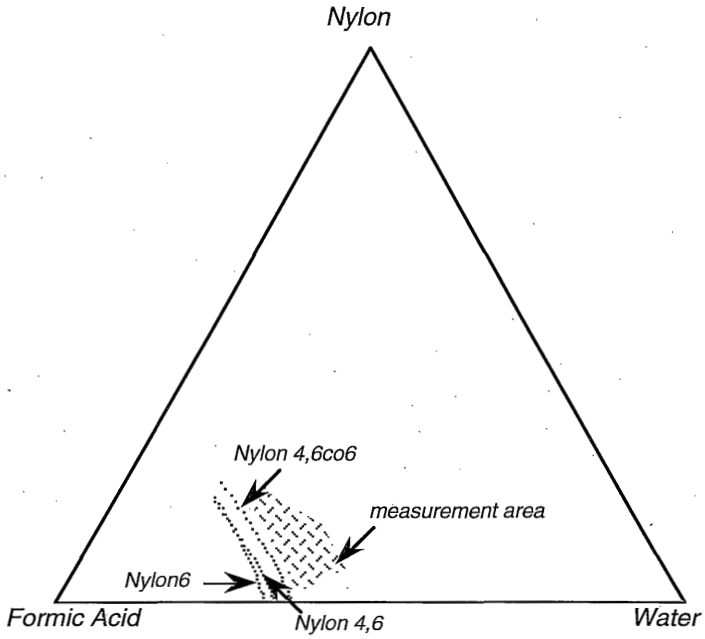

Figure 7. The isothermal crystallization lines at T=30°C of the three different polyamides in the system polyamide/formic acid/water. The measurement area gives the location of the measured melting points at higher tempertures of the ternary samples (figure 6).

An additional problem is that the value of the enthalpy of fusion for the polymer repeating unit is taken as a constant, which might not quite be the case; lower values for ΔH_u give less negative values for g_{23}.
However, it should be realized that equations (14) are partly based on experimental data, from which g_{23} is indirectly determined. Since the range of v_2- values in these data is limited (from about 0.70 to 0.98), care should be taken using these equations outside this area.

Calculation of the ternary phase diagrams

So far, only the isothermal crystallization lines for the different membrane forming systems have been determined. In order to complete the phase diagrams, the binodals must be determined as well. For the calculation the algorithm described by Altena[12] was used. The values for the interaction parameters were taken from equations (10), (11) and (14); The values for the physical constants are given in table 1.

The results of the calculations are shown in figure 8, giving the complete (phase) diagrams for the three membrane forming systems. It should be realized that the exact location of the binodal drawn in figure 8 becomes less certain as the v_2-value decreases. In the case of nylon 6 the crystallization line and the binodal almost cross each other, while in the case of nylon 4,6 and the copolymer there is quite a gap between those lines. This means that thermodynamically for all unstable compositions, crystallization is the most favorable demixing process. In other words, for these systems the binodal has only thermodynamical significance as a *virtual* (hidden) binodal. In membrane formation, however, kinetics plays a very important role as well and the location of the binodal is quite essential for the ultimate membrane morphology.

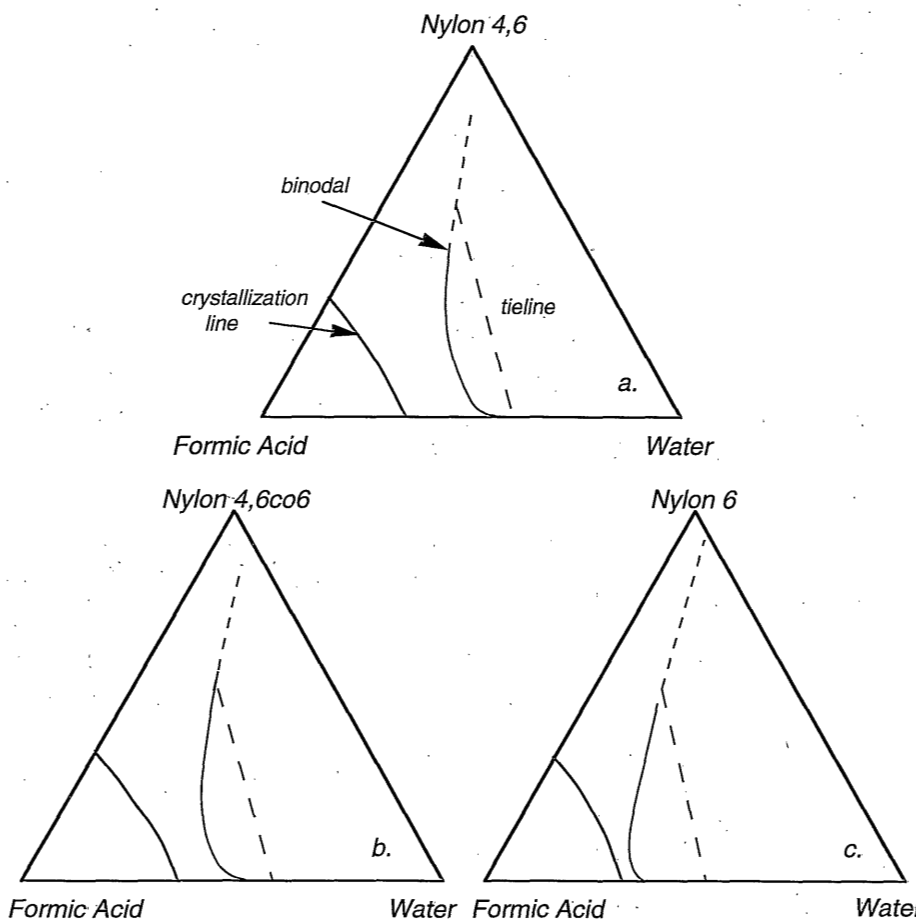

Figure 8: (Phase) diagrams of the three membrane forming systems, a: Nylon 4,6; b: Nylon 4,6co6; c: Nylon 6. The crystallization line is derived from the experimentally determined melting temperatures. De binodal is calculated with the derived Flory-Huggins parameters. It should be noted that for a strict thermodynamic phase diagram the binodals can only be drawn as 'virtual' binodals. The location of the hidden binodals, however, is important for membrane formation.

DISCUSSION

The hypothesis that the crystallization line is positioned more close to the solvent corner than the binodal curve, following from the phenomenological experiments described recently[2], is confirmed by the calculations and experiments in this paper.

Strong interaction between solvent and non-solvent can be expected because of a large contribution of hydrogen bonding and by a partial dissociation of formic acid in water. A relatively large exothermic heat of mixing, which occurs with water and formic acid, contributes to a negative excess free enthalpy of mixing and consequently to negative interaction parameters, g_{12}. Solvent and polymer show a strong intermolecular interaction as well based on hydrogen bonding. From earlier work on membrane formation with Nomex[24], an aromatic polyamide, it is known that dissolution of the polymer in formic acid leads to an increase in temperature, i.e. an exothermic heat of mixing is found.

Cloud points are very often determined from turbidity measurements upon cooling. However, for systems in which it is expected that crystallization is involved, cloud points should be detected by heating turbid mixtures instead of cooling clear solutions. Similar to the determination of melting points in pure polymers the melting temperature and the crystallization temperature may differ by 30 to 50 °C depending on the cooling rate and the crystallization kinetics of the polymer. The experiments confirmed that crystallization is highly influenced by kinetics; solutions with a melting temperature around 30°C or lower did not crystallize within 6 weeks during storage at 8°C. This problem was circumvented by the determination of melting or dissolution temperatures by heating turbid systems and reproducible melting points were obtained.

The shape of the crystallization curves are in agreement with experimentally observed crystallization lines for poly(phenylene oxide)[25] and poly(L-lactide)[26]. The crystallization line will not cross the solvent - non-solvent axis, which is an asymptote for the crystallization line, just as it is for the binodal curve. The calculations carried out by Burghardt[11], which resulted in a crystallization curve with a 'maximum', can be valid only if at intermediate non-solvent concentration a mixture of solvent and non-solvent is a better solving agent for the polymer.

Implications for membrane formation

Both from calculations and from experiments it can be concluded that crystallization or solid - liquid demixing is thermodynamically the most favorable phase separation process for this ternary system. It has been shown, however, that in some cases a membrane morphology has been obtained from these ternary systems which is typical for liquid - liquid demixing[2,11]. Membranes prepared from immersion precipitation are a result of a diffusion induced phase separation process. During the diffusion process the composition in the cast film changes continuously and a thermodynamic equilibrium is never reached during the different stages of the membrane forming process. Both thermodynamic and kinetic parameters thus play a role in the final membrane morphology. In crystallization several kinetic parameters are involved: the (reptation) diffusion of polymer molecules to a growing crystal and the surface reaction of a chain onto the surface. Primary nucleation is dictated by both thermodynamic and kinetic effects. Before crystallization can take place a certain degree of supersaturation or undercooling is necessary. This means that especially for membrane forming systems in which crystallization is involved dynamic phase separation cannot be described by equilibrium thermodynamics alone.
For many membrane forming systems crystallization is a 'slow' process so that it does not involve in membrane formation. Even in turbidity or cloud-point measurements a true crystallization point will not be observed. Phenomena that are not understood are ascribed to a gelation boundary that very well may be a crystallization line in reality for semi-crystalline polymers. For the semi-crystalline polymers poly(phenylene oxide) cellulose acetate and poly(L-lactide) effects of crystallization should not be excluded.

CONCLUSIONS

The melting temperature, measured by cloud point experiments in mixtures of nylons in formic acid and water, is linearly related to the volume fraction of water at constant v_2-values. These experimental data were used to develop a phenomenological relationship between the melting temperature of the mixture as a function of its

composition. It was shown that these relationships provide a satisfactory description of the experimental data; the melting temperature of a ternary mixture of the components mentioned (with $0.75 < v_2 < 0.96$) can be predicted within a range of 1-2 °C.

In order to model the equilibrium thermodynamic conditions of the three components of the membrane forming systems nylon 4,6, nylon 6 and nylon 4,6 *co*6, formic acid and water, the three binary Flory-Huggins interaction parameters were determined. The concentration dependent interaction parameter water - formic acid, g_{12}, was taken from literature; g_{13} which was considered as a constant parameter, was calculated from sorption experiments. These relationships were combined with melting point depression phenomena described with the Flory-Huggins theory making it possible to derive the polymer - solvent interaction parameter g_{23} as a function of v_2. The data needed to calculate the other interaction parameters were acquired from literature. The values found for the interaction parameter polymer - solvent, g_{23}, are highly negative.

The complete isothermal phase diagrams of the three different membrane forming systems at T=30°C could be derived. The isothermal crystallization lines could be calculated directly from the phenomenological relationships. The location of the binodals was calculated, using the earlier derived interaction parameters. Equilibrium crystallization lines and binodal curves can be calculated. For this system the crystallization line is positioned more closely to the solvent corner than the binodal, which is in agreement with the hypothesis stated earlier[2]. Although crystallization is the thermodynamically more favorable process, liquid - liquid demixing may not be excluded because kinetic parameters play an important role in membrane formation.

SYMBOLS

g_{ij}	Flory Huggins interaction parameter between the components i and j [-]
G_M	Free enthalpy of the mixture [J/mole]
ΔG_m	Free enthalpy of mixing [J]
G^E	Excess free enthalpy of mixing [J/mole or Cal/mole]
ΔH	Enthalpy change [J/mole]
M	Molecular weight [g/mole]
n	Number of moles [-]

R	Gas constant [J/mole.K or Cal/mole.K]
ΔS	entropy change [J/mole.K or Cal/mole.K]
r	ratio of the molar volumes of the non-solvent and the polymer (η_1/η_3)
s	ratio of the molar volumes of the non-solvent and the solvent (η_1/η_2)
T	Temperature [K]
T_m	Melting temperature [K]
u_2	$= \phi_2 / (\phi_1 + \phi_2)$
v_2	$= \phi_2 / (\phi_2 + \phi_3)$
x_i	mole fraction of component i [-]
γ_i	activity coefficient of component i [-]
ϕ	volume fraction [-]
χ	Flory Huggins interaction parameter
μ	chemical potential [J/mole or Cal/mole]
η	molar volume [cm^3/mole]
ρ	density [g/cm^3]
Indices	
(c)	crystalline state
(0)	pure (amorphous) state
(1)	non solvent
(2)	solvent
(3)	polymer
(u)	repeating unit in the polymer
(α)	polymer lean phase
(β)	polymer rich phase
(γ)	polymer solution in equilibrium with the crystalline state

ACKNOWLEDGEMENTS

The authors wish to thank DSM the Netherlands for financial and scientific support, and Ir. H. Gankema for his help with the cloud-point measurements.

REFERENCES

1. M.H.V. Mulder, *Basic principles of Membrane Technology*, Kluwer Dordrecht, 1991.
2. A.M.W. Bulte, B. Folkers, M.H.V. Mulder, C.A. Smolders, *J. Appl. Polym.Sci.*, 50, 13-26 (1993).
3. P. Marinaccio, R. Knight, *US Patent* 3 876 738 (1975).
4. D. Pall, *US Patent* 4 340 479 (1982).
5. J. F. Ditter, *WO Patent* 86 / 07544 (1986).
6. P.J. Flory, *Principles of Polymer Chemistry*, Cornell University Press, NY (1953).
7. M. Sawodny, G.I. Asbach, G.G. Kilian, *Polymer*, 31, 1859 (1990).
8. H.G. Kilian, *Makromol. Chemie*, 116, 219 (1968).
9. H.G. Kilian, *Progr. Colloid Polym. Sci.*, 78, 161 (1988).
10. F.W. Altena, J.S. Schröder, R. van de Hulst, C.A. Smolders, *J. Poly,. Sci., Polym. Phys. Ed.*, 24, 1725 (1986).
11. W.R. Burghardt, L. Yilmaz, A.J.McHugh, *Polymer*, 28, 2085 (1987).
12. H. Tompa, *Polymer Solutions*, Butterworths, London (1956).
13. F.W. Altena, C.A.Smolders, *Macromolecules*, 15, 1491 (1982).
14. J.G.Wijmans, F.W. Altena, C.A. Smolders, *J.Polym. Sci., Polym. Phys. Ed.*, 22, 519 (1984).
15. A.J. Reuvers, C.A. Smolders, *J. Membr. Sci.*, 34, 67 (1987).
16. R.M. Boom, Th. van den Boomgaard, C.A. Smolders, *Equilibrium Thermodynamics of a Quaternary Membrane Forming System with Two Polymers*, submitted to *Macromolecules* (1992).
17. W.R. Burghardt, *Macromolecules*, 22, 2482 (1989).
18. I.V. Krasovskii, V.I. Makurina, Russina, *J. Phys. Chem.*, 46, 140 (1972).
19. J. Wisniak, A. Tamir, *Mixing and Excess Thermodynamic Properties*, Elsevier, Amsterdam (1978).
20. A.N. Campbell, A.S.R. Campbell, *Trans. Faraday Soc.*, 30, 1109 (1934).
21. B. Wunderlich, *Macromolecular Physics*, Academic Press, NY, vol 1, *Crystal Structure, Morphology, Defects* (1973), vol. 2 *Crystal Nucleation, Growth, Annealing* (1976), vol. 3, *Crystal Melting* (1980).
22. R.J. Gaymans, D.K. Doeksen, S. Harkema, in *Integration of Fundamental Polymer Science & Technology* (Lemstra, ed.), Elsevier, 573 (1985).
23. J. Brandrup, E.H. Immergut, *Polymer Handbook*, 3rd ed., Wiley, NY (1989).
24. H. Strathmann, internal communication.
25. A.J. Reuvers, PhD thesis University of Twente, Appendix A, Chapter 2 (1987).
26. P.van de Witte, internal communication.

CHAPTER 4

Diffusion Induced Phase Separation with Crystallizable Nylons; I Mass Transfer Processes for Nylon 4,6 and Relation to Final Membrane Morphology.

A.M.W. Bulte, M.H.V. Mulder, C.A. Smolders, H. Strathmann.

SYNOPSIS

Mass transfer during membrane formation by means of phase inversion for a polymeric system with both a solid - liquid and a liquid - liquid equilibrium was studied on the basis of the theory developed by Reuvers and Smolders. During the first moments of immersion in the coagulation bath, the concentrations at the interface between bath and film are governed by the virtual liquid - liquid equilibrium. This equilibrium no longer exists at a larger time scale. The interface concentrations as a result of the local liquid - liquid equilibrium during mass transfer are located deep in the crystallization region or solid - liquid demixing area and after an induction time the solid - liquid phase separation (crystallization) takes place when membranes are formed with an initial polymer concentration of 20% or larger. The calculated initial concentration profiles show a shallow pattern in polymer content for the films with initial concentration of 20 and 25%. A steep increase of the polymer concentration at the interface was observed for the higher concentrated films. It is concluded that a small nucleation density does not influence the overall composition profiles throughout the film. From the calculated initial concentration profiles an isotropic morphology in the final membrane can be expected. A large nucleation density, however, will influence the overall concentration profiles. Enhanced transport of solvent and non-solvent is expected in the porous regions.

INTRODUCTION

Membranes can be prepared by various techniques of which immersion precipitation is widely used[1]. In this process a polymer solution is cast as a thin film and subsequently immersed in a non-solvent bath, thereby inducing diffusional exchange

of solvent and non-solvent, resulting in phase separation. With semi-crystalline polymers, such as aliphatic nylons, two types of phase separation processes may occur. Liquid - liquid demixing resulting in a porous structure with pores that are formed from the nucleated polymer lean phase and solid - liquid demixing with crystalline parts in the membrane. The pores in this case are the voids in between the partly crystalline units.

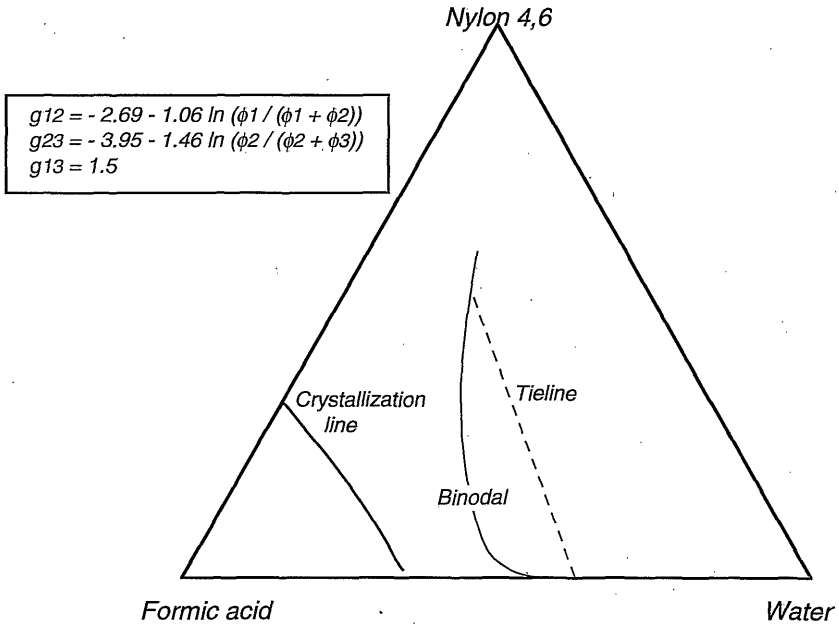

Figure 1. Isothermal (phase) diagram at 30°C for the ternary system water(1), formic acid (2) and nylon 4,6 (3), with the experimentally determined crystallization line and the calculated liquid - liquid demixing gap depicted[3]. The virtual binodal does not represent existing equilibria in this thermodynamic phase diagram. Its location, however, is important for membrane formation.

It has been found that for the ternary system nylon 4,6, formic acid and water crystallization or solid - liquid demixing occurs, resulting in a spherulitic or axialitic morphology of the membrane when the casting solution has a rather high polymer concentration[2]. At lower polymer concentrations the typical cellular morphology,

which is a result of liquid - liquid demixing, has been observed. The equilibrium thermodynamics of this system has been described previously[3]. Thermodynamically, crystallization is the favorable phase inversion process. The phase diagram with the parameters used is given in figure 1.

Knowledge about the thermodynamics of the membrane forming system is a first step towards understanding of the formation of phase inversion membranes. It has been shown, however, that kinetic conditions may result into another phase separation process than predicted by the equilibrium thermodynamic properties of the system[2,3]. In order to understand the mass transfer of the components during the diffusion processes Reuvers and Smolders[4] have developed a model on the basis of earlier work of Cohen and coworkers[5]. Since then a number of papers have been published on mass transfer during a diffusion induced phase separation process[6,7,8]. Two different types of circumstances leading to different types of morphology in the final membranes, in both cases determined by liquid - liquid demixing[9], have been found Firstly, delayed onset of demixing which results in membranes with a dense skin and a porous sub-layer with isolated pores. The second type, instantaneous demixing, being visualized by the occurrence of immediate turbidity in the film after immersion, results in membranes with a porous skin. The model developed by Reuvers et al.[9] allows predictions concerning the type of membrane morphology that can be expected.
In order to develop a further insight concerning the morphology of a membrane, determined by solid - liquid demixing, mass transfer in ternary systems should be studied, while including the crystallization process. Many polymers, such as aliphatic nylons, poly(phenylene oxide) or cellulose acetate, are able to crystallize. While it is known that this influences the properties of the resulting membranes, the crystallization phenomenon has always been neglected in the models describing mass transfer during immersion precipitation, although Koenhen[10] and Altena[11] have studied the thermodynamics of crystallization in binary and ternary systems for poly(phenylene oxide) and cellulose acetate respectively.

The objective for this chapter is to develop a better understanding of the initial concentration profiles of the different components during phase inversion in which crystallization is involved, and to find a relationship between the concentration profiles and the final morphology in the membranes.

THEORY

Mass transfer model

Immersion precipitation is governed by a solvent and a non-solvent flux perpendicular to the film surface as may be deduced from the figures 2 and 3. The final morphology of a membrane is largely influenced by the concentration profile in the film at the moment that the phase separation processes starts.

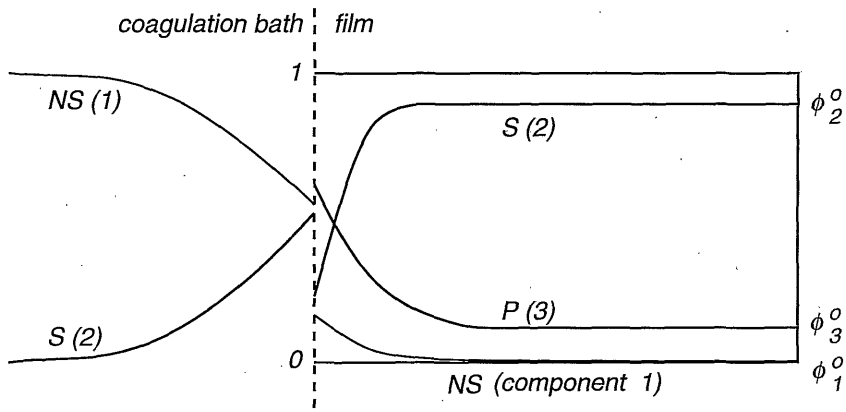

Figure 2. Schematic concentration profiles of the three components in the film, polymer (3) with an initial concentration of ϕ_3^o, solvent (2) with an initial concentration of ϕ_2^o and non-solvent (1) with the initial non-solvent concentration ϕ_1^o equal to zero in this case, and of solvent (2) and non-solvent (1) in the coagulation bath.

Before immersion of the polymer film into the coagulation bath the concentration of polymer is homogeneously distributed in the film and no concentration gradients exist in the coagulation bath. After immersion the in-flow of non-solvent (component 1) into the film and out-flow of solvent (component 2) effects the concentration of all three components in the film. The polymer does not dissolve in the coagulation bath; component (3) stays in the film. Because of a higher flux of solvent (J_2) relative to

the flux of non-solvent (J_1), the polymer concentration in the film generally increases as is indicated schematically in figure 2. The concentration gradients are generally steeper closer to the interface. Mass transfer can only be described if for both the bath and the film differential flux equations are derived. The approach as developed by Reuvers and Smolders[4] will be followed here.

The diffusional equations for the film

Since in most cases $J_1 < J_2$ the film shrinks and therefore the position of the interface is gradually changing in time. Mass transfer must be described with a moving boundary model. The mass transfer is based on a phenomenological model in which a flux is related to thermodynamic driving forces.

$$J_i^c = \sum_{j=1}^{2} L_{ij} X_j$$

$$\text{with} \qquad (1)$$

$$X_j = -\frac{\delta \mu_j}{\delta x}$$

for which μ_j is the chemical potential of component j per kg j and x is the cartesian spatial coordinate perpendicular to the membrane surface, and the L_{ij}'s are the phenomenological coefficients. J_i^c gives the mass flux in kg/m^{2}s.

The coordinates for this system are given in figure 3.
The coordinate x is valid for a laboratory fixed frame of reference. According to Crank[12] a moving boundary problem can be treated by defining the fluxes relative to a polymer fixed frame of reference, since the polymer stays behind in the film, and acts as a reference component.

The fluxes are defined as follows:

$$J_i^c = c_i (\bar{v}_i - \bar{v}_3) \qquad (2)$$

Where $\bar{v}_i$ and $\bar{v}_3$ are the average velocities of component i and 3 relative to the lab fixed frame of reference and c_i is the concentration of component i in kg/m^3.

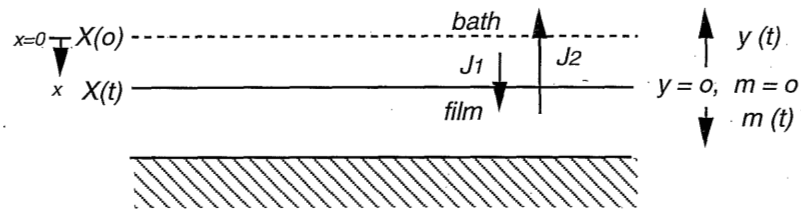

Figure 3. The definition of the coordinates for the mass transfer problem. Three coordinate systems exist: the laboratory fixed frame of reference with coordinate x, the polymer fixed frame of reference with coordinate m for the film and coordinate y for the bath. Capital X gives the position of the interface in the laboratory fixed frame of reference; the location of the interface in the other coordination systems is at position zero by definition. The flux of solvent out of the film is indicated with J_2, the flux of non-solvent into the film is J_1.

For treating the moving boundary problem the coordinate m is introduced according to figure 3. The spatial coordinate m is, according to Crank[12], defined as

$$m\ (x,t\ ) = \int_0^x \phi_3\ (x,t\ )\ dx \qquad (3)$$

The continuity equation for this system can be derived as follows.
For the volume element, dV (figure 4), the mass balance is given as:

$$dV\ d\phi_i\ (t) = (J_{i,\ in}\ (t)\ dt\ - J_{i,\ out}\ (t)\ dt\ )\ A \qquad (4)$$

with

$$dV = A\ dx$$

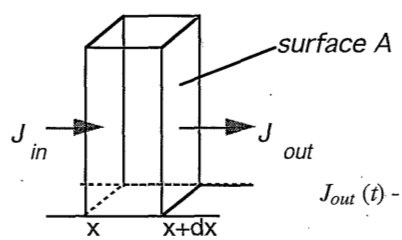

$$J_{out}\ (t) - J_{in}\ (t) = J_{x+dx}\ (t) - J_x\ (t) = d\ J\ (x,t)$$

Figure 4. Mass balance for one component for a differential unit of volume (dV) in the film.

Rewriting this equation gives the continuity equation in terms of volume fluxes (m/s) relative to the laboratory fixed frame of reference.

$$- \frac{\delta \phi_i (x,t)}{\delta t} = \frac{\delta \tilde{J}_i (x,t)}{\delta x} \qquad (5)$$

The tilde ~ denotes that $\tilde{J}_i$ is a flux relative to the laboratory fixed frame of reference.

Equation (5) can be restated according to equation (6).

$$\tilde{J}_i = \phi_i \bar{v}_i \; (= c_i \eta_i \bar{v}_i) \qquad (6)$$

The flux, $\tilde{J}_i$, equals the volume fraction of component i, ϕ_i, multiplied with its velocity, $\bar{v}_i$. The volume fraction can be expressed in the concentration times the partial specific volume, η_i.
It is assumed that the partial specific volumes, η_i, are constant and equal to the specific volume. The volume fixed and the laboratory fixed frames of reference are related to each other by a constant factor. The fluxes $\tilde{J}_i$ (lab fixed frame of reference) and J_i (polymer fixed frame of reference) are related as follows:

$$J_i = \tilde{J}_i - (\phi_i / \phi_3) \tilde{J}_3 \qquad (7)$$

By using the transformation (3) and the continuity equation, equation (1) is transformed to equation (8).

$$J_i = - \sum_{j=1}^{2} \eta_i \phi_3 L_{ij} \frac{\delta \mu_i}{\delta m} \qquad i=1,2 \qquad (8)$$

The relation between the compositions at the directional coordinate m and time t is given by equation (9) with a concentration dependent phenomenological coefficient L_{ij}.

$$\frac{\delta \phi_i / \phi_3}{\delta t} = \frac{\delta}{\delta m} \sum_{j=1}^{2} \eta_i \phi_3 L_{ij} \frac{\delta \mu_i}{\delta m} \qquad i = 1,2 \qquad (9)$$

The fluxes are calculated by integration of the left hand term of equation (9).

The diffusional equations for the coagulation bath

The binary diffusion processes in the coagulation bath can be described by Fick's second law.

$$\frac{\delta \phi_i}{\delta t} = \frac{\delta}{\delta x} \left\{ \mathbb{D} (\phi_i \frac{\delta \phi_i}{\delta x} \right\} \qquad (10)$$

For the bath the position coordinate y is used as is given in figure 3.

$$y = -x + X(t) \qquad (11)$$

Transferring equation (10) with regard to the moving frame gives the differential equations for the bath.

As can be understood easily the change in the interface position ($d X(t) / d t$) relative to the laboratory frame of reference is reflected by the sum of the volume fluxes J_1 and J_2 at $y = 0$, with J_1 being negative relative to the y coordinate. The sum of the fluxes has a positive value in most cases, which implies that the coagulation bath expands and the film shrinks.

$$\frac{\delta \phi_i}{\delta t} = \frac{\delta}{\delta y} \left\{ D(\phi_i) \frac{\delta \phi_i}{\delta y} \right\} - \frac{\delta \phi_i}{\delta y} \frac{\delta X(t)}{\delta t}$$

with (12)

$$\frac{\delta X(t)}{\delta t} = J_1 (y = 0) + J_2 (y = 0)$$

Crystallization in relation to mass transfer

In the previous section the mass transfer model as developed by Reuvers et al.[4] has been explained. This model only deals with one phase separation process, defined by the liquid - liquid demixing boundary, and discusses the mass transfer processes before the actual phase separation process has started. For the membrane forming system discussed in this study two types of phase equilibria are involved: liquid - liquid and solid - liquid demixing boundaries, i.e. the binodal curve and the crystallization line respectively. In this section the process of crystallization will be discussed in relation to mass transfer for this ternary system.

Crystallization always needs some degree of supersaturation, i.e. it does not set in at the moment the equilibrium solid - liquid line in the phase diagram is crossed. First a nucleus with a critical size must be created (thermodynamic reasons) and the crystallization process requires an induction time. The creation of the nuclei or embryos requires the polymer molecules to rearrange in an ordered structure, the crystalline lattice. Examples of schematic drawings of such ordered structures are given in figure 5[13], with the polymer molecules folded back upon themselves. It has been shown that polymers crystallize in spherulites or axialites[14]. For the same considerations as described by Passaglia[15] we do not adopt the fringed micel model. In order to create ordered crystalline structures two steps are involved. Firstly the polymer coil must move to the growing polymer surface and secondly the polymer molecule must fold itself in a specific order in the crystalline lattice, the surface reaction. These kinetic reasons also make clear that crystallization or solid - liquid phase separation needs an induction time.

At the very first moment of immersion of the film in the coagulation bath the crystallization process has not started yet. We assume that from a very small time interval after immersion of the film continuous chemical potential gradients are present (i.e. local equilibrium is assumed)[16]. In case of systems in which a liquid - liquid demixing gap is present the conditions at the interface are clear. A local interfacial equilibrium between the film and the coagulation bath is a liquid - liquid equilibrium that is given by a pair of points on the binodal connected by a tie-line. The composition on the film side is given by a polymer rich phase, the composition in the bath at the interface is the corresponding lean phase (see figure 6).

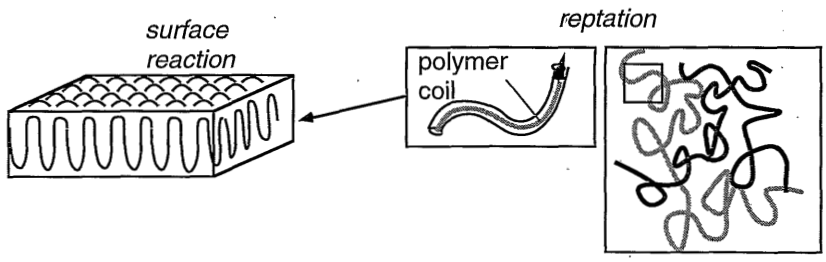

Figure 5. Schematic drawing illustrating the reptation of a polymer molecule out of a random coil structure in a concentrated solution to a growing crystal surface. The crystalline material is organized in a folded chain morphology in a lamella, which is the structural unit for spherulites and axialites[14].

For systems with crystallizable polymers the situation is more complex. At the first moments of immersion two liquid phases are contacted while in later stages (two or three seconds or longer) solid - liquid phase separation takes place. The first moments after immersion cannot be dictated by a solid- liquid demixing border, since the local equilibria at the interface are concerned with a liquid - liquid interface, bath - film.
It has been shown that a binodal curve does exist for the system nylon 4,6, formic acid and water[2], because at the lower concentrations a foam-like morphology has been obtained. This is a clear indication that a liquid-liquid demixing gap is present for this ternary system[2]. It can be assumed that in the first moments after immersion a local liquid - liquid phase equilibrium is present at the interface. The exact composition at both sides of the interface are given by the nodes of a tie-line with the binodal.
These first moments of immersion can be described by the model of Smolders and Reuvers. The parameters for the model are summarized below.

The initial and boundary conditions

The following initial conditions are valid[4]:
at t=0 the compositions of the film and of the coagulation bath are completely homogeneous. The film consists of the original polymer solution and non-solvent eventually added to the solution. The bath has the initial concentration for non-

solvent(and eventually added solvent). The indices b and f stand for the coagulation bath and the film respectively, M gives the site near the glass plate.

$$\begin{aligned} 0 \le m \le M &: \phi_i^f(m, 0) = \phi_i^f \quad i = 1,2,3 \\ y > 0 &: \phi_i^b(y, 0) = \phi_i^b \quad i = 1,2 \end{aligned} \tag{13}$$

These equations are valid for t=0; they state that both in the film and in the bath no concentration gradients are present just before immersion of the film in the bath. For the explanation of the different coordinates, y and m one is referred to figure 3.

At time t>0 after the very first moments of immersion local equilibrium is assumed leading to the boundary conditions at m=0 and y=0:

$$\mu_i^f(m = 0, t) = \mu_i^b(y = 0, t) \quad i = 1,2,3 \tag{14}$$

There is no accumulation of one of the components at the interface. Components that diffuse out of the film, diffuse into the coagulation bath and vice versa. At the interface the following condition is valid:

$$J_i(m = 0, t) = -J_i(y = 0, t) \quad i = 1,2 \tag{15}$$

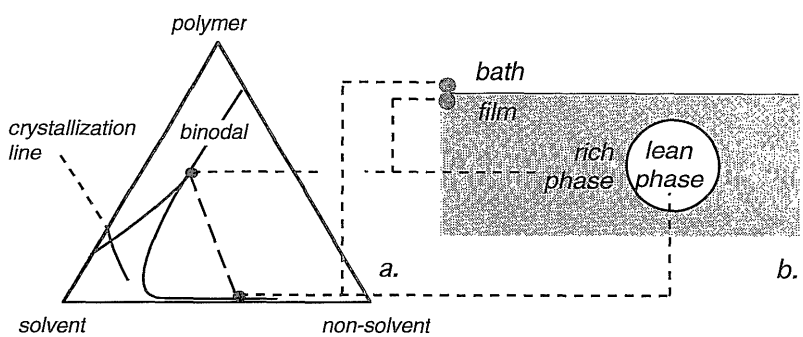

Figure 6. a.) Conditions for local equilibrium at the interface film - coagulation bath and in the nucleus of the polymer lean phase. b.) Part of a film contacted with an immersion bath. Liquid - liquid has taken place. The concentrations of the polymer rich and polymer lean phase and also the film and bath side of the film - bath interface are based on the same equilibrium.

Calculation procedure and assumptions

For describing the chemical potentials in the ternary system the Flory Huggins theory is used[3].
The calculation procedure as described by Reuvers[9] is used.
1. For the boundary conditions at the interface a tieline is chosen on the binodal curve.
2. Solvent and non-solvent fluxes are calculated for the film. Concentration gradients are calculated with equation (9).
3. The value for the sum of the fluxes is used to calculate the non-solvent flux from the coagulation bath. Concentration profiles are calculated for the coagulation bath by means of equation (12).
4. The procedures 1, 2 and 3 are repeated until the flux of non-solvent is equal for both the film and the bath by adjusting the interfacial concentration.

The last step before the concentration profiles for our system can be calculated is the determination of the phenomenological coefficients for the film part and the diffusion coefficient for the calculation of the concentrations in the film.
The same assumptions as have been described by Reuvers[4,9] have been made, in which the phenomenological coefficients L_{ij} are related to the Maxwell Stefan coefficients R_{ij}.
According to Reuvers the following relation is derived:

$$L_{ij} = \begin{vmatrix} L_{11} & L_{12} \\ L_{21} & L_{22} \end{vmatrix} = \begin{bmatrix} \frac{c_1 (c_1 R_{12} + c_3 R_{23})}{\alpha} & \frac{c_1 c_2 R_{12}}{\alpha} \\ \frac{c_1 c_2 R_{12}}{\alpha} & \frac{c_2 (c_2 R_{12} + c_3 R_{13})}{\alpha} \end{bmatrix} \qquad (16)$$

with

$$\alpha = c_3 (c_2 R_{12} R_{23} + c_1 R_{12} R_{13} + c_3 R_{13} R_{23})$$

The Maxwell-Stefan parameters, R_{12} ,R_{13} and R_{23} are binary parameters and can be derived from published binary data or experimentally determined. Furthermore it is assumed that $R_{12} = R_{21}$ (non-solvent - solvent) according to the reciprocity relation. This value is taken as constant and can be related to the binary diffusion

coefficient at infinite dilution, $\mathbb{D}$ ($\phi_1 = 1$). The coefficients R_{13} and R_{23} are concentration dependent. Friction between polymer and solvent can be related to a sedimentation coefficient, s_3 (ϕ_3). The polymer - non-solvent parameter, R_{13}, is assumed to be linearly related to R_{23}.

$$R_{12}(\phi_1) = R_{12}(\phi_1 = 1) = \frac{\eta_1 RT}{M_2 \mathbb{D}(\phi_1 = 1)} \qquad (17)$$

$$R_{23}(\phi_3) = \frac{(1 - \phi_3)\,\eta_3\,(\rho\,\eta_2 - 1)}{\phi_3} \cdot \frac{1}{s_3(\phi_3)} \qquad (18)$$

$$R_{13} = (\eta_1 / \eta_2)\, R_{23} \qquad (19)$$

with η_i and ρ indicating the partial specific volume of component i and the density respectively.

The model system is this case is:
(1.) non-solvent: water
(2.) solvent: formic acid
(3.) membrane forming polymer: nylon 4,6.

The diffusion coefficient of a trace of formic acid in water has been measured with a Taylor capillary[18] and a value of $1.51.10^{-9}$ m^2/s at 30°C was found. With equation (17) the friction coefficient of non-solvent - solvent can then be calculated. Since the values for the density of solvent and polymer lie close to each other a sedimentation or flotation coefficient can not be experimentally determined. Data for sedimentation coefficients of various polyamides in different solvents are listed in the Polymer Handbook[19]. The order of magnitude of the coefficients is similar for all types of polymers. The same concentration dependency is assumed as is found by Reuvers[9] in which the sedimentation coefficients at infinite dilution is taken for an aromatic polyamide with a molecular weight of 25 000 g/mol in dimethylformamide with 3% of LiCl. The sedimentation coefficient of nylon 4,6 in formic acid is estimated in this

way; The inverse value of the sedimentation coefficient ($1/s_3$), which is linearly related to R_{23}, has been plotted in figure 7.

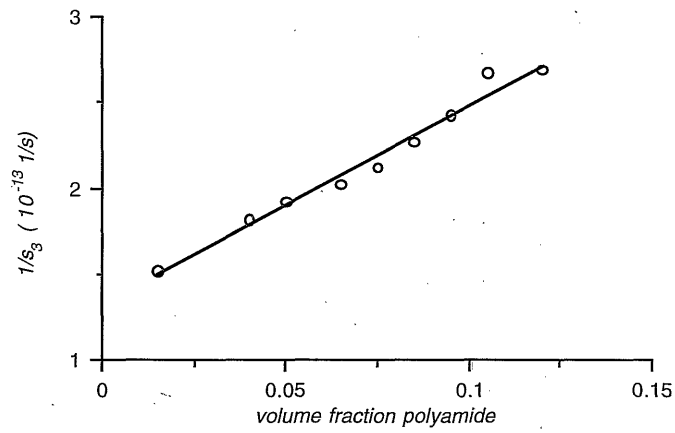

Figure 7. Concentration dependence of $1/s_3$ (the sedimentation coefficient) that is linearly related to the coefficient R_{23} for nylon 4,6 in formic acid as it is estimated from literature data.

In the calculations the following relations are used.

$$F_3 = 0.638 \times 10^{(-8 - 2.97 \times \phi_3)}$$

with (20)

$$R_{23}(\phi_3) = \frac{\eta_3 RT}{M_2 F_3}$$

with the coefficient F_3 inversely proportional to R_{23}, M_2 the molecular weight of component 2 and η_3 the partial specific volume of the polymer.
The calculations are carried out during the first full second. The sensitivity of the calculations towards a change in the values for the friction coefficients will be evaluated.

EXPERIMENTAL

Cryo substitution

Sample preparation

Nylon 4,6 (Stanyl KS 400) kindly supplied by DSM was dissolved at 30 °C in formic acid in the concentrations 20 and 32 wt%. Prior to use the polymer was dried *in vacuo* at 70°C for at least 24 hours. The membranes were cast on a metal plate and immersed in a coagulation bath containing demineralized water. The coagulation process was stopped at different intervals by quick immersion of the metal support with the film into liquid nitrogen. Small samples were cut from the frozen film and immersed in Lowicryl K4M resin at - 20°C in a Balsers FSU 010 cryo-substitution unit. The liquid resin was exchanged several times, because of accumulation of formic acid. The solid components present in the prepolymer were embedded by polymerizing the resin with UV light. The samples were used to prepare thin slices by a microtome for transmission electron microscopy (TEM).

Samples of a film that was completely coagulated were also immersed in the prepolymer resin, in order to prepare TEM samples of the final membrane structure.

Transmission electron microscopy

Microslices were stained with phosphor tungsten acid (PTA), a staining agent, in order to make the lamellae visible in the membranes. Photographs were taken at magnifications between 5000 and 20000 times. The presence and the nature of solid particles as a function of the distance from the interface coagulation bath - film were studied.

RESULTS

The calculation of composition paths

The calculated composition paths starting from various polymer concentrations are given in figure 8. A composition path as it has been defined by Reuvers gives information about the compositions at all positions; it is a curve representing all compositions existing in the polymer solution at one moment, or all compositions at all times at one position in the polymer solution assuming that the polymer solution and the coagulation bath are semi-infinite media under the time scale of consideration. The calculated profiles of the polymer concentration as a function of the position coordinate are given in figure 9.

The binodal curve (only valid when crystallization has not started yet) and the experimental crystallization line are given in figure 8. The composition path 'a' (figure 8) can be considered as a delayed type of demixing in the sense of liquid - liquid demixing, which is consistent with the physical background of the system. The light transmission profiles showed a delay time for this case (see figure 10 a). Crystallization in case 'a' does not take place prior to liquid - liquid phase separation; the membrane cast from a 15% polymer solution (see figure 11a.) shows a cellular morphology as a result of liquid - liquid demixing, even if some of the compositions are inside the crystallization region, The degree of supersaturation for crystallization is apparently not large enough to form nuclei of a critical size. The calculated compositions of curve 'a' are located in a region, in which samples used for determination of the equilibrium melting temperatures[3] showed crystallization only after several hours to several weeks. Crystallization from the melt generally requires at least a degree of undercooling of 30°C or more; the comparison with crystallization from the melt has further been worked out in reference 20.

The composition path 'b' is located deeper into the solid - liquid region (see figure 8). A delay time in the same order of magnitude as for case 'a', 25 to 30 s, (see figure 10b) can be found for the membrane formation with a polymer solution of 20%. In this case the delay time is related to solid-liquid demixing, at least what is observed in

the final morphology (figure 11b). It is very likely, however, that the first turbidity results from early nucleation and growth of a polymer lean phase (liquid - liquid demixing) followed by crystallization. Some remains of an early 'cellular' morphology can be observed in the SEM - photo (figure 11b); the irregularly formed spherulites are connected with each other by ties, which are probably the remains of the 'walls of cells'.

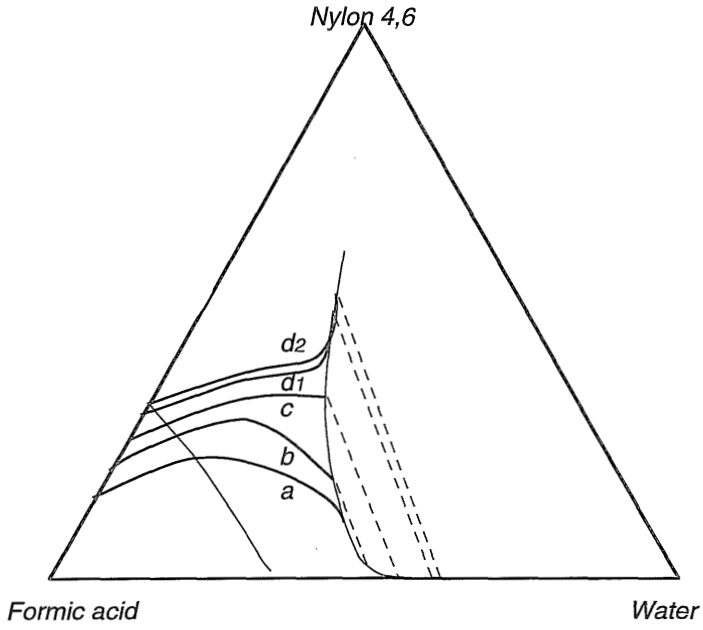

Figure 8. Calculated composition paths for immersion of a film with initial polymer concentration of a: 15%, b: 20%, c:25%, d_1: 30% and d_2: 32%. The experimental crystallization line and the calculated binodal are given as determined in a previous paper[3].

Composition path 'c' (figure 8) has entered the crystallization region deeper compared to case 'b'. The profile as it is calculated according to Reuvers is 'delayed' with respect to liquid - liquid demixing. The values for the delay time in case of membrane formation from a 25% polymer solution (figure 10c) is 6 seconds. Whether

the first turbidity observed is a result of liquid - liquid or of solid - liquid phase separation cannot be concluded from the morphology determined by SEM (figure 11c), because remains of polymer lean nuclei, possibly resulting from liquid - liquid phase separation, have not been found. The delay time for solid - liquid demixing is smaller than the delay time for liquid - liquid demixing The larger degree of supersaturation with respect to crystallization has resulted in the formation of smaller spherulites compared to case 'b'.
Calculation of the concentration profiles during the first second as is described above is justified for the cases 'a', 'b' and 'c', because phase separation or by liquid - liquid or by solid - liquid demixing has not occurred yet. Furthermore it can be concluded that a good correlation has been found between the calculated initial composition paths and the experimental results. In all three cases mass transfer calculations do not predict a large interfacial polymer concentration. The structures of the three corresponding membranes, indeed, show a rather isotropic morphology (see figure 11).

The concentration profiles 'd_1' and 'd_2' as calculated with the mass transfer model are considered as instantaneous with respect to liquid - liquid demixing, which might indicate that the first demixing process is liquid - liquid phase separation. The calculated compositions inside the binodal area are just a result of the calculations, immediate phase separation after immersion into the bath will occur in the case of instanteneous liquid - liquid demixing. Whether instantaneous demixing with respect to liquid - liquid demixing, as it follows from the mass transfer model, takes place as a first phase separation process cannot be concluded from the experimentally obtained results. The immediate turbidity observed in the first second after immersion of the films (figure 10d) can be either due to the onset of liquid - liquid or solid - liquid phase separation. The driving force for crystallization, at the same time, is so large that a large number of nuclei can be created. An eventually formed polymer lean phase in a continuum of a polymer rich phase cannot be found after the crystallites have grown out to their maximum size. In the final morphology of the membrane the so formed crystalline structure dominates, and identification of the phase separation process responsible for the immediate turbidity after immersion is not important. Following the membrane formation visually two stages were observed: 1. the occurrence of an immediate haziness in the film after immersion, followed by 2. the creation of white spots after 2 to 3 seconds spreading out over the whole membrane

area. The large supersaturation in the cases 'd_1' and 'd_2' has resulted in an axialitic morphology in the final membranes because of a large nucleation density as has been described previously[2]. The large nucleation density is a result of a high nucleation frequency[20] in combination with moderate growth. It is not the result of a moderate nucleation frequency with slow growth that also leads to a high nucleation density.

The concentration profiles of the polymer 1 second after immersion of the film into the bath are given in figure 9(1) and the (time normalized) fluxes of solvent and non-solvent through the film - bath interface in figure 9(2). The solvent out-flux is the largest in case of a 15% solution and decreases as the polymer concentration in the initial solution is larger. For the 15% solution the out-flow of solvent is an order of magnitude larger that the inflow of non-solvent. In all cases the flux of solvent is larger than the non-solvent flux. The difference between these fluxes becomes smaller with increasing polymer concentration. As a consequence the non-solvent flux is the largest for the high polymer concentration despite the fact that the resistance for transport must be considerably larger in this case. The in-flux of non-solvent here is hindered to a large extent by the 'counter-current' flux of solvent, which is the largest for the lowest polymer concentration.
From figure 9 it follows that the polymer concentration at and close to the interface is in the cases 'a' and 'b' lower than the 'bulk' polymer concentration. At the higher polymer concentrations (≥25%) this effect does not take place. These results illustrate that a large solvent out-flux (J_2) not necessarily implicates that the interfacial polymer concentration increases compared to the initial polymer concentration. The total compaction of polymer in the film as a result of a larger J_2 relative to J_1 is schematically given by the total area under the curve of a plot of the polymer volume fraction versus the x coordinate (see figure 12a), in which area '2' represents a positive and area '1' a negative value.

Also for the cases 'a' and 'b' in figure 9(1) the area under the curves is positive, which is consistent with the calculated values for the solvent and non-solvent flux through the interface. These calculations are in agreement with the morphology of the membranes observed in the corresponding figures 11a and b. A larger compaction in polymer concentration of the film at the interface that would lead to the formation of a skin is not observed.

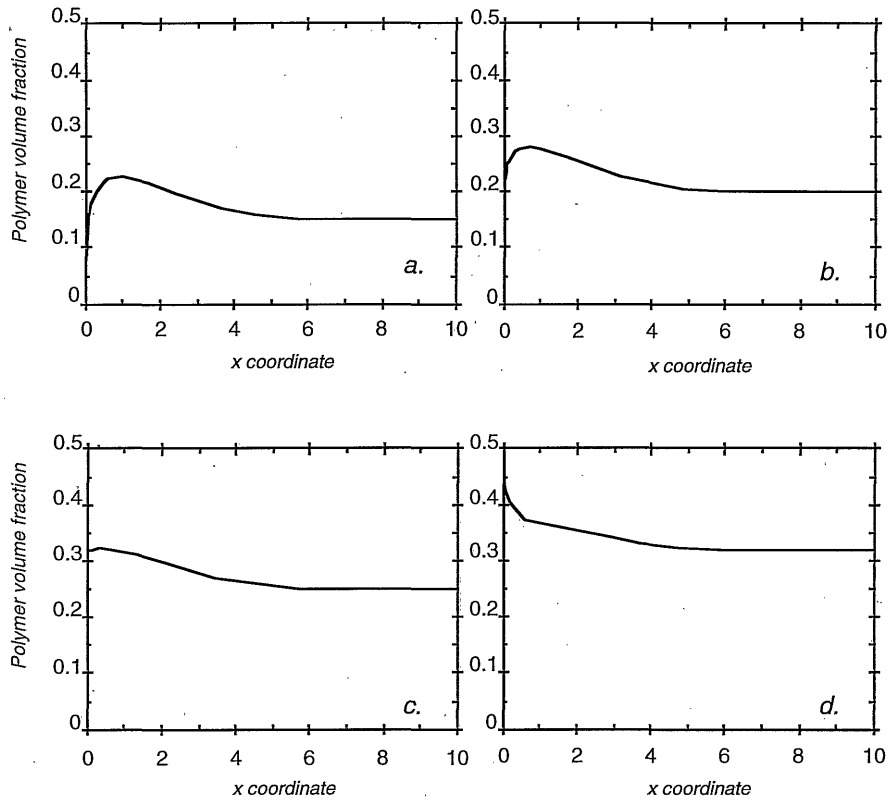

Figure 9. (1) Concentration profiles for the polymer concentration versus the x coordinate (μm) valid for t=1 s after immersion. The initial polymer concentration of the film is a: 15%, b: 20%, c: 25% and d:32%.

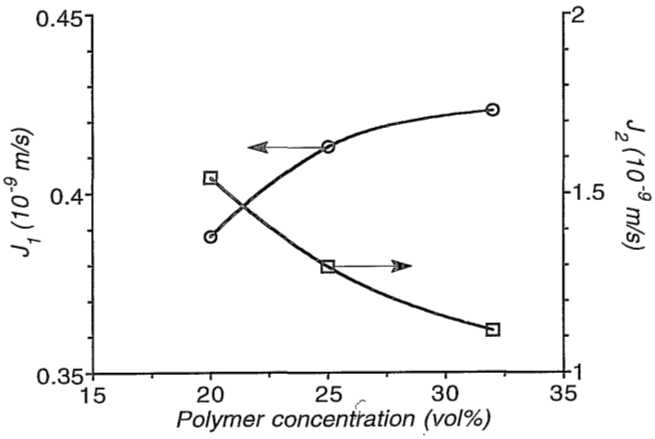

Figure 9 (2) Time normalized fluxes of solvent and non-solvent calculated during t=1s.

For the higher polymer concentrations (curve d_1 and d_2) the surface polymer concentration is much larger. Starting membrane formation with polymer concentrations of 20 ('b') and 25 % ('c') of polymer in the casting solution, an isotropic morphology is observed. The morphology of the membranes cast from a 30 or 32% polymer solution show an asymmetric structure with a higher polymer concentration at the interface, which results in the formation of a skin. An instantaneously demixed film with respect to liquid - liquid phase separation usually gives ultrafiltration membranes with thin top-layers in the membrane with a thickness of 0.2 μm or less. Here, however, ultrafiltration characteristics are not observed. The pore sizes are larger, typically in the microfiltration range[2], probably a result of crystallization. The polymer matrix shows an extra contraction as a result of crystallization, so the voids between the partly crystalline units, the pores, become larger. A detailed photograph of the top of a 32% membrane is given in figure 11d.

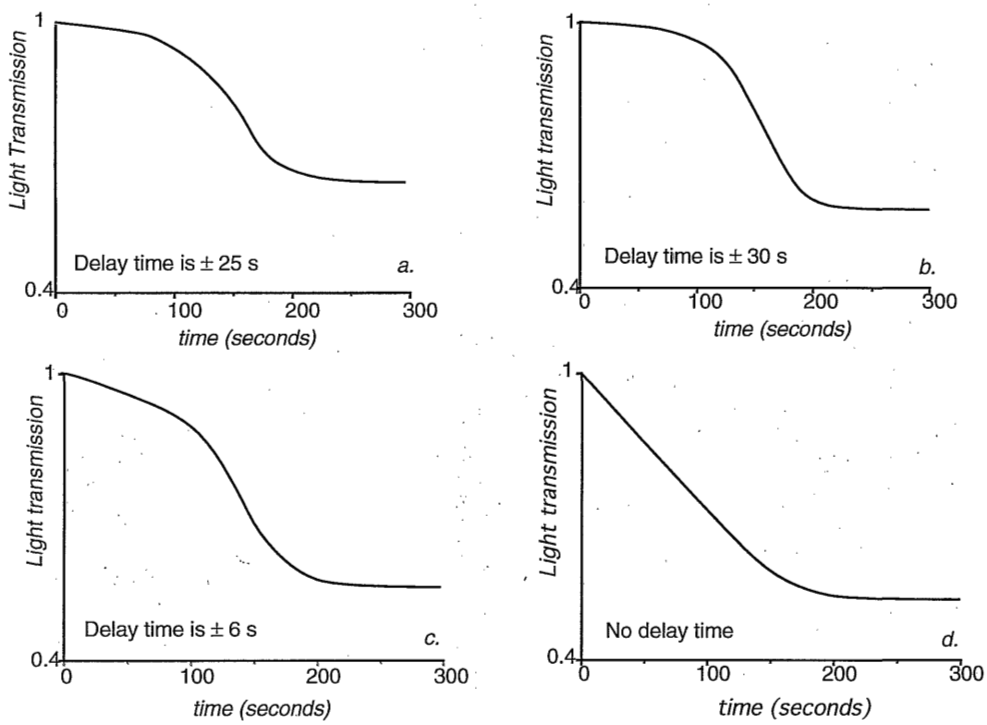

Figure 10. Light transmission through the film as a function of time after immersion in a water bath for a film with initial polymer concentration of a: 15%,b: 20%, c:25% and d: 32%.

The results for the calculated composition paths do not significantly change if other Flory-Huggins interaction parameters are taken for the calculations. The uncertainty in the friction between polymer and solvent was evaluated by changing the 'exponential pre-factor' of equation (20) with a factor of five. The exact location of the composition paths changes to some extent. The choice of a different parameter, however, does not lead to significantly different conclusions. The choice of the R_{23} parameter gave consistent values for the calculated solvent flux (figure 9(2)) compared with the experimentally determined solvent fluxes by casting leaching experiments.

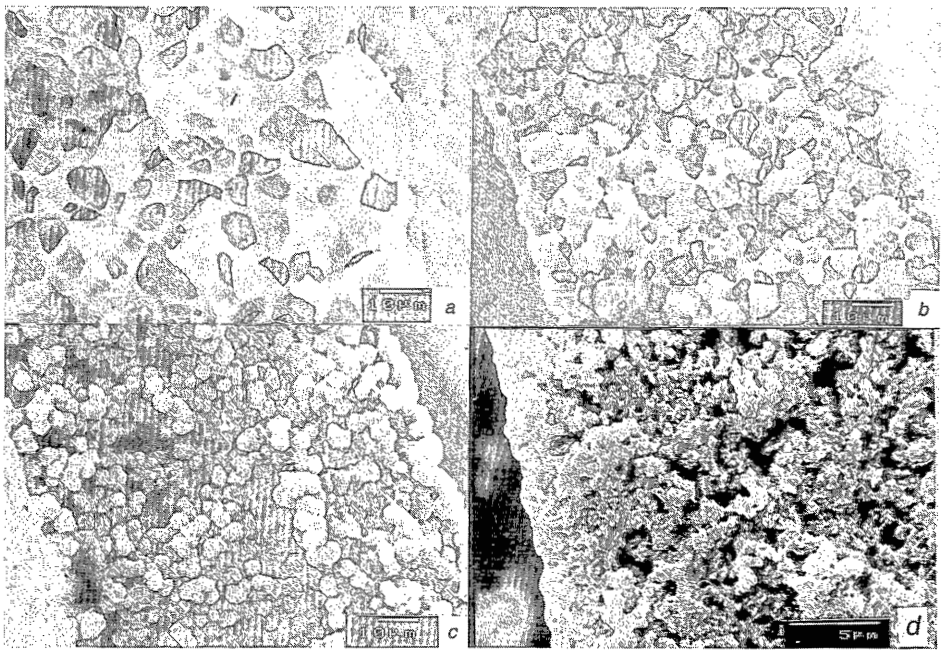

Figure 11. Overview of the final morphology of the membranes cast with an initial polymer concentration of a: 15%, b: 20%, c: 25% and d:32 observed with scanning electron microscopy (SEM)[2].

The calculated concentration profiles may not longer be valid as soon as any kind of phase separation has started. Insight in the intermediate and later stages of membrane formation must be obtained by deduction. The development of the concentration profiles in time passes through different stages. During the whole process the diffusion front enters deeper into the film and shifts to sites further away from the interface. In the early stage the interfacial concentrations are assumed to be constant. During the first second of our calculations this condition is maintained as is assumed by Reuvers[4]. In the later stages, however, the levelling of concentration gradients at the interface, takes place[6]. The driving forces will decline resulting in lower fluxes of solvent and non-solvent. The profiles will become more flattened. These two effects are schematically given in figure 12.

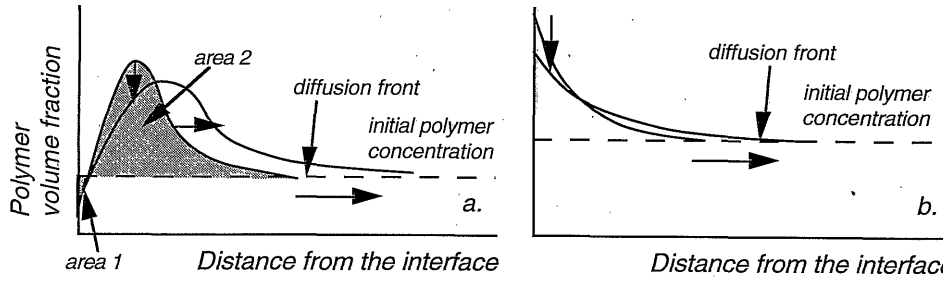

Figure 12. Schematical change of polymer concentration in time. The interface concentration changes; the 'wave' becomes wider and the diffusion front moves away from the interface. The moving interface is not included in this scheme. In case 'a' the situation for lower interfacial polymer concentrations is drawn; 'b' reflects most cases in which the polymer concentration at the interface is higher than the initial polymer concentration. The area under the curve (area 2 - area 1) is a measure for the total compaction of polymer.

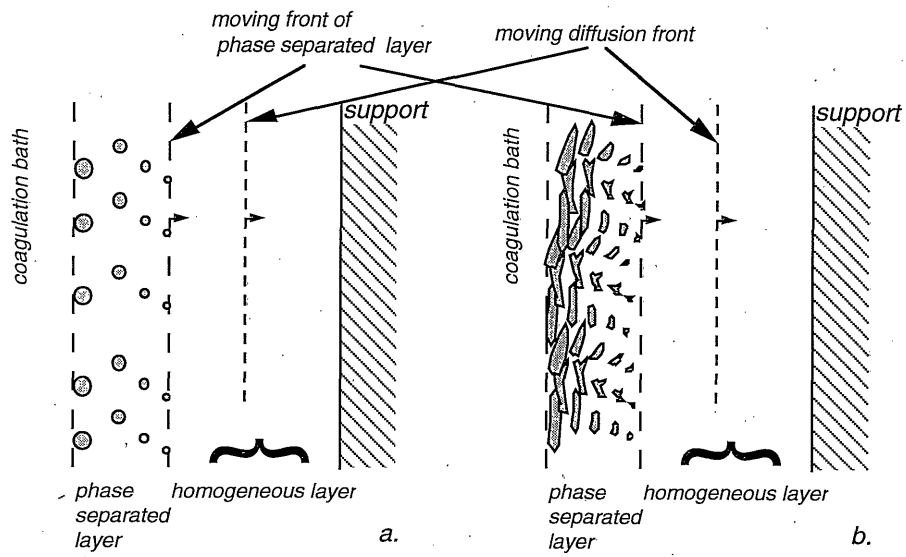

Figure 13. The situation in the film after phase separation has started in the upper layers for a situation with a: a small nucleation density and b: a large nucleation density.

After phase separation has taken place the calculated profiles (as shown in the figures 8 and 9(1)) may no longer be valid. The morphology of the top-layers (the 'slices' near the interface) is determined by the concentration profiles at the moment phase separation sets in. The predictions from the model are only valid for those parts of the membrane that are located close to the interface if turbidity is observed within a few seconds or deeper into the film if it takes place after a longer period of time. Concentration profiles in the still homogeneous layers certainly will develop with a diffusion front proceeding towards the support (see figure 13).

Cryo substitution

Scanning electron micrographs have been used to identify the presence of spherulites in membranes[2]. In order to support the mechanism of spherulitic crystallization during membrane formation transmission electron microcopy (TEM) was used. TEM pictures of a membrane cast from a 20 wt% and from a 32 wt% solution are shown in figure 14. The lamellae, visible in both the spherulitic (20 wt%) and the axialitic (32 wt%) morphology, clearly indicate that spherulites are formed in nylon membranes. The size of the spherulites is in agreement with the results of the SEM pictures[2] (see also figure 11). It can be observed that the centers of both structural units are quite similar in nature, which indicates that the mechanism of spherulitic growth in case of both spherulitic and axialitic morphology is equal. Different mechanism have been reported[21] to explain axialitic and spherulitic morphologies when polymers are crystallized from the melt. Axialites have been observed when the material is crystallized at low undercoolings and spherulites at larger degrees of undercooling. Here, this analogy is not observed since the 20% membrane would be comparable with a low degree of undercooling and the 32% membrane with the largest driving force for crystallization. In these cases the difference can only be explained by a large difference in nucleation density. The axialites simply cannot grow to complete spherulites.

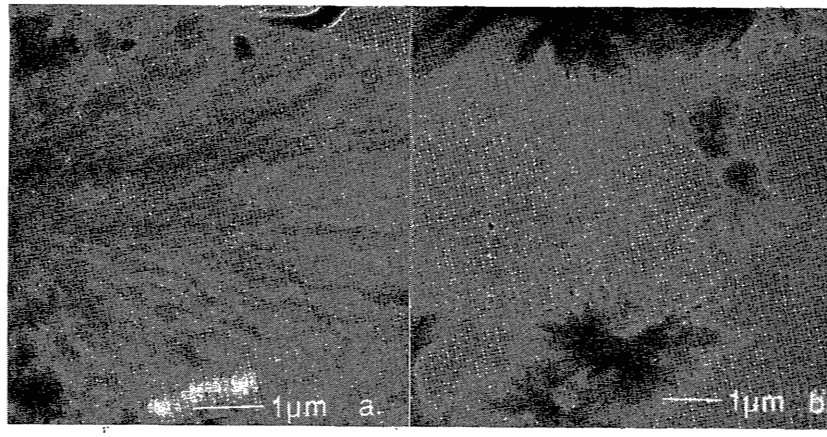

Figure 14. TEM photographs of membranes cast from a 20 wt% solution (a) and a 32 wt% solution (b).

The presence and nature of solid particles present during membrane formation has been further studied as a function of coagulation time and of the distance from the interface. The results of two casting solutions with a polymer concentration of 20 and 32 wt% are schematically shown in figure 15 and 16 respectively. TEM pictures were prepared from samples at different sites: from sites near the top-layer to sites closer to the support layer.

The transmission curves during the formation of these membranes are shown in figure 10 b and d respectively.
For the 20 wt% casting solution the first stage after 90 s shows the larger spherulites formed near the top with a size of spherulites of 5 - 15 µm, as observed in the final membrane(figure 11b). Smaller spherulites are found in the middle of the membrane, and some axialitic structures near the bottom. After 180 seconds the larger spherulites can be found deeper in the membrane and smaller spheres near the metal plate. Then after 240 s the spherulite size deeper in the film has increased and in the final stage a uniformly distributed spherulite size is observed. In combination with the light transmission profile it can be seen that after 240 s the line is bending towards a horizontal direction just at the moment that the morphology has almost reached its final state.

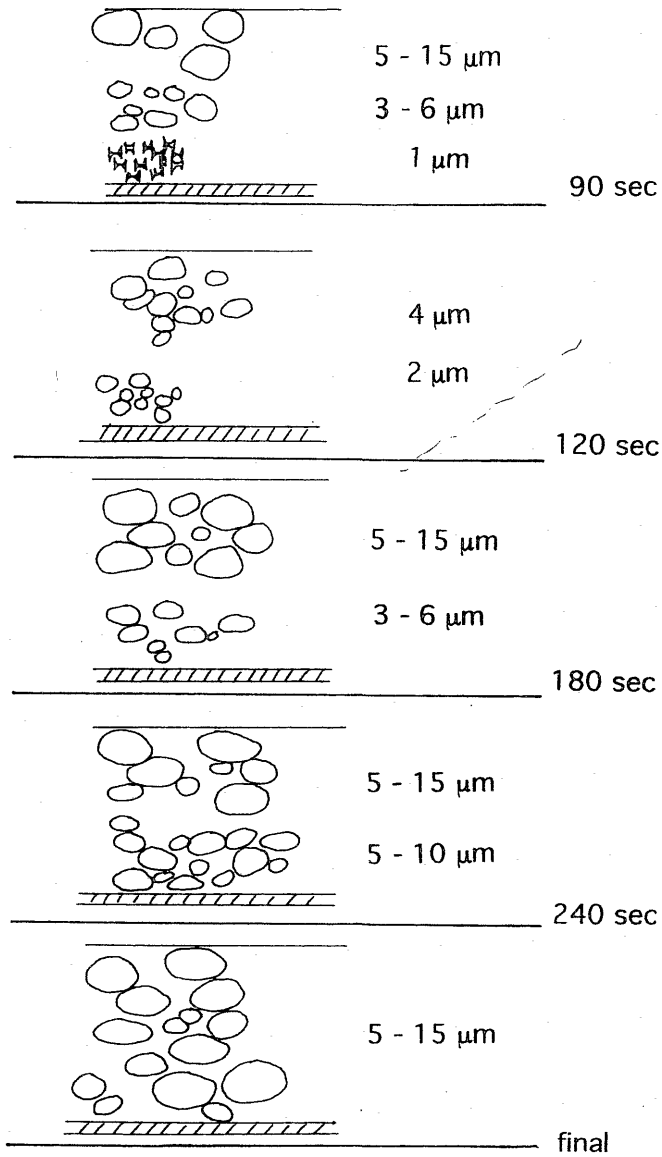

Figure 15. An overview of the results obtained from the cryo-substitution experiments with membranes cast from a 20% solution of nylon 4,6 in formic acid, with the circles representing the spherulites and the 'clock houses' representing the axialites. The sizes of the solid particles and the coagulation times are given in the right hand column.

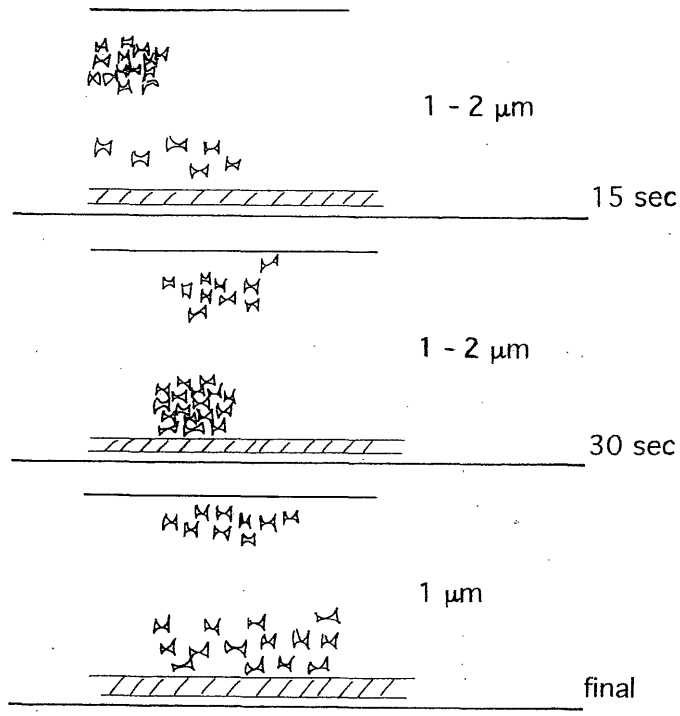

Figure 16. An overview of the results obtained from the cryo-substitution experiments with membranes cast from a 32% solution of nylon 4,6 in formic acid, with the 'clock houses' representing the axialites. The sizes of the solid particles and the coagulation times are given in the right hand column.

This uniform morphology is not a result of simultaneously nucleated and grown spherulites. During the progress of the diffusion processes nucleation takes first place near the interface. The differences in size of the spherulites in the first stages of the membrane formation process are levelled out during the later stages. The density of the spherulite population is not consistent over the whole result. This might be caused by some disturbance of the nucleation during the quenching and the substitution processes.

Phase separation in the membranes cast from a 32 wt% solution sets in during a much shorter time scale compared to a 20 wt% solution. During the membrane formation all stages show axialites through the membrane. The bottom side of the film was still 'sticky' after melting of the cryogenically frozen sample in a water bath at room temperature, which is an indication that up to 45 s demixing in the layers close to the bottom part of the film was still far from complete.

DISCUSSION

Explaining the morphology in the sub-layer formed after phase separation has set-in in the upper layers still remains a problem. A continuous 'interplay' exists between the proceeding of the phase separated layer (which is not equal to the moving diffusion front in case of delayed onset of demixing or if solid-liquid demixing takes place) and the proceeding of the diffusion pattern. A concentration profile near the growing crystals superimposed on the overall concentration profile exists. Several cases are schematically given in figure 17. The conditions at the interface of a growing crystal unit is dictated by the solid - liquid equilibrium. At the crystal-side of the interface the polymer concentration is one, at the liquid side the composition is given by a point at the crystallization line. At a semi-infinite distance from this growing surface the composition is dictated by the overall concentration profile, which continuously changes. The two cases examined with the cryo-substitution experiments will be worked out. The first one is for a spherulitic morphology; the second in case an axialitic morphology is obtained.

Spherulitic morphology

According to the results of the cryo-substitution the average rate of spherulitic growth is in the order of 2 - 5 μm/min. With a spherulite size of 10 μm it takes approximately 2 - 5 minutes before they impinge for this specific case. From the calculated concentration profiles the rate of movement of the diffusion front is in the order of 5 μm per square root of time (5 μm / $t^{-1/2}$). The layer in which phase separation sets-in will stay in a stage in which spherulites still can grow freely before they impinge after 2 to 5 minutes. With an average spherulite size of 10 μm the

nuclei, formed in earlier stages of the membrane formation process, have an average distance of 10 μm from each other. In the first stages of immersion (30s) the main part of the layer where crystallization has taken place is still in the 'homogeneous' composition dictated by the overall concentration profile (see also figure 13a.). The propagation of the concentration profiles through the film is then hardly influenced by the already started phase separation. Since the composition path of the 20% solution (case 'b' in the figures 8, 10 and 11) is already rather shallow it will become even more levelled out in time; the morphology of the final membrane can be thus expected to be quite homogeneous as indeed is observed.

Two conditions can cause spherulites to stop growing.
1. They touch upon neighboring spherulites
2. The surrounding matrix is depleted of polymer.
When spherulites impinge, it is not necessary that the growth of the spherulite completely stops. In other directions than the site of contact there would still be a possibility to continue growth.
Around the contact-points of the spherulites the crystallization process continues; the points of fusion must give the membrane its mechanical strength. It can be concluded that the growth of spherulites is ceased by the absence of more polymer molecule, because a precipitated film is porous. The entire space will not be filled up with polymeric material as is the case for crystallization from the melt.

Axialitic morphology

This morphology is observed for the membrane cast from a 32% polymer solution. Almost immediately after immersion the growth of a layer consisting of crystalline units starts. In the concentration profiles of figure 9 it can be observed that the interfacial polymer concentration is almost 50%. The concentration at the growing crystal surface, as given by the crystallization line, gives an equilibrium concentration with a lower polymer content. The high nucleation density results in growing centers that are very close to each other (see also figure 13b.).

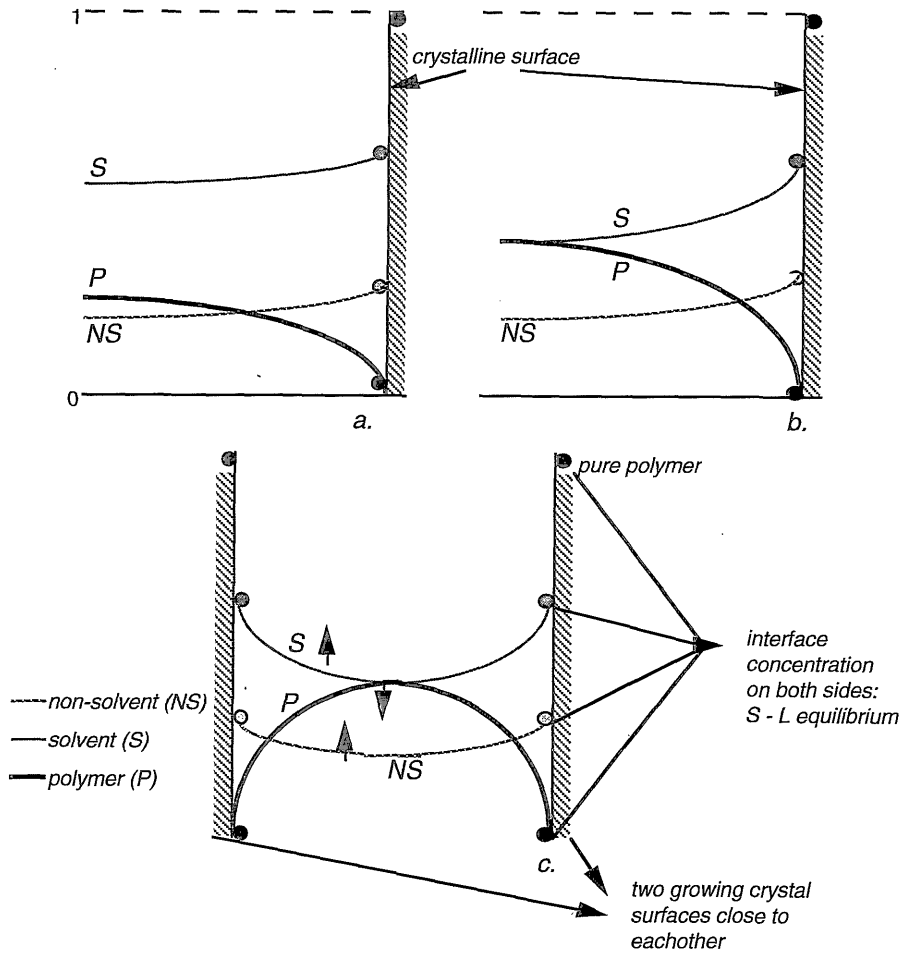

Figure 17. Concentration profiles in the presence of a growing crystal surface, with concentrations at the interface that are given by the solid - liquid equilibrium. A schematic profile for a crystalline unit grown from a film with initial polymer concentration of a.) 20%, b.) for 32% and c.) when two surfaces grow in the vicinity of each other; in the latter case the layer between the growing crystal surfaces is exhausted in polymer, therefore the solvent and non-solvent concentration will increase. This will effect the overall composition throughout the film. The local equilibria are schematically drawn on the same scale.

In figure 17c it is shown how the concentration profiles near these surfaces can no longer be considered as 'semi-infinite' in the first stages. The profiles between two growing centers are largely influenced by crystallization, and will be 'refreshed' by the newly set overall concentration profiles as given for the whole film, that on their turn are strongly influenced by these local phenomena. Polymer molecules will tend to diffuse towards growing crystal surfaces; polymer diffusion may also take place from the still homogeneous layer. Compared to diffusion of low molecular weight components, however, diffusion of macromolecules is relatively slow. In the regions between the growing crystal centers (figure 17c) both the solvent and the non-solvent concentration have increased, which will enhance solvent and non-solvent transport by an increase of driving forces. It can be considered as an iterative process each superimposed on the preceding stage. The concentration profiles can undergo iterative changes, with the initial profile, however, propagating in every stage. A steady state growth of the phase separated layer can be expected, with the upper layer, which contains in their pores only solvent and non-solvent, hardly contributing to resistance for solvent and non-solvent transport. Actually the 'porous' part of the upper layer can then be considered as part of the coagulation bath. The growth of the porous layer can be compared to a linearly grown oxidation layer, that also is porous or cracked in nature[22]. This contrary to parabolic oxidation, known from corrosion theories[21], in which the dense oxidation layer grows with the square root of time. Parabolic oxidation kinetics leads to the formation of impervious adherent oxide layer, protecting metals against further degeneration. This analogy might be of importance for formation of a porous sub-layer, when a thick skin is formed as a result of the diffusion processes.
The concentrations at which nucleation takes place are the same throughout the immersion of the film in the water bath. A sub-layer in such cases will have a isotropic morphology.

Interface & roughness of the surface of the membrane

An important characteristic of the final membrane is the morphology, i.e. roughness, of the top-layer. The typical separation properties of the membrane are determined by the pore size and the largest resistance for transport in a separation system. It is relevant to consider in more detail the mechanism of formation of this top-layer. A

crystal surface near the interface has a similar concentration profile as given in figure 17. The difference, however, is that no semi-infinite 'bulk' concentration of polymer is present. The polymer concentration must drop to zero at the interface film - bath, since the coagulation bath does not contain polymer. During growth of the crystal surface the film near the interface gradually is exhausted in polymer. Two phases, the coagulation bath and the polymer lean phase in the film with both only low molecular weight components will merge. The top-layer of the membrane is composed of surfaces that are grown in this way. Such a surface never is smooth because growing surfaces of the structural crystalline units have axialitic or spherulitic geometrical forms, that are reflected in the surface at the top. A roughness of the surface is a characteristic for membranes that are determined by crystallization or solid - liquid phase separation.

CONCLUSIONS

Mass transfer of the three components during membrane formation has been studied during the first moments of immersion of a nylon 4,6 solution in formic acid into the coagulation bath containing water. The results are related to the final state of the membrane morphology.

The types of mechanisms, delayed liquid - liquid demixing and solid - liquid demixing with an induction time, lead in most cases to a membrane with a morphology controlled by crystallization. The nucleation of crystalline material is highly dependent on the degree of supersaturation. Smaller spherulite size is a result of a larger nucleation density followed from a larger degree of supersaturation. If the supersaturation is too low crystallization of the polymer takes place after the cellular morphology was formed; nuclei of a crystalline phase could not be created on a short time scale. This type of morphology then is the result of liquid - liquid phase separation.

Concentration profiles by solvent / non-solvent exchange develop more or less independently from the starting crystallization if the nucleation density is small. The flat composition paths (figure 8), which are calculated for 20 and 25% of initial

polymer concentration in the film, give rise to an isotropic morphology in the final membrane. Cryo-substitution experiments show that the nucleation of a crystalline phase and the growth of spherulites continues throughout the membrane. In earlier stages a gradient in spherulite size exists, which levels out in later stages. The growth of spherulites is limited by depletion of polymer.

With a large nucleation density the concentration profiles are influenced by crystallization process. The exchange rate of solvent for non-solvent is not hindered in those layers which contain mainly low molecular weight components in the pores. Despite the fact that the calculated concentration profile for the polymer shows a rather high polymer concentration at the interface, the morphology in most parts of the membrane (the sub-layer) is more or less isotropic. A close look to the situation at the top shows a very thin denser layer (see figure 11d).

In these cases nucleation density and the existence of a steep or a flat polymer concentration profile cannot be varied independently, but are two parameters in membrane formation in which crystallization is involved.

It can be concluded that a further insight is developed in membrane formation in which crystallization is involved. The type of morphology, cellular, spherulitic or axialitic is mainly dependent on the degree of supersaturation that is a result of exchange of non-solvent and solvent. Calculation of the initial composition path is therefore an essential procedure for understanding and predicting the membrane morphology.

SYMBOLS

A	surface [m^2]
c_i	concentration component i [kg/m^3]
$\mathbb{D}$	Fickian diffusion coefficient [m^2/s]
F_3	coefficient [m^2/s]
g_{ij}	Flory-Huggins interaction parameter between the components i and j
J_i	volume flux of component i relative to the polymer volume frame of reference [m/s]
$\tilde{J}_i$	volume flux of component i relative to the fixed frame of reference [m/s]
J_i^c	mass flux of component i relative to the polymer volume frame of reference [kg/m^2 s]

L_{ij}	phenomenological coefficient for transport of i in j [kg.s/m^3]
m	place volume coordinate for the polymer volume frame of reference
M	total volume of component 3
M_2	molecular weight of component 2 [kg/mol]
NS	non-solvent
P	polymer
R	gas constant [J/mole.K]
R_{ij}	Maxwell-Stefan coefficient between component i and j [m^3/(kg.s)]
S	solvent
s_3	sedimentation coefficient [s]
t	time [s]
T	temperature [K]
V	volume [m^3]
$\overline{v}_i$	average velocity of component i relative to the fixed frame of reference [m/s]
x	coordinate in the fixed frame of reference in the film [m]
y	coordinate in the polymer volume frame of reference in the coagulation bath [m]
ϕ_i	volume fraction of component i [-]
μ_i	chemical potential of component i [J/kg = m^2/s^2]
η_i	partial specific volume of component i [m^3/kg]

indices

(1)	non-solvent; water
(2)	solvent; formic acid
(3)	polymer; nylon 4,6
(b)	coagulation bath
(f)	*film*

ACKNOWLEDGEMENTS

The authors wish to thank the Computer Information Center of the University of Twente for help with the model calculation, Dr Ir R.M. Boom for explanation and handing over the computer programs and stimulating discussions, to Mrs. Ir H. Vermeiren and Dr R. Deblieck of D.S.M. the Netherlands for their pleasant cooperation and stimulating ideas concerning the cryo-substitution experiments and to D.S.M. the Netherlands for funding of this project.

REFERENCES

1. M. H. V. Mulder, *Basic Principles of Membrane Technology,* Kluwer Dordrecht, 1991.
2. A.M.W. Bulte, B. Folkers, M.H.V. Mulder, C.A. Smolders, *J. Appl. Polym. Sci.,* 50, 13-26 (1993).
3. A.M.W. Bulte, *Equilibrium Thermodynamics of the Ternary Membrane Forming System Nylon 4,6, Formic Acid and Water, Chapter 3 of this thesis.*
4. A.J. Reuvers, J.W.A. van den Berg, C.A.Smolders, *J. Membrane Sci.,* 34, 45, 1987.
5. C. Cohen, G.B. Tanny, S. Prager, *J. Polym.Sci., Polym. Phys. Ed.,* 17, 477, 1979.
6. S.C. Tsay, A.J. McHugh, *J. Polym. Sci., Polym. Phys. Ed.,* 28, 1327 (1990).
7. Ph. Radovanovics, S.W. Thiel, S.-T. Hwang, *J. Membr.Sci.,* 65, 213, 1992.
8. K. Kimmerle, *Quantitative Betrachtung de Phaseninversionsprozesses bei der Herstellung von Membranen,* PhD thesis University of Stuttgart, 1988.
9. A.J. Reuvers, C.A. Smolders, *J. Membrane Sci.,* 34, 67, 1987.
10. D.M. Koenhen, C.A. Smolders, *J. Polym.Sci., Polym. Phys. Ed.,* 15, 155 (1977).
11. F.W. Altena, C.A. Smolders, *J. Polym. Sci., Polym. Symp.,* 69, 1 (1981).
12. J.Crank, *The Mathematics of Diffusion,* 2nd ed., Clarendon Press, Oxford, 1975.
13. A. Keller, *Philos. Mag.,* 2, 1171 (1957).
14. H.D. Keith and F.J. Padden Jr., *J. Appl. Phys.*, 34, 2409 (1963).
15. F. Khoury, E. Passaglia, *The Morphology of Crystalline Synthetic Polymers, Treatise on Solid State Chemistry, Vol. 3, Crystalline and Non-Crystalline Solids (Ed. N.B. Hannay), Chapter 6, The Morphology of Crystalline Synthetic Polymers, Plenum Press, NY,* 1976.

16. S.R. De Groot, P. Mazur, *Non-equilibrium thermodynamics*, North-Holland Publ. Co., Amsterdam, 1962.

17. R.M. Boom, *Mass Transfer and Thermodynamics during Immersion Precipitation for a Four-Component System with Two Polymers, PhD thesis,* University of Twente, Chapter 3, Enschede, 1992.

18. E.D. Snijders, M.J.M. ter Hiele, van Swaay, submitted to AIChE Journal, 1993.

19. J. Brandrup, E.H. Immergut, *Polymer Handbook,* 3rd ed., Wiley, NY (1989).

20. A.M.W. Bulte, *Diffusion Induced Phase Separation with Crystallizable Nylons; II Kinetic and Thermodynamic Parameters for Membrane Formation,* Chapter 5 of this thesis. (1993).

21. J.D. Hoffman, G.Th. Davis, J.I. Lauritzen, Jr., *The Rate of Crystallization of Linear Polymers with Chain Folding, Treatise on Solid State Chemistry, Vol. 3, Crystalline and Non-Crystalline Solids (Ed. N.B. Hannay), Chapter 6, The Morphology of Crystalline Synthetic Polymers,* Plenum Press, NY, 1976.

22. P.J. Gellings, *Introduction to Corrosion Prevention and Control,* Delft University Press, Delft, 1985.

CHAPTER 5

Diffusion Induced Phase Separation with Crystallizable Nylons; II Kinetic and Thermodynamic Parameters for Membrane Formation with Nylon 4,6

A.M.W. Bulte, B. Folkers, M.H.V. Mulder,
C.A. Smolders, H. Strathmann

SYNOPSIS

The effects of changes in the membrane forming parameters for the preparation of phase inversion membranes on the mass transfer processes that take place during the first moments of immersion were studied. It was found that the membrane morphology is mainly determined by the degree of supersaturation with respect to crystallization. Not only thermodynamic factors not only determined the morphology. Also the composition of the initial casting solution seems to be a parameter for the nucleation of crystalline material.

INTRODUCTION

Specific membrane applications require membranes with optimal separation characteristics. Frequently the optimal casting conditions for a phase inversion membrane with desirable separation properties have been found empirically. It is difficult to oversee all the effects the change of one parameter has on the final morphology of a membrane. From the early start of membrane preparation by means of phase inversion[1] several attempts have been made in order to obtain more insight in this process of diffusion induced phase separation[2-7]. Structural morphology of the membrane can be related to predictions made from the model.
The model developed by Reuvers and Smolders[4] allows to predict qualitatively the

type of demixing process and consequently the membrane morphology. Two general types of demixing processes can be distinguished when only liquid - liquid demixing occurs: (i) instantaneous demixing and (ii) delayed onset of demixing. In the first case generally an ultrafiltration membrane is obtained with a porous skin; the second type of membrane has a gas tight skin with a porous support. Reuvers[4] showed that the choice of solvent - non-solvent pair was the most important parameter. Several improvements on the model have been made[6,9] which allows a better description of the mass transfer during the immersion precipitation process in later stages. The authors claim that the polymer concentration at the interface decreases after a longer immersion time.

For a system in which a semi-crystalline polymer is used, crystallization may take place as the dominating phase separation process, depending on the thermodynamic and kinetic properties. It has been shown that for the ternary membrane forming system nylon 4,6, formic acid and water, crystallization or solid - liquid demixing is the thermodynamically favorable process[10]; the thermodynamics of this ternary system is given in figure 1.[10]. Also for other polymers used in order to prepare phase inversion membranes such a thermodynamic situation is reported[11,12].

In order to describe mass transfer in systems in which crystallization is involved some assumptions are necessary concerning the local equilibrium at the interface[13]. It has been discussed how in the first moments of immersion local interface concentrations are given by some tie-lines on the thermodynamically virtual binodal. Crystallization of the polymer only occurs after an induction time, and will only set in if a certain degree of supersaturation has been created by diffusion.

In chapter 4 of this thesis[13] two characteristics have been discussed leading to the final morphology of the membrane: 1. the diffusion profile, 2. nucleation density and crystallization kinetics. It has been shown that both are related to each other and cannot be changed independently[13]. The relation between the membrane forming parameters, the kinetically determined parameters and the final membrane morphology is schematically given in figure 2.

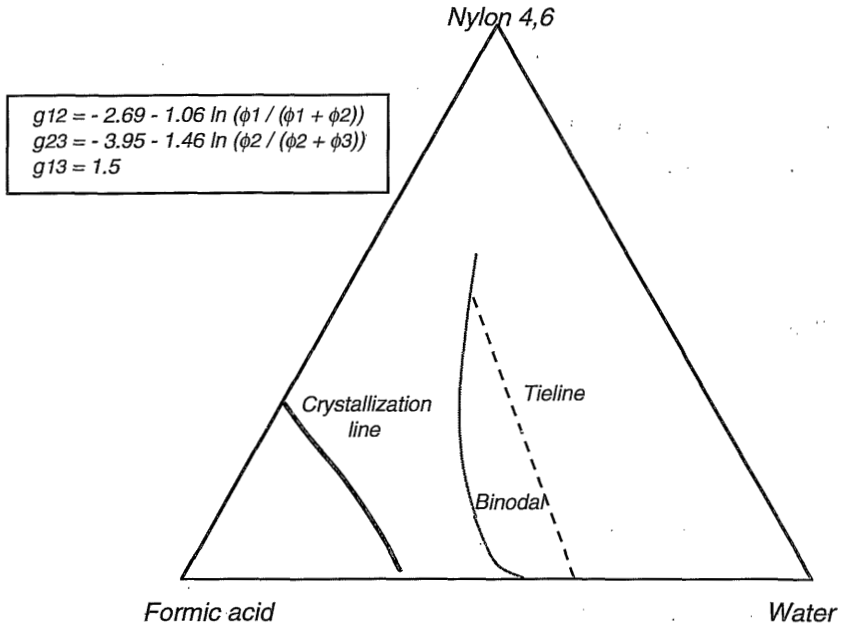

Figure 1. (Phase) diagram of the ternary membrane forming system nylon 4,6, formic acid and water[10].

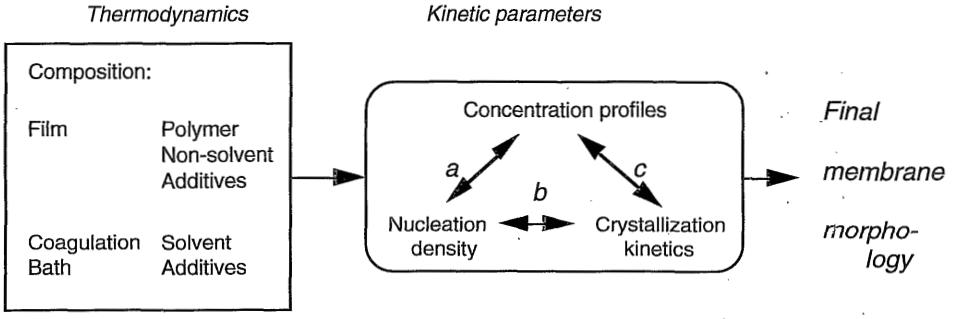

Figure 2. Thermodynamic and kinetic parameters following from the choice of the membrane forming system.The choice of the polymer system determines the final membrane morphology according to the indicated pathway.

In this paper it will be shown how the thermodynamics are correlated to the kinetic parameters. In this chapter particularly the relation between the concentration profiles and the nucleation density will be emphasized. Since the crystallization kinetics very often depends on the type of polymer a comparison of results with other aliphatic polyamides will be described.

THEORY

Concentration profiles

In immersion precipitation an interface has been created between the polymer solution and the non-solvent bath. A driving force has been generated, since there is a chemical potential difference across the interface for each component. After immersion a local equilibrium is assumed (the values for the chemical potential at both sides of the interface are equal). Gradients in chemical potential cause propagation of diffusion of solvent and non-solvent until the final membrane has been formed.
The composition path as it is calculated according to the model of Reuvers and Smolders[4] gives the compositions for polymer, non-solvent and solvent.
It has been shown[8] that an increase in polymer concentration together with a delayed type of demixing resulted in a membrane morphology with a gas tight skin. For the instantaneous type of demixing very often an increase in polymer concentration at the interface has been observed resulting in a skinned ultrafiltration type of membrane. For the present system membranes with a tight skin could not be prepared. Mainly microfiltration membranes have been prepared[14], in which crystallization plays a dominant role. The concentration of polymer near the interface is important for the morphology of the separating skin.
In a thermodynamic situation that predicts crystallization to take place preferably the polymer concentration near the interface not only is important for the morphology of the skin, but also gives rise to a certain degree of supersaturation towards crystallization. This degree of supersaturation is one of the factors that determines the morphology. A large degree results in an axialitic morphology, whereas a smaller degree of supersaturation leads to a spherulitic morphology[13]. In case the degree of

supersaturation is very low even liquid - liquid demixing is competitive[13,14].

Consequences for the final morphology are due to the differences in profiles:
1. Is a composition path of the delayed type or not. The question is if crystallization or solid - liquid demixing is competitive if instantaneous demixing occurs.
2. The steepness of the composition path leads to a certain degree of supersaturation, the more the profile tends to a larger interfacial polymer concentration the larger the degree of supersaturation is. More and smaller structural units in the final membrane can be observed and spherulites will be smaller or even remain in the axialitic form.
3. The steepness of the composition path and thus the polymer concentration at the interface together with a certain delay time dependent on the crystallization kinetics may give a membrane with a skin. The interfacial polymer concentration is related to the final membrane morphology.

Nucleation density and crystallization kinetics

The term nucleation density comes from theories developed for crystallization from the melt[15]. It gives a phenomenological value that can directly be obtained from electron micrographs of the samples. Nucleation density is defined as the total number of nuclei (N) formed per unit of volume as has been shown recently[14]. It gives the total number of structural units (axialites of spherulites) assuming that one nucleus grows out into one structural unit. The more nuclei are being created the smaller are the structural crystalline units in the membrane.
The nucleation density is a function of supersaturation, type of polymer and eventually seeding or heterogeneous nucleation.
Nucleation density must not be confused with the nucleation frequency. The latter parameter is the number of nuclei created per unit of volume per unit of time. A high nucleation density can be a result of a large nucleation frequency and a moderate growth or a moderate nucleation frequency with a slow nucleus growth. In the latter case there is a longer time available for still non-crystallized polymer molecules to create new nuclei. The integral of nucleation frequency (as a function of time) in time is equal to the nucleation density.

Crystallization from the melt

Spherulitic crystallization is the dominant morphological characteristic when polymers are crystallized from the melt[15]. Spherulites in polymers are generally microscopic in size (100 μm or less in diameter). The size of the spherulites grown is generally dependent on the magnitude of the undercooling, since at high undercooling more nuclei are formed per unit volume. The degree of undercooling reflects the difference between the equilibrium melting temperature and the crystallization temperature and is usually set at 20 to 150 °C. The morphology of a material crystallized from the melt is not a porous one. The entire space will be filled up with polymeric material.

A similar degree of undercooling for different polymers does not necessarily indicate that the nucleation density will be equal. The critical nucleus size for example is also dependent on the lateral surface free energy and the fold surface free energy[16]. These values can be considered as material characteristics and hence the nucleation density also is dependent on the choice of the system.

Crystallization in a binary situation

Lloyd and coworkers have reported the influence of crystallization on the membrane morphology in a number of papers[17-24]. The systems studied were: polyethylene and isotactic polypropylene in mineral oil, isotactic polypropylene in tetradecane (C14), eicosane (C20) and dotriacontane (C32) as aliphatic hydrocarbons and pentadecanoic acid and eicosanoic acid as fatty acids. In the studied systems both liquid - liquid phase separation and solid - liquid phase separation can occur, as well as crystallization from the diluent phase. If the morphology of the film resulted from nucleation and growth of the polymer lean phase or of spinodal decomposition the vitrification of the film was caused by crystallization. A spherulitic structure has been reported to superimpose on an already phase separated sample[17,19].

Three of the papers are mainly focussed on spherulitic crystallization of isotactic polypropylene in these binary cases[20,21,24]. The nucleation density has been reported to be dependent on the degree of undercooling. The spherulite size decreased with increasing undercooling both in non-isothermal and isothermal situation. The use of a nucleating agent also reduced the size of spherulites considerably. A more fundamental study on spherulitic crystallization has been published recently[24]. The spherulitic growth rate of the polymer has been studied for polymer concentrations between 10 and 100 wt%. The spherulitic growth rate at

constant crystallization temperatures is higher at higher polymer concentrations . The degree of undercooling for the cases, however, was not the same.
The morphology of the films in all cases was a porous one. The remaining diluent phase was extracted from the films, leaving the porous matrix as the final membrane. Unlike the situation from the melt spherulites can impinge or form interspherulitic lamellae, so that material between spherulites is interconnected, giving the membrane its mechanical strength. Spherulites grown in the presence of a diluent phase leave porosity inside the spherulites and between the spherulites.

Crystallization in a ternary (isothermal) system

For a binary system nucleation is a result of the undercooling or the rate of cooling. For an immersion precipitation process in a ternary system supersaturation is the result of diffusion processes. It is clear that a relationship exists between nucleation density and the composition profile. (see figure 2 relation a.; the creation of thermodynamic driving forces for crystallization). Two other factors (kinetic factors for nucleation and growth) are: 1. the ability of the polymer to rearrange into the necessary critical nucleus size and 2. heterogeneous nucleation or seeding.

Crystallization kinetics

Nucleation density and crystallization kinetics are closely related. The description of crystallization in kinetic terms is a more fundamental approach. Usually crystallization involves the nucleation and growth of polymer molecules into an ordered crystal lattice.

The nucleation of a nucleus depends on
1. The thermodynamic driving force. Nuclei with a size larger than the critical nucleus size are called stable nuclei. The free enthalpy barrier to crystallization can only be overcome by local random fluctuations. The larger the required size of the nucleus, the longer will be the time needed for the nucleation process, and the smaller is the nucleation frequency. The critical lamella thickness, l, is related to the surface free energy, σ, the melting temperature T_m, the heat of fusion, Δh_f, the undercooling, $\Delta T=T_m-T$, and the density, ρ, according to:

$$l = 2\,\sigma_e T_m / (\Delta h_f \Delta T\,\rho) + \delta l$$

with the free surface energy σ_e at the folding ends (see also figure 3). With typical values T_m =600K, Δh_f = 200 J/g, ρ = 1 g/cm^3, σ_e = 100 10^{-3}N / m and δl =4 nm, the critical dimensions are e.g. 600, 60, 28, 16, 10 and 8 nm for undercoolings of 1, 10, 25, 50, 100 and 150 °C respectively.

At low undercoolings relatively thick lamellae must be created in order to allow continuation of crystallization. The larger the degree of undercooling (supersaturation) is, the smaller the required critical nucleus size. With increasing undercooling the probability an embryo grows out is much larger. This factor again determines the relation 'a' in figure 2.

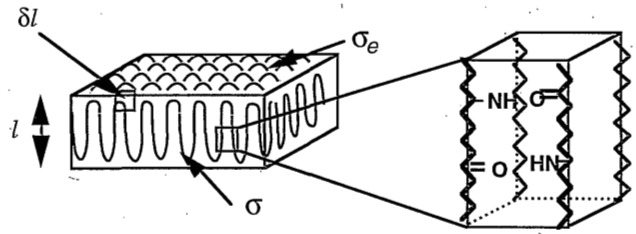

Figure 3. Folded chains in a crystalline structure with the folded surface free energy, σ_e, and the lateral free energy, σ; δl is the size necessary for the fold (left-hand side), and a schematic unit cell for a nylon (right-hand side).

2. The surface free energies, σ_e and σ (see figure 3) are other factors involved in nucleation.(The lateral free energy of a lamellae, σ is in the order of 10 10^{-3}N / m and will not be of first influence for nucleation.) The folded surface free energy, σ_e, is a material property depending on the choice of the system.

3. The ability of a polymer molecule to rearrange in an ordered embryonic structure during the creation of the nucleus.

The growth of a nucleus depends on

1. The thermodynamic driving force (or supersaturation).

2. The ability of a polymer chain to reorganize into an ordered structure. In this factor chain regularity and chain flexibility is involved.

3. The possibilities and restrictions of the polymer molecules to move towards the growing crystal side by reptation. This diffusion of polymer is not the rate limiting

step for the growth of the crystalline entities when spherulites are grown from the melt at moderate temperatures. It is limited by the 'surface reaction' or the reorganization of the polymer chain at the interface. It has been observed in several studies on spherulitic crystallization[16,17] that the radius of the spherulites increases linearly with time during growth. Different mechanisms of spherulitic crystallization have been reported, with either the evolution of a crystalline entity to a symmetrical spherulite or the occurrence of incompletely grown units that stop growing before they attain the spherically symmetric growth stage. When crystallized from the melt an axialitic morphology results from a change in mechanism, that has specifically been worked out for polyethylene[25].

4. The viscosity of the still amorphous phase. When polymers are crystallized at temperatures close to or beneath the glass transition temperature, reptation diffusion of polymer molecules will become a rate limiting step for crystallization, resulting in a dramatically decreasing crystallization rate. Hoffmann et al.[16] express the influence of reptation of polymer molecules as a function of temperature in a retardation factor, β, which governs the rate of transport of polymer molecules to the site of crystallization. Polymers can often be undercooled more than 100°C below their melting temperatures at which they become extremely viscous. β is strongly dependent on temperature; it decreases more than exponentially over 100°C and drops to very low values near the glass transition temperature. In binary or ternary systems the transport factor is mainly influenced by the total polymer concentration.

The total crystallization rate, the transition from polymers in the amorphous state to the crystalline state is a function of both nucleation and growth. The crystallization rate in systems crystallized from the melt first increases as a function of undercooling, because of a strong increase of the nucleation rate; when the crystallization temperature is further lowered, the total crystallization rate decreases again, due to the retarded transport of polymer molecules to the growing crystal site during growth. The overall crystallization rate as a function of undercooling goes through a maximum.

In binary systems, in which crystallization is also induced by a temperature step the effect of retarded diffusion of polymer molecules will influence the total crystallization rate as well when crystallized at temperatures far below the crystallization temperature. Isothermal crystallization in ternary systems, of course is

not influenced by diffusion rates as a function of temperature. In such cases transport of polymer molecules is only a function of polymer concentration.

This chapter mainly will emphasize the relation between the thermodynamic driving force (the degree of supersaturation) and nucleation density. The different morphological aspects are discussed in relation to the concentration profiles that result from diffusion of solvent and non-solvent.

EXPERIMENTAL AND CALCULATIONS

Membrane preparation

Nylon 4,6 (Stanyl KS 400), nylon 6 (Ultramid B3) and nylon 4,6 *co* 6 (Stanyl KS 611), kindly supplied by D.S.M. the Netherlands were dried *in vacuo* for at least 24 hours at 70°C for nylon 4,6 and the copolymer and 30°C for nylon 6 and dissolved in formic acid (Merck analytical grade 98%) in a concentration range of 15 to 32 wt%. Formic acid was used without further purification. Polymer solutions were cast on a glass plate with a thickness of 0.3 mm. The glass plate with the cast polymer solution was immediately immersed in a coagulation bath, containing water and 0 to 50 vol% of formic acid. After a sufficient coagulation time (15 - 30 minutes) the membranes were removed from the glass plate, rolled in filter paper and washed with demineralized water for at least 24 hours.
The morphology of the membranes was examined by Scanning Electron Microscopy (Jeol JSM T 220A). The samples were wetted in ethanol, cryogenically broken and dried *in vacuo* for at least 6 hours. A thin layer of gold was deposited on top of the sample with a Balzer Union SCD 040 sputtering apparatus (sputtering conditions: 25 mA for 2 minutes).

Calculation procedure

The method of Reuvers and Smolders is used[4] for calculation of the composition paths and the concentration profiles and adapted to the situation in which crystallization is involved as has been described in a preceding paper[13]. The thermodynamics of this system has been described recently[10]. Isotherms in the ternary system at various temperatures can be derived from the experimental data. and the temperature belonging to the interface concentration is so calculated from the Flory - Huggins equations and melting point depression relations[10]. The diffusion induced degree of supersaturation can be expressed as an undercooling, which is given by the difference between the *(virtual) temperature* of points on the composition path and the actual temperature at which membrane formation takes place (30°C). When the calculated temperatures are located above 100°C, the boiling points of formic acid and water, these temperatures must be considered as virtual.

Composition paths for the systems nylon 6, formic acid and water, and nylon 4,6*co*6 (a copolymer of nylon 4,6 and 6 containing 95% of nylon 4, units), formic acid and water are calculated using the derived thermodynamic relations for these systems[10] and somewhat lower (friction) coefficients, since the viscosity of the solutions was experimentally found to be a factor 2 to 3 lower. The diffusivity factor F as described by Reuvers[4] used to derive the phenomenological coefficient for polymer in solvent is given by for the copolymer: $0.9*10\text{^}(-8*2.97\phi_3)$, and for nylon 6: $1.9*10\text{^}(-8*2.97\phi_3)$[13]. The same concentration dependency as for nylon 4,6 was assumed, only the absolute values are a factor 2 - 3 larger.

RESULTS AND DISCUSSION

Effect of the initial polymer concentration

This effect has been described in chapter 4 of this thesis. An increase of the polymer concentration in the starting solution leads to a larger concentration at the interface. At low initial concentrations a cellular membrane morphology is obtained, whereas at

medium concentrations spherulitic structures are found. The higher polymer concentrations give membranes with an axialitic morphology[13,14], as a result of a larger degree of supersaturation The same mechanism for crystallization is valid for both the spherulitic and the axialitic morphology[13].

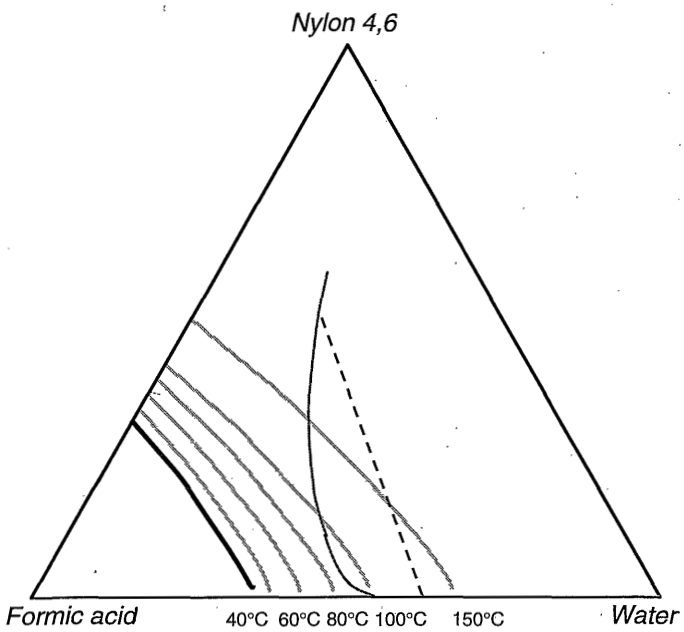

Figure 4. Calculated (virtual) isotherms for the crystallization lines and the binodal curve at 30°C from the ternary system nylon 4,6, formic acid and water[10].

In order to correlate the concentration profile with the nucleation density, the (virtual) melting temperatures belonging to the points on the composition paths can be calculated according to the melting point depression relation as was described previously[10]. With the same data for the thermodynamic Flory-Huggins interaction parameters an equilibrium temperature can be calculated. The difference between this temperature and the isotherm at 30°C, at which these diffusion processes take place, gives some indication of the magnitude of supersaturation which is expressed here as a degree of undercooling (the difference between the calculated (virtual) melting temperature and the temperature of 30°C, see figure 4).
The supersaturation can also be expressed in terms of a chemical potential difference.

Using a (virtual) melting temperature, however, could give more insight and makes comparison to a situation with crystallization from the melt possible.
By comparing all the corresponding (virtual) melting temperatures of a composition path it is found that the closer a point is located near the interface the higher is its temperature, i.e. the larger is the undercooling. The point at the virtual binodal has the largest degree of undercooling, even for the cases in which the polymer concentration decreases. The (virtual) temperature at the interface is taken as a first indication of the degree of undercooling. The relation between the nucleation density, described in earlier work[14], and the interfacial equilibrium melting temperature minus the 30°C isotherm is given in table 1.

It can be concluded that the larger the degree of undercooling the finer is the membrane structure. Whether the nucleation density is a result of a larger nucleation frequency can only be concluded if compared with other situations.

Effect of addition of non-solvent to the casting solution

The effect of adding water to the casting solution follows a similar trend as is found for the effect of different initial polymer concentrations as can be seen in table 1. The final morphology of the membranes was studied in earlier work[14]. Addition of non-solvent to the casting solution gives rise to an increase of polymer concentration at the interface (see figure 5). Larger polymer concentrations at the interface and as a result a larger degree of supersaturation ('undercooling'), when more water to the initial solution has been added, gives a larger nucleation density and a shift from a spherulitic morphology to an axialitic structure. The changes in composition paths are comparable to the results found by Reuvers[8].
The calculations predict a shift from a delayed type of demixing to instantaneous demixing (see figure 5). The morphology observed in the final membrane is still controlled by crystallization and clear experimental evidence for the occurence of a first instantaneous L-L demixing cannot be given. It cannot be excluded, however, that liquid - liquid demixing can take place as a first step, followed by the nucleation of crystalline nuclei in a much larger density compared to the nuclei of the polymer lean phase a few moments later.

Table 1. The relation between the nucleation density in number (N) per μm^2 found on a scanning electron micrograph and the calculated (virtual) melting temperature; as a function of a: initial polymer concentration b: initial water concentration in the film with a polymer concentration of 15% and c: initial water concentration in the film with an initial polymer concentration of 25% [10,14]. The effective undercooling is the (virtual) melting temperature minus 30°C.

a.

Initial Polymer concentration (%)	Nucleation density (N /μm^2)	(Virtual) Melting Temperature (°C)	Effective Undercooling (°C)
15	0.02 (L-L)	80 - 100	50 - 70
20	0.02	100	70
25	0.04	150	120
32	1.2	200	170

b.

Initial Water concentration in film (%)	Nucleation density (N /μm^2)	Virtual Melting Temperature (°C)	Effective Undercooling (°C)
0	0.02 (L-L)	80 - 100	50 - 70
5	0.05	80 - 100	50 - 70
10	0.1	100	70
15	1.0	120	90

c.

Initial Water concentration in film (%)	Nucleation density (N /μm^2)	Virtual Melting Temperature (°C)	Effective Undercooling (°C)
0	0.04	150	120
5	0.3	170	140
10	1.0	190	170

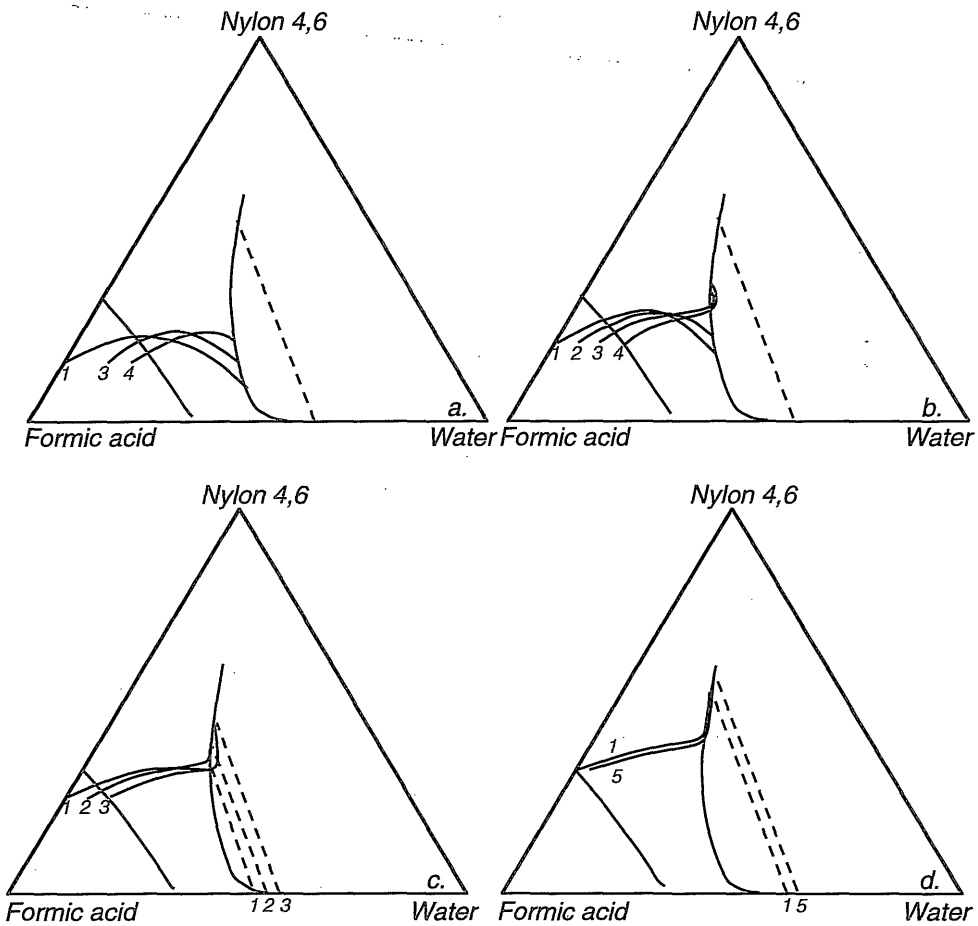

Figure 5. Composition paths for films with an initial polymer concentration of a: 15%, b: 20%, c: 25% and d: 32% with increasing water content in the initial solution 1) 0%, 2) 5%, 3) 10%, 4) 15% and 5) 3% of water. The thick drawn line is the crystallization curve, the dashed line the binodal with tielines and the dotted lines are the composition paths.

The final morphology is overruled by the growth of the crystalline nuclei into axialites. In the case of membrane formation from a 20% and 25% polymer solutions to which 10% water was added, an axialitic morphology is observed[14]. A higher polymer concentration at the interface will give a membrane with a smaller pore size and smaller water fluxes[14].

The effect of addition of solvent to the coagulation bath

The effect of solvent addition to the bath is investigated for two systems. The first one is a 25% polymer solution with a spherulitic morphology when immersed in pure water. The second system is a 25% polymer solution with the addition of 10% of water with an axialitic morphology after coagulation in a water bath. The composition paths are shown in figure 6 for coagulation baths containing 0 - 40% formic acid. The final morphology of the membranes is shown in figures 7a and b.

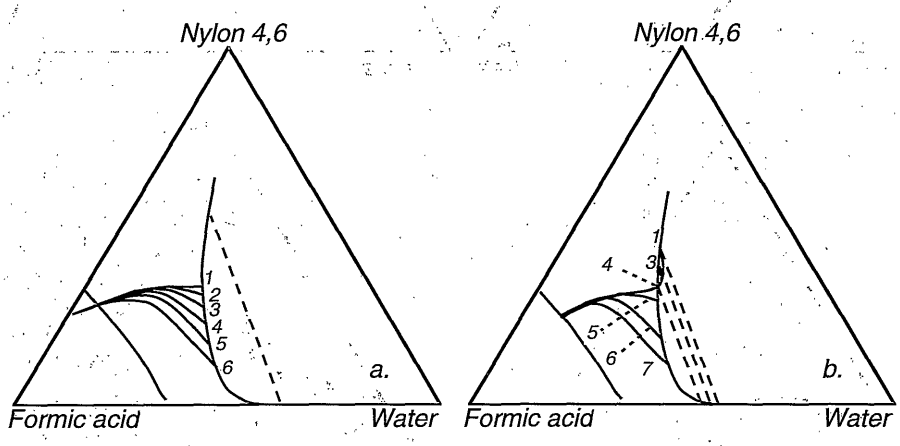

Figure 6. Composition paths for (a) a film with an initial polymer concentration of 25% and (b) a film with an initial concentration of 25% polymer solution and 10% water both immersed in a coagulation bath containing water and: 1) 0% 2) 5% 3) 10% 4) 15% 5)20% 6) 30% and 7) 40% of formic acid.Crystallization line and binodal are given according to reference 10.

Light transmission through the film, recorded during membrane formation, gives information about the moment turbidity sets in, i.e. direct data of the delay times are obtained. The light transmission profiles for the two systems, a 25% polymer solution and a 25% polymer solution with 10% of water both coagulated in a bath containing various concentrations of solvent, are shown in figure 8.

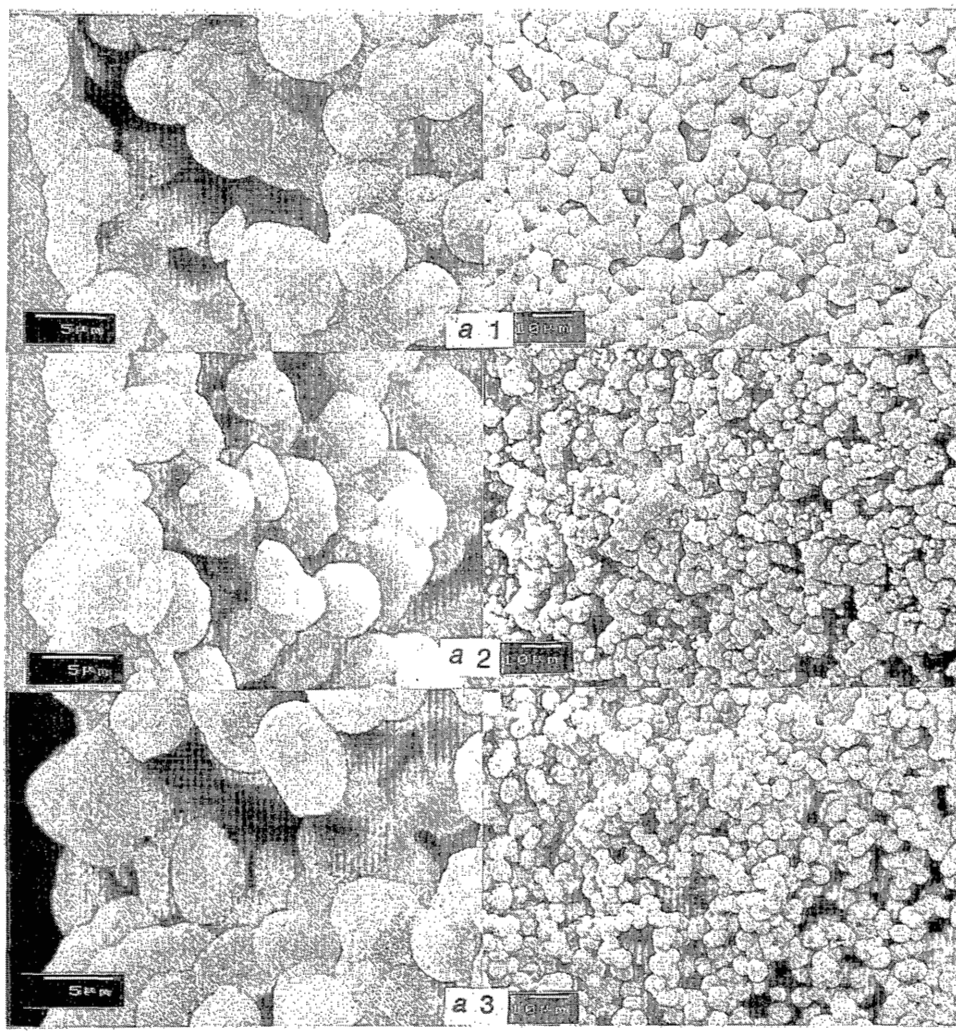

Figure 7a. Final morphology of the cross-section (left-handed) and the surface (right-handed) observed with scanning electron microscopy for a film with an initial concentration of 25% polymer solution immersed in a coagulation bath containing water and: 1) 0% 2) 15% 3) 30% of formic acid.

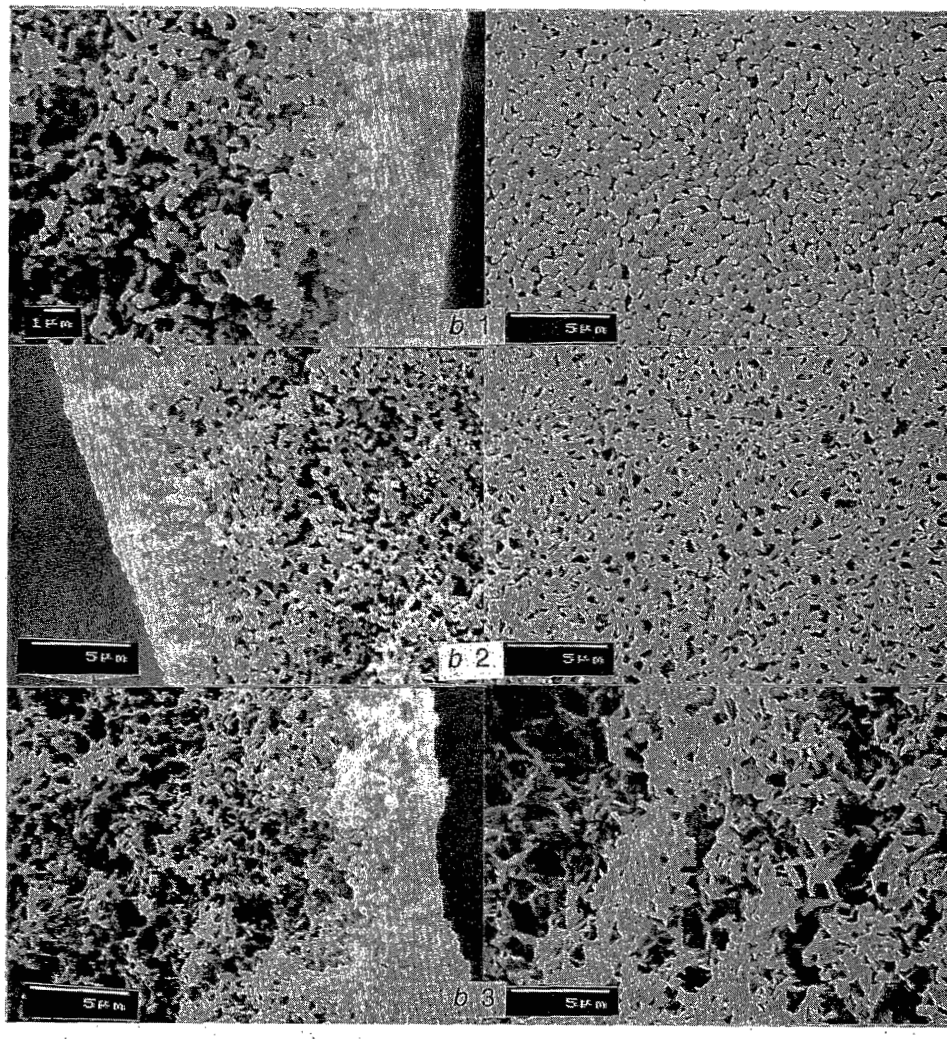

Figure 7b. Final morphology of the cross-section (left-handed) and the surface (right-handed) observed with scanning electron microscopy for a film with an initial concentration of 25% polymer solution and 10% water immersed in a coagulation bath containing water and: 1) 0% 2) 25% 3) 40% of formic acid.

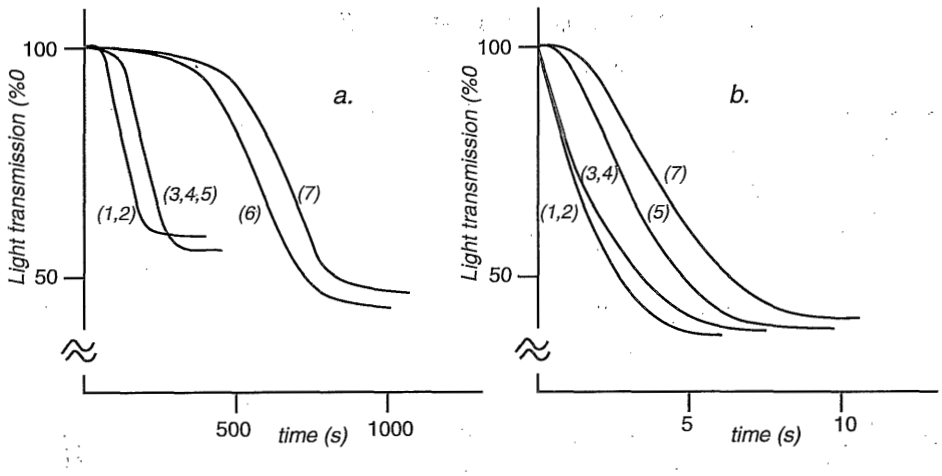

Figure 8. Light transmission profiles during membrane formation for films with (a) an initial polymer concentration of 25% and (b) an initial concentration of 25% polymer solution and 10% water both immersed in a coagulation bath containing water and: 1) 0% 2) 5% 3) 10% 4) 15% 5)20% 6) 30% and 7) 40% of formic acid.

The more solvent is added to the coagulation bath the slower is the coagulation process. In addition the interfacial polymer concentration drops. The film cast from a 25% of polymer solution already showed a delay time[13]. Upon addition of solvent in the bath the delay time (figure 8a) increases furthermore. An immediate turbidity occurred upon immersion of a films with a casting solution containing 25% of polymer and 10% of water in a coagulation bath containing 0 - 15 % of solvent. A shift from an instantaneous demixing to a delayed type of demixing was calculated from the mass transfer equations (compare cases 4 and 5 in figure 6b) This shift corresponds to the light transmission profiles (figure 8b), in which case '4' shows an immediate decrease in light transmission and case '5' shows a delay time. A change from instantaneous to delayed demixing may be correlated with an induction time in the light transmission experiments. In the morphology, however, no clear changes are observed. Whether the immediate occurrence of turbidity in the film is caused by an instantaneous type of L-L demixing or by crystallization (S-L demixing) with a negligible induction time cannot be concluded from the data available.

An increase of the solvent concentration in the bath gives a gradual change from an axialitic morphology to a more 'leafy', dendritic, type. The axialites are more stretched out and show less branched crystalline entities. Such a morphology is very well known for poly(lactic acid) membranes cast from a solution in chloroform with methanol as a non-solvent[26,27].

For the two cases worked out in the figures 6 to 8 the degree of undercooling can be determined for the different concentration profiles by making use of the isotherms of figure 4. These data are given in table 2.

Table 2. Degree of undercooling as a function of solvent in the bath (a) an initial polymer concentration of 25% and (b) an initial concentration of 25% polymer solution and 10% water both immersed in a coagulation bath containing water and: 1) 0% 2) 5% 3) 10% 4) 15% 5)20% 6) 30% and 7) 40% of formic acid.

	Formic acid in bath (vol%)	Virtual Melting Temperature (°C)	Under-cooling (°C)
(1)	0	150	120
(2)	5	145	115
(3)	10	130	100
(4)	15	120	90
(5)	20	110	80
(6)	30	90	60

a.

	Formic acid in bath (vol%)	Virtual Melting Temperature (°C)	Under-cooling(°C)
(1)	0	190	160
(2)	5	180	150
(3)	10	170	140
(4)	15	155	125
(5)	20	140	110
(6)	30	110	80
(7)	40	100	70

b.

If nucleation would be only dependent on thermodynamic driving force it could be expected that the lower the degree of undercooling, the smaller is the number of nuclei. The growth rate is smaller as well since it is also dependent on the thermodynamic driving force. Generally the size of the crystalline units remains the same; a spherulite size of approximately 5 μm is observed for membranes cast from the 25% polymer solution (figure 7a) and the axialites and later dendrites for membranes cast from the 25% of polymer and 10% of water solution (figure 7b) do

not exhibit significant differences in size. The nucleation density as it can be deduced from SEM - photos (defined in reference 14) seems to remain the same. Figure 9 c and d shows a decrease of solvent flux, J_2, up to a factor 3 in the most extreme case (the non-solvent flux, J_1, is up to 15% larger) The degree of supersaturation ('undercooling') is smaller (see figure 6 and table 2) with more solvent in the bath, leading to a smaller nucleation frequency. The time available for crystallization, however, is larger (see also the declining steepness of the transmission profiles of figure 8). Nucleation density is the integral in time of the nucleation frequency (see section 'crystallization in ternary isothermal systems'), and can therefore not directly be related to the thermodynamic driving force if the crystallization time in different cases is not of the same order. Also factors, such as the total polymer concentration and the diffusivity of polymer molecules, are of importance for the nucleation frequency and nucleus growth.
It is very likely that the formation of nuclei is also controlled by the composition of the initial solution, since small precursor nuclei may already be present in the solution. The concentration of precursors can very well be a function of the composition of the starting solution. It is remarkable that the sizes of the crystalline entities in the final membrane remained the same upon changing the formic acid content in the coagulation bath. It was indeed observed that conditions for the preparation of the polymer solution were of influence for the reproducibility of membrane formation.

It can be observed in figure 9 that the solvent flux into the coagulation bath drops drastically with increasing content of formic acid in the bath. At the same time it is possible that the water fluxes increase as a result of the lower dragging forces of the solvent velocities. For this reason the interfacial polymer concentration is lower the more solvent is present in the coagulation bath. This can also be observed from scanning electron micrographs (see figure 7). The crystalline units are more and more loosely packed and finally the film degenerates to a compact powder, from which the surface is easily removed.

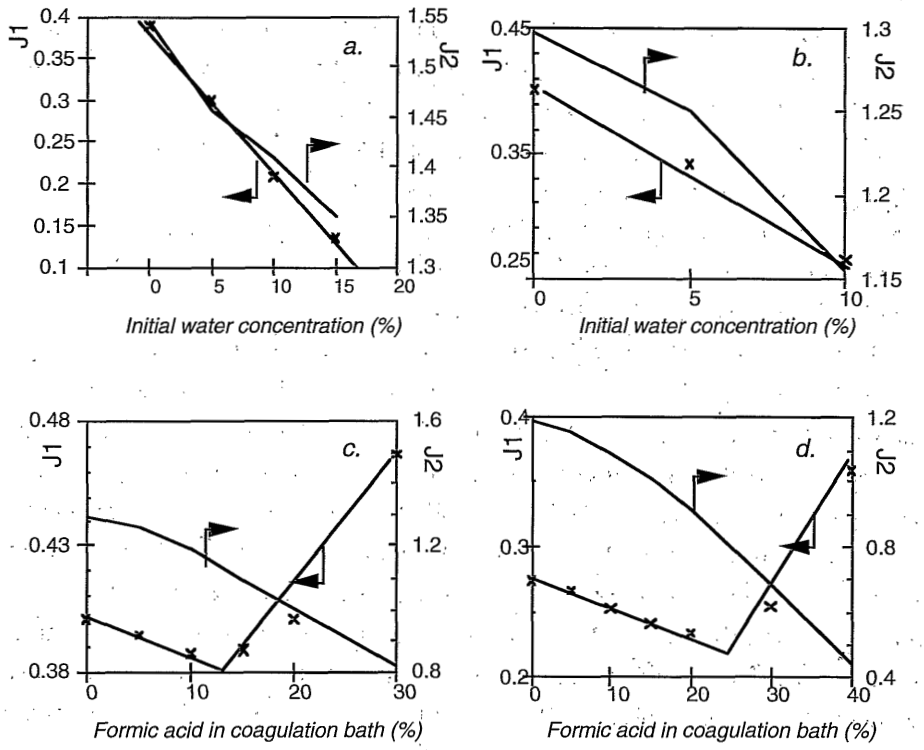

Figure 9. Calculated non-solvent flux (J_1) and solvent flux (J_2) in 10^{-9}m/s during the first second of immersion for films with the following initial concentrations: a) 20% with various non-solvent concentrations, b) 25% polymer and various non-solvent concentrations, c) 25% polymer and 0% non-solvent, d) 25% polymer and 10% of non-solvent; in the cases c and d the content of formic acid in the bath is varied.

Nylon 4,6 compared to nylon 6 and nylon 4,6 co 6

The composition paths for the 32% solutions of nylon 6 and nylon 4,6*co*6 copolymer are given in figure 10. It was found[28] that both systems gave delayed onset of demixing. Also the calculated concentration profiles show a delayed type of

phase separation. The morphology of the membranes cast from a 32% solution of both polymers is shown in figure 11.
For nylon 6 a cellular morphology occurred. Apparently the degree of supersaturation for crystallization is not large enough. The delayed character of the demixing promotes the evolution of a skin. Crystallization only takes place after nucleation and growth of a polymer lean phase. The location of the binodal closer to the crystallization line[10] compared to the situation for nylon 4,6 determined this behavior. A direct comparison between the crystallization kinetics of nylon 6 and nylon 4,6 is not possible in this case, since the changes in thermodynamics and mass transfer already give rise to completely different situations.
The membranes cast from a nylon 4,6 *co* 6 solution (32%) give a spherulitic morphology in the sub-layer. The delayed character of this phase separation process leads to the evolution of a skin. In this densified skin also spherulites, with a similar size as it is found in the sublayer, can be observed. The binodals of nylon 4,6 and nylon 4,6 *co* 6 are rather close[10]. The crystallization line for the copolymer, however, is located more into the direction of the polymer - non-solvent axis (the homogeneous region is larger). This means that relative to the case of nylon 4,6 the copolymer exhibits a smaller degree of supersaturation upon immersion compared to nylon 4,6. The location of the binodals of both systems do not differ much; as a result the distance between crystallization line and binodal is smaller for the copolymer. This 'distance' determines the magnitude of supersaturation. As a result a smaller number of nuclei and thus larger crystalline entities are formed in the film leading to a membrane morphology with complete spherulites.

Liquid liquid demixing versus solid - liquid demixing

Whether solid - liquid demixing takes place or not is dependent on a number of factors:
1. Location of the equilibrium crystallization line relative to the binodal (the thermodynamics of the chosen ternary system).
2. The diffusion induced degree of supersaturation (the composition path).

If the degree of supersaturation as a result of the diffusion process is large enough

(for comparison: for crystallization from the melt a degree of supercooling of at least 30 to 50 °C is necessary) crystallization can take place. The process of crystallization and especially the nucleation, must be fast enough. For a ternary system both the polymer and the non-solvent concentration can be varied. It has been observed[10] that for samples with an equilibrium melting temperature of 80°C at least a few hours were necessary to induce crystallization at 8°C. From this observation it is not surprising that films with an initial concentration of 15% of nylon 4,6 with an interfacial concentration located on an isotherm between 80 and 100°C did not show a specific crystalline morphology.

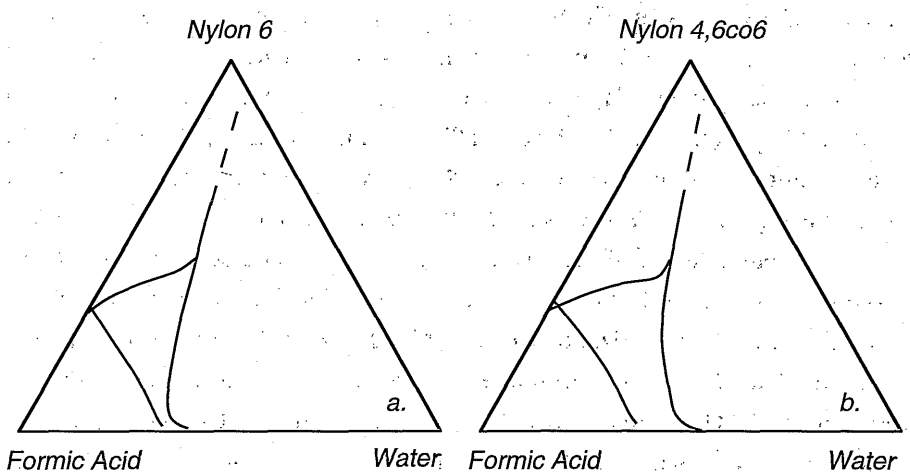

Figure 10. Composition paths for 32% polymer solutions with (a) nylon 6 and (b) nylon 4,6co6.

It cannot be excluded that instantaneous demixing occurs in the sense of liquid - liquid demixing, but that the final morphology is overruled by crystallization. It can be hypothesized that phase separation starts as liquid - liquid demixing and nuclei of a polymer lean phase are created. In the polymer rich phase crystallization can set in. A crystalline unit will stop to grow if it enters a polymer lean phase region or if no more polymer molecules are present. The resulting final morphology of the membrane shows crystalline units.

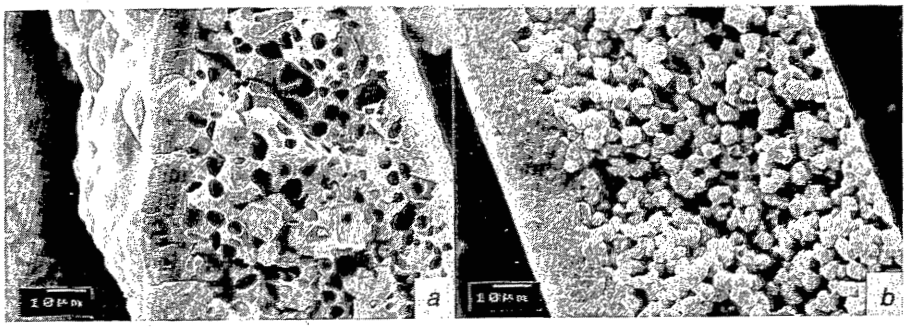

Figure 11. Final morphology observed with scanning electron microscopy for 32% polymer solutions with (a) nylon 6 and (b) nylon 4,6 co 6.

In case of a cellular morphology the degree of supersaturation was far too low to allow crystallization to take place prior to nucleation and growth of the polymer lean phase. The vitrification of the walls of the cells will occur by crystallization finally. The development of a spherulite around a polymer lean phase is schematically indicated in figure 12a. If creation of new nuclei does not occur crystallization continues by secondary nucleation onto an already growing spherulite. The effect on the final morphology can be observed in figure 12b, showing the bottom structure of a nylon 6 membrane with spherulites grown around a polymer lean phase, the pores. This phenomenon has earlier been observed also by Lloyd[17], Inaba[29] and van de Witte[30]. There is no glass transition for this ternary system at 30 °C, since a little water present has already dropped the glass transition temperature to -20°C. This is analogous to the system poly (lactic acid), dioxane and water. A membrane is never formed if amorphous poly (lactic acid) is used ; the film remains in the liquid state as a sort of stable emulsion[30].

A possible third factor determining the membrane morphology may be added now:

3. The location of the glass transition temperature.

If the composition of the film passes the glass transition temperature before crystallization sets in the cellular morphology is preserved. Some crystallization still can take place, but it is hindered because of the slower diffusion of polymer molecules in this 'frozen state'.

4. Polymer chain flexibility and chain regularity; these factors determine how easy it

is for a molecule to rearrange into an ordered folded structure. This is a last factor taken into account. It is reflected in the crystallization kinetics of a system. We observed that it was not possible to examine this factor independently, i.e. to keep the thermodynamics and mass transfer processes unchanged. It should be mentioned, however, that if diffusion of polymer molecules or the crystallization surface reaction is hindered in one way or another, the evolution of crystalline entities in the membrane morphology will not occur.

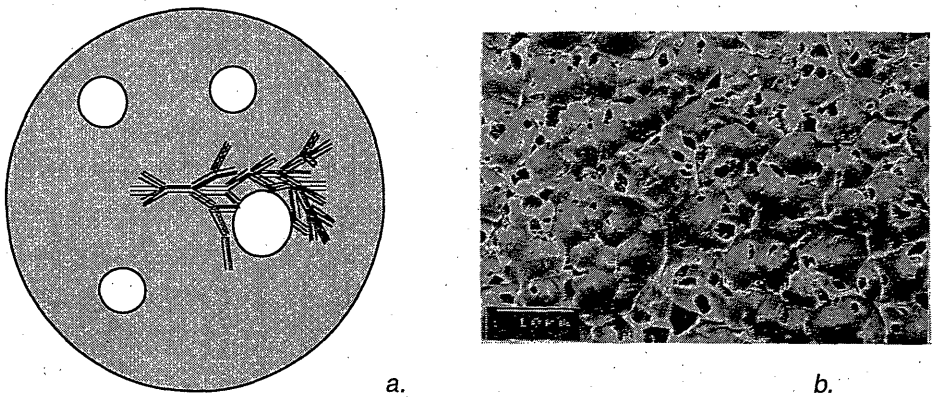

a. b.

Figure 12.(a.) Schematic drawing illustrating the development of spherulites after liquid - liquid phase separation occurred and (b.) bottom structure of a nylon 6 membrane cast from a 32% solution observed with scanning electron microscopy . The spherulites are grown around the polymer lean phase, the pores, which is not covered with gold and thus not visible in a SEM photograph.

CONCLUSIONS

Composition paths for the system nylon (nylon 4,6 nylon 4,6 *co* 6 or nylon 6), formic acid and water calculated during the first second can be related to nucleation density in the final membrane. The larger the degree of supersaturation expressed in (virtual) melting isotherms, the larger is the total number of nuclei. The total number of nuclei is not implicitly related to the supersaturation, although in most cases a good correlation was found. It was concluded that also the composition of the initial

solution influences the process of nucleation, probably by heterogeneous nucleation. Addition of water to the casting solution leads to an increase of polymer concentration at the interface. Membranes resulting from these solutions showed a skinned morphology. An increase of polymer concentration means at the same time an increase in degree of supersaturation; smaller spherulites and axialites can be found back in the structures.

Addition of formic acid to the coagulation bath resulted in a lower polymer concentration at the interface and at the same time a lower degree of supersaturation. Membranes cast with an increasing formic acid content in the bath indeed showed a morphology with a more and more open top layer. Finally the films did not have mechanical strength and a kind of powder-like film was obtained.

A shift from a delayed type of demixing to an instantaneous composition path occurred from the mass transfer calculations when the initial polymer concentration is larger or when more water was added to the casting solution. These shifts are also observed during membrane formation: immediate turbidity of films with corresponding initial compositions occurred after immersion in the water bath. Increasing the solvent content in the coagulation bath results in a shift from an immediate to a delayed occurrence of turbidity. The final morphology of the membranes, however, is only related to the degree of supersaturation. In cases of the instantaneously demixed solutions the degree of supersaturation is so large that a large number of nuclei is formed. The growth of the crystalline structures completely dominates the growth of possible nuclei of a polymer lean phase; a cellular morphology is not observed.

The effect of crystallization kinetics of three nylons, nylon 4,6 nylon 6 and a copolymer of the two could not be studied independently. We observed that the morphology was mainly determined by the thermodynamics of the three membrane forming systems.

ACKNOWLEDGEMENTS

The authors wish to thank dr ir R.M. Boom and ir E.M Naafs for the enlightening discussions, and D.S.M. the Netherlands for funding of this project.

REFERENCES

1. S. Loeb, S. Sourirajan, *Advan. Chem. Ser.*, 38, 117 (1962).
2. C. Cohen, G.B. Tanny, S. Prager, *J. Polym. Sci., Polym. Phys. Ed.*, 17, 477 (1977).
3. J. G. Wijmans, F.W. Altena, C.A. Smolders, *J. Polym. Sci., Polym. Phys. Ed.*, 22, 519 (1984).
4. A. J. Reuvers, J.W.A. van den Berg, C.A. Smolders, *J. Membr. Sci.*, 34, 45 (1987).
5. K. Kimmerle, *Quantitative Betrachtung des Phaseninversionsprozesses bei der Herstellung von Membranen, PhD thesis*, University of Stuttgart, Stuttgart, 1988.
6. A.J. McHugh, L. Yilmaz, *J. Membr. Sci.*, 43, 319 (1989).
7. Ph. Radovanovics, S.W. Thiel, S.-T. Hwang, *J. Membrane Sci.*, 65, 213 and 231 (1992).
8. A.J. Reuvers, C.A. Smolders, *J. Membr. Sci.*, 34, 67 (1987).
9. C.S. Tsay, A.J. McHugh, *J. Polym. Sci., Polym. Phys. Ed.*, 28, 1327 (1990).
10. A.M.W. Bulte, E. Naafs, F. van Eeten, M.H.V. Mulder, C.A. Smolders, H. Strathmann, *Equilibrium Thermodynamics of the Ternary Membrane Forming System Nylon, Formic Acid and Water*, Chapter 3 of this thesis.
11. W.R. Burghardt, L. Yilmaz, A.J. McHugh, *Polymer*, 28, 2085 (1987).
12. A.J. Reuvers, PhD thesis, *appendix A of Chapter 2* (1987).
13. A.M.W. Bulte, M.H.V. Mulder, C.A. Smolders, H. Strathmann, *Diffusion Induced Phase Separation with Crystallizable Nylons; I Mass Transfer Processes fro Nylon 4,6 and Relation to Final Morphology*, Chapter 4 of this thesis.
14. A.M.W. Bulte, B. Folkers, M.H.V. Mulder, C.A. Smolders, *J. Appl. Polym. Sci.*, in press 1993. (Chapter 2 of this thesis)
15. F. Khoury, E. Passaglia, *Treatise of Solid State Chemistry (Ed. N.B. Hannay), The morphology of Crystalline Synthetic Polymers*, Chapter 6, Plenum Press, NY (1977).
16. J.D. Hoffman, G.Th. Davis, J.I. Lauritzen, Jr., *Treatise of Solid State Chemistry* (Ed. N.B. Hannay), *The Rate of Crystallization of Linear Polymers with Chain Folding*, Chapter 7, Plenum Press, NY (1977).
17. D.R. Lloyd, J.W. Barlow, K.E. Kinzer, *AIChE Symposium Series*, 261, 28 (1988).
18. D.R. Lloyd, K.E. Kinzer, H. Tseng, *J. Membr. Sci.*, 52, 239 (1990).
19. D.R. Lloyd, S.S. Kim, K.E. Kinzer, *J. Membr. Sci.*, 64, 1 (1991).
20. S.S. Kim, D.R. Lloyd, *J.Membr. Sci.*, 64, 13 (1991).
21. G.B.A. Lim, S.S. Kim, Q. Ye, Y.F. Wang, D.R. Lloyd, *J.Membr. Sci.*, 64, 31 (1991).
22. S.S. Kim, G.B.A. Lim, A.A. Alwattari, Y.F. Wang, D.R. Lloyd, *J. Membr. Sci.*, 64, 41 (1991).
23. A.A. Alwattari, D.R. Lloyd, *J. Membr. Sci.*, 64, 55 (1991).
24. Y.F. Wang, D.R. Lloyd, *Polymer*, 34, 2324 (1993).
25. L.H. Sperling, *Introduction to Physical Polymer Science*, Wiley & Sons, NY, 1986.

26. H. Esselbrugge, *PhD thesis* University of Twente, Enschede The Netherlands, 1992.

27. P. van de Witte, H. Esselbrugge, A.M.P. Peters, P.J. Dijkstra, J. Feijen, R.J.J. Groenewegen, J. Smid, J. Olijslager, J.M. Schakenraad, M.J.D. Eenink, A.P. Sam, *J. Controlled. Release*, 24, 61 (1993).

28. A.M.W. Bulte, J.J. Krol, M.H.V. Mulder, C.A. Smolders, H. Strathmann, *The Influence of Blending on Structure and Performance of Nylon 4,6 Membranes*, chapter 6 of this thesis.

29. N. Inaba, T. Yamada, *Macromolecules*, 21, 407 (1988).

30. P. van de Witte, *internal communication*, University of Twente.

CHAPTER 6

The Influence of Blending on Morphology and Performance of Nylon 4,6 Membranes

A.M.W. Bulte, J.J. Krol, M.H.V. Mulder, C.A. Smolders, H. Strathmann

SYNOPSIS

The quaternary membrane forming system consisting of nylon 4,6 with either nylon 6 or a copolymer of nylon 4,6 and nylon 6 as polymers, formic acid as a solvent and water as a non-solvent was studied. The blend membranes prepared from nylon 4,6 and nylon 6 with less than 50% of nylon 6 mainly resemble the nylon 4,6 membranes, showing a thin skin and an axialitic morphology. With more than 50% of nylon 6 the membranes exhibited thick top-layers, similar to the pure nylon 6 membranes. The morphology of the sub-layer gradually changed from an axialitic to a cellular structure as a function of increasing nylon 6 content in the nylon 6 / nylon 4,6 blend membranes. The copolymer, containing 5% of nylon 6 units in the nylon 4,6 polymer chain did not influence the membrane structure unless the blend with nylon 4,6 contained more than 95% of this copolymer. The morphology then changed to a spherulitic structure with a thick top-layer.

INTRODUCTION

Nylon 4,6 shows promising characteristics as a membrane material especially in non-aqueous media. This is partly due to the high crystalline content. Previously it has been described that nylon 4,6 membranes can be prepared by immersion precipitation[1], resulting in a pore size typically in the micro- and upper ultrafiltration range with pores larger than 50 nm. In most cases crystallization plays a dominant part in the formation of nylon 4,6 membranes[1-3]. At low initial polymer

concentrations of the casting solution the 'cellular' membrane morphology is determined by liquid - liquid phase separation, whereas at higher initial polymer concentrations membranes with a typical crystalline morphology are obtained[1]. Both a spherulitic and an axialitic structure have been observed depending on the diffusion induced degree of supersaturation that occurs after immersion of the film into the non-solvent bath. A high degree of supersaturation, which typically occurs for films with a high initial polymer concentration, results in a high nucleation density. The total number of nuclei per unit of volume is so large, that the crystalline structures cannot grow to complete spherulites and an axialitic morphology is formed.
In the membrane top-layer large spherulites are present which hinder the formation of a well-defined top-layer. It appeared that the roughness of the surface is a result of the merging of the coagulation bath and the polymer lean phase around the growing spherulites[2]. These spherulites are believed to be too large to leave pores in the lower ultrafiltration range, i.e. smaller than ±50 nm.
Ultrafiltration membranes are often used as support layers in composite membranes. A good support layer should have a high permeability in order to minimize the resistance towards permeation through the composite membrane. The pore size of the support however must not be too large, otherwise no defect-free coating layer can be applied. The nylon 4,6 membranes prepared so far do not possess the requirements of an ultrafiltration membrane or support layer.

The crystallization behavior of a polymer can be considerably modified by the presence of a second (macromolecular) component. Crystallization in these blends is very complex which makes it generally difficult to predict the effect of the second component. This second component may either retard, enhance or not affect the crystallization of the polymer. The use of two crystallizable nylons for membrane formation has been described in a Domnick Hunter[4] patent. Mechanical strength of the membrane was improved, probably because a better connectivity between the crystalline units was achieved.

In this chapter the influence of the presence of a second crystallizable polymer on the formation of nylon 4,6 membranes is investigated. This work is focused on the effect of this second component on the crystallization behavior. In order to prepare a

nylon 4,6 based membrane suitable as an ultrafiltration membrane or a support layer in composite membranes especially the morphology of the top-layer must be controlled. For maintaining the nylon 4,6 properties the second polymer must also exhibit a similar chemical stability. The polymers that are chosen for blending with nylon 4,6 are nylon 6 and a nylon copolymer which consists of 95% of nylon 4,6 and 5% of nylon 6. Crystallizable nylons are chosen because the crystallinity is essential for the chemical resistance of the membranes.

THEORY

Polymer blends

In the polymeric industry an increasing diversity of polymer blends has appeared[5]. The basic reason for blending is the ability to develop materials with improved properties and performance and is mostly based on economical considerations.
Polymer blends can be classified into miscible and immiscible blends. Polymer blends are called miscible when the blend is homogeneous down to the molecular level[5].
Two polymers are miscible if their free enthalpy of mixing (ΔG_m) is smaller than zero; the free enthalpy of mixing is a result of the entropy of mixing (ΔS_m) and the enthalpy of mixing (ΔH_m) according to:

$$\Delta G_m = \Delta H_m - T\Delta S_m$$

with T representing the temperature. A negative ΔG_m can be accomplished by either a negative ΔH_m or a positive ΔS_m. In most systems in which two components are mixed the entropy change is positive. For two polymers, however, the entropy change is very small, because the number of different arrangements for the two macromolecular components hardly increases. Miscibility of two polymers in most cases is governed by a negative enthalpy of mixing. In other words specific interactions between the two polymers must exist.
The presence of a single glass transition temperature is generally taken as an indication of complete miscibility. Any polymer system showing two glass transition

temperatures located at the same glass transition temperatures of the single polymers may be considered as an immiscible polymer blend combination. Separate domains of each component will be present.

Literature about polymer blends refers almost exclusively to amorphous polymers prepared from the melt. In this situation the state of the blend is not very complex; the two components form a homogeneous amorphous phase or not. Ong[6] and Ellis[7] have investigated the compatibility of nylons in the amorphous phase. Except for the system nylon 6 / nylon 6,6 heterogeneous amorphous phases are formed from the melt. No information about crystallization is available.

When a blend is formed of a semi-crystalline polymer and an amorphous polymer, a more complex situation exists. When a blend is cooled down from the melt, the semi-crystalline polymer may crystallize. Substances tend to crystallize in a pure form; additives are normally expelled from the growing crystals. For polymer blends this means that, independent of the miscibility in the liquid state, phase separation occurs at the crystallization temperatures. Crystallization generates two phases of this polymer: an amorphous and a crystalline phase. The amorphous phase in the blend can again be either homogeneous or not.

The crystallization behavior of a semi-crystalline polymer can be largely influenced by the presence of a second, non-crystallizable, component. Various authors[8-11] have reported that the crystal growth rate of a polymer decreased by the presence of a second amorphous polymer due to a reduction of the mobility of the crystallizable polymer chains in the melt. On the other hand Cimmino[12] has found that the presence of amorphous poly(vinyl methylene ether) increased the crystal growth rate of iso- and syndiotactic polystyrene (PS) as a result of an increased mobility of the PS chains in the melt.

The system is even more complex in the case of two crystallizable polymers. Generally the two components crystallize separately; co-crystallization of two polymers into isomorphic crystalline cells seldomly occurs[5]. The crystallization behavior of each component can be influenced by crystallization of the other polymer. General trends cannot be given in such cases, because crystallization of both polymers is affected by a large number of parameters. Literature about polymer blends of two semi-crystalline polymers is limited. Verma[13] has studied the solution crystallization of nylon 6 and nylon 12 and has found that individual crystals were formed; no crystals containing both nylon 6 and nylon 12 chains were observed.

Kitao[14] has investigated blends prepared from the melt of nylon 6 with poly (ethylene terephtalate) (PET) and other nylons. PET, a semi crystalline material, remained in the amorphous state because of the much higher crystallization rate of nylon 6. The nylon 6 / nylon 6,6 combination showed that the minor component in the blend did not crystallize; only in the 50/50 blend both components were able to crystallize. Differential thermal analysis on the nylon 6 / nylon 11 and nylon 6 / nylon 12 blends showed that both components crystallized at all compositions. The melting temperatures of the two nylons in these blends were slightly lower than of the two homopolymers and almost independent of blend composition. Nadkarni and Jog[15] have published a literature review about the melt crystallization behavior in polymer blends which confirms the complexity of this process. They conclude that a variety of critical factors exists that govern the extent and direction of change in the crystallization behavior and the crystalline morphology of a polymer in a blend. Factors included are the glass transition temperature and melting points of both polymers, their relative melt viscosities, chemical compatibility, inherent crystallizability and the phase morphology in the as-compounded pellets.
It has been described recently that crystallization induced by diffusional processes in membrane formation can be compared to crystallization from the melt[3] in terms of undercoolings. Diffusion of solvent and non-solvent, however, create gradients of the three components in the film leading to a more complex situation. Based on literature data, as described above, it is expected that nylon 4,6 and nylon 6 crystallize separately. Since quaternary mixtures at low polymer concentrations could be prepared a homogeneous region must exist, in which the two polymers are miscible.

Blending in membrane formation

Information about the effect on phase separation phenomena of blending in membrane formation is very limited. Boom et al.[16-18] fundamentally studied blend membranes of the two amorphous polymers polyethersulfone (PES) and poly (vinyl pyrrolidone) (PVP). It was found that in the first moments of immersion the polymers could be considered as one component. On a larger time scale phase separation of the two polymers occurred. Kesting[19] used an amorphous polyamide terpolymer for the preparation of nylon 6,6 membranes. The resulting membrane was more flexible

and much stronger, suitable for application in micro- and ultrafiltration. Membrane formation with incompatible block-copolymers has been reported by Hugl et al.[20] The copolymer consisted of polyether and polycarbonate segments. The membrane surface showed a domained structure, indicating that the two polymer blocks were phase separated.

In this work nylon 4,6 blend membranes were investigated using nylon 6 and a nylon copolymer as the second polymer. Nylon 6 and the copolymer are both semi-crystalline polymers. This chapter is focused on:

1. The possible creation of separate crystalline structures of the two polymers and the implications for the morphology of the final membrane.
2. The morphology of the top-layer and the relation to the membrane performance.
3. The conclusions to be drawn concerning the thermodynamics and mass transfer of these (quasi) quaternary systems in relation to membrane formation.

EXPERIMENTAL

Membrane preparation

Nylon 4,6 (DSM, Stanyl KS400) was dissolved together with nylon 6 (DSM Ultramid B3) or a nylon copolymer, nylon 4,6 *co* 6, (DSM KS611, which consists for 95% of nylon 4,6 and 5% of nylon 6) in formic acid (Merck, analytical grade) at 30 °C. Prior to use nylon 4,6 and the copolymer were dried *in vacuo* at 70°C and nylon 6 at 30°C. The total polymer concentration in all solutions was 32 wt% but the ratio of the two nylons was varied. Solutions were stirred one day for homogenization and kept unstirred for another day for degassing.

Polymer solutions were cast with a thickness of 0.3 mm on a glass plate and immersed in a coagulation bath containing demineralized water. After a sufficient coagulation time (± 20 min) the membranes were removed from the glass plate, rolled in filter paper and washed with demineralized water for at least 24 hours.

Blend membranes were also prepared from casting solutions containing 32 wt% polymer, 3 wt% demineralized water and 65 wt% formic acid.

Flux measurements

Pure water flux (reverse osmosis water) measurements were performed using an Amicon set-up at an applied pressure difference of 2 bars.

Coulter® porometry

Pore size analysis was performed on a Coulter® Porometer II (ASTM F316-80, 1980; BS 6410:1984). The membranes were dried for at least 18 hours at 80 °C prior to use. Coulter® Porofil was used as a wetting liquid. The sample holder had a diameter of 25 mm.

Scanning Electron Microscopy (SEM)

The morphology of the membranes was examined by SEM (Jeol JSM T 220A). The membranes were dried for at least 18 h at 80 °C prior to sample preparation. Cross-sections of the samples were obtained by breaking a small membrane strip in liquid nitrogen after being wetted by ethanol; top and bottom surface samples were prepared by adhering a small piece of membrane to the sample holder with the use of conductive carbon. A thin gold layer was applied on the sample, using a Balzer Union SCD 040 sputtering apparatus at 25 mA for 2.5 minutes.

Differential Scanning Calorimetry (DSC) & Wide-Angle X-ray Scattering (WAXS)

In order to study the crystalline nature of the membranes DSC measurements were performed with a Perkin Elmer DSC-4 calorimeter with a scanning velocity of 15°C per minute. The membranes were dried as described above. The weight of the samples varied from 5 to 9 mg.
WAXS measurements on the prepared membranes were kindly performed at the DSM laboratories with a Philips diffractometer (Cu K-α radiation, 50 kV, 40 mA).

RESULTS

Membrane preparation

When a polymer solution is cast on a glass plate and immersed in a coagulation bath, the transparency of the polymer film changes as soon as phase separation starts. Figure 1 shows the time between immersion of the cast film and the appearance of turbidity (delay time) as a function of composition. The delay times were determined visually.

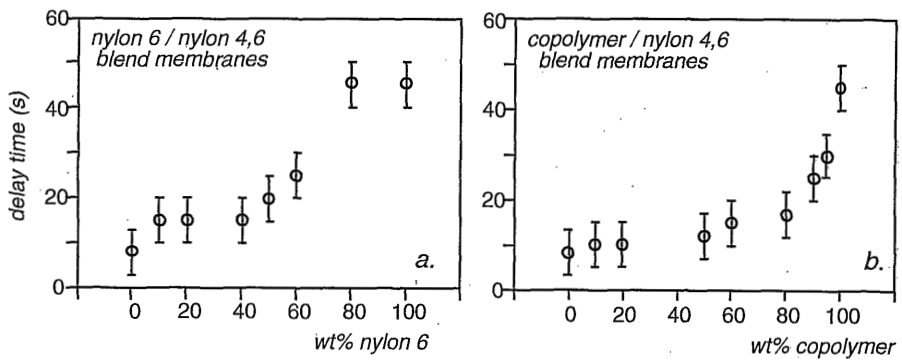

Figure 1. Delay time measurements for demixing of the blend membranes prepared. (a: nylon 6 / nylon 4,6 blend membranes; b: nylon copolymer / nylon 4,6 blend membranes)

The delay time measurements for demixing of the membranes prepared from nylon 6 / nylon 4,6 blends showed a gradual increase in delay time. Immediate occurrence of turbidity for a pure nylon 4,6 film shifted to delay times in the order of 50 seconds for membranes prepared from both pure nylon 6 (figure 1a) and the 'pure' copolymer (figure 1b). The transition to significantly larger delay times occurred near 50% of nylon 6 in the nylon 6 / nylon 4,6 blends and near 90% of the copolymer in the nylon 4,6 *co* 6 / nylon 4,6 blends. Membranes prepared with water in the casting solution showed a similar sequence, with values 5 to 10 seconds lower than those

shown in figure 1. It was shown earlier[3] that theoretically the addition of water to the casting solution should increase the degree of supersaturation and that consequently the induction time should be lowered.

SEM: morphology of the membranes

All membranes prepared were characterized with electron microscopy. As the nylon 6 content in the nylon 6 / nylon 4,6 blend membranes increased, the top-surface morphology changed from a rather irregularly packed layer of separate spherulites (or aggregates consisting of a few spherulites) to a dense layer in which hardly any spacing between the spherulites is visible anymore. The last described morphology occurred when 50 wt% nylon 6 or more was present (see figure 2). At the same time large top-layer thicknesses were observed. In addition the spherulite diameter in the top-layer increased. In the substructure, a gradual change from an axialitic to a cellular structure occurred with an increasing nylon 6 content. The axialitic morphology is a result of spherulitic crystallization in which the nucleation density was too high for the growth of complete spherulites[1]. The cellular morphology results from nucleation and growth of a polymer lean phase, typically for liquid - liquid phase separation.
Membranes prepared with water in the casting solution showed a much denser and finer structure (see figure 3). The overall morphology in the cross section was not significantly altered compared to changes observed in figure 2. The top-structure of a blend membrane with water was considerably improved for support applications, since it showed much smaller cavities that could disturb a coating process.

A transition from an axialitic to a spherulitic structure of the sub-layer can be observed for the copolymer / nylon 4,6 blend membranes (see figure 4). The various results for the membranes from this blend showed that the presence of the copolymer only effected the membrane structure when a large amount of copolymer ($\geq$ 80wt%) was present. Then a change was observed from an axialitic to a spherulitic morphology.

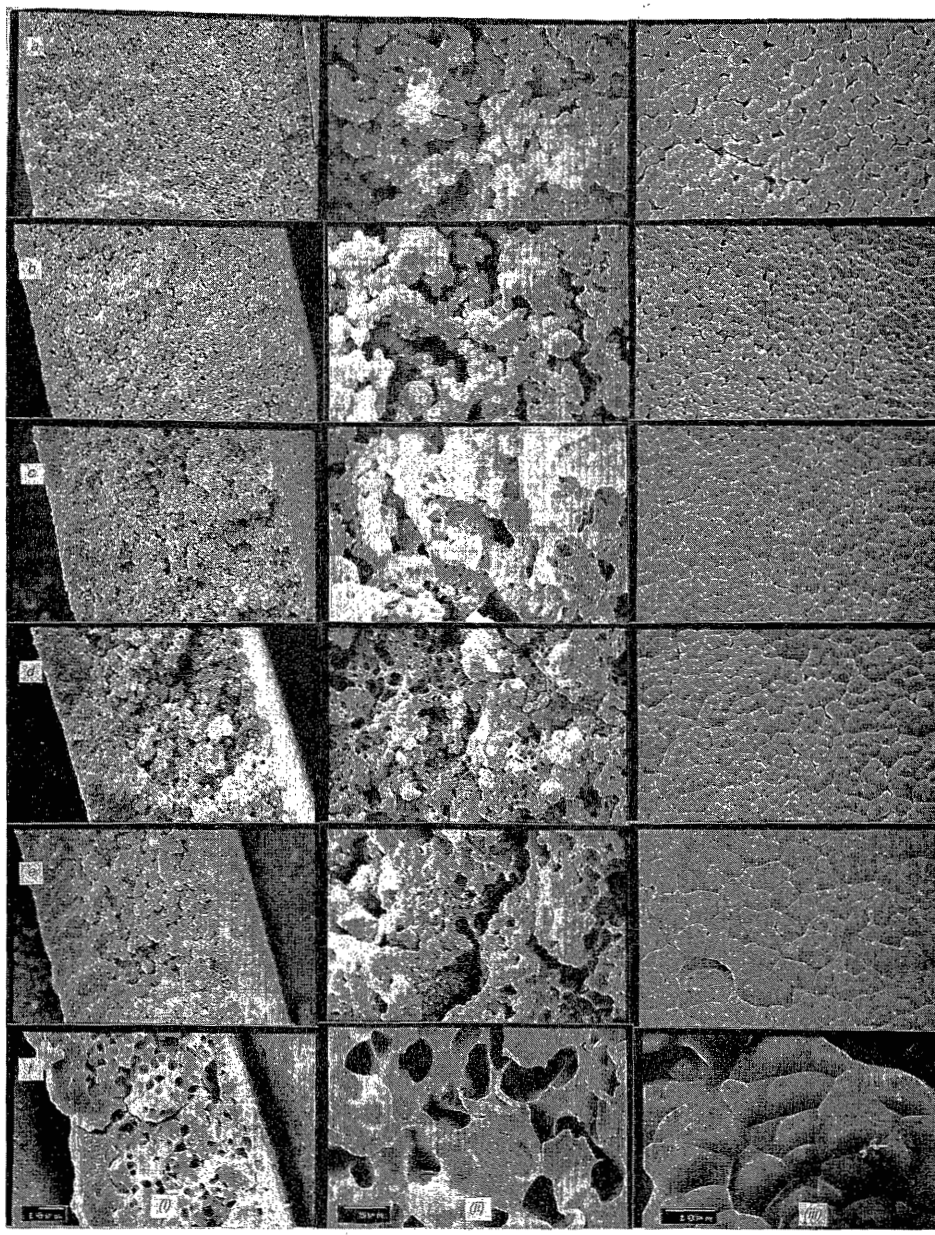

Figure 2. SEM of cross-sections (i and ii) and top-surfaces (iii) of nylon 6 / nylon 4,6 blend membranes prepared with various ratios nylon 6 / nylon 4,6: a: 0/100, b: 40/60, c: 50/50, d: 60/40, e: 80/20, f: 100/0).

Pure water flux

The pure water flux of the blend membranes was measured. The flux varied between 500 and 900 L/(m^2.h.bar) for membranes with 0 - 30 wt% of nylon 6 in the nylon 6 / nylon 4,6 blend membranes, while lower values were measured for the membranes prepared with water in the casting solution (see figure 5, flux of approximately 200 L/(m^2.h.bar)). Between 30 and 50 wt% of nylon 6 a decrease was observed for all membranes. At concentrations > 50 wt% a very low flux was measured (smaller than approximately 10 L/(m^2.h.bar)).
The copolymer / nylon 4,6 blend membranes showed values for the water flux between 300 and 800 L/(m^2.h.bar) for membranes with 0 - 95 wt% of copolymer. Again the values were lower for the blend membranes prepared with water in the casting solution; values for the water flux between 200 and 400 L/(m^2.h.bar) were measured. Between 95 and 100 wt% copolymer a sharp decrease in flux was observed, and with 100% of the copolymer the membrane exhibited a flux smaller than 10 L/(m^2.h.bar).

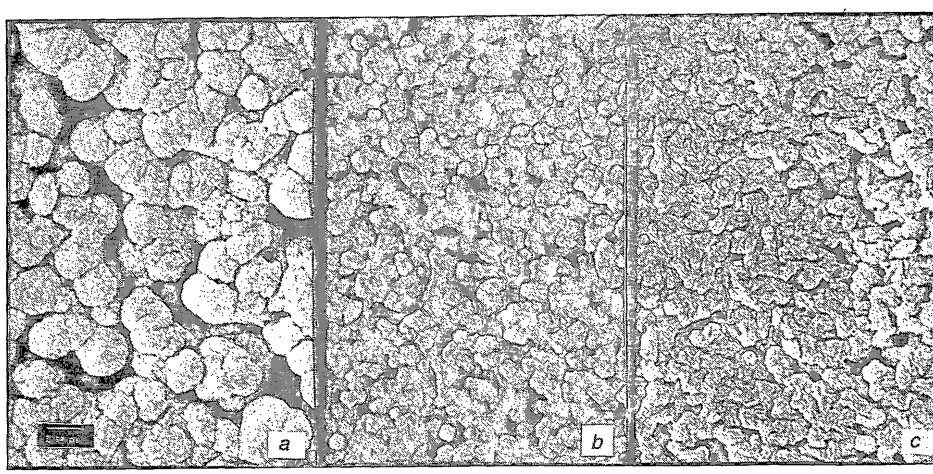

Figure 3. SEM of top-surfaces of (a) nylon 4,6 membrane, (b) nylon 4,6 membrane prepared with water in the initial casting solution and (c) blend membrane of nylon 6 / nylon 4,6 is 35 / 65 with 3 wt% of water in the initial casting solution. The total initial polymer concentration in all cases was 32 wt%. The photos were taken at the same magnification.

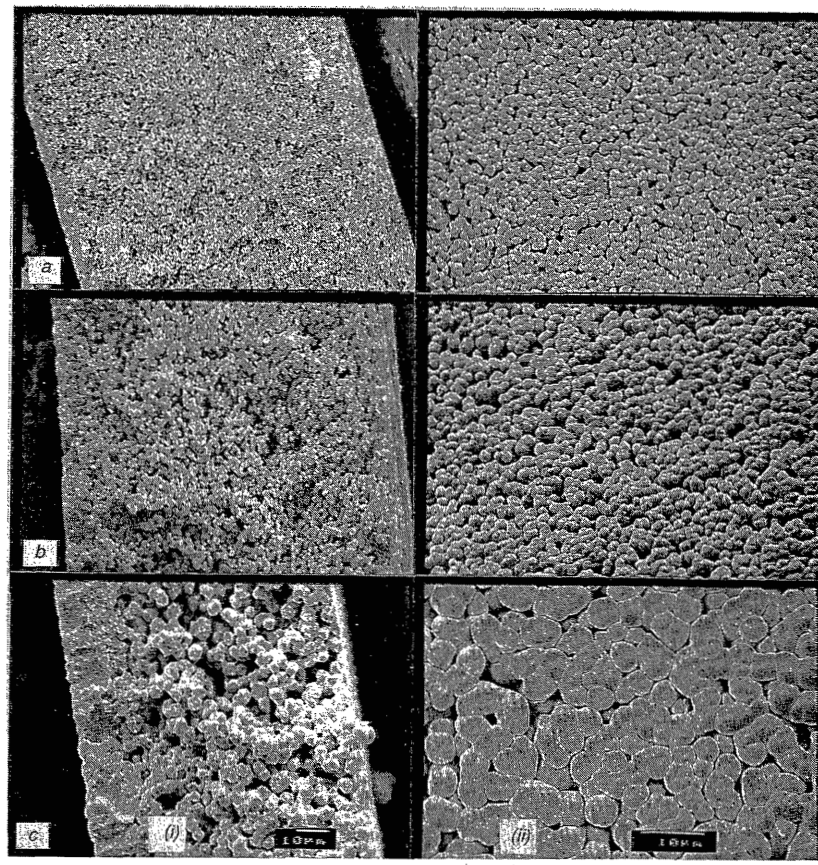

Figure 4. SEM of cross-sections (i) and of top-surfaces (ii) of copolymer / nylon 4,6 blend membranes in various ratios copolymer / nylon 4,6: a: 10/90, b: 90/10 and c: 100/0.

Coulter® porometry

The pore size distribution of three membranes prepared from a 32 wt% solution of nylon 4,6, of nylon 4,6 with 3 wt% of water in the casting solution and of a blend membrane with nylon 6 / nylon 4,6 is 35 / 65 with 3 wt% of water in the casting solution with a total polymer concentration of 32 wt%, is given in figure 6. For nylon 6 / nylon 4,6 blend membranes with 0 - 50 wt% of nylon 6 the maximum pore size

6 / nylon 4,6 blend membranes with 0 - 50 wt% of nylon 6 the maximum pore size was typically in the microfiltration range, varying between 0.25 and 0.45 μm (see figure 7a). The air permeability of these membranes was in the range of 0.5 and 2.0 L/(cm^2.min) at standard temperature and pressure (STP). The membranes prepared with water in the casting solution showed smaller values, with pore sizes still in the microfiltration range. When 50 wt% or more nylon 6 was present, the pore size became too small to be determined by this technique, i.e. the pores were smaller than approximately 70 nm, and no air flow could be detected anymore (figure 7c). SEM pictures showed that addition of water to the casting solution resulted in membranes with much finer and more dense structures, but similar trends in morphological changes were observed (axialitic / cellular and the occurence of thick top-layers). This implies that, by addition of water to the casting solution, pore size and water flux are systematically lower.

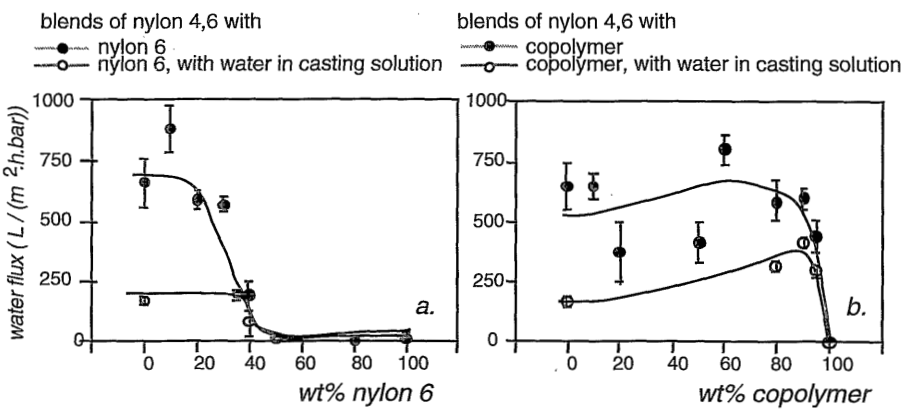

Figure 5. Initial pure water flux as a function of membrane composition in the nylon 4,6 blend membranes with a: addition of nylon 6 and b: addition of nylon 4,6 co 6. Two curves are presented in both graphs, one for membranes cast without and membranes cast with water in the casting solution.

The copolymer / nylon 4,6 blend membranes also contained pores in the microfiltration range, between 0.15 and 0.40 μm, while the air permeability varied from 0.5 to 1.5 L/(cm^2.min), STP (figure 8). The pore size of the pure copolymer membrane was too small to be determined, while no gas flow could be detected either.

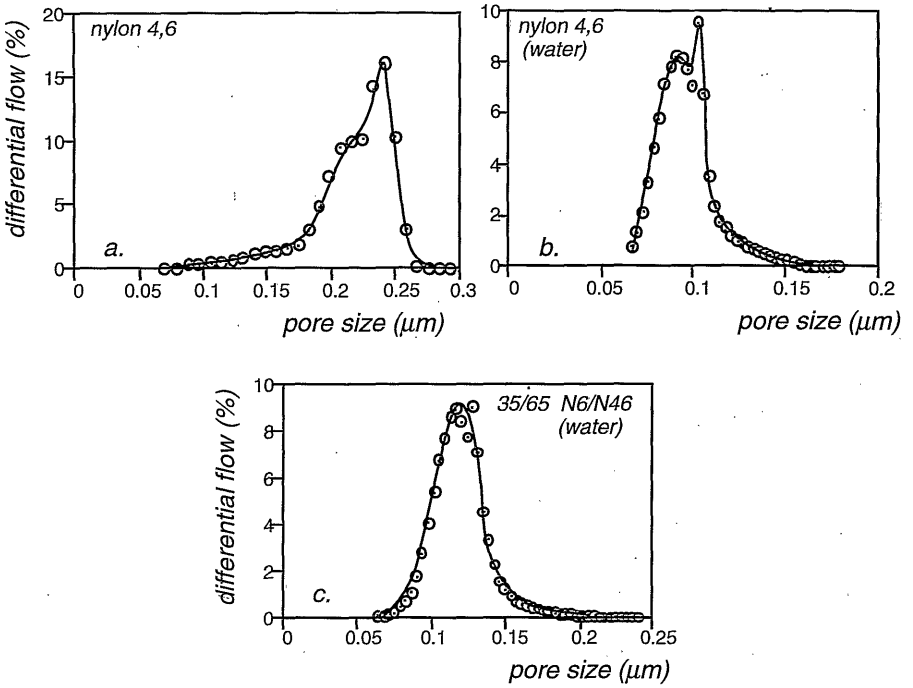

Figure 6. Typical pore size distributions obtained by Coulter porometry (a: pure nylon 4,6 membrane; b: nylon 4,6 membrane with water in the casting solution; c: blend membrane of 35 wt% nylon 6 and 65 wt% nylon 4,6 with water in the casting solution).

Performance & Morphology

The effect of addition of nylon 6 to a casting solution containing nylon 4,6 on the structure of the blend membranes, corresponds to the results of the pore size and pure water flux measurements. The pure water flux and pore size were about equal for membranes with 0 - 40% of nylon 6. At 50 wt% nylon 6 and more, the blend membranes were so dense that pore size decreased to a value less than 70 nm, the detection limit of the porometer. This means that these membranes possibly contain pores in the lower ultrafiltration range.

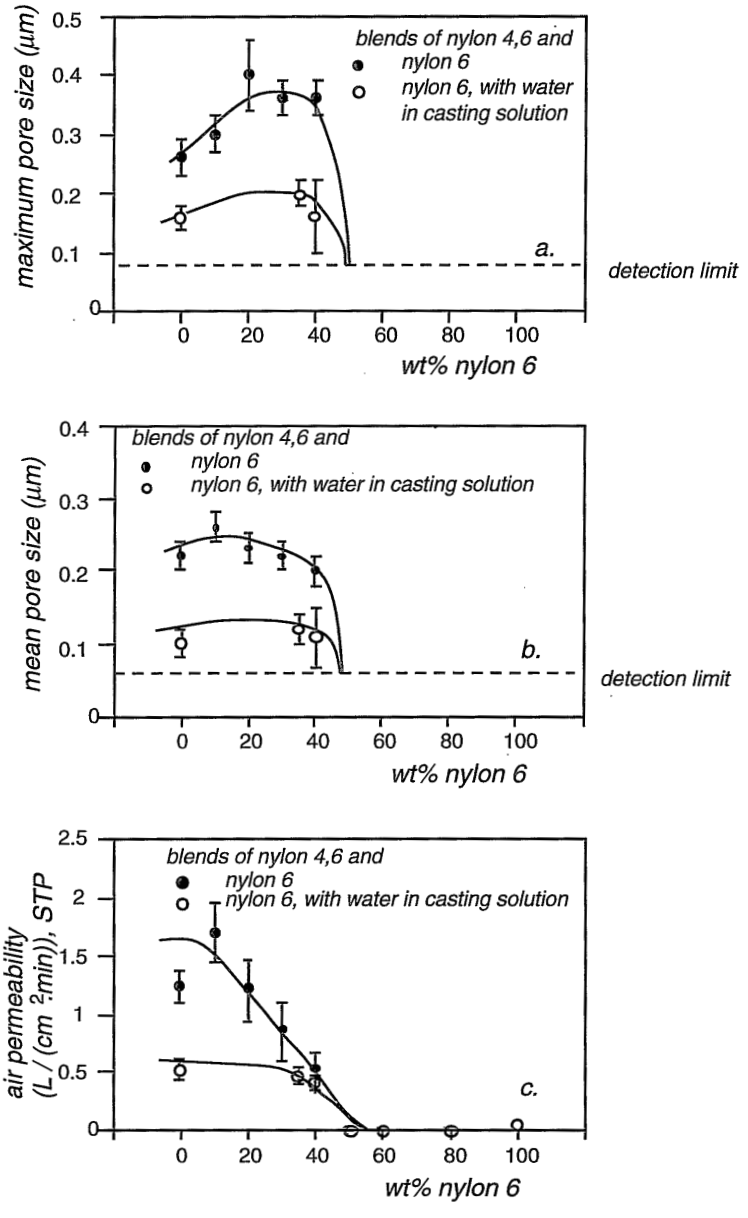

Figure 7. Coulter porometry for nylon 6 / nylon 4,6 blend membranes, a: maximum pore size, b: mean pore size and c: air permeability for membranes cast without and with 3wt% of water in the casting solution.

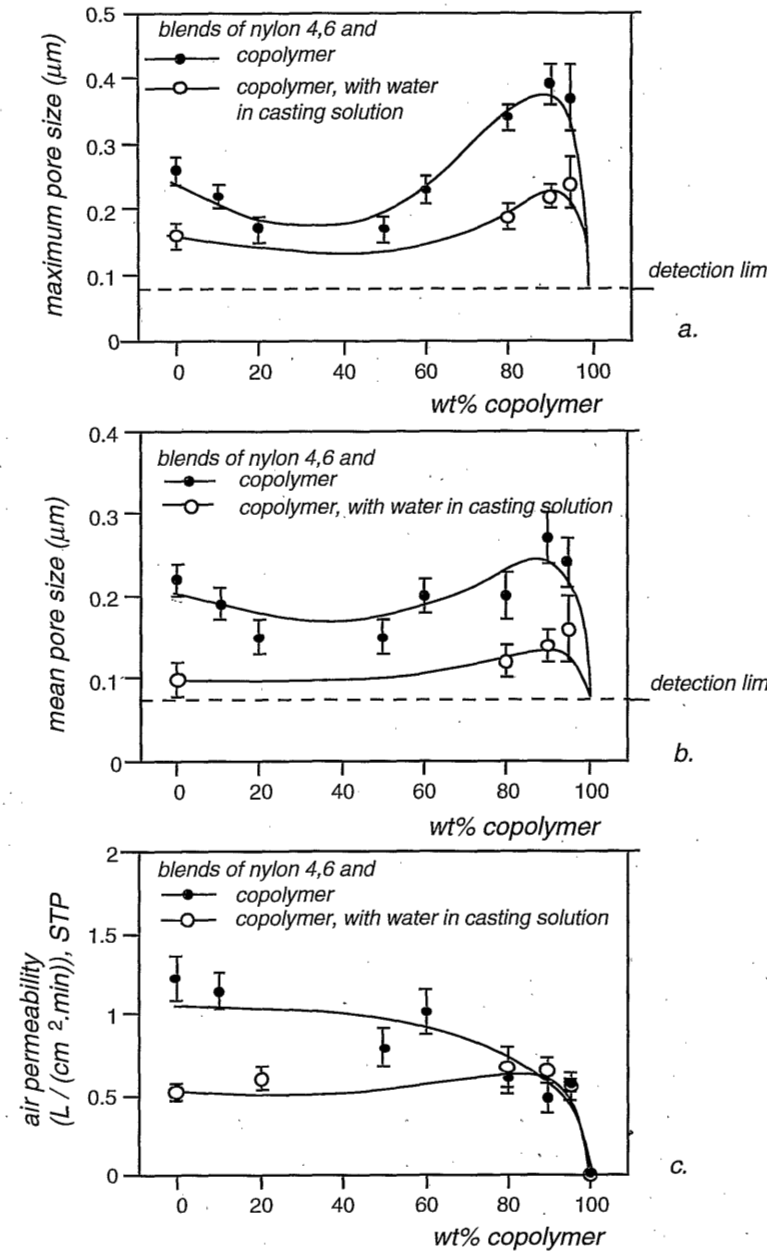

Figure 8. Coulter porometry for nylon copolymer / nylon 4,6 blend membranes, a: maximum pore size, b: mean pore size and c: air permeability for membranes cast without and with 3 wt% of water in the casting solution.

However, due to the large top-layer thickness, the resistance towards permeation is so large that hardly any pure water flux could be measured making these membranes unsuitable for ultrafiltration applications. These observations explain the search for skinless membranes in the patent literature concerning nylon microfiltration membranes[4,21], because the nylon skins apparently are rather impermeable. In order to prepare nylon 6 or nylon 6,6 membranes with a reasonable permeability a rather large concentration of solvent (formic acid) in the coagulation bath was used or membranes were prepared from the vapor phase; membranes that exhibited a skin were rejected for any practical application.

The spacing between the spherulites in the top-surface is much larger than the pore size obtained with the porometer especially for an open top-surface. For instance, the nylon 4,6 membrane with spacings between the spherulites in the top of 0.5 to 1 μm (figure 2) can be compared to the results obtained with Coulter porometry in which a pore size of 0.2 μm was observed (figure 6). Obviously below the open top-layer a much denser layer is present that determines the pore size and hence the separation performance of these membranes.

Similar trends were observed for the blend membranes with a copolymer content of 95 to 100%. Because of the thick densified top-layer of the pure copolymer, hardly any water flux could be measured, which means that this membrane is not suitable as an ultrafiltration membrane.

The effect of water in the casting solution for the copolymer / nylon 4,6 blends is similar to what was found for the nylon 4,6 / nylon 6 blend membranes. Water caused a decrease in crystallite size present in the membranes without changing other aspects of the overall membrane morphology.
A considerable improvement of the surface morphology was found for the blend of nylon 4,6, and nylon 6 when the membrane was prepared with water already present in the casting solution. The pore size distribution of this blend membrane is comparable to the nylon 4,6 membrane cast with water, but at the top-surface the 'dome-like' appearance (see figure 3a-b and also figure 4ii) has disappeared, making it more suitable for coating with a thin selective layer[22]. The differences between a nylon 4,6 membrane and a blend membrane is shown in figure 9. An EPDM (Keltan

478, DSM) coating was applied from a 1% solution in n-hexane on carefully dried membranes dried by a liquid exchange method. The membranes must be dried between glass plates to prevent irregular shrinkage. The observed selectivity for carbondioxide / methane mixtures was 3.9 after 7 coating steps for the nylon 4,6 membrane and 4.1 after 5 coating steps for the blend membrane. The intrinsic selectivity of EPDM for carbondioxide / methane is 4.3. A thinner and better coating could be applied on the blend membrane. No penetration of the EPDM solution in the membrane was found (see figure 9); this penetration occurred for the nylon 4,6 membrane.

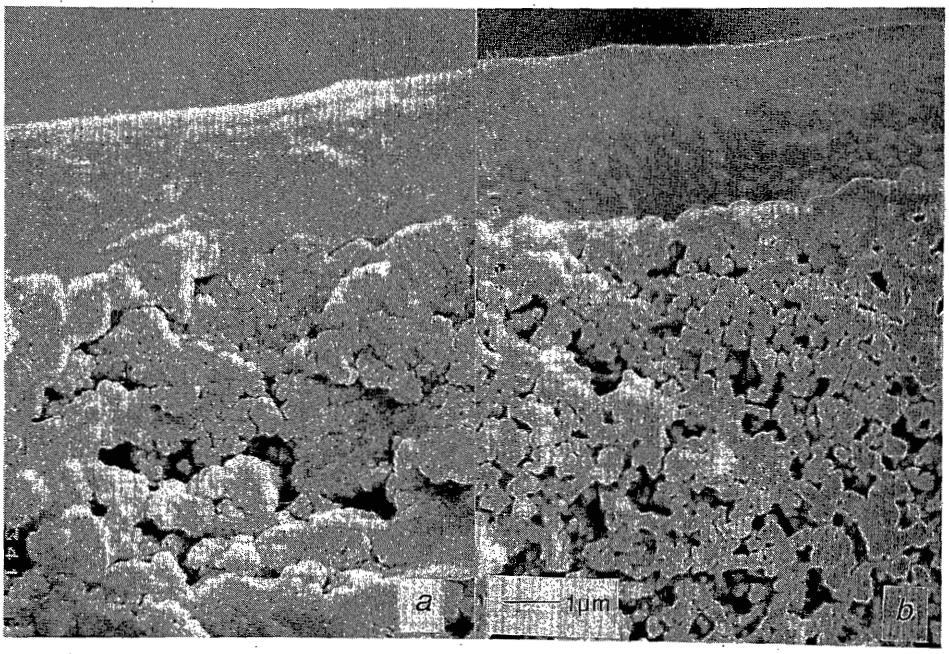

Figure 9. SEM of the cross-section of two composite membranes for a: a nylon 4,6 membrane prepared form a 32wt% solution on which the EPDM coating was applied after 7 coating steps, and b: a nylon 6 / nylon 4,6 blend membrane prepared from a 32wt% of total polymer concentration and 3 wt% of water with nylon 6 / nylon 4,6 is 35 / 65.

DSC and WAXS

Typical DSC curves for membranes prepared from a ternary system each containing one of the polymers, nylon 4,6, nylon 6 or nylon 4,6 *co* 6 are presented in the figures 10a, 10b and 10c respectively. The DSC curves for the blend membranes, for which a typical example is given in figure 10d, clearly showed that both nylon 6 and nylon 4,6 crystallized independently during the membrane formation.

1. Crystallization of nylon 6 in nylon 6 / nylon 4,6 blends

Nylon 6 exhibited a double melting endotherm at all blend compositions. There was a clear change visible with nylon 6 content in the double melting endotherm at ± 200 °C: the ratio of the first to second peak of this double melting endotherm decreased with increasing nylon 6 concentration. This is schematically depicted in figure 11d.

The total heat of fusion showed an increase from 55 to 90 J / (g of nylon 6) upon increasing the nylon 6 content in the blend membrane.

Double melting endotherms can be caused by the presence of two different crystal structures or by the presence of crystals with a distribution of lamellar thickness which gives rise to melting and recrystallization at different temperatures.

Nylon 6 can show two crystal structures, α and γ. The α structure is the most common structure and is dominant[23] over the γ structure for crystallization from the melt or from solution. The melting point of the α structure is ± 220 °C and for the γ structure it is ± 215 °C . The γ structure can be obtained from the α structure when specific salts, like LiBr and LiCl, are present during crystallization[24] or when the α nylon 6 is treated with an iodine - potassium iodide aqueous solution[23,25]. WAXS diffractograms of pure nylon 4,6, pure nylon 6 and of the blend membranes (figure 12) were identical and showed two α-peaks for all membranes at reflection angles of 20.2 and 24.2°. No γ phase, which would show a reflection peak at 22°, was observed for the nylon 6 crystals in the blend membranes. The presence of different crystal structure, both α and γ, is excluded; only the α structure is observed for these membranes.

The differences in peak height thus must be caused by the distribution of the lamellar thickness and (re)crystallization of the thinnest lamellae after melting. The WAXS experiments show a clear separation of the two peaks for both nylon 4,6 and nylon

6, indicating that a rather perfect ordering exists on the level of the unit-cells of the crystals. The resolution obtained here is only matched by slow crystallization form diluted solutions; samples crystallized from the melt give much more diffuse peaks.

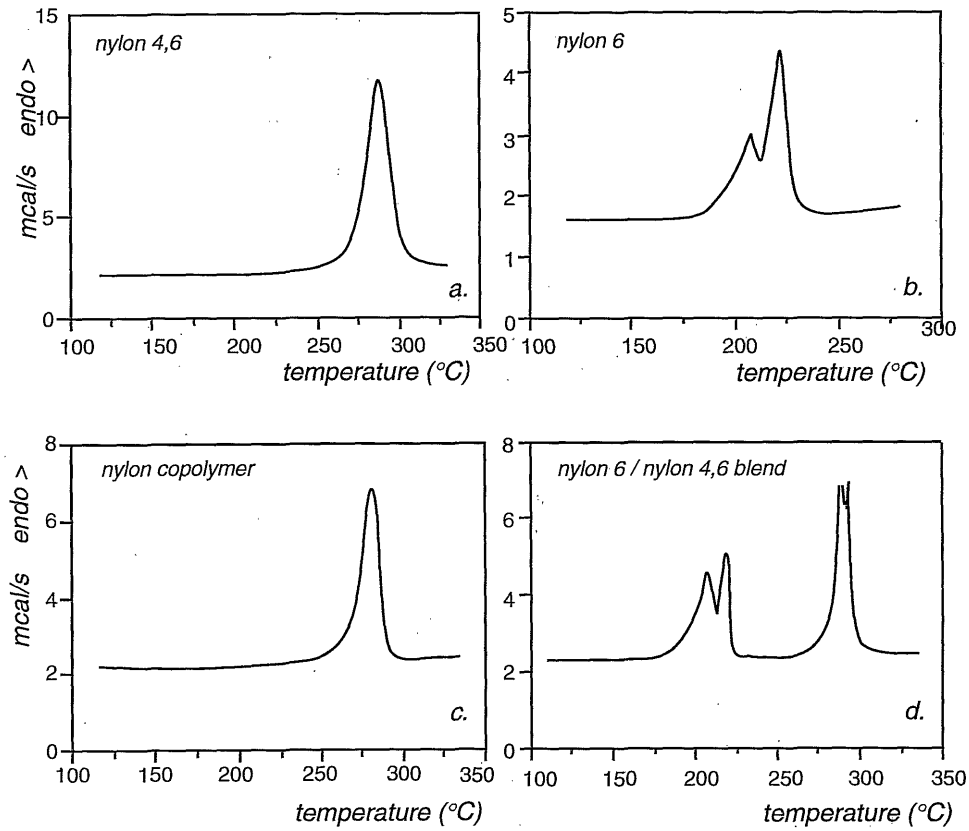

Figure 10. Typical DSC curves for membranes prepared from a ternary system each containing the polymers, nylon 4,6 (a), nylon 6 (b) and nylon 4,6 co 6 (c). The blend membrane shown in figure d consists for 50% of nylon 6 and 50% of nylon 4,6.

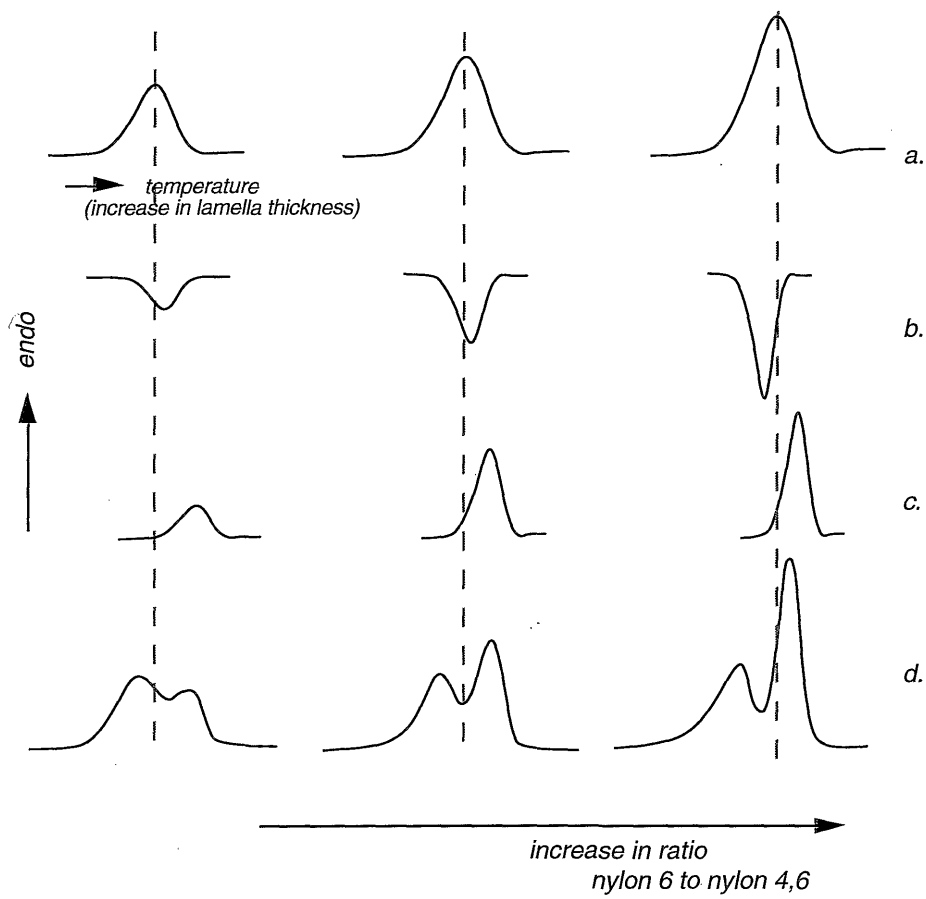

Figure 11. Reconstruction of a DSC curve from (a) melting of the originally present crystalline material; (b) (re)crystallization of molten and amorphous material and (c) the remelting peak of the in 'b' crystallized material, both occurring during the DSC heating scan. Figure (d) reflects the schematic representation of the change in shape of the double nylon 6 melting endotherm with an increase in the nylon 6 content in the nylon 6 / nylon 4,6 blend membranes.

2. Crystallization of nylon 4,6 in nylon 6 / nylon 4,6 blends.

The nylon 4,6 peak in the blend membranes did not show such clear changes as was observed for the nylon 6 peak in these blend membranes. Some membranes did show, not very clearly though, a double nylon 4,6 melting endotherm while it was often

observed that a second sample only showed one nylon 4,6 melting peak in the DSC scan. The heat of fusion was approximately constant at all compositions. The heat of fusion for nylon 4,6 crystals with infinitely large lamellae, ΔH_f^o, is equal to 210 J/g[26]. With an observed heat of fusion of approximately 105 J/g, a crystallinity of ± 50% can be calculated for nylon 4,6 which seems rather high regarding the crystallization conditions. However, a similar degree of crystallinity was obtained in previous work with nylon 4,6 membranes[1]. The presence of nylon 6 apparently did not influence the crystallinity of nylon 4,6 in the final membrane.

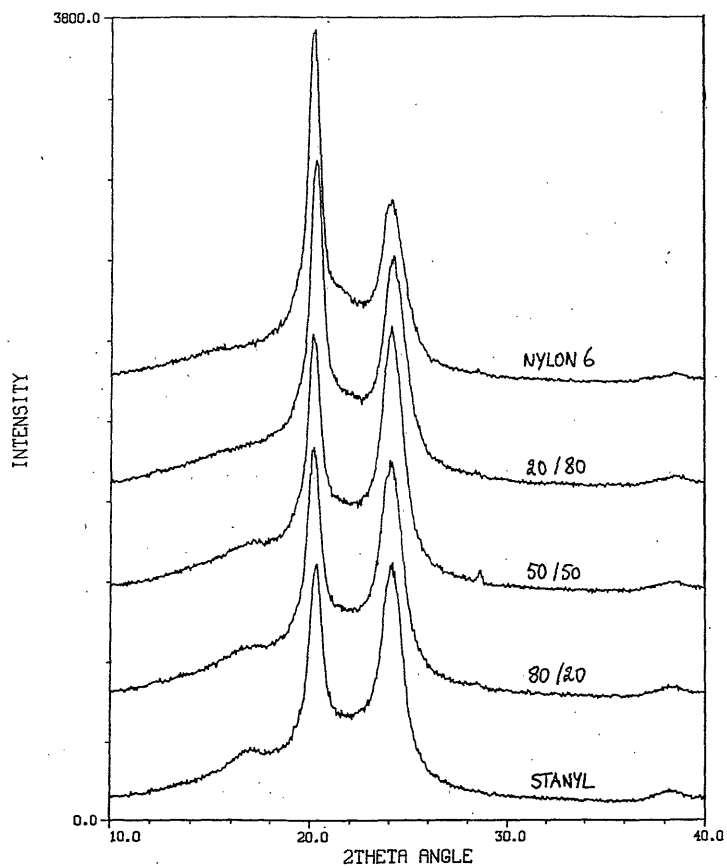

Figure 12. Wide-angle X-ray scattering of nylon 6 / nylon 4,6 blend membranes with different composition. (Stanyl is the tradename for nylon 4,6).

3. Crystallization in nylon 4,6 *co* 6 / nylon 4,6 blends

The DSC scans of the nylon copolymer and nylon 4,6 as received showed that the copolymer resembled nylon 4,6 to a large extent, with a melting temperature just a few degrees lower. The membranes prepared from both nylon 4,6 and the copolymer gave similar results. Blend membranes of nylon 4,6 and the copolymer generally showed only one melting endotherm at peak temperatures of 280 - 290°C; the separate melting peaks of both components overlap in the DSC curves. The heat of fusion was approximately constant at all compositions, indicating that an equal amount of polymer has crystallized during membrane formation.

DISCUSSION

Nylon 6 / nylon 4,6 blend membranes

Morphology in relation to mass transfer

The gradual change from an immediate to a delayed occurrence of turbidity after immersion in the non-solvent bath supports the assumption made by Boom et al.[16] that in a quaternary membrane forming system the two polymers can be considered as one polymeric component in the first stages of immersion, i.e. the mutual diffusivity of the two polymers is low compared to the diffusivities of the low molecular weight components. Phase separation between the two polymers takes place on a larger time scale. In our case phase separation did not occur independently; if the nylon 4,6 molecules would show an independent behavior with respect to nylon 6 molecules then the delay times (figure 1) would be equal to the delay time of pure nylon 4,6 solutions at all composition, except for 100% nylon 6. As can be concluded from figure 1 this was not the case; a gradual increase in delay time was observed.

It was shown from mass transfer calculations that for both nylon 4,6 and nylon 6 the interfacial polymer concentration in the first moments of immersion precipitation was quite large, up to 50 - 60% of polymer[3]. Nylon 4,6 exhibits immediate phase separation upon immersion in the coagulation bath. Nylon 6 demixing, governed by liquid - liquid phase separation, is delayed. The longer the delay time (before demixing starts), the longer the time for the top-layer to become thicker. A larger

delay time then is related to a thicker and more concentrated top-layer. The crystallization process in such concentrated top-layers that originates from this delay type resembles crystallization from the melt. Spherulites can grow without spacing in between the crystalline material. (see figure 2 (iii)). We can also observe that the total shrinkage of the films with respect to the final membrane thickness is larger the longer the demixing is retarded. The first nuclei created near the top for the pure nylon 6 membrane can only grow in the direction in which polymer is still present. The appearance of the top-surface of these layers resembles the top of a 'dome' and a rather irregular surface can be observed (see figure 2f).

The sub-layer of the nylon 4,6 membrane is axialitic, of the nylon 6 membrane cellular, with the appearance of large spherulites superimposed on the cellular morphology[3]. In the latter case liquid - liquid phase separation takes place before crystallization can occur. In case of the blend membranes the substructure showed a more cellular type of morphology with increasing content of nylon 6 (see figure 2 (ii)).

The nucleation and growth mechanism in liquid - liquid phase separation can continue until the polymer matrix is soldified by passing the glass transition of the polymer or by crystallization. In this membrane forming system soldification can only take place by crystallization, since the glass transition is located beneath 30°C. The cells become larger the longer is the crystallization time, since the polymer lean nuclei are believed to exhibit structure coarsening by anomalous growth[27]. In the blend membranes soldification of the cellular morphology occurring by liquid - liquid phase separation can take place by the crystallization of the nylon 4,6 molecules prior to nylon 6 crystallization, because crystallization of nylon 4,6 sets in faster than for nylon 6. Therefore the presence of a finer cellular morphology can be explained by the faster crystallization of the polymer matrix. This means that with increasing nylon 6 content in the initial casting solution the cellular morphology becomes more dominant over the axialitic morphology, giving cell growth less chances to proceed. At these higher nylon 6 concentrations less spherulites per unit of volume are visible in the top-surface while the size of the spherulites increases. This indicates that, compared to the situation in which only nylon 4,6 is present, in the presence of nylon 6 the number of nuclei that are created in time per unit of volume is lower. A lower nucleation density (total number of nuclei per unit of volume) means that less nuclei are formed per unit of volume and consequently these can grow further before they

reach a neighboring crystallite. This may explain the observed increase in spherulite size in the membrane top-layer. Since nucleation is hindered at higher nylon 6 content and the delay times increase liquid-liquid demixing becomes more competitive to solid-liquid demixing even though the time available for crystallization increases.

Crystallization behavior

The reconstruction of the 'double' melting peaks for three different blend compositions, which originate from a recrystallization process during the DSC scan[28-30], is schematically depicted in the figures 11a-c. The peaks shown in 'a' originate from the original crystalline content of the membrane. The area under the peak is a measure of the energy required for melting the crystalline structure. The larger the energy is, the better the crystalline material is ordered in more thermodynamically stable configurations. These can be a result of a better arrangement of the polymer chains on the scale of the unit cell of the lattice and / or the presence of thicker lamellae. The more stable forms show melting at higher temperatures.

The peaks shown in 'b' reflect the (re)crystallization of molten crystals that already have melted in peak 'a' and crystallization of neighboring amorphous material near the lamellae in the spherulite or axialite. Melting of the (re)crystallized material results in the melting endotherm shown in 'c'. What is (re)crystallized in 'b' must be (re)melted in 'c'. The observed pattern for the changes in melting peaks for the blend membranes shown in figure 11d can be obtained if peak 'b' becomes larger with an increasing ratio nylon 6 to nylon 4,6. Then peak 'c' also shows a larger surface and the reconstruction of the total energy effect during a DSC measurement (figure 11d) can be constructed.

1. The rearrangement of crystalline nylon 6 in nylon 6 / nylon 4,6 blends. In the pure nylon 6 membrane reorganization of crystalline structures during a DSC heating curve is most pronounced. For a blend membrane with a relatively large nylon 4,6 content compared to the nylon 6 content less reorganization during melting occurs. Apparently, reorganization of nylon 6 molecules after melting of the 'thinnest' lamellae is more hindered in the presence of nylon 4,6 molecules. It is not likely that a more stable crystal lattice is formed (see figure 12), since WAXS already showed a rather perfect organization on a crystallographic scale. It is also not expected that at

low nylon 6 content significantly thinner lamellae have been nucleated, because this factor is related to the thermodynamic driving force, the degree of supersaturation. The lower extent of rearrangement of crystalline nylon 6 at low nylon 6 content will thus originate mainly from a hindered crystallization of amorphous nylon 6 in the presence of mainly nylon 4,6 molecules.

SEM did not reveal whether separate nylon 4,6 and nylon 6 crystals are formed. Spherulites are multi-crystals, since they consist of separate lamellae. It seems possible that, starting from a nylon 4,6 nucleus, nylon 6 uses this surface for its own nucleation and hence that nylon 4,6 and nylon 6 chains might be present in the same spherulite or axialite. No information in literature is found about this phenomenon. A spherulitic structure consisting of lamellae of both nylon 4,6 and nylon 6 is schematically depicted in figure 13. (Parts of) polymer molecules, still in the amorphous state can be found closely attached to the lamellae, the interlamellar links, and in relatively large regions precipitated between the radially grown fibrils. In the originally porous samples migration of (segments of) polymer molecules over a distance larger than the spherulite (or axialite) size during a DSC scan is not expected to occur. (See figure 2 ii: the distance would be in the order of 5 μm.) Rearrangement of polymeric material will take place within the spherulitic or axialitic region. It must be concluded that (re)crystallization of nylon 6 during a DSC scan is hindered in the presence of large quantities of nylon 4,6. This means that the hindrance for reorganization must take place within a spherulitic or axialitic structure, and bi-component spherulites or axialites must have been formed in these membranes.

2. Rearrangement of crystalline nylon 4,6. The melting behavior of nylon 4,6 crystals in a blend membrane was not largely influenced by the presence of nylon 6. 'Double' melting peaks originating from recrystallization have not been observed. This does not mean, however, that this phenomenon did not take place. Successive melting (figure 11a), (re)crystallization (figure 11b) and (re)melting (figure 11c) can take place such that the peaks partly or completely overlap in the observed peak. In practice the reorganization will then not be observed.

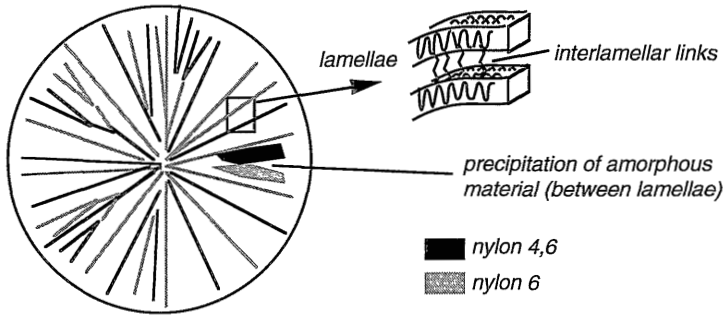

Figure 13. Schematic representation of a spherulite consisting of both nylon 4,6 and nylon 6 in the crystalline and amorphous state. Note that a similar structure also can occur in an axialite.

3. Crystallization and melting of both nylon 6 and nylon 4,6 in the blend. Upon increasing the ratio nylon 6 to nylon 4,6 a gradual shift from an axialitic to a cellular morphology occurred. Crystallization of nylon 4,6 takes place prior to nylon 6 crystallization. This means that nylon 6 is still in the liquid state during crystallization of nylon 4,6. Therefore nylon 4,6 crystallization is not largely influenced by the presence of nylon 6. Crystallization of nylon 6 takes place when part of the nylon 4,6 chains already are in the solid (crystalline) state. Nylon 6 crystallization is thus hindered when nylon 4,6 molecules are present.

It is generally concluded that phase separation between the two polymers has taken place into the two corresponding crystalline phases. The lattices of both crystalline structures are well organized (observed by WAXS). It is deduced that the phase separation between the two polymers occurs at a local scale, i.e. within a spherulitic or an axialite, and that phase separation between the two polymers into crystalline material is incomplete. Nylon 4,6 chains might be entangled in interlamellar amorphous parts. After melting of nylon 6 crystals the nylon 6 system under strain can rearrange and recrystallize without the nylon 4,6 molecules being trapped.
These phenomena are comparable to the situation with amorphous quaternary systems, such as polyethersulfone (PES), polystyrene (PS) in n-methylpyrolidone (NMP) and water[18]. These two polymers are incompatible and expected to exhibit complete phase separation. When samples were heated for a DSC scan a large relaxation peak was observed above the first glass transition of PS at 107°C.

Apparently, polymer molecules of one phase were trapped in the other. Only after the possibility of enhanced chain mobility at higher temperatures after the first glass transition the phase separation could be further completed.

Mass Transfer

It was shown earlier in which way the location of the binodal is of importance for membrane formation[2,3]. In the case of polymer blends of crystallizable nylons we may assume that in the first moments of immersion the two polymers can be considered as one component. For the two ternary systems studied the location of the binodal was completely located inside the solid-liquid region[3,31]. Also for the quaternary systems *virtual (hidden) binodals* are present giving the boundary conditions for mass transfer[3]. The degree of supersaturation is then schematically given by the composition path with its interfacial composition located at the binodal compared to the location of the crystallization line. At low nylon 6 concentration the dominating phase separation is solid - liquid demixing resulting in an axialitic morphology with a thin porous layer. Nucleation of nylon 4,6 crystals takes place, being the first step in the phase separation between nylon 4,6 and nylon 6. In a later stage nylon 6 can crystallize near and in between the nylon 4,6 axialites.
At high nylon 6 content the degree of supersaturation for both nylon 6 and nylon 4,6 is not large enough to induce crystallization and liquid - liquid phase separation is the prime demixing process. A polymer rich phase is then created around polymer lean liquid nuclei. The phase separation between the two polymers will take place after this liquid - liquid phase separation by nucleation and growth of a polymer lean phase, with nylon 4,6 having the highest tendency towards crystallization. The phase separation between the two polymers in crystal structures is present on a very local scale, since clear differences in morphology on a larger scale were not observed. It is expected that the amorphous phases of the two components are highly entangled. This is probably one of the reasons why blend membranes have shown[4,19] better mechanical properties when one or both components can crystallize. Smaller crystalline entities of the two phases act as 'cross-links' for the polymer chains which are entangled in the amorphous phase.

Nylon copolymer / nylon 4,6 blend membranes

The membranes of the pure polymers, nylon 4,6 and the copolymer, showed a different behavior. Both membranes are formed according to a solid-liquid demixing mechanism. The sub-layer structure of the nylon 4,6 membrane consists of axialites while the copolymer clearly showed the presence of spherulites (see figure 4). The nucleation density for the copolymer is lower than for nylon 4,6; because the crystallization line is located further away from solvent corner; i.e. the degree of supersaturation is less for the copolymer. This lower nucleation density is thus related to the thermodynamics of the systems[3,31]. Because less copolymer nuclei are formed they can keep growing until the spherical growth stage has been reached. In the case of nylon 4,6 many more nuclei are formed and only the intermediate stage in the development of a spherulite is reached. The lower nucleation density for the copolymer can also be deduced from the fact that less spherulites can be seen in the top-surface SEM pictures (figure 3), while the size of these spherulites is larger than for nylon 4,6.

The same considerations as discussed for the nylon 6 / nylon 4,6 membranes concerning the thermodynamics and mass transfer for this quaternary systems are of importance for this combination of polymers, although the presence of the separate corresponding crystal structure could not be confirmed. Unlike the situation in nylon 6 / nylon 4,6 blends, the copolymer resembling nylon 4,6 to a large extent, is expected to co-crystallize with pure nylon 4,6 molecules. The transition from a nylon 4,6 determined morphology to a nylon 4,6 *co* 6 determined structure occurs at a much higher copolymer content (95%); 5% of nylon 4,6 homopolymer is enough to make the system mainly resemble the ternary system with only nylon 4,6. The pure copolymer also showed the presence of a large top-layer thickness, resulting from a delayed solid-liquid demixing. As has been described in chapter 5[3], it is possible that a thick and highly concentrated layer at the film-bath interface is formed before demixing starts by liquid - liquid or by solid - liquid phase separation in this case. Separate spherulites are visible at the top-surface of the copolymer membrane although delayed phase separation has taken place. The reason for this difference in top-surface morphology may be attributed to the lower interfacial polymer concentration and less shrinkage of the film during immersion precipitation.

CONCLUSIONS

The preparation and characterization of blend membranes of nylon 4,6 / nylon 6 and of nylon 4,6 / nylon copolymer were investigated. The pure nylon 4,6 membrane had an axialitic structure resulting from solid-liquid demixing while nylon 6 showed a cellular structure that resulted from liquid-liquid demixing. In the nylon 4,6 / nylon 6 blend membranes it was found that the membrane structure changed gradually from an axialitic to a cellular morphology as the nylon 6 content increased. The shift from a nylon 4,6 determined to a nylon 6 determined morphology occurred at approximately 50% of nylon 6 in the membrane. The increased top-layer thickness is caused by a more delayed phase separation process. This large top-layer thickness results in a very low water flux which makes these membranes unsuitable for ultrafiltration applications.

DSC and WAXS showed that both nylon 6 and nylon 4,6 crystallize during membrane formation. As the prime phase separation mechanism for nylon 6 appears to be liquid-liquid demixing, this means that nylon 6 crystallizes after the solution has separated into two liquid phases. Indications were found that probably the two nylons crystallize in separate lamellae, but inside the same spherulite or axialite. The better mechanical properties observed in literature for blend membranes of different nylons compared to the pure nylon membranes can be explained by the mutual entanglements between the two polymers near their lamellae, as is deduced from these measurements. Phase separation between the two corresponding crystalline phase must occur at a very local scale.

Both nylon 4,6 and the copolymer membranes are formed according to a solid-liquid phase separation mechanism. The copolymer / nylon 4,6 blend membranes showed a transition from axialitic to spherulitic morphology at high copolymer content (more than 90 wt%). The water flux and pore size of the membranes were in the microfiltration range. Only in the case of the pure copolymer, pores in the microfiltration range were no longer observed. The large top-layer thickness of this membrane resulted in a very low water flux not suitable for ultrafiltration applications. It seems probable that nylon 4,6 and the copolymer co-crystallize in the same lamellae, in contrast to the nylon 6 / nylon 4,6 system.

Improvement concerning the use of nylon membranes as support layers was achieved. The typical 'dome' structure of the top-layers was avoided by preparing nylon 4,6 / nylon 6 blend membranes with water in the casting solution.

ACKNOWLEDGEMENTS

The authors acknowledge financial support by D.S.M. the Netherlands. They are also indepted to Ir. Stephan Eltink for the performance of the WAXS experiments and to Ir. G.W. Meindersma of D.S.M. the Netherlands for supplying the polymers and to both for their pleasant cooperation.

REFERENCES

1. A.M.W. Bulte, B. Folkers, M.H.V. Mulder, C.A. Smolders, *J. Appl. Polym. Sci.*, 50, 13-26 (1993).
2. A.M.W. Bulte, *Diffusion Induced Phase Separation with Crystallizable Nylons, I Mass Transfer Processes for Nylon 4,6 and Relation to Final Morphology*, chapter 4 of this thesis.
3. A.M.W. Bulte, *Diffusion Induced Phase Separation with Crystallizable Nylons, II Kinetic Parameters for Membrane Formation with Nylon 4,6,* chapter 5 of this thesis.
4. R. Curry, *US patent* 4788226 (1988), *WO patent* 87 / 07849 (1987) (Domnick Hunter).
5. L.A. Utracki, *Polymer Alloys and Blends, Thermodynamics and Rheology*, Oxford University Press, NY (1990).
6. E. S. Ong, Y. Kim, *J. Appl. Pol. Sci.*, 31, 367 (1986).
7. T.S. Ellis, *Polymer*, 33, 1469 (1992).
8. J. Runt, D.M. Miley, *Macromolecules*, 25, 1929 (1992).
9. H. Saito, T. Okada, *Macromolecules*, 24, 4446 (1991).
10. G.C. Alfonso, V. Chiappa, *Eur. Polym. J.*, 27, 795 (1991).
11. Wei Li, Rongjiang Yan, J. *Macromol. Sci. - Phys.*, B31 (2), 239 (1992).
12. S. Cimmino, *Pol. Communications*, 32, no. 8, (1991).
13. Verma, B.L. Deopura, *J. Appl. Pol. Sci.*, 31, 747 (1986).
14. T. Kitao, H. Kobayashi, *J. Polym. Sci.: Pol. Chem. Ed.*, 11, 2633 (1973).
15. L.A. Utracki, in *"Two-Phase Polymer Systems"*, Carl Hanser Verlag, München, 1991.
16. R.M. Boom, Th. van den Boomgaard, C.A. Smolders, accepted by *J. Membr. Sci.*, (1992).
17. R.M. Boom, *Membranes Prepared from a Polymeric Blend Part I: Membranes from Poly(Ether Sulfone) and Poly(vinyl Pyrrolidone)*, chapter 4, PhD Thesis University of Twente (1992).
18. R.M. Boom, *Membranes Prepared from a Polymeric Blend Part II: Membranes Prepared from PES and PS; Comparison with the PES - PVP System*, chapter 5, PhD Thesis University of Twente (1992).
19. R. Kesting, *US patent* 4450126 (1984).
20. H. Hugl, R. Rhein, H.Göhl, *A Tailormade Polymer for Biocompatible Dialysis Membranes*, Proceedings

ICOM Heidelberg, 1993.

21. D.B. Pall, *US patent* 4340479 (1982), *EP patent* 0005536 A2 (1979) (Pall).
22. J.J Krol, *The Influence of blending on structure and performance of nylon 4,6 membranes*, M Thesis, University of Twente, Enschede (1993).
23. K.H. Illers, H. Haberkorn, *Macromol. Chem.*, 158, 285 (1972).
24. B. Valenti, E. Bianchi, *J. Phys. Chem.*, 7, no. 3, (1973).
25. H. Arimoto, *J. Polymer Sci.*, 2, 2283 (1964).
26. R.J. Gaymans, in *"Integration of Fundamental Polymer Science and Technology"*, Elsevier Publishers, 573 (1985).
27. R.M. Boom, unpublished results University of Twente, 1992.
28. G. E. Sweet, *J. Polymer Sci. - A2*, 10, 1273 (1972).
29. M. Todoki, T. Kawaguchi, *J. Polymer Sci.*, 15, 1067 (1977).
30. R.C. Roberts, *J. Pol. Sci. B-8*, 381 (1970).
31. A.M.W. Bulte, *Equilibrium Thermodynamics of the Ternary Membrane Forming System Nylon, Formic acid and Water*, Chapter 3 of this thesis.

Summary

Nylon 4,6, a new member in the family of aliphatic polyamides, has been studied for the application as membrane material. The membranes were prepared by the technique of immersion precipitation, which involves the immersion of a cast polymer film into a coagulation bath containing a non-solvent. Upon exchange of solvent and non-solvent the composition of the film changes and becomes instable. The morphology of the resulting membranes is dependent on the type of phase separation process that takes place. The manufacture of membranes with the membrane forming system nylon 4,6, formic acid as a solvent and water as a non-solvent has been studied in relation to performance and morphology in chapter 2. Typical microfiltration membranes were prepared with pores from 50 nm to 1 μm. The influence of crystallization of the polymer was very pronounced. The morphology of most nylon 4,6 membranes was spherulitic or axialitic of nature, while for most other membrane forming systems a cellular structure is found. The spherulitic and axialitic morphology is a result of solid - liquid (S-L) phase separation with spherulitic crystallization of the polymer; a cellular morphology is a result of liquid - liquid (L-L) phase separation. Thermodynamic and kinetic effects of both S-L phase separation and L-L phase separation are considered to be major parameters.

The performance of nylon 4,6 membranes in non-aqueous media is described in the first appendix to chapter 2. In the second appendix to chapter 2 the influence of metal halides as an additive to the casting solution has been studied. This additive was added to control the crystallization process. Addition of salts can change the morphology from spherulitic to axialitic and vice versa. In some specific cases the pore sizes of the membranes could be reduced considerably. The third appendix to chapter 2 describes another membrane forming system for nylons: ethanol or methanol with calcium chloride as a solvent system with various liquids as non-solvent. A wide range of pore sizes and types of morphology has been obtained.

The equilibrium thermodynamics of this ternary membrane forming system, nylon 4,6, formic acid and water, at 30 °C has been worked out in chapter 3. Melting points of ternary mixtures were determined between 35 and 85°C giving the isothermal crystallization line at 30°C by extrapolation. Melting point depression of the

polymer has been described by means of a modified Flory-Huggins theory. The three binary interaction parameters have been derived from literature data, swelling values and these experimental melting points. The binodal for this membrane forming system has been calculated from these three interaction parameters. The binodal is completely located within the S-L region. For this system thermodynamically crystallization or S-L phase separation is favorable over L-L demixing. Beside nylon 4,6 nylon 6 and a copolymer of the two polymers with 5% nylon 6 has been studied as well.

Mass transfer of solvent and non-solvent during membrane formation for this system has been described according to the mass transfer model of Reuvers and Smolders in chapter 4. Initial composition paths have been calculated in the assumption that at a small time scale the local equilibrium is given by the virtual binodal, located in the S-L region. As a result of the diffusion induced degree of supersaturation, crystallization takes place. The calculated degree of supersaturation for various cases is correlated to a cellular, a spherulitic or an axialitic morphology. A cellular morphology occurs when the degree of supersaturation is too low to induce crystallization on a small time scale. A moderate degree of supersaturation combined with a shallow composition path results in a isotropic spherulitic membrane morphology. An axialitic morphology occurs when the degree of supersaturation is large. Simultaneously an increase of polymer concentration at the interface is induced, resulting in the formation of a skin. The crystalline nature of spherulites and axialites is confirmed by transmission electron microscopy for which the samples were stained. Different stages of the coagulation process have been experimentally investigated by using a cryo-substitution technique.

Chapter 5 describes the correlation between the thermodynamic driving force for crystallization and the membrane morphology in terms of a virtual melting temperature. Heterogeneous nucleation of crystalline material is probably involved in the formation of crystalline structures in the membrane.

In chapter 6 the influences of the macromolecular additives, nylon 6 and a copolymer of nylon 6 and nylon 4,6, on the membrane morphology have been described. For the use of nylon membranes as support layers for composite membranes a regularly formed toplayer with smaller pores is required. The use of blends of nylon 4,6 and nylon 6 avoids the typical 'dome structure' and a dense selective coating layer on the support layer could be acquired. During the first stages of membrane formation the polymer system can be considered as one component, while phase separation

between the two semi-crystalline polymers takes place on a larger time-scale. Both polymeric components of the blends showed crystallization.

This thesis has described both the use of nylon 4,6 as a membrane material from a practical point of view and the effect of polymer crystallization during immersion precipitation for which the ternary system nylon 4,6, formic acid and water is used as a model system.

Samenvatting

Nylon 4,6, een nieuw polymeer in the familie van alifatische polyamiden, is bestudeerd voor de toepassing als membraan materiaal. De membranen zijn vervaardigd met behulp van immersie precipitatie; een gestreken polymeeroplossing wordt geprecipiteerd in een coagulatiebad, dat een niet-oplosmiddel bevat. Door uitwisseling van oplosmiddel en niet-oplosmiddel verandert de samenstelling van de film, die instabiel wordt. De morfologie van de resulterende membranen is afhankelijk van het type fase scheidingsproces. Membranen vervaardigd met het membraanvormende systeem nylon 4,6, mierezuur en water zijn bestudeerd op hun filtratiekarakteristieken en hun morfologie. Dit staat beschreven in hoofdstuk 2. De verkregen microfiltratiemembranen hebben poriën van 50 nm tot 1 µm. Kristallisatie van het polymeer had een uitgesproken invloed op de membraanstructuur, die in de meeste gevallen sferulitisch of axialitisch was, terwijl de meeste andere uit de literatuur bekende membraanvormende systemen een cellulaire structuur vertonen. De sferulitische en axialitische morfologie is het resultaat van vast - vloeistof (S-L) fasescheiding met sferulitische kristallisatie van het polymeer, terwijl een cellulaire morfologie het resultaat is van vloeistof - vloeistof (L-L) ontmenging. Thermodynamische en kinetische effecten van S-L fase scheiding naast L-L fase scheiding worden als belangrijke parameters besproken.

Het gebruik van nylon 4,6 membranen in niet-waterig milieu is bestudeerd en beschreven in de eerste appendix van hoofdstuk 2. In de tweede appendix van hoofdstuk 2 zijn de effecten van toevoeging van metaalhaliden aan de polymeeroplossing beschreven met als doel het kristallisatieproces te beïnvloeden. Toevoeging van zout kan de morfologie veranderen van sferulitisch naar axialitisch en vice versa. In sommige specifieke omstandigheden kon de poriegrootte aanzienlijk worden gereduceerd. De derde appendix van hoofdstuk 2 beschrijft een ander membraanvormend systeem met ethanol of methanol in combinatie met calciumchloride als een oplosmiddel systeem; verschillende vloeistoffen zijn gebruikt als niet-oplosmiddel. Membranen met een variëteit aan poriegrootten en soorten morfologie konden worden verkregen.

De evenwichtsthermodynamica van het membraanvormende systeem, nylon 4,6,

mierezuur en water bij 30 °C is uitgewerkt in hoofdstuk 3. Smelttemperaturen van ternaire mengsels zijn bepaald tussen 35 en 85°C en de smeltpuntverlaging van het polymeer is beschreven met een gemodificeerde Flory-Huggins theorie. De isotherm bij 30°C kan worden bepaald door extrapolatie. De drie binaire interactie parameters zijn afgeleid uit de literatuur, uit sorptie-experimenten en uit de experimenteel bepaalde smeltpunten. De binodaal van dit membraanvormende systeem is berekend met behulp van de drie interactie parameters en ligt volledig in het S-L gebied. Kristallisatie zal thermodynamisch gezien de voorkeur hebben boven L-L ontmenging. Naast nylon 4,6 zijn de polymeren nylon 6 en een copolymeer van de twee bestudeerd.

Massatransport van oplosmiddel en niet-oplosmiddel voor dit systeem is uitgewerkt in hoofdstuk 4 met behulp van het model beschreven door Reuvers en Smolders. Initiële compositiepaden zijn berekend onder de aanname dat het locale evenwicht op het grensvlak in een kort tijdsinterval gegeven wordt door de virtuele binodaal, die is gelegen in het S-L gebied. Kristallisatie vindt plaats als een resultaat van de diffusie-geïnduceerde graad van oververzadiging. De berekende graad van oververzadiging is gecorreleerd aan het voorkomen van een cellulaire, een sferulitische of een axialitische morfologie voor verschillende omstandigheden. Een cellulaire morfologie wordt waargenomen wanneer de oververzadiging te klein is om kristallisatie binnen een korte tijd te laten plaats vinden. Een matige oververzadigingsgraad in combinatie met een vlak compositiepad geeft een isotrope sferulitsche membranen. Axialitische morfologie wordt waargenomen bij een hoge oververzadiging, die geïnduceerd wordt in combinatie met een hoge polymeerconcentratie op het grensvlak. Dit type membraan heeft een dunne toplaag. De kristallijne aard van de waargenomen sferulieten en axialieten is bevestigd door transmissie electronen microscopie. De verschillende stadia van het coagulatie proces zijn experimenteel bestudeerd met behulp van een cryo-substitutie techniek.

Hoofdstuk 5 beschrijft de correlatie tussen de thermodynamische drijvende kracht voor kristallisatie en de waargenomen membraanmorfologie met behulp van virtuele smeltpunttemperaturen. Heterogene kiemvorming van kristallijne structuren is hoogstwaarschijnlijk van invloed op de membraanmorfologie.

In hoofdstuk 6 wordt de invloed van de macromoleculaire additieven nylon 6 en een copolymeer van nylon 6 en nylon 4,6 op de membraanmorfologie bestudeerd. Een regelmatig gevormde toplaag met ultrafiltratie poriën is noodzakelijk voor de toepassing van deze nylon membranen als onderlaag voor composiet membranen.

Door gebruik te maken van nylon 6 kan de voor deze nylon membranen typische 'koepel-structuur' in de toplaag worden vermeden. Een composiet membraan met een selectieve coating laag kon worden verkregen. Gedurende de eerste stadia van de membraanvorming kan de polymere blend worden beschouwd als één polymeer systeem, terwijl de faseschеiding tussen de twee semi-kristallijne polymeren plaats vindt in een grote tijdsinterval. Beide polymere komponenten vertoonden kristallisatie.

Dit proefschrift heeft zowel de practische betekenis van het gebruik van nylon 4,6 als de effecten van polymeer kristallisatie tijdens immersieprecipitatie beschreven vanuit het ternaire systeem nylon 4,6, mierezuur en water.

Levensloop

Astrid Bulte werd geboren op 21 oktober 1964 te Oldenzaal, alwaar zij in 1983 haar VWO diploma behaalde aan het Twents Carmellyceum. In hetzelfde jaar begon zij haar studie Chemische Technologie aan de Universiteit Twente te Enschede. Haar doctoraalstage vervulde zij bij DOW Chemical te Rheinmünster (Duitsland), waar zij heeft gewerkt aan de vervaardiging van epoxyharsen. In het kader van de internationale studiereizen heeft zij in 1988 meegewerkt aan de door C.T.S.G. Alembic georganiseerde reis naar Japan. In 1989 verrichtte zij haar doctoraalopdracht in de vakgroep Biomedische Materiaal Techniek bij prof. Feijen met als onderwerp "Synthesis and Characterization of Biodegradable Block-copolymers", waarmee zij haar doctoraaldiploma Chemische Technologie met lof behaalde.

In de periode van 1 november 1989 tot 1 november 1993 was zij werkzaam als assistent in opleiding bij de onderzoeksgroep Membraantechnologie en verrichtte zij het onderzoek beschreven in dit proefschrift.

ISBN 90-9006884-8